The synergistic interaction between dithiophosphate and frothers at the air-water and mineral-water interface

Dandré Pienaar

A thesis submitted to the Faculty of Engineering and the Built Environment, University of Cape Town, in fulfilment of the requirement for the degree of

Doctor of Philosophy

Centre of Minerals Research

Department of Chemical Engineering

University of Cape Town

August 2021

Plagiarism declaration

I, **Dandré Pienaar**, hereby declare that the work on which this thesis is based is my original work (except where acknowledgements indicate otherwise) and that neither the whole work nor any part of it has been, is being, or is to be submitted for any other degree in this or any other university. I authorise the University to reproduce for the purpose of research either the whole or any portion of the contents in any manner whatsoever.

Signed by candidate

Signature: _____ Date: 2022/02/21

Acknowledgements

I would like to acknowledge the following people for contributing to the success of this project:

- My supervisors A/Professor Belinda McFadzean and Professor Cyril O'Connor. My time under your supervision has evoked curiosity. Thank you for your open-doors, long discussions, expertise, and insights. They were invaluable to the success of this project.
- A/Professor Kirsten Corin and Dr Nora Schreithofer. Thank you for the opportunity and funding to go to Finland. It was an amazing experience. Thank you Nora for being an incredible host.
- The team in Finland – Professor Rodrigo Serna, Dr Robert Hartmann, Dr Ted Nuorivaara, and the late Omar Martinez. Thank you everyone for your hospitality. My time spent there was truly memorable.
- The CMR staff – Gary, Shireen, Kenneth, Monde, Refilwe, Nqobile, Keshree and Lorrain. Thank you for help and support through various aspects of this project.
- Students in the CMR labs – Sebia, Andrea, Shoki, Jestos, and Noli. Special thank you to Andrea for feedback on my document.
- My friends in the chemical engineering department - Dawid, Olga and CK. Thank you for discussions over lunch. These helped me persevere when I felt unsure about myself.
- My parents, Madré and Danie Pienaar. Thank you for your support, pride, and encouragement.
- My grandparents. Thank you for your help and support.
- My partner, Channon Perry. Thank you for your endless patience. Thank you for putting up with my craziness. Thank you for listening to me talk about mineral processing. Thank you for your help and continuous support. I love you.
- My cats, Wednesday and Forest. Thank you for keeping being there when things got very stressful. Squeezing a cat always helped.

I would also like to acknowledge the National Research Foundation (NRF), South African Minerals to Metals Research Institute (SAMMRI), Department of Science and Innovation (DSI) and the Chemical Engineering Department. Thank you for the funding and the input into this work.

List of publications and presentations

1. McFadzean, B., Jordaan, T., Pienaar, D. & O'Connor, C. 2018. Interactive effects between frothers and dithiophosphate collectors in sulfide mineral flotation. *Proceedings of the XXIX International Mineral Processing Congress, Moscow, Russia*
2. Pienaar, D., Jordaan, T., McFadzean, B. & O'Connor, C. 2019. The synergistic interaction between dithiophosphate collectors and frothers at the air-water and sulphide mineral interface. *Minerals Engineering*. 138:125-132.
3. Pienaar, D., McFadzean, B., O'Connor, C. & Schreithofer, N. 2019. The interactions of thiol collectors with frothers on pyrite, quartz and chalcocite. *Proceedings of the MEI Flotation Conference*. Including oral presentation.
4. Pienaar, D., McFadzean, B. & O'Connor, C. 2020. Molecular interactions between thiol collectors and non-ionic frothers in mixed monolayers at the air-water interface using a regular solution theory approach. *Proceedings of the XXX International Mineral Processing Congress, Cape Town, South Africa*

Abstract

Collectors and frothers are reagents in the flotation process that are thought to have separate roles. Collectors selectively hydrophobized the mineral surface and frothers adsorb onto bubbles inhibiting bubble coalescence and stabilizing the froth. Interactions between these molecules have been previously reported in literature (Leja & Schulman, 1954; Lekki & Laskowski, 1971; Dai, Bradshaw & Harris, 2001; Jordaan, 2018). These interactions have been shown to improve sulphide mineral recovery.

Dithiophosphate (DTP) is a collector in sulphide mineral flotation which has been shown to synergistically increase flotation recovery in the presence of frothers (Pienaar et al., 2018) but it has also been shown that DTP does not adsorb onto the sulphide mineral surface (Nagaraj & Brinen, 2001; McFadzean & O'Connor, 2014; Petrus et al., 2011; Grano et al., 1997; Guler et al., 2006; Taguta, O'Connor & McFadzean, 2017) as occurs with conventional collectors. If DTP does not adsorb onto the mineral surface and improve hydrophobicity it was not clear what the role of DTP is in the flotation process. The main objective of this research was to identify the role of DTP in sulphide mineral flotation.

Each of the respective interfaces were investigated for the adsorption of dithiophosphate (DTP). The adsorption of DTP on galena, pyrite, chalcopyrite and chalcocite was measured by UV-Vis spectrophotometry and isothermal titration calorimetry. Adsorption tests in the presence of aeration were used to determine if DTP dynamically transferred from the air-water to the mineral-water interface. At the air-water interface a regular solution theory approach, critical coalescence experiments and foam stability tests were used to quantify the interactions between DTP and frothers and compare them to xanthate and frothers. Microflotation and induction time experiments were performed to determine the effect of the collectors, frothers and their mixtures on mineral recovery and bubble-particle attachment

It was found that DTP in the presence of a non-ionic frother synergistically improved sulphide mineral recovery. This improvement was attributed to attractive molecular interactions which were found to occur between the collector and the frother at the air-water interface. The interaction facilitated the transfer of the frother between the air-water and mineral-water interface, which destabilised the film between the bubble and the particle, improving film thinning kinetics and synergistically enhanced mineral recovery. When DTP did not adsorb onto the mineral surface, the collector co-adsorbed with the frother at the air-water interface and transferred with the frother onto the mineral surface during bubble-particle collision.

Table of Contents

List of figures

List of Tables

Abbreviations and acronyms

ACTA – Automated contact time apparatus

BET - Brunner-Emmett-Teller

BMS – Base metal sulphide

CCC – Critical coalescence concentration

DLVO - Derjaguin-Landau-Verwey-Overbeek

DRIFT - Diffuse Reflectance Fourier Transform Infrared

DTC – Dithiocarbamate

DTP – Dithiophosphate

IEP – Isoelectric point

ITC – Isothermal Titration calorimetry

PAX – Potassium amyl xanthate

PGM – Platinum group minerals

PNBX – Potassium n-butyl xanthate

PPG – poly propylene glycol

SAS – Surface active substances

SD(I)BDTP – Sodium di-iso-butyl dithiophosphate

SD(N)BDTP – Sodium di-n-butyl dithiophosphate

SD(N)HDTP – Sodium di-n-butyl dithiophosphate

SDEDTP - Sodium diethyl dithiophosphate

SEX – Sodium ethyl xanthate

SIBDTPINA – Sodium di-iso-butyl dithiophosphinate

SIBX – Sodium iso-butyl xanthate

ToF-SIMS – Time of flight secondary ion mass spectrometry

UV-Vis – Ultraviolet visible

1. Introduction

Froth flotation is a crucial beneficiation step in the recovery of minerals where differences in mineral surface hydrophobicity are exploited to separate valuable minerals from gangue in a 3-phase system. Even though there are many important inter-related variables that govern the froth flotation process, the chemistry is the basis on which the valuable mineral surface is selectively hydrophobized, so that it can attach to the bubble and rise to the froth phase where it can be recovered into the concentrate.

1.1 Background

Thiol collectors are the reagents that are used in base-metal sulphide (BMS) and platinum group mineral (PGM) flotation to selectively hydrophobize sulphide minerals. Xanthates and dithiophosphates (DTP) are the most common thiol collectors used in sulphide mineral flotation. These collectors are typically used as a mixture of xanthate and DTP, where it has been reported that these mixtures of collectors synergistically improve the recovery of sulphide minerals (Corin, Bezuidenhout & O'Connor, 2012; Bradshaw & O'Connor, 1994). Primarily, collectors are present on the mineral surface, but DTP has exhibited froth modification properties suggesting that it is active at the air-water interface (Lotter & Bradshaw, 2010).

DTP has been shown not to adsorb onto the sulphide mineral surface under conditions of high pH and for certain mineral types (Nagaraj & Brinen, 2001; McFadzean & O'Connor, 2014; Petrus et al., 2011; Grano et al., 1997; Guler et al., 2006; Taguta, O'Connor & McFadzean, 2017). Hence DTP does not appear to behave as a classical collector, where the collectors adsorb at the mineral surface to increase hydrophobicity and facilitate the attachment of the bubble to the particle.

A recent investigation has shown that even though DTP does not adsorb onto the surface of pyrite and galena, a synergistic improvement (the ultimate effect is greater than the effect of the weighted sum of the individual components) in mineral flotation performance was observed with DTP in the presence of a non-ionic frother, rather than in the presence of a co-collector (Jordaan, 2018). Leja & Schulman (1954) theorized that the improvements in flotation performance observed for mixtures of collectors and frothers are due to molecular interactions between these reagents at the air-water and mineral-water interface.

There have been a limited few that have suggested that molecular interactions may occur between DTP and frothers (Jordaan, 2018; Dai, Bradshaw & Harris, 2001). Similar studies with xanthate-frother mixtures have shown conflicting results, where the improvement in recovery observed may not be due to interactions between the xanthate and the frother, but

due to the collector and frother having separate roles, where the collector enhances the mineral surface hydrophobicity, and the frother improves the film thinning kinetics between the bubble and the particle by transferring from the air-water interface to the mineral-water interface (Lekki & Laskowski, 1971; Dai, Bradshaw & Harris, 2001). These effects thus represent separate and parallel roles of the two reagents.

Further investigation into the role of DTP at the air-water interface, and its interactions with non-ionic frother is thus required to elucidate the mechanism by which DTP improves pulp phase recovery.

The main objective of this study is to understand the mechanism whereby DTP-frother interactions synergistically improve sulphide mineral recovery.

1.2 Problem statement

DTP has been shown to synergistically increase flotation recovery in the presence of frothers (Jordaan, 2018) but it has also been shown that DTP does not adsorb onto the sulphide mineral surface (Nagaraj & Brinen, 2001; McFadzean & O'Connor, 2014; Petrus et al., 2011; Grano et al., 1997; Guler et al., 2006; Taguta, O'Connor & McFadzean, 2017) as occurs with conventional collectors. The role that DTP plays in the flotation process is thus not clear and often controversial. Further investigations are thus required to understand the role which DTP plays in flotation both on its own and in the presence of frothers. Such an improved understanding may well lead to the development of better reagent suites which will improve flotation performance.

1.3 Scope and project approach

1. This project aims to investigate the molecular interactions between thiol collectors and non-ionic frothers at the air-water and sulphide mineral-water interface. Furthermore, the mechanism by which the molecular interactions between these reagents synergistically improve sulphide minerals will be investigated. The primary thiol collectors that will be used are DTP and xanthate. Xanthate will be used as a benchmark to compare the behaviour of DTP. This investigation will be carried out by the following three studies:Characterization of the effect of collectors, frothers and collector-frother mixtures on bubble-particle attachment and sulphide mineral recovery using a Glembodsky device and a microflotation device. The Glembodsky device decouples bubble-particle attachment where the effect of chemical environment on the attachment sub-process is revealed. The microflotation device decouples froth-phase effects from the overall flotation process, and only bubble-particle attachment is measured.

2. Characterization of the adsorption behaviour of DTP and DTP-frother mixtures at the air-water interface and at the sulphide mineral interface through foam stability, surface tension, pulp bubble coalescence and UV-Vis spectrophotometry. The adsorption behaviour of DTP will also be studied in the presence of aeration to determine if the collector transfers from the air-water interface to the mineral-water interface.
3. Qualitative and quantitative characterisation of the molecular interactions between collector and frothers at the air-water interface through a combination of foam stability, surface tension, pulp bubble coalescence experiments and the regular solution theory model.

The outcomes of these studies will be used to understand the mechanism whereby DTP-frother mixtures synergistically enhance sulphide mineral recovery.

2 Literature review

2.1 Overview

The froth flotation process can be separated into two zones: The froth zone and the pulp zone is depicted in Figure 2.1. In the pulp zone the selectively hydrophobized particles attach to the air bubble and moves up to the froth zone where the particles are recovered. The particles are hydrophobized by collectors and the frothers stabilize the froth by inhibiting bubble coalescence.

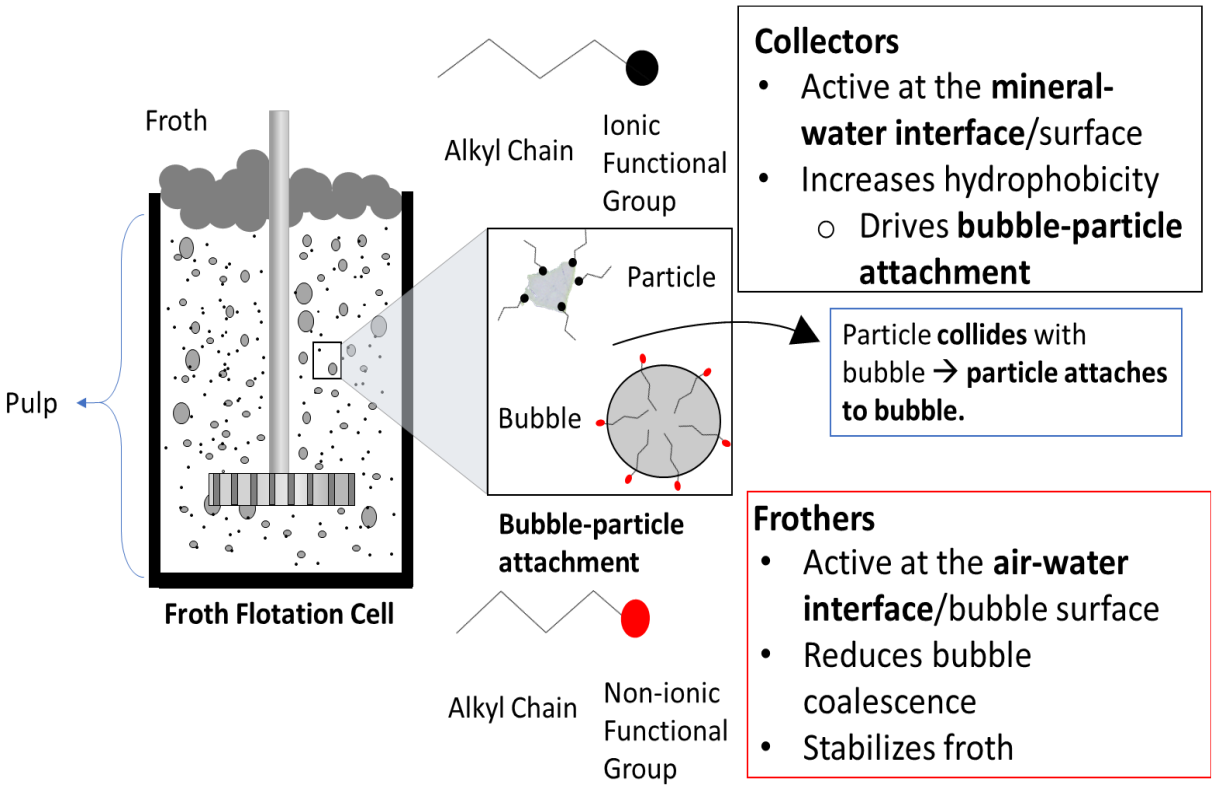

Figure 2.1: Froth flotation process and overview of literature review

This review primarily focuses on the bubble-particle attachment process that occurs in the pulp phase, and how collectors and frothers, and mixtures of these reagents affect this process.

2.2 Sub-processes of bubble-particle attachment

2.2.1 Flotation probability

One of the most important steps for successful flotation is bubble-particle attachment in the pulp (Albijanic et al., 2010). The dynamics of the bubble-particle attachment process can be expressed as:

$$P = P_c\, P_a\, P_s \qquad \text{Equation 1}$$

where P_c is the probability of a collision occurring between the bubble and the particle, P_a is the probability that the particle attaches to the bubble, and P_s is the probability that a stable bubble-particle aggregate forms.

The probability of collision is mainly governed by the relative velocity of the bubbles and the particles in the hydrodynamic pulp phase. The probability that the bubble-particle aggregate that is formed is stable is influenced by the hydrodynamics but is mainly a function of the contact angle formed between air-water and mineral-water interface.

For successful flotation to occur the particle needs to attach to the bubble. During the attachment subprocess an intervening water film between the bubble and mineral surface needs to be displaced in order for the particle to attach to the bubble. In the first step of this subprocess, the wetting film between the bubble and particle thins to critical thickness. At this point the surface forces between these interfaces govern the stability of the wetting film. These forces are due to the surface properties of each of the interfaces. If there is a net attractive surface force between these interfaces, the film will become unstable. If the wetting film becomes unstable, the thin film of water ruptures. A three-phase contact line is formed, where the mineral-water, air-water and air-mineral interfaces are present. The air-mineral interface spreads out and forms a stable wetting perimeter (Nguyen, Schulze & Ralston, 1997).

The time scale of this process is known as the bubble-particle attachment time, which is often referred to as the induction time. For successful attachment to occur, the attachment time must be shorter than the time that the bubble and particle are in contact with each other (Albijanic et al., 2010). The attachment process which is governed by the thinning kinetics and stability of the thin film between the bubble and the particle is mainly controlled by the interfacial chemistry of these two surfaces.

2.2.2 Surface forces

The surface forces which influence the stability of thin liquid films between air bubbles and mineral surfaces can be described by extended Derjaguin-Landau-Verwey-Overbeek (DLVO) forces, which are the double-layer (electrostatic), van der Waals and hydrophobic forces. Van der Waals forces are repulsive under flotation conditions. In the case where the electrostatic double-layer force is repulsive, the hydrophobic force is responsible for the attraction between bubbles and mineral particles (Laskowski & Kitchener, 1969). When the hydrophobic force is weak and the double-layer force is attractive, the electrostatic force is responsible for attraction between bubbles and mineral particles, which results in contactless flotation (Derjaguin & Dukhin, 1961).

The adsorption of collector at the mineral-water interface controls the hydrophobicity of the mineral surface, which is responsible for the attractive force between the bubbles and mineral particles (Laskowski & Kitchener, 1969).

2.3 Collectors

Collectors are surface active reagents (surfactants) which are used in mineral processing for selective hydrophobization of valuable minerals. A schematic showing the interaction of the

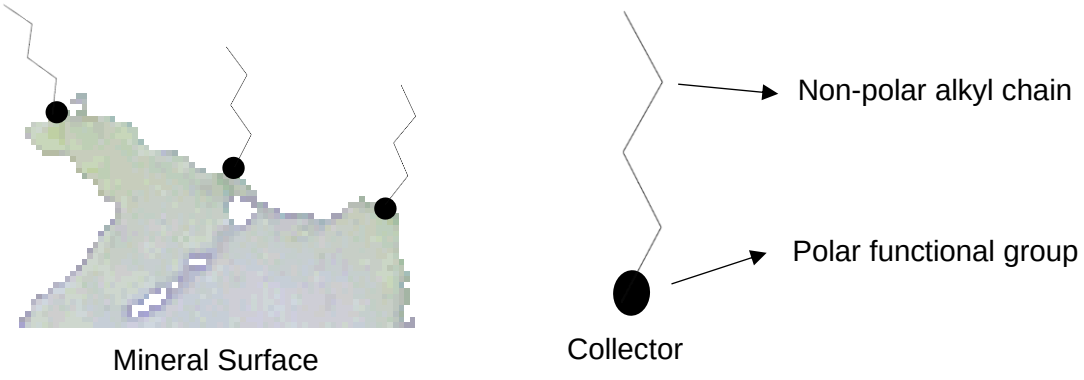

Figure 2.2: Schematic diagram of collector structure and orientation on mineral surface

collector with the mineral surface is illustrated in Figure 2.2. From Figure 2.2 it can be seen that the collector consists of two portions, a polar functional group/ligand and a non-polar alkyl chain. The ligand portion selectively interacts with the mineral surface. For thiol collectors, primarily used for sulphide mineral flotation, the functional group is anionic. The alkyl chain portion is hydrophobic by nature due to water not being able to interact with the chain via hydrogen bonding.

2.3.1 Mechanisms of collector adsorption

The adsorption of thiol collectors onto sulfide minerals has been observed to be electrochemical in nature. The process involves an anodic oxidation reaction on the mineral surface involving the collector, with a simultaneous cathodic reduction of oxygen. As sulfide minerals are semiconductors, they provide a pathway for the transfer of the electrons from the oxidation site to the reduction site (Rao, 2013:482).

The nature of the adsorbed species on the mineral surface depends on the pulp potential. Mainly chemisorbed thiolates, metal thiolates, or dithiolates are the species responsible for the mineral hydrophobicity. Each of these species induces a different degree of hydrophobicity on the mineral surface.

2.3.1.1 Chemisorption

The chemisorption of thiol collector onto the mineral surface follows an anodic charge transfer described by Equation 2:

$$X^- \leftrightarrow X_{adsorbed} + e^- \quad \text{Equation 2}$$

Where X is the thiolate species which bonds to a metal atom in the surface lattice structure of the mineral. The bond of the thiolate species with the metal atom does not change the lattice structure of the mineral (Buckley & Woods, 1993). The coupled oxygen reduction is described in Equation 3**:**

$$O_2 + 2H_2O + 4e^- \leftrightarrow 4OH^- \quad \text{Equation 3}$$

The chemisorbed thiolate forms at potentials below the reversible potential for the formation of the metal thiolate, and only monolayer coverages are possible (Allison et al., 1972).

2.3.1.2 Metal thiolate formation

The formation of metal thiolate compounds follows a coupled electrochemical and chemical reaction at the mineral surface.

First the mineral surface is oxidized in the reaction described in Equation 4:

$$MS + 4H_2O \leftrightarrow MSO_4 + 8H^+ + 8e^- \quad \text{Equation 4}$$

The mineral surface oxidation reaction is coupled with the same oxygen reduction reaction described in Equation 3. Following these reactions there is an ion exchange process between the thiolate and the surface oxidation products in Equation 5:

$$MSO_4 + 2X^- \leftrightarrow MX_2 + SO_4^{2-} \quad \text{Equation 5}$$

The metal thiolates species show decreasing hydrophobicity with increasing electronegativity of the metal ion or increasing solubility of the metal thiolate compound (Rao, 2013:483).

2.3.1.3 Catalytic oxidation for dithiolate formation

The thiol collector can be further oxidized to form a dithiolate, depending on the pulp potential. The oxidation of the thiol collector to the dithiolate is typically quite slow, but the presence of the mineral can catalyze the reaction, improving the reaction rate. The thiol oxidation reaction is as follows:

$$2X^- \rightarrow X_2 + 2e^- \quad \text{Equation 6}$$

The oxygen reduction reaction occurs at the mineral surface according to Equation 3:

The neutral dithiolate molecule is highly insoluble and has the highest degree of hydrophobic character compared to all the other thiolate species that form. The dithiolate is held weakly at

the mineral surface through physisorption and can form multilayers on the mineral surface (Rao, 2013:296,318)

If the rest potential of the mineral is higher than the oxidation potential for the formation of the dithiolate, the primary species found on the mineral surface is the dithiolate, whereas if the rest potential of the mineral is below the oxidation potential, the primary species is the metal thiolate (Allison et al., 1972). The oxidation potential of diethyl DTP is significantly lower, viz. -0.255 V (Kakovskii, Ryazantseva & Serebryakova, 1959) compared to that of ethyl xanthate, viz. 0.060 V (Winter & Woods, 1973), thus the formation of the DTP dithiolate is less likely than for xanthate.

2.3.2 Dithiophosphate adsorption

DTP is a thiol collector that is typically used as a co-collector with xanthate. DTP is known for its selectivity against pyrite and galena, where is it used to selectively float copper sulfides.

2.3.2.1 Chalcopyrite

Diffuse Reflectance Infrared Fourier Transform (DRIFT) spectroscopy on chalcopyrite under varying pH and potential conditions showed that the potential at the mineral surface was not a critical variable in determining the resultant surface species of diethyl DTP. It was rather found that pH had a strong influence on the adsorption of these species onto the mineral surface. At acidic to neutral pH's the metal thiolate and dithiolate DTP species was dominant, whereas at alkaline pH barely any species of DTP was detected on the surface of chalcopyrite (Güler et al., 2005). These results were supported by contact angle tests, revealing lower contact angles obtained at alkaline conditions, compared to neutral and acidic conditions (Güler & Hiçyilmaz, 2004).

Similar results were obtained by Petrus et al. (2011), where ultraviolet – visible (UV-Vis) spectrophotometry analysed the remaining concentration of diethyl DTP in the pulp after contacting with the mineral, at pH 9. After DTP was contacted with chalcopyrite under alkaline conditions, the residual concentrations of DTP remaining in the pulp was virtually unchanged from the concentrations in the absence of the mineral. This illustrates that DTP is not adsorbing onto the surface of chalcopyrite.

Grano et al. (1997) simulated the oxidation of the chalcopyrite surface through the addition of Fe^{3+} ions which adsorb onto the mineral surface forming iron oxyhydroxide species. UV-vis spectrophotometric analysis showed that at basic pH's there was a lower affinity of sodium dicresyl DTP for the oxidized chalcopyrite surface. All authors (Güler et al., 2005; Petrus et al., 2011; Grano et al., 1997) concluded that the adsorption of DTP onto the chalcopyrite surface is strongly dependent on the pulp pH which can affect the surface state of the mineral.

At an alkaline pH the formation of iron oxyhydroxide species inhibits the adsorption of DTP, as depicted in Figure 2.3.

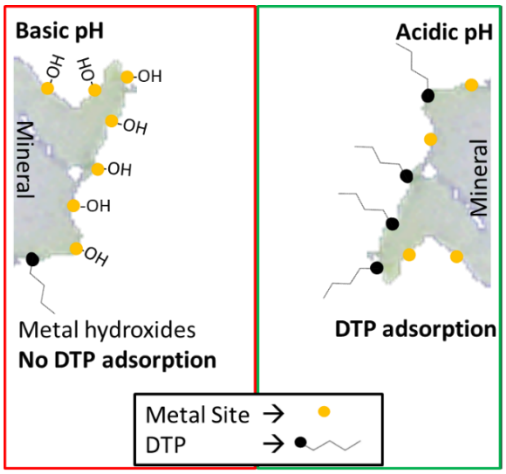

Figure 2.3: Formation of oxyhydroxide species on the mineral surface

Taguta, O'Connor & McFadzean (2017) used isothermal titration calorimetry (ITC) to characterise the adsorption energy of thiol collectors onto sulphide minerals at pH 9. The authors found that diethyl DTP showed very low adsorption energies onto chalcopyrite (-4.9 kJ/mol) compared to that of ethyl xanthate (-33.4 kJ/mol), corresponding to the previous studies where low to negligible adsorption was observed (Güler et al., 2005; Petrus et al., 2011; Grano et al., 1997).

2.3.2.2 Iron sulphides

On other minerals such as pyrrhotite and pyrite, low adsorption energies were observed for diethyl DTP at pH 9 (Taguta, O'Connor & McFadzean, 2017). These results are supported by ToF-SIMS surface studies performed on pyrite, where low adsorption densities of an iron hydroxyl di-iso-butyl DTP complex was detected relative to the adsorption densities of other thiol collectors on the mineral surface (Nagaraj & Brinen, 2001). These findings are consistent with industry practice as DTP's are generally used for their selectivity against pyrite and pyrrhotite (Lotter & Bradshaw, 2010).

2.3.2.3 Galena

McFadzean & O'Connor (2014) used ITC to show that diethyl DTP produced very low heats of adsorption when titrated into a pH 9 slurry of galena, which indicated that there was negligible adsorption of DTP onto the mineral. Further investigation by McFadzean & O'Connor (2014) with UV-Vis spectrophotometry supported this when the concentration of residual DTP remaining in the pulp did not change within the detection limits of the apparatus.

These findings are in line with those of Wark & Cox (1934). They found the critical pH, which is the pH below which collector adsorption occurs, of the diethyl DTP-galena system was 6.2 according to contact angle measurements. Sutherland & Wark (1955) analysed the residual concentration of ethyl DTP remaining in the pulp after contact with galena and determined the critical pH to be 6.0, similar to Wark & Cox (1934).

In addition, cyclic voltammetry and Auger electron spectroscopy tests investigated the adsorption of diethyl DTP onto galena at pH 5 (below the critical pH of galena) and with the pulp saturated with air. These tests showed that there was no interaction of the collector with the mineral surface for conditioning times less than an hour, indicating extremely poor adsorption onto galena, even at low pH's (Buckley & Woods, 1991).

2.3.2.4 Chalcocite

The chalcocite-DTP system behaves differently to the other minerals reviewed so far. Buckley & Woods (1993) performed cyclic voltammetry and Auger electron spectroscopy tests to investigate the mechanism of how diethyl DTP interacts with the chalcocite at alkaline conditions and varying pulp potentials. It was found that diethyl DTP chemisorbed onto the mineral at potentials below the formation of the metal thiolate.

Compared to the adsorption of dithiophosphate, the other thiol collectors such as xanthate readily adsorb onto sulphide minerals and in the presence of oxygen will form multilayers of dixanthogen on the mineral surface (Rao, 2013:296).

2.3.3 Donor atoms and thiol collector reactivity at the sulphide mineral-water interface

One of the governing factors influencing the reactivity, and thus selectivity of thiol collectors to the sulphide mineral is the presence of electron withdrawing or donating groups that control the electron density around the sulphur donor atoms. Dialkyl dithiophosphates do not bond as strongly with the mineral surface due to the two electron-withdrawing oxygen atoms attached to the phosphate (Lotter & Bradshaw, 2010; Somasundaran & Nagaraj, 1984), as illustrated in Figure 2.4 (c). In contrast, dithiocarbamates (DTC) have an electron-donating nitrogen atom attached to the carbon (Figure 2.4 (a)), resulting in a higher electron density in the dithiol headgroup, which creates a stronger bond with the mineral surface. In this context of reactivity, xanthates are intermediate between DTP and DTC in terms of bonding strength.

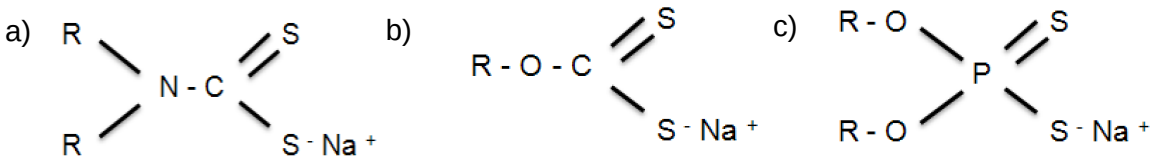

Figure 2.4: Chemical structure of thiol collectors. (a) Dithiocarbamate , (b) Xanthate and (c). Dithiophosphate (R represents the alkyl chain)

The reactivity of thiol collectors is reflected in their pK_a values – the acid dissociation constant. The equilibrium dissociation reaction for the collector is represented by:

$$HX \leftrightharpoons H^+ + X^- \qquad \text{Equation 7}$$

With K_a is represented by:

$$K_a = \frac{[H^+][X^-]}{[HX]} \qquad \text{Equation 8}$$

Where X represents the collector, and H is hydrogen. The pK_a is the negative logarithm of K_a. The pK_a values for ethyl chain length thiol collectors are shown in Table 2.1. The pK_a of the collector represents the tendency of the collector to donate electrons to a metal atom and form a metal thiolate. DTP has the lowest pK_a value of the thiol collectors, which is due to electron withdrawing inductive effect of the electronegative oxygens, stabilizing the DTP anion, making it a more selective collector than xanthate and DTC (Somasundaran & Nagaraj, 1984).

Table 2.1: pK_a values for various thiol collectors

Collector	pK_a	Reference
Diethyl DTP	~ 0	Rao (2013:431)
Ethyl Xanthate	2.20	Hayashi et al, (1984)
Diethyl DTC	4.62	Hayashi et al, (1984)

The polarizability of these collectors follows the reverse order of their pK_a:

DTC > Xanthate > DTP

with DTC being the most polarized and DTP exhibiting the greatest non-ionic character. (Somasundaran & Nagaraj, 1984).

2.3.4 Effect of DTP on flotation recovery

A comparison between coverage of the collector on the sulfide mineral surface and flotation recovery has shown that low coverages of collector (10% monolayer) is often sufficient to induce hydrophobicity to a significant degree whereby flotation recovery is improved

compared to collectorless flotation (Woods, Kim & Yoon, 1993). The hydrophobicity that the collector induces is influenced by many factors such as the surface species that are formed, the metal with which the collector forms a complex, oxidation state of the mineral surface, and collector chain length. Thus, pulp phase recovery is often the easiest and most direct way to measure the effectiveness of a collector.

Even though adsorption studies of DTP indicate selective adsorption, further examination of its effect on recovery is required to understand whether DTP has other effects during the flotation process.

2.3.4.1 Batch flotation recovery

McFadzean, Mhlanga & O'Connor (2013) conducted batch flotation tests using pure pyrite and galena at pH 9. The use of diethyl DTP in pyrite flotation did not significantly increase recovery compared to collectorless recovery (29.31% - collectorless, and 33.58% - diethyl DTP). It thus follows that DTP is usually used for its selectivity against pyrite, and it does not interact with the pyrite mineral surface.

For galena a significant improvement in recovery was observed upon addition of diethyl DTP. Recoveries improved from 44% for the baseline collectorless case, to 89% recovery when DTP was used. Ethyl xanthate only showed an improvement in recovery to 76%. The results are contrary to the proposals by McFadzean & O'Connor (2014), that ethyl xanthate adsorbed onto galena and formed the metal thiolate on the mineral surface. In the same microcalorimetric study it was shown that ethyl DTP exhibited no detectable interaction.

Batch flotation tests performed on Cu-Ni-Pt ores at alkaline pH by Manono et al. (2020) and Kloppers et al. (2016) both showed that diethyl DTP significantly improved the recovery of copper and nickel compared to the case of collectorless recovery and recovery using isobutyl xanthate. The majority of the copper mineral in the Kloppers et al. (2016) study was found to be chalcopyrite, which has been shown not to interact with DTP at high pH (Güler et al., 2005; Petrus et al., 2011; Grano et al., 1997).

Table 2.2: Summary of batch flotation results performed on a Cu-Ni-Pt Merensky Reef ore (Adapted from Kloppers et al, (2016))

	Recovery (%)		Grade (%)	
	Cu	Ni	Cu	Ni
Collectorless	88	22.5	0.43	0.32
Isobutyl Xanthate	90	54.8	0.41	0.58
Ethyl DTP	95.7	64.4	0.14	0.3

Table 2.2 shows that even though recoveries were improved with diethyl DTP for this ore, there is a significant decrease in the grade of copper and nickel compared to the grades obtained when using SIBX, which indicates that it may simply be an increased mass pull effect.

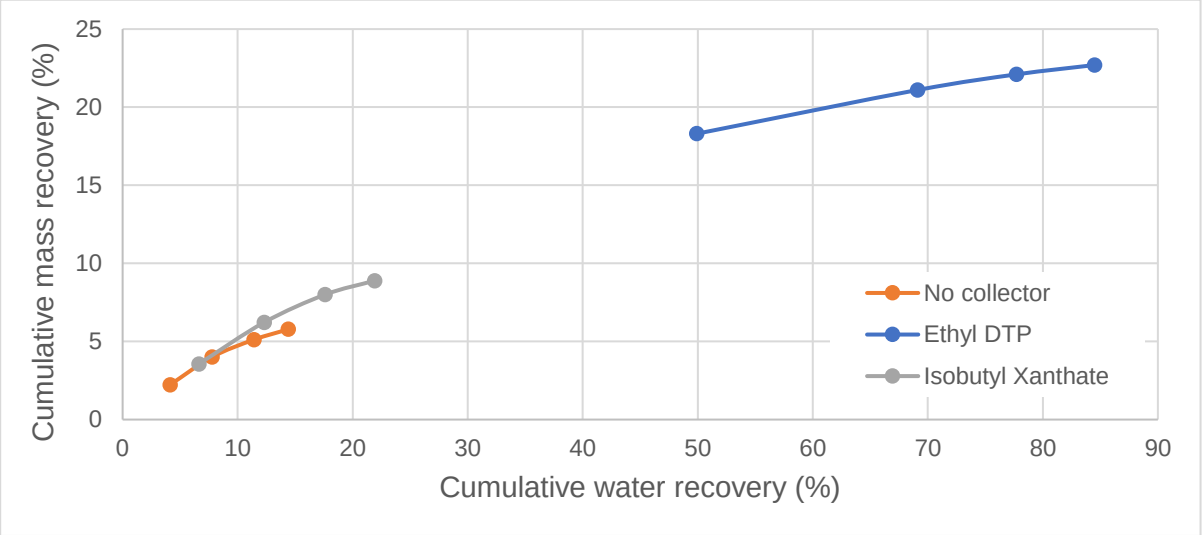

Figure 2.5: Mass vs water recovery for ethyl DTP and isobutyl xanthate (Adapted from Kloppers et al (2016))

The low grades observed in both of these studies (Manono et al., 2020; Kloppers et al., 2016) were attributed to significantly higher water/solids recoveries obtained as illustrated in Figure 2.5. Corin, Bezuidenhout & O'Connor (2012) ascribed the higher mass-water recoveries observed when using DTP, to this reagent having frothing effects, suggesting that the reagent might be active at the air-water interface.

The effect of thiol collectors at the air-water interface has been addressed in some important studies. Figure 2.6

Figure 2.6 compares the air-water interface activity of standard thiol collectors to a typical glycol frother blend used in flotation. Ethyl xanthate was shown to have no effect on surface tension even at concentrations much higher than typical flotation concentration ranges (Jordaan, 2018). This confirmed results reported in other studies (Manev and Pugh, 1993, Buckenham and Schulman, 1963). The surface tension measurements showed that DTP was active at the air-water interface but was much weaker than the typical frothers used in flotation.

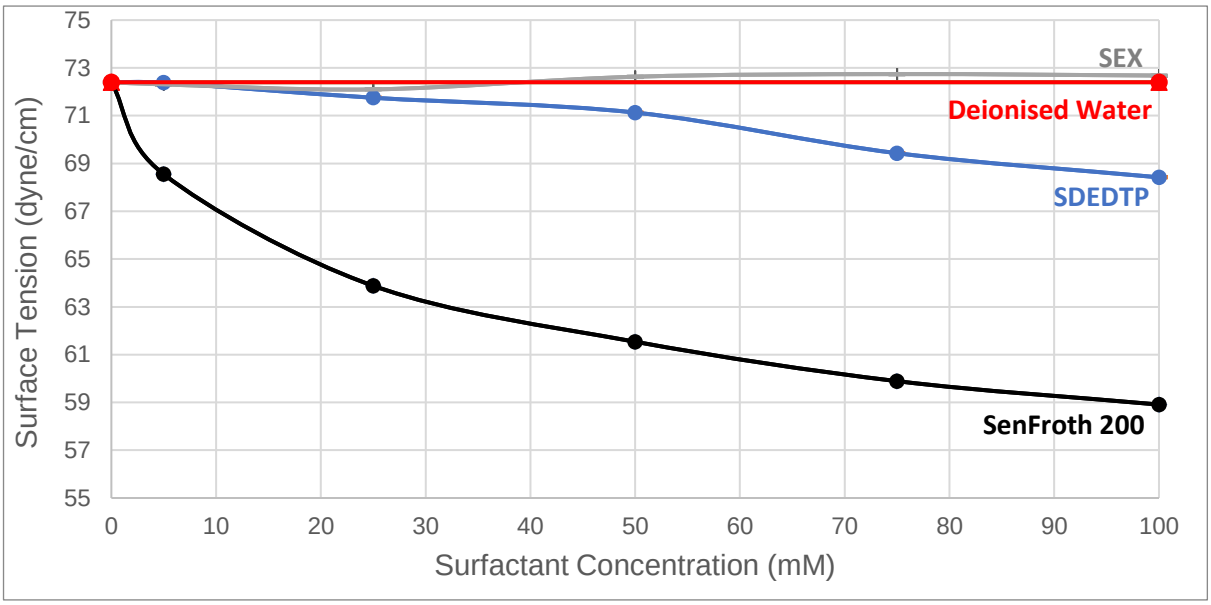

Figure 2.6: The effect of typical sulfide mineral flotation reagents on surface tension (Figure adapted from Jordaan (2018))

The difference in the activity between xanthate and DTP at the air-water interface could be attributed to the pK_a values of the collectors and the polarizability of their anion. As can be seen from Table 2.1, a higher pK_a value for xanthate shows the anion of the collector is more polarized than that of DTP, which has more non-ionic character. This may affect the electrostatic repulsion between the anion headgroups when they are adsorbed at the air-water interface. The DTP anion produces less electrostatic repulsion at the air-water interface than the xanthate anion, allowing for greater adsorption density.

The weak surface activity of DTP collectors relative to the activity of non-ionic frothers may correspond to the charge on short chain ionic surfactants inductively counteracting the hydrophobic effect of the alkyl chain. This is prevalent in carbon molecules neighboring the polar head group of the molecule. The charge can inductively change the electron density around the non-polar chain making it more polar in character (Rao, 2013:163).

Some reports have attributed the activity of DTP at the air-water interface to be due to residual reactants remaining after the synthesis of DTP. Dialkyl dithiophosphoric acid is produced by the following reaction:

$$P_2S_5 + 4\,ROH \rightarrow 2(RO)_2PS_2H + H_2S \qquad \text{Equation 9}$$

where the dithiophosphate salt is produced by neutralizing the acid with a base. The reaction is performed in excess alcohol and thus further purification of the collector is required. It has been proposed that the residual alcohol present in the product mixture may be the cause of the air-water interface activity observed when using DTP (Corin, Bezuidenhout & O'Connor, 2012).

Measurement of the stability of the froth can indicate whether DTP has froth stabilizing properties like frothers. Jordaan (2018) conducted 2 phase and 3 phase, foam and froth stability tests on mixtures of diethyl DTP and SenFroth 200 (a polyglycol frother blend). Figure 2.7 indicates that ethyl DTP on its own provides slight foam and froth stability compared to the frother. Two phase tests show that these reagents improve foam stability synergistically viz. to a greater extent than the sum of the individual components, but this improvement is absent in the presence of particles, as can be seen from 3 phase froth stability. Similar results have been reported by Bezuidenhout (2011) for 3 phase tests. The improved foam stability may be from collector-frother interactions which have been shown to produce synergistic effects in pulps and froths (Leja & Schulman, 1954).

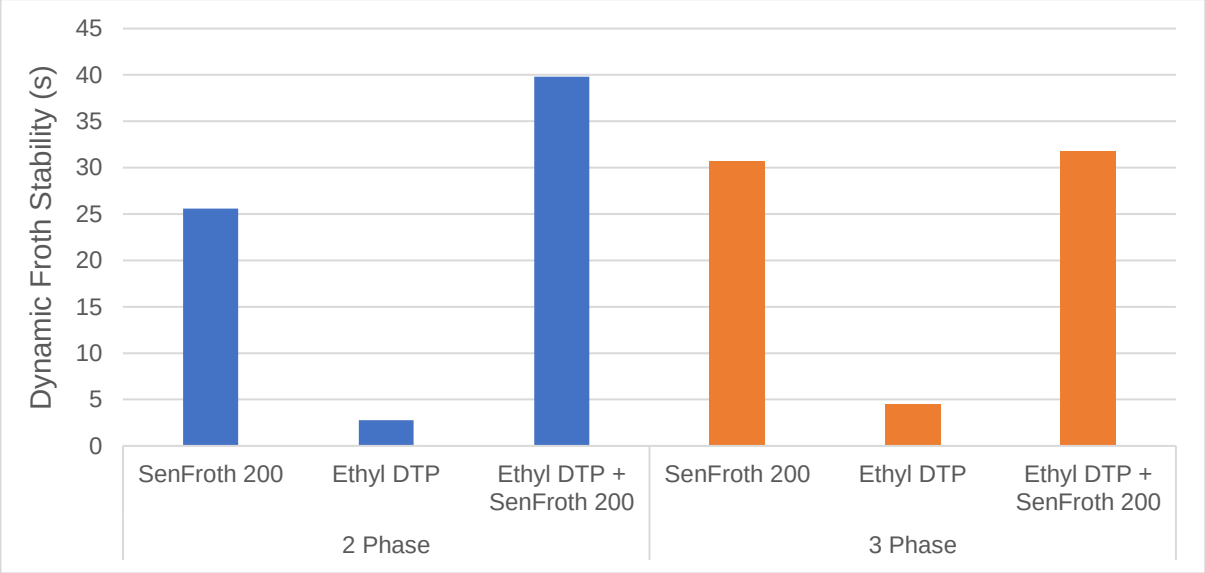

Figure 2.7: Dynamic foam and froth stability for 2 phase and 3 phase systems using DTP - frother mixtures. (Data adapted from Jordaan (2018))

Particles play an important role in the froth stability and can have a much greater effect on froth stability than the frother, which minimizes the effects produced by the DTP-frother mixture. Furthermore, the presence of particles may influence whether DTP adsorption occurs at the air-water interface or mineral-water interface. This can change the mechanism of interaction observed in two phase froths.

There are many conflicting results reported in the literature when DTP has been used in batch flotation studies. High water recoveries and surface tension data suggest that DTP is active at the air-water interface rather than the mineral water interface, and that there could be an interaction between DTP and frothers as shown by 2 phase foam stability tests. Contrary to this, 3 phase froth stability tests show no improvements in froth stability when DTP was used. The results of the experiments reviewed in this section appear to show that DTP behaves like a collector for galena and chalcopyrite even though it does not interact with these minerals.

2.3.5 Pulp phase recovery

Frothers which are typically active at the air-water interface have shown improvements in pulp phase recovery and bubble-particle attachment kinetics (Dai, Bradshaw & Harris, 2001; Jordaan, 2018; Lekki & Laskowski, 1971). Since DTP has been shown not to interact with some minerals and is active at the air-water interface, it is possible that DTP could enhance pulp phase recovery by a similar mechanism. Microflotation decouples froth phase effects from pulp phase effects so that the bubble-particle attachment process can be better understood.

The effect of ethyl DTP on pulp-phase recovery is summarized for various sulfide minerals in Figure 2.8. For pyrrhotite and pyrite no significant improvements in recovery are observed when using DTP (Taguta, O'Connor & McFadzean, 2017; Jordaan, 2018), which is supported by adsorption data, which showed that there was no detectable interaction between DTP and these minerals (Taguta, O'Connor & McFadzean, 2017). Furthermore batch flotation results with pyrite showed no significant improvements in recovery (McFadzean, Mhlanga & O'Connor, 2013).

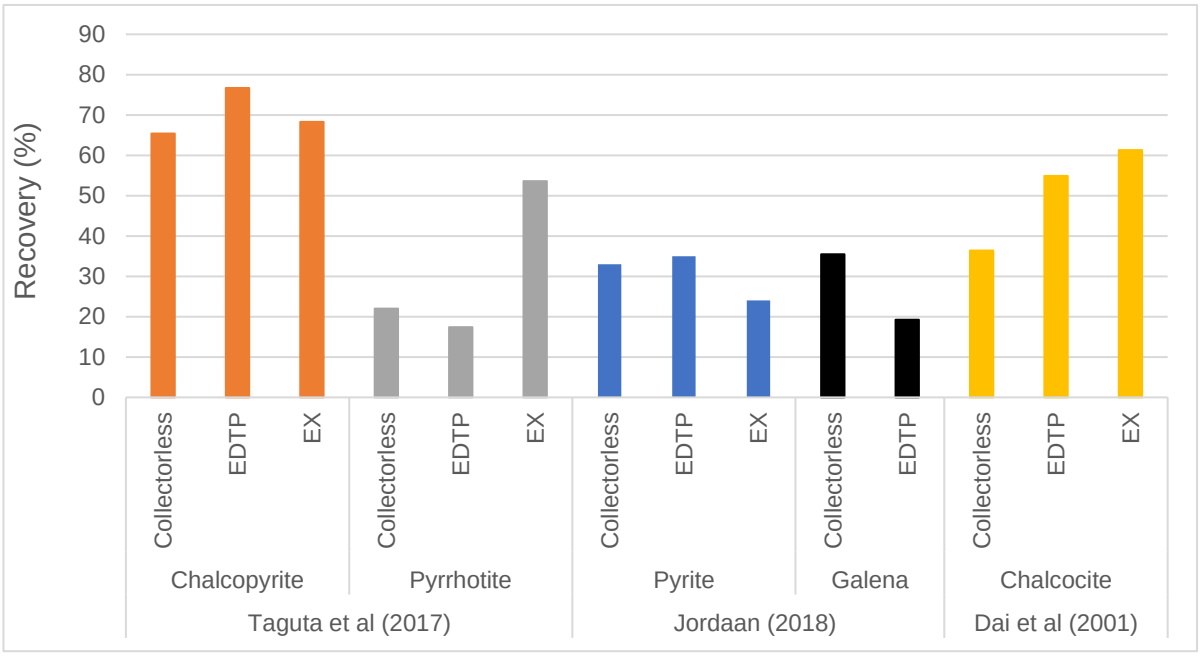

Figure 2.8: The effect of ethyl DTP and xanthate on sulfide mineral recovery (Adapted from Taguta, O'Connor & McFadzean (2017), Jordaan (2018) and Dai, Bradshaw & Harris (2001).

Ethyl DTP improved the recovery of chalcocite (Dai, Bradshaw & Harris, 2001), which is expected as DTP does interact with the chalcocite mineral surface (Buckley & Woods, 1993), and coverages as low as 10% can produce recoveries of 50% in 1 minute (Woods et al 1993).

Even though negligible interaction of ethyl DTP with the chalcopyrite surface was observed by Güler et al. (2005), Petrus et al. (2011) and Taguta, O'Connor & McFadzean (2017), Figure

2.8 presents the results reported by Taguta, O'Connor & McFadzean (2017) who observed an increase in chalcopyrite recovery at pH 9.2. The recovery increased from 65.4% to 76.6% with the addition of ethyl DTP.

Galena showed a synergistic improvement in batch flotation recovery when using ethyl DTP (McFadzean, Mhlanga & O'Connor, 2013), but in the microflotation cell DTP does not improve recovery as demonstrated in Figure 2.8. The microflotation results by Taguta (2015), and McFadzean, Castelyn & O'Connor (2012) for DTP and galena similarly showed no improvement in recovery. Adsorption results support the microflotation results, viz. that DTP does not interact with the mineral surface (McFadzean & O'Connor, 2014; Buckley & Wood, 1991; Taguta, O'Connor & McFadzean, 2017).

The question then remains as to what conditions in the batch flotation cell could lead to DTP improving the recovery for galena, but not improve the recovery in the microflotation cell? Frothers are used in batch flotation cell to stabilize the froth and reduce bubble size in the pulp. They are not typically used in microflotation cells as bubble coalescence is not as severe. This is due to the single stream of bubbles generated in the microflotation cell (Cho & Laskowski, 2002) and the difference in the energy input into the microflotation cell compared to the batch cell. In addition, there is no froth to stabilize. Therefore, the synergistic improvements observed for galena and ethyl DTP in the batch flotation system may be due to synergistic interactions between collectors and frothers. These synergistic interactions between these reagents have been shown to facilitate bubble-particle attachment and improve pulp phase recovery (Leja & Schulman, 1954).

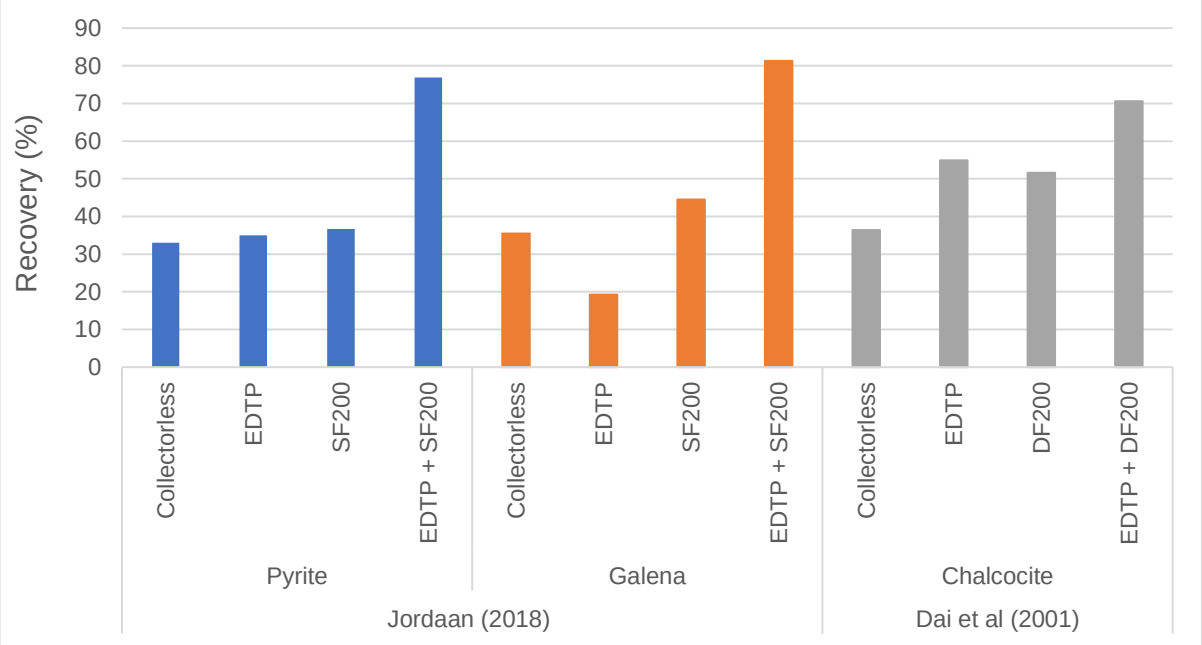

Figure 2.9: The effect of ethyl DTP and polyglycol frothers on sulfide mineral recovery (Adapted from Jordaan (2018) and Dai, Bradshaw & Harris (2001))

A study done by Jordaan (2018) showed that when a polypropylene glycol frother was used with diethyl DTP in a microflotation cell, synergistic improvements in pulp phase recovery for galena and pyrite (Figure 2.9) were observed. Notwithstanding these results, DTP showed no interaction with these mineral surfaces which is reaffirmed by no improvement in the microflotation recovery when only the collector is used. When the frother was added the recovery doubled for both pyrite and galena, using the recovery of frother as a baseline (the frother was chosen as a baseline as it gave a higher recovery than the DTP collector). The author speculated that the interaction between the collector and frother facilitated the improved recoveries observed with galena and pyrite (Jordaan, 2018). Comparing the recovery with frother alone to the collectorless condition however showed no significant change for pyrite and a 25% improvement for galena.

The response of chalcocite to the ethyl DTP-Dowfroth 200 mixture was not as significant as that observed for galena and pyrite, as is demonstrated in Figure 2.9. The mixture of collector and frother showed a significant improvement in the recovery compared to the baseline of ethyl DTP or the frother (Dai, Bradshaw & Harris, 2001). Furthermore, both ethyl DTP and the frother showed a significant improvement in the recovery compared to the baseline collectorless recovery.

In the case of chalcocite, it appears that both the collector and frother have separate roles in improving the microflotation recovery. Ethyl DTP is known to interact with the chalcocite surface improving the surface hydrophobicity (Woods, Kim & Yoon, 1993). Frothers have been shown to improve bubble-particle attachment (Lekki & Laskowski, 1973) in the pulp phase, which can be attributed to effects frothers have on bubble rise velocity (Nguyen and Schulze, 2004), bubble size (Wang et al., 2005; Gu et al., 2004) and surface forces present between the bubble and the particle (Leja & He, 1984). Thus, the improvements observed may possibly not be due to synergistic interactions between these reagents but to the individual effects of the collector and frother.

Comparing the behavior of ethyl xanthate (EX) and ethyl DTP on pyrite, the mixture of xanthate and frother only marginally improved the recovery of pyrite (Figure 2.10), compared to the recovery of the ethyl DTP-frother mixture which improved the recovery of pyrite 2-fold (Figure 2.9). Ethyl xanthate is known to form dixanthogen on the pyrite surface (Usul & Tolun, 1973), which is contrary to the behavior of ethyl DTP which does not interact with the mineral. The differences in recoveries for the DTP-frother and xanthate-frother mixtures might thus be attributed to the activity of ethyl DTP at the air-water interface (Figure 2.6), which is the interface where the frother is active. Jordaan (2018) suggested that an interaction between

the collector and the frother is at the air-water interface, and that this interaction was improving the recovery of pyrite and galena.

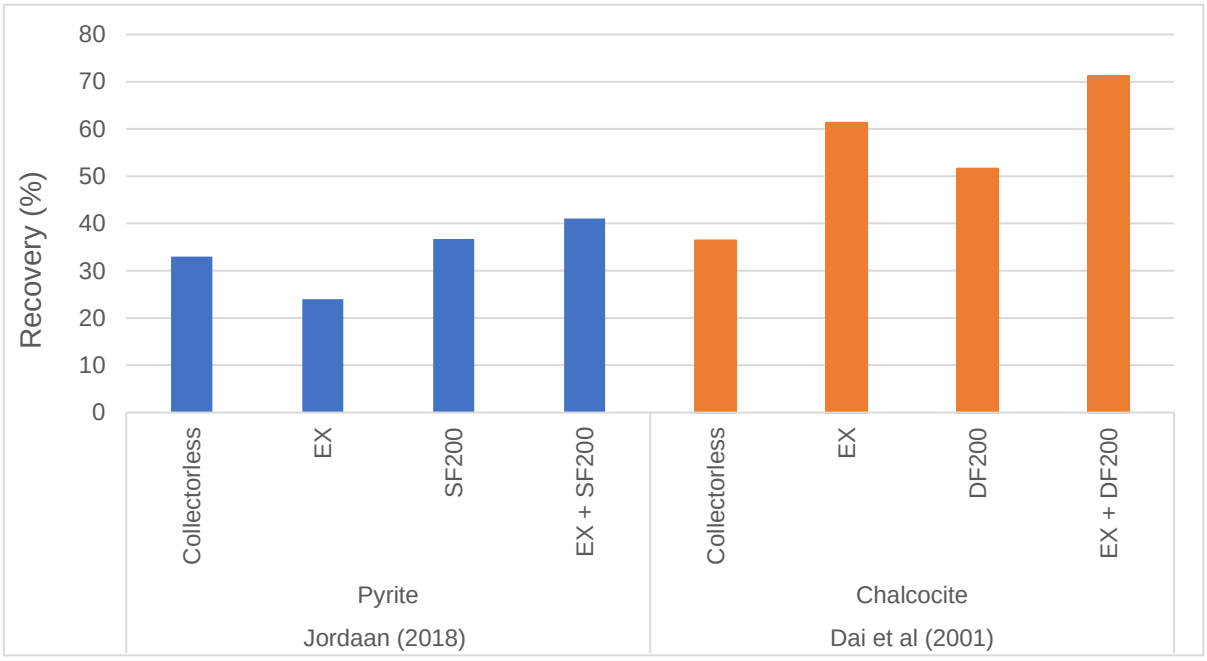

Figure 2.10: The effect of ethyl xanthate and polyglycol frothers on sulfide mineral recovery (Adapted from Jordaan (2018) and Dai, Bradshaw & Harris (2001))

The behavior of ethyl xanthate-frother mixture exhibits analogous behavior to the ethyl DTP-frother mixture on chalcocite. Significant improvements in recovery for the addition of the collector, the frother, and the collector-frother mixture indicate that the collector and frother might have different mechanisms for improving the pulp-phase recovery.

2.3.6 Collector transfer between the air-water and mineral-water interface

Derjaguin & Dukhin (1961) proposed that when a particle coated with collector comes into contact with a bubble, the collector will desorb from the mineral surface and diffuse from the mineral surface to the bubble. Subsequently the collector will adsorb onto the bubble surface. This occurs when the bubble and the particle are in a non-equilibrium state with respect to the concentration of collector at each interface.

Some authors (e.g. Fuerstenau, 2001; Yan, 2016; Wang & Miller, 2018) have found that when low concentrations of collector adsorb at the mineral surface, the remaining collector in the pulp can transfer from the air-water to the mineral-water interface as the bubble and particle collide. This has only been observed for amine-based collectors on quartz.

Rao (2013:652) argued that the diffusion of the collector through the thin film between the bubble and the particle would not significantly influence the induction time but proposed that the presence of a second type of surfactant may significantly improve the induction time. Further it was argued that the typical collectors used in flotation adsorb strongly at the mineral

surface and are likely immobilized. Meaning that it is unlikely that the collector desorbs off the surface of the mineral.

This mechanism whereby collectors transfer between interfaces may be the mechanism by which DTP functions as a collector in certain systems.

2.4 Frothers

Frothers, like collectors, are surfactants but are active at the air-water interface. The structure can contain a polar group, which in sulphide mineral flotation is non-ionic, and a non-polar alkyl chain. The chain is preferentially orientated at the air side of the interface, with the polar group at the water side.

Typical types of frothers include alcohols, or polyglycols which have a heterogenous distribution of polar and non-polar components.

2.4.1 Activity and effects of frothers at the air-water interface

Thermodynamics dictate whether the high energy surface of air-bubbles in water will coalesce upon interaction with each other. Frothers which are active at the air-water interface will lower the surface tension which means that the bubbles are more thermodynamically stable due to the lowering of surface free energy. At the concentrations which are typically used in flotation no surface tension change occurs as illustrated in Figure 2.11 (Comley et al., 2002; Sweet et al., 1997). Yet there is still a reduction in bubble coalescence. It is proposed that frothers create a kinetic resistance to the drainage of the thin film during a bubble-bubble interaction

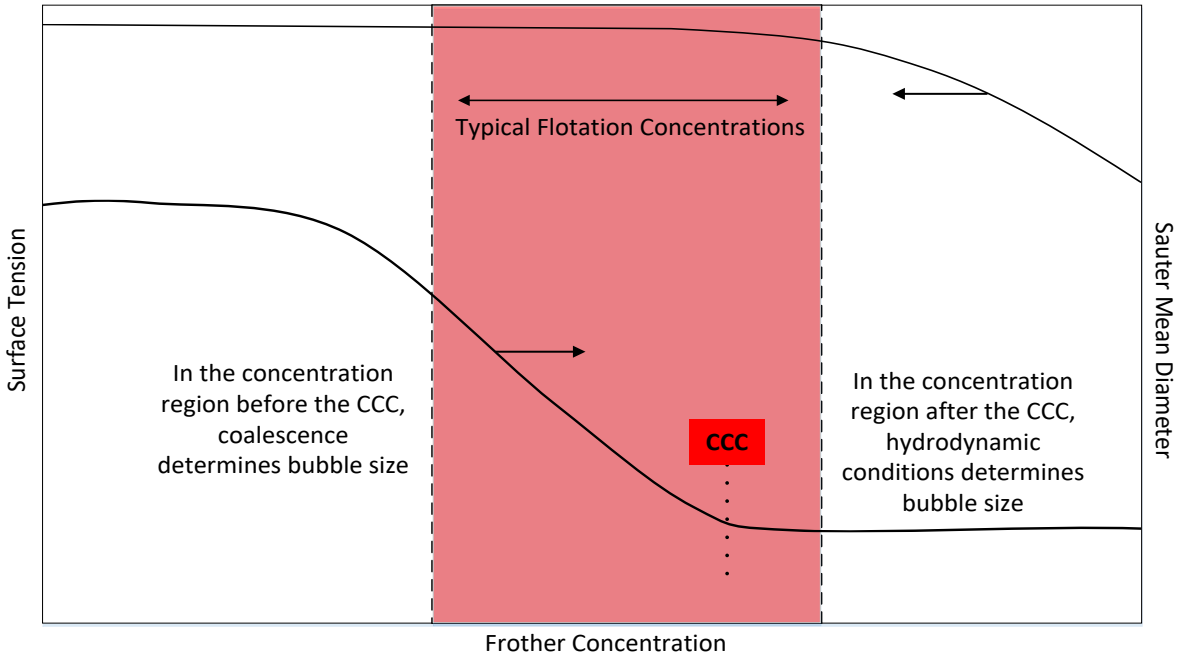

Figure 2.11: Change in surface tension and Sauter mean bubble diameter with increasing frother concentration (Figure adapted from Comley et al., (2002) and Cho & Laskowski (2001))

by forming a thin stable film around the bubble. This happens due to hydrogen bonding between the polar group of the frother and water molecules, which form a stable immobile film around the bubble that can resist bubble coalescence in the pulp and in the froth (Rödel, 1981).

2.4.1.1 Bubble Coalescence

Typically, coalescence determines the bubble size in the pulp of a flotation cell, and the presence of low concentrations of frothers inhibit bubble coalescence. The critical coalescence concentration (CCC) is known as the concentration at which coalescence is completely inhibited (Figure 2.11), and the bubble size is only controlled by sparger geometry (Cho & Laskowski, 2001; Grau, Laskowski & Heiskanen, 2005).

A decrease in bubble size is associated with an increase in collision efficiency between bubble and the particle (Yoon & Luttrell, 1989). The first order rate constant is also directly proportional to the bubble surface area, which is inversely proportional to the diameter of the bubble. This results in improved recoveries in the presence of frothers which generate smaller bubbles by inhibiting bubble coalescence.

2.4.2 Activity of frothers at solid-water interfaces

Non-ionic surfactants used as frothers are assumed to be mainly active at the air-water interface, but studies with mercury electrodes have shown aliphatic alcohols adsorb at the mercury electrode surface close to the isoelectric point (IEP) (Zembala & Pomianowski, 1970).

Lekki & Laskowski (1971) used zeta potential to show that α-terpineol interacts with the chalcocite surface at potentials of between -10 and -50 mV, and that potential control of the mineral-water interface through changing pH, or adsorption of collector at the mineral surface can control the potential conditions at the surface to allow either adsorption or desorption of the non-ionic frother molecule. This adsorption process was thought to be the mechanism behind the improvement of bubble-particle attachment kinetics in the presence of a frother.

The desorption of the frother at the mineral-water interface was also hypothesized to be promoted by the change in surface potential (away from the IEP) occurring as the film thins between the bubble and the particle (Lekki & Laskowski, 1976)

2.4.3 The role of non-ionic frothers in bubble-particle attachment kinetics

Frothers are typically used to stabilize the water film at the air-water interface, and when bubbles collide these films can resist drainage and inhibit bubble coalescence. Contrary to this mechanism of stabilization during bubble-bubble collision, when a bubble collides with a

sulfide mineral particle in the presence of a frother, film thinning kinetics are improved (Lekki & Laskowski, 1971; Leja & He, 1984).

2.4.3.1 Polarization of frothers

Under typical flotation conditions, the air-water and mineral-water interface generally carry a similar charge which will make the electrostatic force between them repulsive. Leja & He (1984) hypothesized that as the bubble and particle approach each other, the dipole of the polar portion of the non-ionic frother can be orientationally polarized in the electrostatic field of the particle. The time that this process takes to occur is called the principal dielectric relaxation time. This time is on the order of 10^{-12} s and depending on the state (gaseous, condensed or solidified) can vary by several orders of magnitude (Dannhauser, 1968).

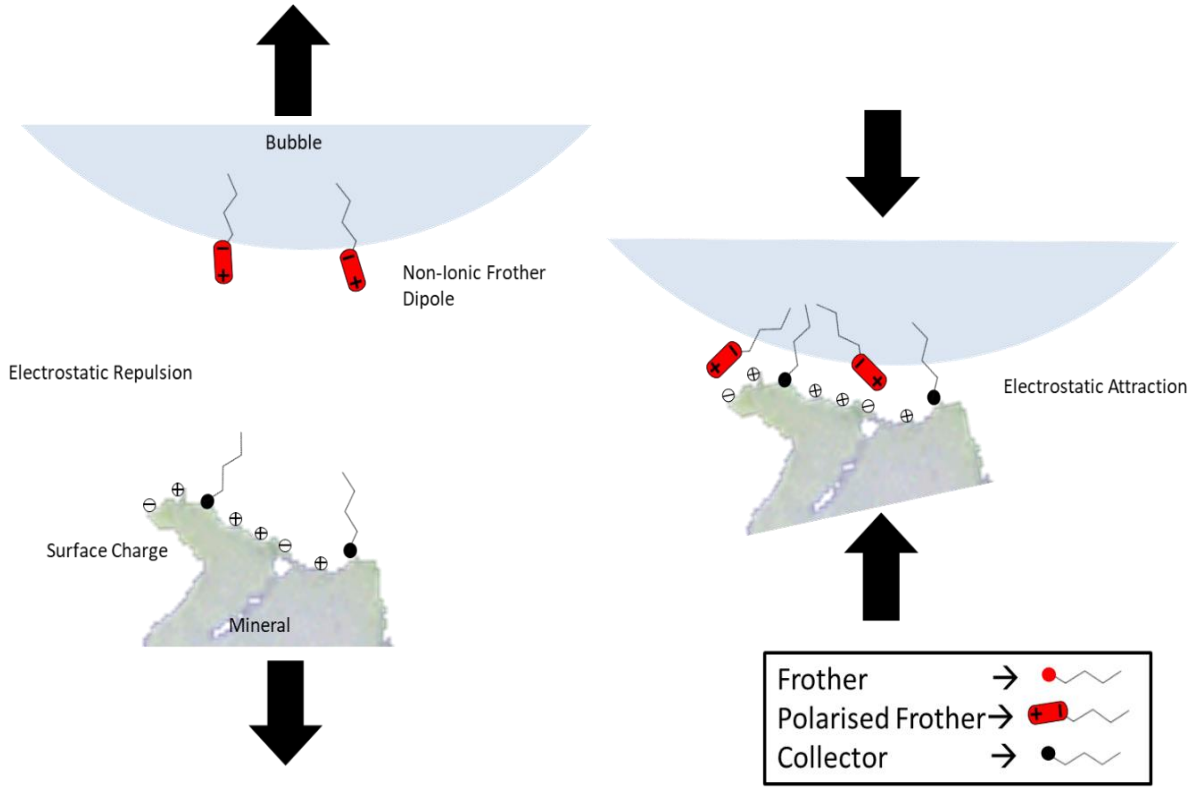

Figure 2.12: Reduction of electrostatic repulsion between the air-water and mineral-water interface in the presence of a polarized frother

The polarized portion of the frother molecule can interact with charges on the mineral surface, and dynamically alter the double-layer forces between the particle and the bubble from repulsive to attractive, enhancing the film thinning kinetics (depicted in Figure 2.12). For attachment to occur the principal dielectric relaxation time needs to be shorter than the contact time (Leja & He, 1984).

If high concentrations of frother are used, the state of the air-water interface can change from diffuse to condensed, which can increase the relaxation time by orders of magnitude to the point that the relaxation time is greater than the contact time. This can slow down the altering

of the double-layer forces between the particle and bubble and inhibit attachment within the contact time.

2.4.3.2 Frother transfer through films and between interfaces

The flotation system is generally a non-equilibrium system. Bubbles are not homogenously coated in surface active substances (SAS), and due to hydrodynamics, these SAS can be swept around and can be concentrated or diffuse on different portions of the bubble.

Lekki & Laskowski (1971) proposed that frother molecules can adsorb and desorb from the mineral surface depending on the potential at the mineral surface. During bubble-particle collision, the air-water and mineral-water interface can be in a non-equilibrium state with respect to the concentration of the frother at each interface. This promotes transfer of the frother molecule between these interfaces, and the movement of the frother through the thin film between the bubble and the particle, can destabilize the thin film – enhancing bubble-particle attachment kinetics.

Frothers, specifically alcohols, are sparingly soluble in water as the non-polar part of the molecule cannot form hydrogen bonding with the water molecules. When the frother is present in these thin films they can disrupt the hydrogen bonding network between the water molecules. Lekki & Laskowski (1971) observed that in the presence of higher concentrations of α-terpineol, the thickness of the fluid film on a chalcocite electrode decreased significantly.

2.4.3.3 Microbubbles at the solid-water interface

Kosior et al. (2013) observed that the time for the formation of 3 phase contact (induction time) between a hydrophobic Teflon plate and a bubble was increased in the presence of non-ionic flotation frothers. It was theorized that when a hydrophobic solid is immersed in water, small pockets of air on the scale of nano or micro bubbles can be trapped in the surface roughness. Flotation frothers can be adsorbed both onto these entrapped bubbles, and on the colliding bubble. During collision the entrapped bubbles and colliding bubble can resist drainage of the thin film, increasing the time for the formation of 3 phase contact. It was found that the concentrations at which this happened was within the range of the critical coalescence concentrations of the frother (Kosior et al., 2013). This supports the theory that the entrapped bubbles at the hydrophobic surface, and the colliding bubble resist coalescence during collision which can increase the time for the thin film to drain.

2.4.3.4 Bubble rise velocity

A bubble rising through a liquid without any surfactant has a mobile surface which flows downward as the bubble rises, but in the presence of a frother, the frother molecules (which makes the film partially immobile) are swept to the back of the bubble, creating a surface

tension gradient. This surface tension gradient, which is highest in the front of the bubble and lowest at the bottom, results in a net force towards the front of the bubble due the Marangoni effect. This force resists the tangential shear stress due to the partially immobile surface of the bubble, creating drag and lowering the bubble rise velocity (Dukhin, Miller & Loglio, 1998; Finch, Nesset & Acuña, 2008). The lowered rise velocity of the bubble can enhance the bubble-particle attachment probability as it lengthens the sliding contact time of a bubble over a particle (Nguyen & Schulze, 2004).

2.4.4 Microflotation recovery

Tests using a microflotation cell, which decouple froth phase effects, can show the effect of frothers on bubble-particle attachment in the pulp zone. Jordaan (2018) performed microflotation tests on pyrite and galena, using a polyglycol ether frother at a concentration of 10^{-4} M (Figure 2.13). The addition of the frother to galena at pH 4 and pyrite at pH 9 showed small improvements in recovery, whereas pyrite at pH 4 showed an increase in recovery from 24% (where no reagents are used) to 65%.

At pH 9 pyrite shows greater natural floatability than at pH 4, yet the frother improves the floatability of at pH 4 to a much greater extent. As the pyrite surface charge is much closer to the IEP at pH 4 and becomes increasingly negative at pH 9 (Fornasiero, Eijt & Ralston, 1992), the presence of the frother molecule on the mineral surface is more likely at pH 4. The improvement in recovery could be ascribed to the mechanism proposed by Lekki & Laskowski (1973).

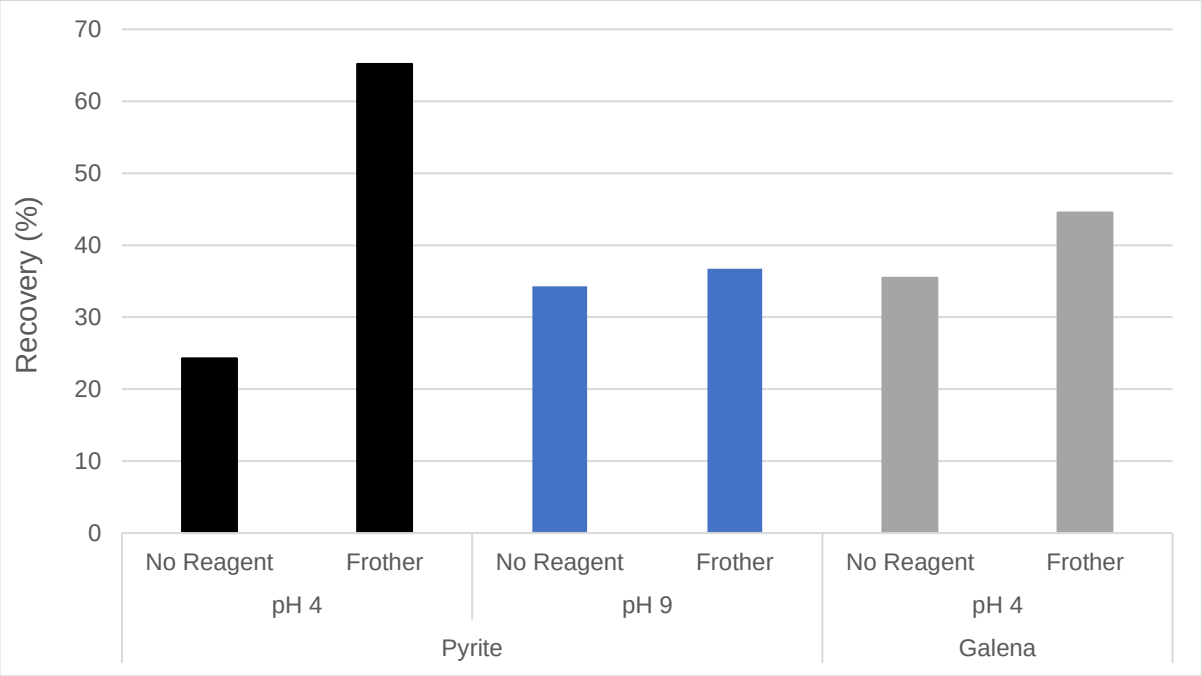

Figure 2.13: Microflotation recovery for pyrite and galena in the presence of SenFroth 200 (Adapted form Jordaan (2018))

Microflotation tests performed on chalcocite showed that frothers such as methyl iso-butyl carbinol (MIBC), DowFroth 200, and α-terpineol improved the recoveries compared to the baseline case when no reagents are present, and with increasing frother concentration, as demonstrated in Figure 2.14 (Dai, Bradshaw & Harris, 2001), recoveries increased. Lekki & Laskowski (1971) similarly showed that increasing the concentration of α-terpineol in the presence of ethyl xanthate, increased the recovery of chalcocite.

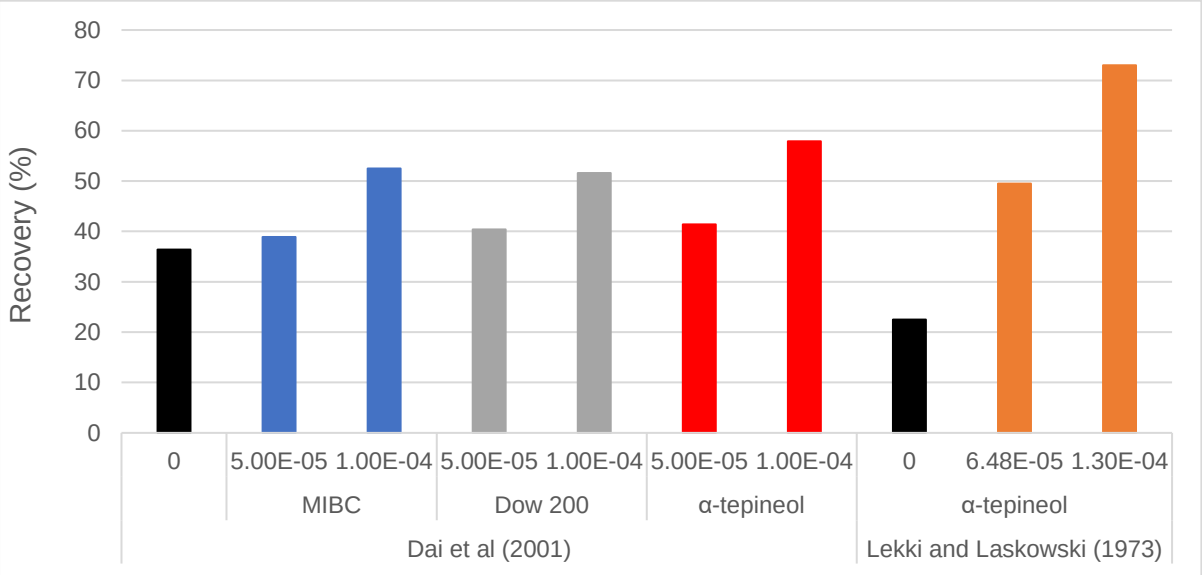

Figure 2.14: Microflotation recovery after 2 minutes for chalcocite in the presence of various non-ionic frothers (Adapted from Dai, Bradshaw & Harris (2001) and Lekki and Laskowski (1973))

The differences in improved recoveries observed upon addition of α-terpineol between the results reported by Dai, Bradshaw & Harris (2001) and those of Lekki & Laskowski (1973), Figure 2.14, might be attributed to the different microflotation cell designs. The Hallimond cell used in the Lekki & Laskowski (1971) study, which can decouple the effects of the froth from the pulp, uses a glass frit of approximately the same diameter as the cell to produce a swarm of bubbles which have a high probability of coalescence as depicted Figure 2.15. The large increases in recovery upon addition of the frother, which would inhibit bubble coalescence, and hence result in smaller bubbles and greater bubble surface area would increase first order flotation kinetics and also result in higher recoveries. The UCT microflotation cell (used in the Dai, Bradshaw & Harris (2001) study) used a needle to produce a single stream of bubbles, which may have a lower probability of coalescence, as demonstrated from the schematic in Figure 2.15. To understand the effect that frothers have on hydrodynamics (bubble size and velocity) and the surfaces forces present between the particle and the bubble, equipment design may play an important role in decoupling these effects.

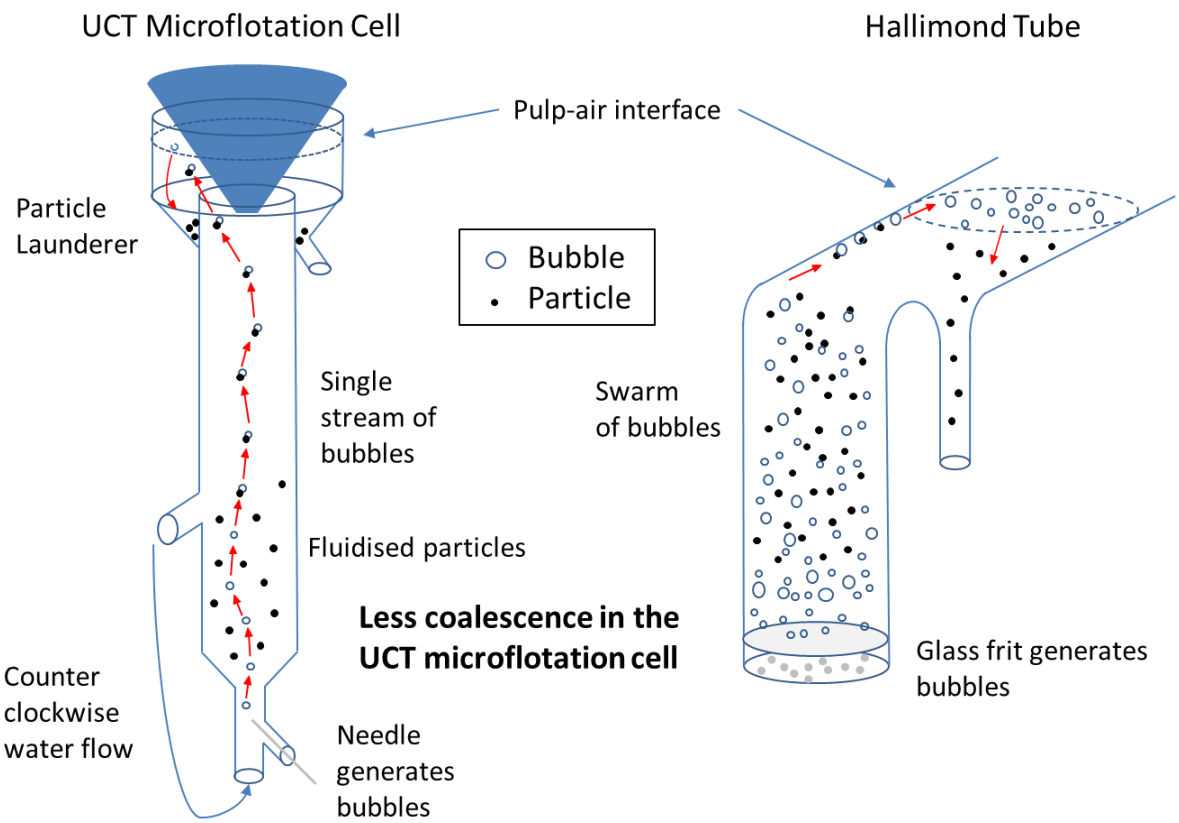

Figure 2.15: Schematic diagrams of the UCT microflotation cell and Hallimond microflotation cell

2.4.5 Glembotsky devices

Microflotation tests incorporate both the hydrodynamic effects that frothers have on bubble-particle attachment, and the surface forces between the bubble and the particle. To fully understand how frothers affect the surface forces between the bubble and the particle, the hydrodynamic and surface forces need to be decoupled.

A Glembotsky device is a device in which a captive bubble at the end of a capillary tube is moved towards and away from a bed of particles which are prepared in the chemical solution of interest (Glembotsky, 1953). These devices allow for control of approach and receding velocities, bubble size and contact time, so that the surface forces between the bubble and the particle can be studied.

Typically, it is thought that smaller bubble size improves flotation recovery increasing the available surface area flux for particle capture, but smaller bubbles have been shown to decrease the induction time for bubble-particle attachment in a Glembotsky device (Figure 2.16).

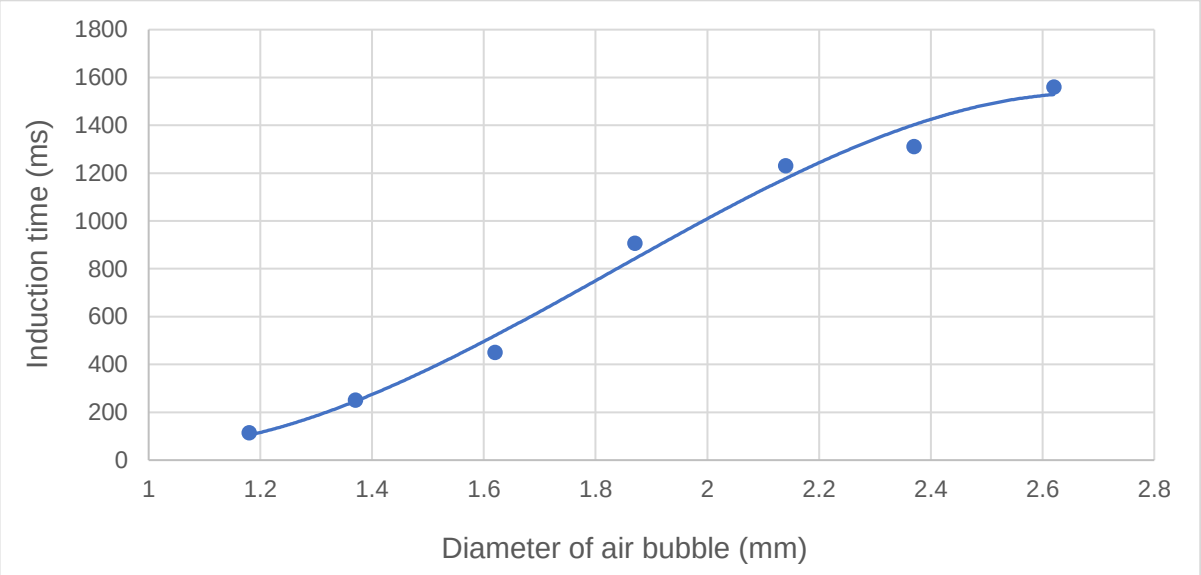

Figure 2.16: Induction time as a function of bubble diameter (Gu et al., 2003)

Lekki and Laskowski (1971) used a Glembotsky device to observe the effect of α-terpineol concentration on the induction time for chalcocite hydrophobized with potassium ethyl xanthate (KEX) at pH 9.7. Figure 2.17 shows that increasing frother concentration exponentially decreases the induction time. These results show that frothers have a kinetic effect on the film thinning process during bubble-particle attachment.

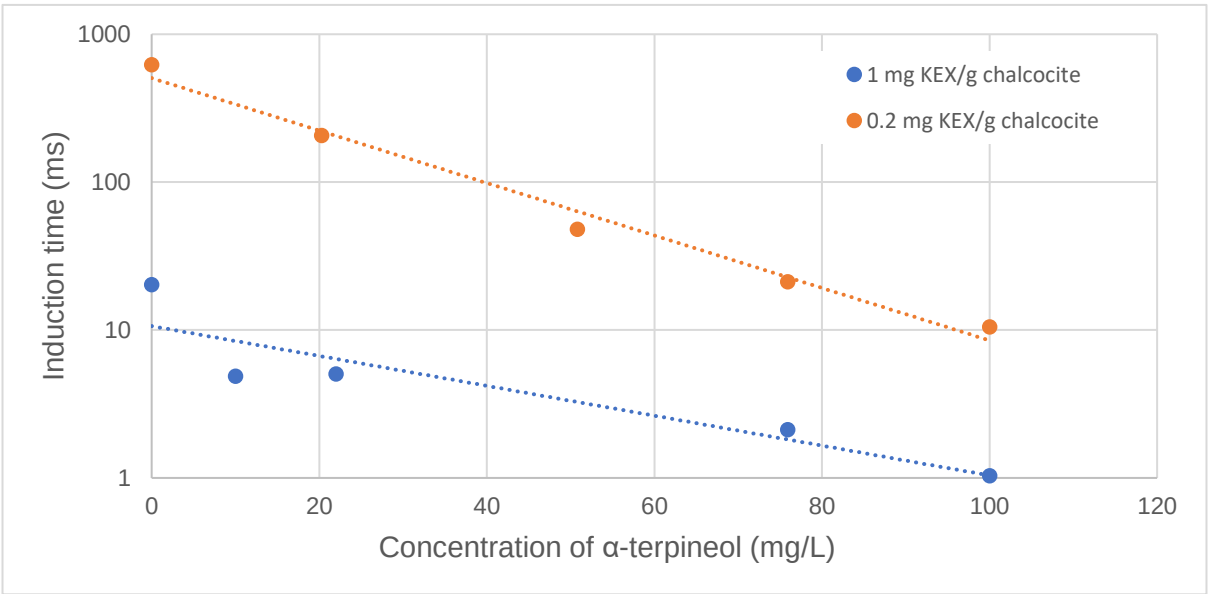

Figure 2.17: Induction time for bubble-chalcocite particle attachment at pH 9.7 as a function of increasing concentration of α-terpineol concentration (Adapted from Lekki and Laskowski (1973))

Lekki & Laskowski (1971) proposed that the decrease in attachment time was due to the transfer of frother between the air-water and mineral-water interface. Hadler, Aktas & Cilliers (2005) showed that frothers do not adsorb onto the mineral surface without the presence of a

collector on the mineral surface. The experiments performed by Lekki & Laskowski (1971) were performed in the presence of a collector, so the improved film thinning kinetics may be due to collector-frother molecular interactions (Leja & Schulman, 1954). Baseline tests with only the presence of the frother would reveal if the improved film thinning kinetics observed in the Lekki & Laskowski (1971) study were due to the effect of the frother or due to synergistic interactions between the collector and the frother.

2.5 Collector-frother interactions

2.5.1 Surfactant interactions

In general, surfactants are often used in mixtures as molecular interactions between surfactants in mixtures produce synergistic improvements in performance over the use of a surfactant on its own (Rosen, 1986). The molecular interactions that are generally encountered are due to electrostatic interactions between the polar groups, ion-dipole interactions between ionic and nonionic polar groups, hydrogen bonding between hydrogen acceptor and donor groups, van der Waals interactions between nonpolar groups, and steric interactions between polar and non-polar groups (Zhou & Rosen, 2003).

In flotation the collector and frother surfactants used are usually present at different interfaces, where they have separate roles, but interactions have been observed through co-adsorption of these surfactants at each of the interfaces, which lead to improved pulp phase recoveries and froth stability (Leja & Schulman, 1954).

2.5.1.1 Surfactant interactions between collectors and frothers

Tests performed using the Langmuir trough and surface tension at the air-water interface have indicated that complexes can be formed between frothers and xanthates. These complexes arise from molecular interactions due to the association between the nonpolar and polar parts of the two amphiphilic molecules, with these interactions being more prominent with increasing alkyl chain lengths of the respective reagents. It is hypothesized that these complexes have different properties and functions compared to the pure components from which they are constituted (Leja & Schulman, 1954; Buckenham & Schulman, 1963)

Bradshaw & O'Connor (1998) proposed that frothers are held at the mineral surface by Van der Waals forces between the alkyl chains of the frother and the adsorbed collector, or that frothers can form hydrogen bonding with the oxygen atom contained in functional groups of the thiol collector. There is thus a likelihood that DTP may interact with frothers in the same way as xanthates do.

2.5.2 Collector-frother interactions at the air-water interface

The study of thin liquid films appears to show that ethyl xanthate has an antagonistic effect in the presence of polypropylene glycol frother, where the equilibrium film thickness was decreased and a higher concentration of frother was required to produce a stable film that will not rupture (Manev & Pugh, 1993). It was also observed that ethyl xanthate had no effect on surface tension and thus no activity at the air-water interface (Manev & Pugh, 1993; Jordaan, 2018). However, tests on longer chain insoluble xanthates and frothers did show interactions. Lauryl xanthate was shown to be stabilized at the air-water interface by hexadecyl alcohol in Langmuir trough experiments, forming a mixed film of collector and frother, which produced an excess surface pressure, greater than the surface pressures of the pure components combined (Leja & Schulman, 1954).

From Figure 2.18 it is evident that SDEDTP has weak activity at the air-water interface (Jordaan, 2018). The addition of Dowfroth 200 showed a greater reduction in surface tension compared to that of the frother on its own, but it is challenging to qualitatively discern if the effects are due to synergistic interactions, or if the effects are equal to the sum of the contribution of each of the components. Further investigation by Dai, Bradshaw & Harris (2001) demonstrated similar interactions between the longer chain length sodium di-isobutyl DTP (SDIBDTP) and the frothers, MIBC and Dow200, using surface tension and frothability tests, which was not observed with sodium isobutyl xanthate (SIBX) which has the same alkyl chain structure.

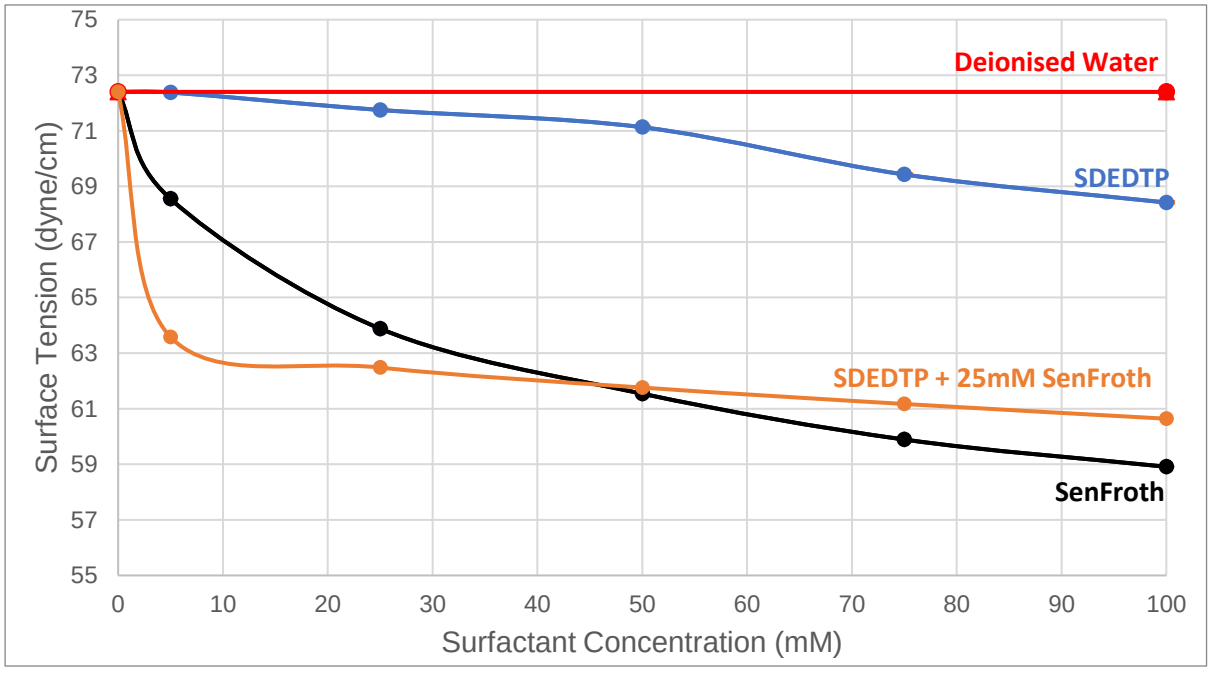

Figure 2.18: The effect of typical sulfide mineral flotation reagents on surface tension (Figure adapted from Jordaan (2018))

2.5.3 Collector-frother interactions at the mineral-water interface

A study done by Mukai, Wakamatsu & Takahashi (1972) showed that alcohol frothers interact at a water-mercury interface by reducing interfacial surface tension, but only in the presence of potassium ethyl xanthate (KEX). Longer amyl chain lengths produced a greater reduction in surface tension than the ethyl chain length frothers. Without the collector present there was no reduction in surface tension with increasing frother concentration.

Hadler, Aktas & Cilliers (2005) analyzed the supernatant of a PGM ore for residual polyglycol ether frother and isobutyl xanthate, using photocatalytic oxidation and a total organic carbon analyzer, and UV-Vis spectrophotometry. A decrease of 20% frother concentration was observed in the presence of isobutyl xanthate, where no decrease was observed without the presence of a collector. This implied that 20% of the frother adsorbed onto the mineral surface in the presence of collector.

The co-adsorption of the frother at the mineral-water interface is dependent on the presence of the collector at that interface. The molecular interactions between the collector and the frother acts as an “anchor” so that the frother can co-adsorb onto the mineral surface, whereas when there is no collector present on the mineral surface there is no “anchor” for the frother to interact with and thus it does not co-adsorb.

Even though frothers co-adsorb at the mineral surface in the presence of collectors, studies have shown that the contact angle of diffuse films of collector do not change with the addition of frother at the mineral surface, indicating that the mineral surface hydrophobicity has not increased (Rao, 2013:667).

2.5.4 Quantified interactions parameter for surfactant interactions

As discussed in section 2.5.2, collector-frother mixtures show a reduction in surface tension but it is challenging to qualitatively discern if these are due to molecular interactions or if these effects are due to the sum of the contribution of the effect of each reagent.

2.5.4.1 Regular solution theory approach

Regular solution theory has been used to capture non-ideal interactions at the gas-liquid interface between surfactants (Kunjappu & Rosen, 2013). The theory assumes that the excess energy in the mixed reagent system is equal to the excess enthalpy produced upon mixing. The excess enthalpy produced upon mixing is due to the interaction energy between each reagent in solution. This approach can be applied to surfactants mixing at interfaces.

A dimensionless β parameter is derived from the regular solution theory model which describes the interactions between binary mixtures of surfactants. This parameter can be

readily obtained from interfacial tension data (Kunjappu & Rosen, 2013). Two of the main assumptions of this approach are that the molar surface area at the interface upon mixing is similar to that of the individual surfactants, and that the solution is in equilibrium with the interface (Kunjappu & Rosen, 2013). The approach is described in section 3.5.3.

The β parameters obtained from this analysis provides quantitative information on the interaction between the different components in the surfactant mixture, relative to the interaction of the component with itself (Kunjappu & Rosen, 2013). A negative value of the parameter β indicates that there is attraction between the components of the surfactant mixture relative to the component with itself, whereas a positive value indicates a repulsive interaction.

2.5.5 Penetration theory

The main theory that attempts to explain collector-frother synergy in terms of molecular interactions is known as penetration theory and was proposed by Leja & Schulman (1954). This theory is based on a diffuse mixed monolayer of collectors and frothers forming at the air-water and mineral water interface due to interactions occurring between these molecules. When the particle contacts the bubble, the diffuse monolayers at the air-water and mineral-water interface interpenetrate each other (as depicted in Figure 2.19), increasing the concentration of collector on the mineral surface, stabilizing bubble-particle attachment and synergistically enhancing recovery and froth stability.

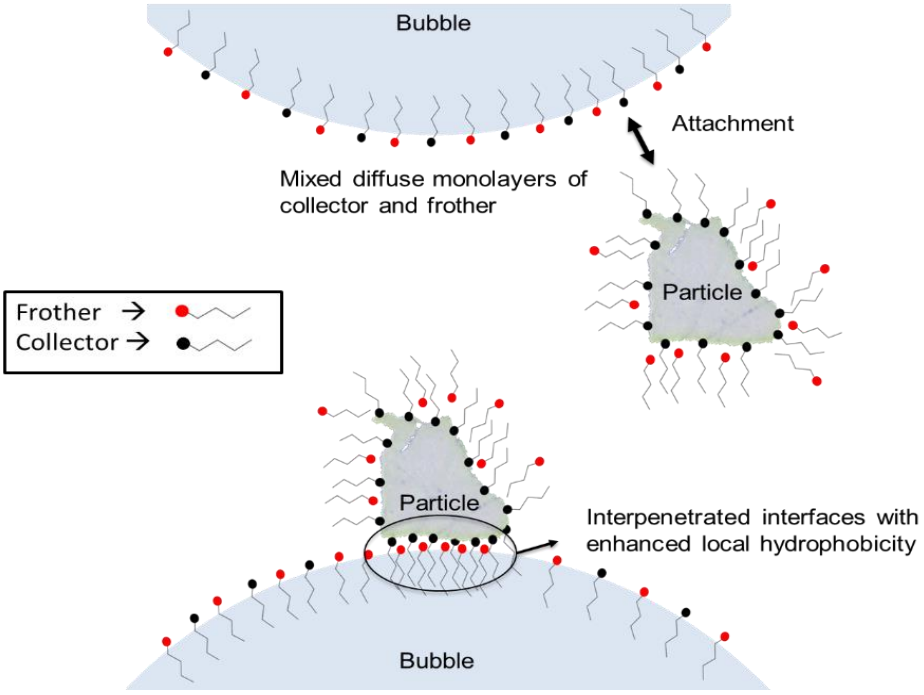

Figure 2.19: Penetration theory schematic depiction

If the air-water and mineral-water interfaces are highly condensed with collector and frother, the formation of a bimolecular-leaflet micelle will occur which inhibits bubble-particle attachment (Leja & Schulman, 1954).

2.6 Summary of critical literature

Jordaan (2018) is one of few studies that has shown that a collector-frother mixture synergistically enhanced valuable mineral recovery even though, under the conditions used, DTP is not typically present at the mineral-water interface. Considering that DTP does not adsorb onto most minerals (Petrus et al., 2011; McFadzean & O'Connor, 2014; Taguta, O'Connor & McFadzean, 2017; Nagaraj & Brinen, 2001), the interaction between DTP and frothers can likely be present at the air-water interface. Alternatively, DTP may adsorb onto the mineral surface in the presence of non-ionic frothers. However, this has not been reported to date in published literature.

There is limited literature that shows that there is a synergistic interaction between thiol collectors and non-ionic frothers at the air-water interface, but this was mostly observed for insoluble longer chain length reagents (Leja & Schulman, 1954), with the shorter ethyl chain length xanthates exhibiting no activity at the air-water interface, and no interactions with frothers (Jordaan, 2018; Manev & Pugh, 1993). Two studies (Jordaan, 2018; Dai, Bradshaw & Harris, 2001) have shown that di-ethyl DTP and di-isobutyl DTP are both active at the air-water interface, but the interpretation of the DTP-frother mixture results qualitatively do not

give a clear indication that there are molecular interactions between DTP and frothers. Models are required to give quantitative information about these interactions.

The dynamic mechanism whereby flotation reagents can transfer between the air-water and mineral-water interface during bubble-particle attachment described in literature (Derjaguin & Dukhin, 1961; Fuerstenau, 2001; Yan, 2016; Wang & Miller, 2018; Lekki & Laskowski, 1973) may explain how DTP and frother synergistically improve mineral recovery.

Interactions between xanthates and non-ionic frothers were also observed at the mineral-water interface, with greater interactions observed for longer chain length frothers (Mukai, Wakamatsu & Takahashi, 1972; Hadler, Aktas & Cilliers, 2005). Considering that residual xanthate in the pulp is usually negligible when using sub monolayer dosages, xanthate-frother interactions are not possible at the air-water interface, indicating that xanthate interactions must occur at the mineral-water interface.

It is unclear how the interaction between these surfactants at the respective interfaces synergistically enhances recovery according to the surface forces present between the bubble and the particle. Frothers have been shown to improve mineral recovery (Dai, Bradshaw & Harris, 2001; Jordaan, 2018) and it is well established and understood that collectors improve mineral recovery. It could be that the role of the collector is, as is well known, to enhance the hydrophobicity at the mineral surface, and the role of the frother is to reduce the double layer force between the bubble and the particle (Leja & He, 1984), and that these two separate effects enhance the recovery additively.

There have been limited reports on how the structural differences of xanthate and DTP contribute to the interactions between these collectors and non-ionic frothers. Bradshaw & O'Connor (1998) proposed that the interactions between the non-polar portions of the thiol collectors and non-ionic frothers are due to hydrogen bonding with the oxygen atom contained in the functional group of the thiol collector.

The role of DTP in the flotation process remains unclear. As already referred to, the collector does not behave as a classical collector by adsorbing at the mineral-water interface, enhancing surface hydrophobicity.

2.7 Hypotheses and key questions

The main mechanism which by collectors and frothers interact are through molecular interactions between the two surfactants (Rosen, 1986; Zhou & Rosen, 2003; Leja & Schulman, 1954). Bradshaw & O'Connor (1998) proposed that these interactions occur between thiol collectors and frothers due to the molecular structure of the thiol head group. It

is proposed that the interactions between DTP and frothers occur via these molecular interactions due to the molecular structure of DTP.

Hypothesis I: DTP forms a complex with non-ionic frothers due to the association between the nonpolar and polar parts of the two amphiphilic molecules. The interactions between the molecules are due to hydrogen-bonding between the oxygen atoms on the functional group of DTP and the non-polar part of the frother. The polar parts of the molecule associates through the Van der Waals force, which increases with alkyl chain lengths of the respective reagents.

Key questions to be addressed in investigating the validity of this hypothesis:

- Do DTP-frother show greater attractive attractions at the air-water interface compared to xanthate-frother mixtures according to the regular solution theory model?
- Are the collector-frother interactions dependent on the collector species that forms on the mineral surface?

The interactions observed by previous authors (Rosen, 1986; Zhou & Rosen, 2003; Leja & Schulman, 1954) allow for improved adsorption of collector molecules at the air-water interface in the presence of frothers (Dai, Bradshaw & Harris, 2001) and frother molecules at the mineral-liquid interface in the presence of collectors (Mukai, Wakamatsu & Takahashi, 1972; Hadler, Aktas & Cilliers, 2005; Lekki & Laskowski, 1971).

Hypothesis II: The formation of DTP-non-ionic frother complexes promotes the co-adsorption of DTP at the air-water interface through molecular interactions between the collector and the frother.

Key questions to be addressed in investigating the validity of this hypothesis:

- Do DTP-frother or xanthate-frother mixtures show attractive or repulsive interactions according to the regular solution theory model?
- Do DTP-frother or xanthate-frother mixtures lower the CCC with reference to the CCC of the pure components?
- Does DTP or xanthate adsorb onto the mineral surface to a greater extent in the presence of non-ionic frothers?

Considering that DTP has shown weak adsorption onto most sulphide minerals studied (Petrus et al., 2011; McFadzean & O'Connor, 2014; Taguta, O'Connor & McFadzean, 2017; Nagaraj & Brinen, 2001), but has shown interaction at the air-water interface in some studies (Jordaan, 2018; Dai, Bradshaw & Harris, 2001), it is postulated that there may be a transfer of the collector from the air-water interface to the mineral-liquid interface as has been observed

by Derjaguin & Dukhin (1961), Fuerstenau (2001). Yan (2016), Wang & Miller (2018), Lekki & Laskowski, (1973).

Hypothesis III: When DTP co-adsorbs with non-ionic frothers at the air-water interface, the collector-frother complex can transfer from the air-water interface to the mineral-water interface as the bubble collides with the particle, enhancing the kinetics of film thinning between the bubble and the particle, synergistically enhancing flotation recovery.

Key questions:

- Does aeration reduce the amount of DTP remaining in the pulp in the presence of a non-ionic frother?
- Do DTP-frother or xanthate-frother mixtures synergistically enhance the pulp zone recovery compared to the recoveries obtained for the individual reagents?
- Do DTP-frother or xanthate-frother mixtures synergistically enhance the attachment probability in a Glembotsky device, where the hydrodynamic effects of frothers are not present, compared to the attachment probabilities of the pure reagents?

3 Experimental Approach

3.1 Approach and experimental design

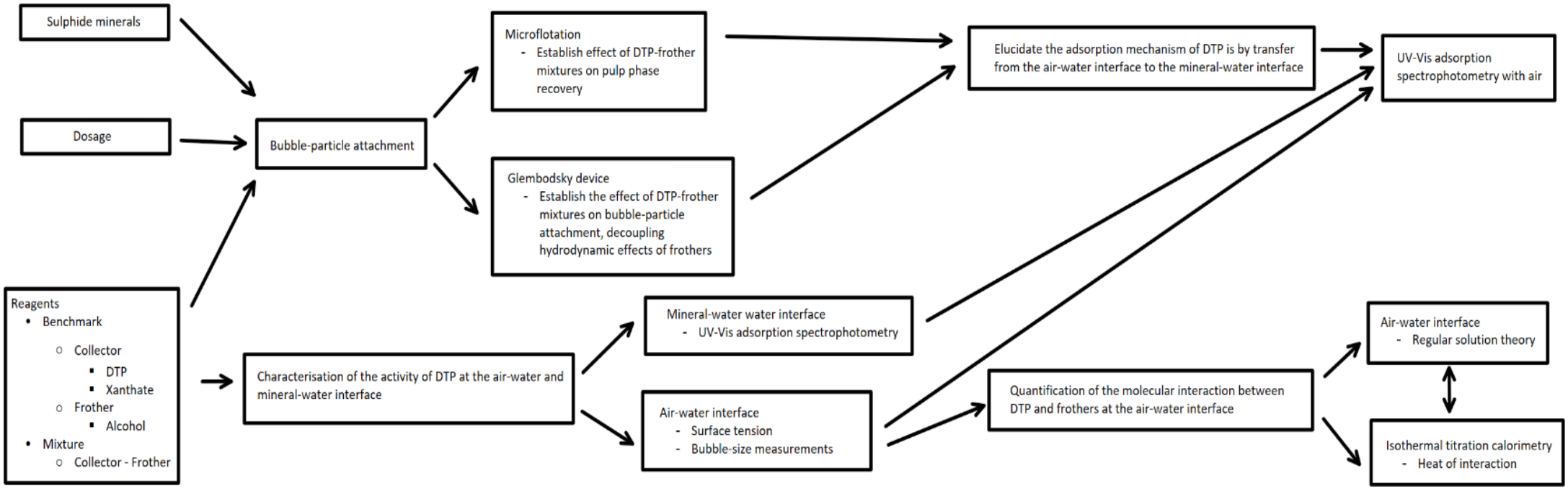

Figure 3.1: Overall experimental programme.

The main aim of the experimental programme is to understand the mechanism of how DTP and frothers synergistically improve sulfide mineral recovery, which is outlined in Figure 3.1. This is approached by quantifying the effect of the frother and the collector, respectively, on the bubble-particle attachment process with a view to understand if these reagents have separate roles, or if there is a molecular interaction between DTP and frothers that would produce synergistic improvements in recovery.

Since frothers affect many of the sub-processes of bubble-particle attachment, a Glembotsky device is used to decouple the hydrodynamic effects of frothers so as to understand how frothers affect the attachment between a bubble and a particle in terms of the surface forces present between the bubble and the particle.

Once it is established what the effect of DTP-frother mixtures is on bubble-particle attachment, synergistic or otherwise, the adsorption and interaction of these reagents are characterized at the air-water and mineral-water interface to understand the mechanism of how DTP-frother mixtures synergistically improve sulfide mineral recovery.

3.2 Mineral preparation, reagents and reagent dosages

3.2.1 Mineral preparation

Pyrite, pyrrhotite, galena, and chalcopyrite samples were sourced from Ward's Natural Science Establishment, Rochester, New York and chalcocite was sourced from BGRIMM Technology Group. The samples were received in chunks of 150mm diameter. The samples were crushed to about 10mm and then pulverized in a Sieb mill for 15 seconds. The samples were dry sieved for 20 min on a shaker into three fractions, viz. -125+106µm, -106+38µm, -38µm (Quartz samples were sieved into a -106+75 µm size fraction).

Samples were stored under nitrogen at -30ºC to minimize surface oxidation.

3.2.2 Mineral purity

The purity of the mineral samples was an important factor in this work, as impurities can lead to complex interactions occurring. X-ray diffraction (XRD) was performed to determine the purity of each mineral. The Malvern Panalytical Aeris benchtop XRD equipped with a CO tube was used for the analysis. The Bruker EVA software was used to identify the minerals. Rietman refinement was used to obtain quantification data. The Crystallographic Open Database was used to obtain crystal structure information for mineral quantification.

Table 3.1 presents the purities for galena, pyrite, chalcopyrite and chalcocite. The galena was very pure containing less that 1% by mass impurities. In pyrite and chalcopyrite, the main impurities were not sulphide minerals. It was assumed that these minerals would not

significantly influence the outcomes of any tests. Chalcocite contained the most significant amount of impurities, but most of this was digenite which is also a copper sulfide mineral. It was assumed that the behaviour of digenite would be similar to that of chalcocite. The next major impurity in chalcocite was the quartz which is known not to interact with thiol collectors (Nagaraj & Brinen, 1996), so it was assumed that the quartz would not significantly influence experimental results.

Table 3.1: Mineral sample purities for galena, pyrite, chalcopyrite and chalcocite as determined by X-Ray Diffraction)

Mineral sample	XRD analysis results		
	Mineral sample composition	Chemical Formula	Mass %
Galena	Galena	PbS	99.8
	Hydrocerrusite	$Pb_3(CO_3)_2(OH)_2$	0.2
Pyrite	Pyrite	FeS_2	97.1
	Muscovite	$KAl_3Si_3O_{10}(OH)_{1.8}F_{0.2}$	1.6
	Chlorite	ClO_2	0.7
	Gypsum	$Ca(SO_4)•2(H_2O)$	0.6
Chalcopyrite	Chalcopyrite	$CuFeS_2$	94.3
	Magnetite	Fe_3O_4	3.6
	Chlorite	ClO_2	2.2
Chalcocite	Chalcocite	Cu_2S	87.0
	Digenite	Cu_9S_5	6.9
	Quartz	SiO_2	3.2
	Hematite	Fe_2O_3	0.8
	Covellite	CuS	0.7
	Chalcopyrite	$CuFeS_2$	0.5

3.2.3 Quartz preparation and methylation

The cleaning procedure outlined in Diggins, Fokkink & Ralston (1990) was followed in which the -106+75 µm size fraction of quartz was boiled in concentrated nitric acid for 3 hours, and then rinsed with deionized water until the pH became neutral. The quartz was then immersed in a 30% (by weight) KOH solution for 1 minute, and then rinsed with deionized water until the pH became neutral.

The procedure outlined by Blake & Ralston (1985) was used for the methylation of quartz. Quartz particles were contacted with a 4×10^{-5} M solution of trimethyl chlorosilane (TMCS) in cyclohexane, which were contacted with the solution for 3 hours to ensure maximum uptake

of the TMCS. The dosage of TMCS was based on a 50% surface coverage, which was calculated from the specific surface area of the mineral (Estimated by the Malvern Mastersizer 3000) and the 2.6 active sites per nm^2 on the surface of quartz (Blake & Ralston, 1985).

The TMCS and cyclohexane used for the methylation of quartz were obtained from Sigma Aldrich.

3.2.4 Collectors

The collectors that were used in this study was provided by Senmin (Pty) Ltd., South Africa. Xanthates were received as pure powders. DTP's were received in a high pH solution. Gas chromatography (GC) analysis was performed on the DTP samples to confirm their purity. Aerophine 3418A was obtained from Cytec Industries (Solvay), which was received in a 50% by weight water solution.

Since DTP's are usually synthesized using alcohols, residual alcohols may be present with the collector. These residual alcohols may induce a synergistic effect with DTP for baseline tests without frother present. It was important to verify the purity of the collector, and the presence of these alcohols. Table 3.2 shows the purity information of all the collectors used in this study.

Table 3.2: Thiol collectors used in this study.

Collector	Abbreviation	Purity by active component (%)	Molecular Mass (g/mol)
Sodium diethyl DTP	SDEDTP	95.66	208.21
Sodium di-n-butyl DTP	SD(N)BDTP	91.38	264.3
Sodium di-iso-butyl DTP	SD(I)BDTP	90.32	264.3
Sodium di-n-hexyl DTP	SD(N)HDTP	86.53	172.2
Sodium ethyl xanthate	SEX	100	144.18
Potassium butyl xanthate	PNBX	100	188.4
Sodium iso-butyl xanthate	SIBX	100	172.2
Potassium amyl xanthate	PAX	100	202.3
Sodium di-iso-butyl dithiophosphinate (Aerophine 3418A)	SIBDTPINA	100	232.3

The purity of all DTP's used were greater than 90% and contained undetectable amounts of alcohols, except for the SDHDTP which contained 7% residual hexanol. The results of GC analysis are shown in Appendix 8.6.

Stock solutions of collectors were made up with deionised water each day.

3.2.4.1 Collector dosage

The collector dosages were based on a theoretical monolayer coverage of the mineral surface. These calculations require an estimate for the surface area of the mineral and the molecular footprint area of the collector molecule.

Brunner-Emmett-Teller (BET) analysis was performed on all samples to determine mineral surface area. Table 3.3 shows the surface area for each mineral at each size fraction, normalized by the mass.

The molecular footprint of the DTP headgroup has been experimentally determined to be 35.4 $Å^2$, (Matsuoka and Ichikoku, 1982). Grano et al. (1997) determined that this value was very close to the theoretically calculated value of 36.6 $Å^2$. The molecular footprint of xanthate was 28.8 $Å^2$ (Grano et al., 1997).

Table 3.3: Mineral surface areas obtained from BET analysis

Mineral	Surface area of each size fraction (m^2/g)		
	-125+106 µm	-106+38 µm	-38 µm
Galena	0.0132	0.0688	0.3158
Pyrite	0.253	0.2927	0.9052
Chalcopyrite	0.0832	0.2327	0.7026
Chalcocite	0.1535	0.2966	2.1197

The pH of the mineral slurry was adjusted to pH 9 before dosage of the collector. A pH 9 was chosen as it is the pH where DTP did not adsorb onto most of the minerals reviewed. It will also be easier to gain understanding of how DTP improves mineral recovery even though it is not adsorbing onto the surface.

The collector was dosed to give the equivalent of a 50% theoretical monolayer coverage on the mineral surface. This dosage was chosen since Leja & Schulman (1954) proposed that frother-collector interaction would only occur in the case of diffuse monolayers.

The number of moles of collector dosed was calculated according to Equation 10.

$$N_{Collector} = \frac{F_{Area}\ Area_{BET}\ m_{mineral}}{N_A\ Area_{collector}} \qquad \text{Equation 10}$$

where F_{Area} is the fractional area of the mineral surface covered with collector, $Area_{BET}$ is the BET surface area in m^2/grams, $m_{mineral}$ is the mass of mineral in grams, N_A is Avogradro's constant ($6.2214 * 10^{23}$), and $Area_{Collector}$ is the molecular footprint of the collector molecule or the area that the headgroup of the molecule occupies in m^2/molecule.

Since DTP was not adsorbed onto some mineral surfaces, a fixed pulp concentration dosage for DTP was used in some experiments. The dosage was chosen as 0.1 mM, which is within the concentration range in which frothers inhibit bubble coalescence in the pulp.

Table 3.4: Summary of concentrations used for SDEDTP and SEX in each of the experimental methods where the collectors were dosed at a 50% monolayer coverage.

SDEDTP	Galena	Pyrite	Chalcopyrite	Chalcocite
Microflotation concentration [mM]	0.01	0.04	0.03	0.04
Residual adsorption test concentration [mM]	0.04	0.02	0.13	0.05
Induction time test concentrations [mM]	0.01	0.11	0.04	0.08
SEX	Galena	Pyrite	Chalcopyrite	Chalcocite
Microflotation concentration [mM]	0.01	0.05	0.04	0.05
Residual adsorption test concentration [mM]	0.04	0.03	0.16	0.06
Induction time test concentration [mM]	0.01	0.13	0.04	0.08

Table 3.4 shows the concentrations used in each of the experimental methods where the collectors were dosed at a 50% monolayer coverage. Most of the concentrations are within the same order of magnitude, approximately 0.01 mM.

3.2.5 Frothers

The frothers used in this study were obtained from Sigma Aldrich. An alcohol (1-Hexanol) and polypropylene glycol (PPG425) frother was used where 425 indicates the approximate molecular weight of the frother. The purity of hexanol and PPG425 were both ≥99% by volume.

The frother concentrations used were above the critical coalescence concentration, which was 0.12 mM for hexanol and 0.014 mM for PPG425.

3.3 Bubble-particle attachment

The effects of collectors, frothers, and their mixtures were studied on pulp phase recovery and attachment probability.

3.3.1 Microflotation

The UCT microflotation cell described in Bradshaw & O'Connor (1996), was used to measure the effects of the reagents on pulp phase recovery. This device is depicted in Figure 3.2. The microflotation cell was designed to create a quiescent flotation environment minimizing hydrodynamic effects caused by agitation. A peristaltic pump was used to create a loosely fluidized bed of particles, through which through a single stream of bubbles (generated by a micro syringe) can move. A secondary pump was used to supply a constant flow rate of air to the syringe for bubble generation. This method of single-stream bubble generation is used to minimize bubble coalescence, as bubble size is inversely proportional to first order flotation

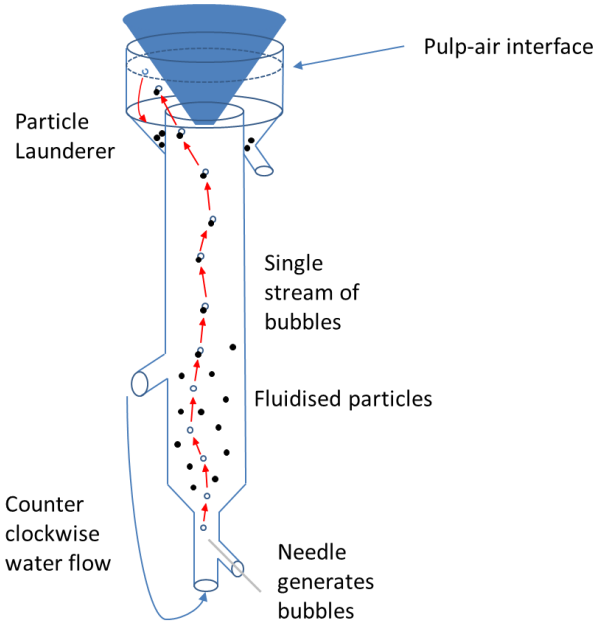

Figure 3.2: Microflotation setup

kinetics. A comparison between a single-stream device and a multi-stream device showed that coalescence was minimal in a single-stream device (Cho and Laskowski, 2002).

For each experiment, 3g of the mineral (-106+38µm size fraction) was sonicated in 50 mL of deionized water for 30 seconds. The pH was adjusted to 9 using a 0.1 M solution of sodium hydroxide (NaOH). When collector was used the slurry was conditioned with the collector for 5 minutes. The slurry was added to the microflotation cell, which was topped up with deionized water at pH 9. When frother was used in the cell, it was added to the make-up water. Each time a concentrate was collected the cell was topped up with the relevant make-up water.

Air flowrate was controlled at 7 mL/min. Concentrates were collected cumulatively at 2, 6, 12 and 20 minutes. The experiments were performed in duplicate and error bars are shown in

the figures. Rate data was obtained using the Klimpel rate equation (Equation 11) using the least squares method on the recovery vs time data.

$$R = R_{\infty}\left((1-\frac{1}{kt})(1-e^{-kt})\right) \qquad \text{Equation 11}$$

where k is the first order rate constant, t is time, R is recovery and R_{∞} is maximum possible recovery of the mineral.

3.3.2 Attachment probability measurements – Automated contact time apparatus

The Automated Contact Time Apparatus (ACTA) is a device that is used to determine the bubble-particle attachment probability under various chemical conditions (Aspiala, Schreithofer & Serna-Guerrero, 2018). The device is based on the Glembotsky device in which a captive bubble at the end of a capillary tube is moved towards and away from the bed of mineral particles which are prepared in the chemical solution of interest (Glembotsky, 1953). The contact time is the amount of time which the bubble is in contact with the particle bed. One of the main features that sets the ACTA apart from other devices that have similar functionality, is that it has an array of 6 needles which contacts the particle bed in 66 different places. This allows for 396 bubble-particle attachment opportunities, whereas in previous devices there is usually one needle which is contacted 10 times with the particle bed.

A schematic and an image of the prototype is illustrated in Figure 3.3 a) and b). The device has two motors, one for horizontal movement of the needle array to different points on the particle bed, and one for programmable vertical movement of the needle array to bring the bubbles into contact with the particle bed. The ACTA allows control of the approach and retreat velocity of the bubble to and from the particle bed, the contact time of the bubble with the particle bed, the amount of time air is pumped into the bubbles, and the compression against the particle bed (as an overstep parameter).

Pictures of the bubbles are taken after each contact cycle. Figure 3.3, c) and d) shows the bubbles before and after attachment. Optical fiber backlighting is used to aid the detection of particles on the bubble surface. Attached particles can be observed on Figure 3.3 d) as black specks. Images are also taken to analyze the bubble size (Figure 3.3 e)). The bubble sizes were determined using the canny edge detection algorithm to detect the edges of the bubbles and the Hough circle transform to find the center of the bubbles. Julia was used to perform this analysis. The code used to do this is shown in section 8.7. After imaging of the bubbles, the particles were deposited in a particle bin which can be used for further analysis.

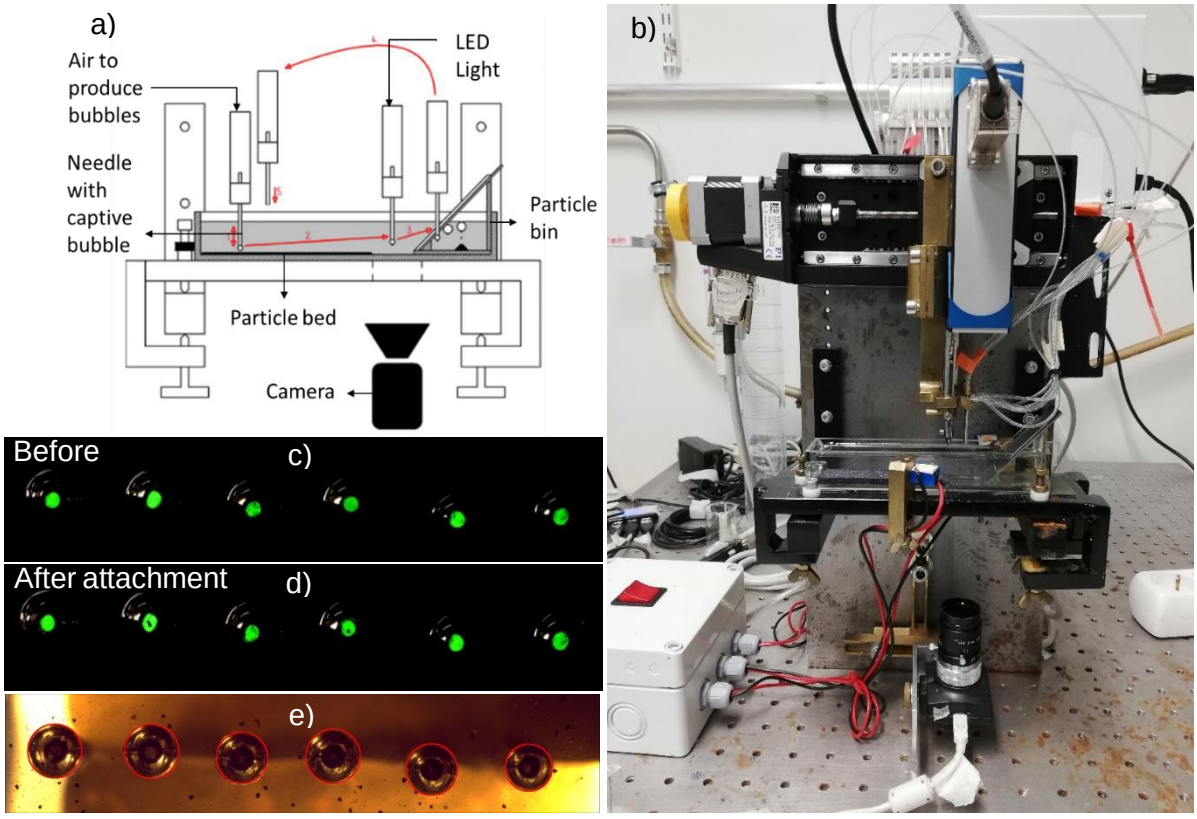

Figure 3.3: a) Schematic diagram of ACTA b) Picture of ACTA prototype c) Bubble image before attachment (enhanced with fiber optic) d) Bubble images after attachment (Particle on needle 2 and needle 4) e) Bubble image for detection of bubble edges and bubble diameter

3.3.2.1 Parameter settings

The approach and retreat velocities were set a 50 mm/s, and the overstep was set to 0.1 mm. These settings were used as the default parameters recommended by Bellers (2017). The pumping time was set at 1.2 seconds to produce an average bubble diameter of 1.77 mm. The contact time was selected for each mineral so that a difference in attachment probabilities could be observed for different chemical conditions.

3.3.2.2 Bubble size filtering and attachment probability calculation

Bubbles that had a diameter greater than 1.9 mm or less than 1.6 mm were removed from the data set. Bubble diameters smaller than 1.6 mm did not touch the particle bed and cannot result in an attachment. Bubble diameters greater than 1.9 mm would squeeze onto the particle bed and result in greater attachment probabilities.

The attachment probability was calculated as the total number of bubbles with particles on them that fall within the bubble size range divided by the total number of bubbles that fall within the bubble size range.

3.3.2.3 Particle preparation

Mineral particles in the -125 + 106 µm size range were used to make the particle bed. For each experiment 18 grams of mineral was used. Before each experiment the particles were sonicated for 5 minutes, and then wet screened over a 106 µm screen to remove any fines (The fines tend to make the water murky which causes issues with imaging the bubble). The particles were conditioned in 100 mL of deionized water, which was adjusted to pH 9. The same dosages for collector and frother was used as in the microflotation experiments.

The ACTA will be used to understand the effects of collector-frother mixtures on the interaction between the bubble and the particle in a quiescent environment where there are no hydrodynamic effects. Add further explanations around contact time and how calculations were performed. Also add why induction times were different.

3.4 Adsorption at the mineral-water interface

3.4.1 UV-Vis spectrophotometry

The residual concentration of collector remaining in solution was measured using UV-Vis spectrophotometry, to determine the amount of collector that accumulated on the mineral surface.

0.5 grams of mineral (-38 µm size fraction) was added to 50 mL of deionized water, which was adjusted to pH 9. The collector was added to the solution, where a 50% theoretical monolayer dosage was used, similar to microflotation test and ACTA tests. The solution was placed in a temperature-controlled water bath shaker set to 25^{o}C. After 20 minutes the slurry was filtered through a 0.22µm syringe filter, and the supernatant was collected. The supernatant was analyzed in the Ultrospec 4300 Pro. The characteristic adsorption wavelength of 225 nm was used for DTP and 301 nm for xanthate. The experiments were performed in duplicate.

Adsorption tests were also performed in the presence of air bubbles to determine if the collector transfers from the air-water interface to the mineral surface during the bubble-particle collision process. The adsorption with air tests were performed in a 0.5 L bottom driven mechanical batch flotation cell. The air flowrate was 1.8 L/min and the impeller speed was 125 rpm. 5g of mineral was used and SDEDTP was dosed at 0.05 mM. The experiments were performed in duplicate.

3.5 Activity at the air-water interface

3.5.1 Bubble size measurements

Frothers inhibit bubble coalescence at very low concentrations, which are typically employed in flotation. These concentrations are generally lower than the sensitivity of surface tension measurements to detect, which is why bubble size measurements were also carried out. The critical coalescence concentration (CCC) is known as the concentration at which coalescence is completely inhibited, and the bubble size is only controlled by sparger geometry (Cho & Laskowski, 2001).

Since the literature indicates that DTP is active at the air-water interface (Dai, Bradshaw & Harris, 2001; Jordaan, 2018), CCC measurements were used to measure the activity of DTP at the concentrations that are used in flotation. Furthermore, the CCC of mixtures of collectors and frothers were used to observe if there were any observable synergistic interactions at these typical flotation concentrations.

Bubble size was measured using the Anglo Platinum Bubble Sizer (APBS), which is based on the McGill design described in Hernandez-Aguilar et al. (2004). An 8 L bottom driven mechanical flotation cell was used as a bubble generation device. The complete setup can be observed in Figure 3.4. The same concentrations of reagents were used in the bubble sizer as in the flotation cell.

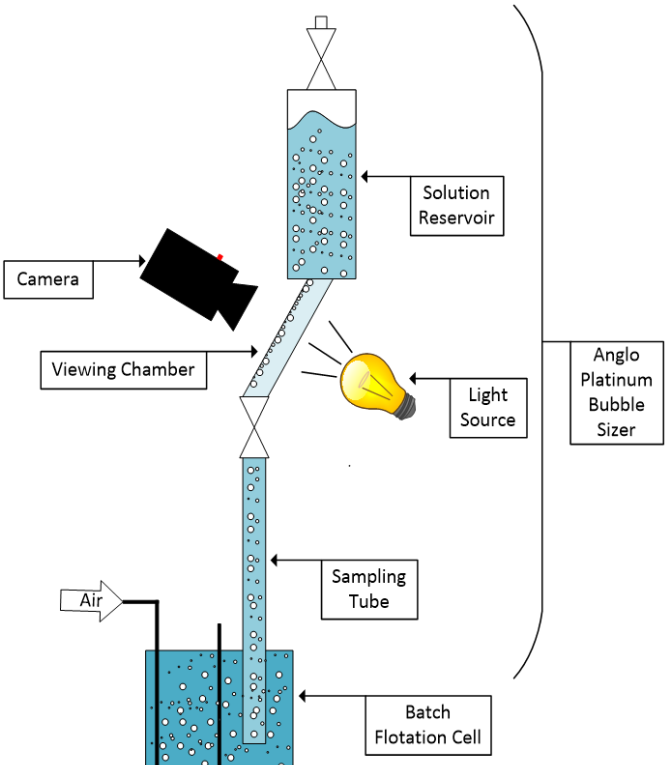

Figure 3.4: Experimental setup of Anglo Platinum Bubble Sizer and batch flotation cell

The CCC95 was calculated by the least square's method using Equation 12 and the bubble size vs surfactant concentration data.

$$d_{32} = d_L + (d_0 + d_L)\exp\left(-B\left(\frac{C}{C_{95}}\right)\right) \qquad \text{Equation 12}$$

d_{32} is the Sauter mean diameter, d_L is the Sauter mean diameter with no surfactant in the system, d_0 is the Sauter mean diameter at concentrations where bubble coalescence has been completely inhibited, C is the concentration, C_{95} is the concentration at which the bubble size has been reduced by 95% compared to d_L, and B is a constant.

3.5.2 Foam stability tests

Similar to bubble coalescence in the pulp, frothers inhibit bubble coalescence in the froth at concentrations lower than the sensitivity that surface tension can detect (Comley et al., 2002). Foam stability tests were conducted to observe if there are any synergistic interactions between collectors and frothers at the air-water interface at the concentrations typically used in flotation.

Concentrations were chosen to be between 0.26 mM and 0.53 mM of collector or frother which corresponds to dosages between 50 and 100 g/ton at 35% solids. The experimental setup for measuring foam stability is shown in Figure 3.5. A 10 cm Perspex column was used for the

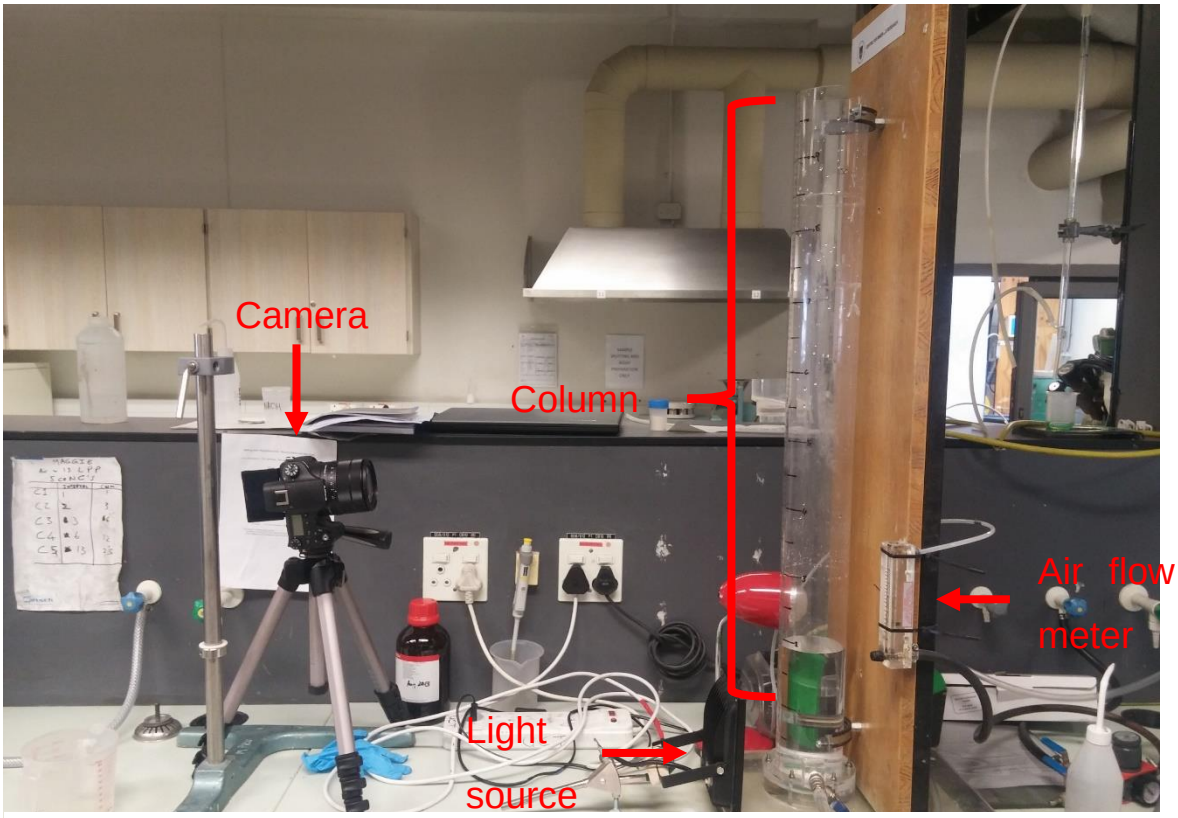

Figure 3.5: Foam stability measurement setup

foam stability measurements with a glass frit. The column was filled with 3L of water-reagent mixture for each experiment.

An air flowrate of 7 L/min was used. Medical grade air was used for all the experiments. The flow meter was calibrated using a soap bubble meter. A DSLR camera was used to track the growth of foam. LED lights were used to track the pulp-foam interface and the height of the foam.

The Bikerman (1973) test was used to determine the dynamic foam stability of the mixtures. The test uses the ratio of the steady-state foam volume to gas flowrate to determine a factor ∑. The factor represents the average amount of time that the gas is entrained in the foam (Barbian, Ventura-Median, & Cilliers, 2003). The equation to determine this factor is represented in Equation 13.

$$\sum = \frac{H_{max}\, A}{Q} \qquad \text{Equation 13}$$

where H_{max} is the maximum height the foam reaches, A is the cross-sectional area of the column, and Q is the volumetric flowrate of the air. All experiments were performed in duplicate.

3.5.3 Regular solution theory

The β parameter from the regular solution theory approach will be used to describe the interactions between collector and frother mixtures using interfacial surface tension data. The approach described in Zhou & Rosen (2003) was used.

Equation 15 and 15 are used to calculate the β parameter for the mixed monolayer of surfactants using the surface tension in data in Figure 3.6.

$$\frac{X_1 \ln\left(\frac{\alpha_1 C_{12}}{X_1 C_1^0}\right)}{(1-X_1)^2 \ln\left[\frac{(1-\alpha_1)C_{12}}{(1-X_1)C_2^0}\right]} = 1 \qquad \text{Equation 14}$$

$$\beta^{\sigma} = \frac{\ln\left(\frac{\alpha_1 C_{12}}{X_1 C_1^0}\right)}{(1-X_1)^2} \qquad \text{Equation 15}$$

C_1, C_2, and C_{12} are the concentrations of the surfactant 1, surfactant 2, and the mixture of the surfactants. X_1 is the mole fraction of surfactant 1 at the air-water interface, in the mixture. α_1 is the mole fraction of the first component, on a surfactant basis, not taking into account the bulk solution.

The first equation is numerically solved for the surface mole fraction (X_1), where the concentrations of C_1, C_2, and C_{12} are obtained from Figure 3.6 at a fixed surface tension. Once X_1 is obtained it can be used in Equation 15 to calculated β^{σ}.

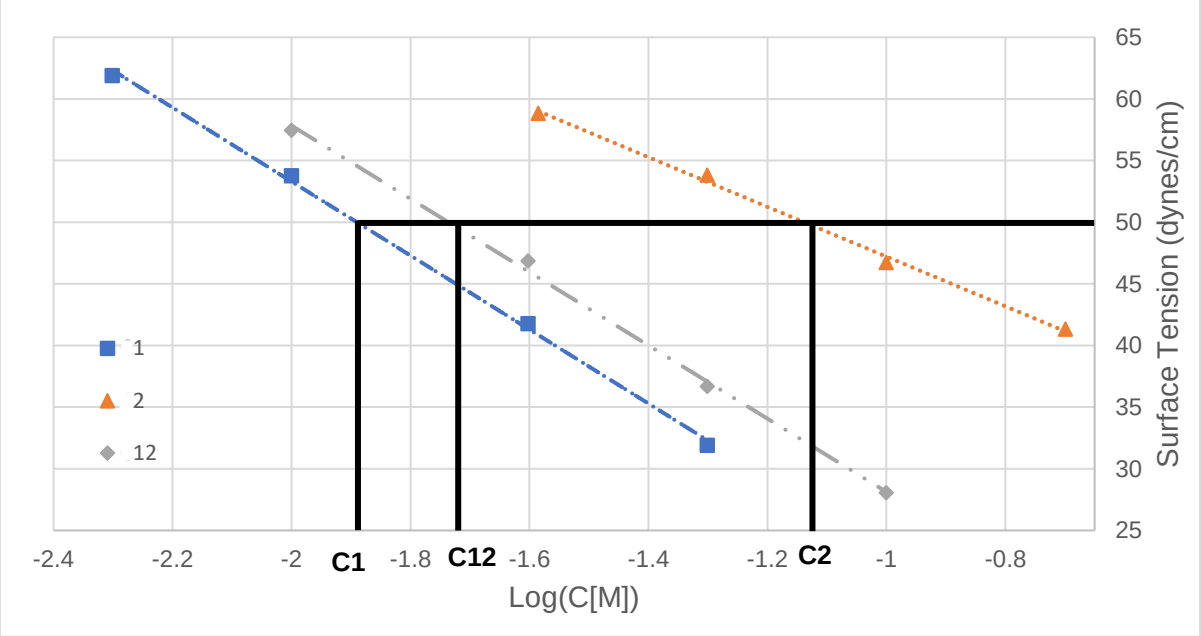

Figure 3.6: Surface tension vs log concentration for single surfactants (1,2) and surfactant mixture (12)

3.5.3.1 Dynamic surface tension

Dynamic surface tension measurements were performed with the Kruss BP2 bubble pressure tensiometer. Temperature was controlled at 25.0 ± 0.5 °C. The tests were performed at surface ages from 10ms to 1000ms, and it was found that at surface age of 1000ms the values for surface tension became constant. The surface tension values at 1000ms were used as a pseudo equilibrium surface tension measurement.

The solutions were made up with a 0.1 M NaCl solution as a background electrolyte. The pH was not adjusted but was recorded at a pH of 11 for collector, and collector-frother mixtures, and a pH of 6.8 for frother solutions. Jordaan (2018) showed that the pH had no effect on surface tension.

3.5.3.2 Surface excess and minimum surface areas

The surface excess was determined using the Gibbs adsorption isotherm (Kunjappu & Rosen, 2013) from Equation 16 and the slope of the lines in the surface tension (γ) vs log bulk concentration (LogC) plot (Figure 3.6).

$$\Gamma = -\frac{1}{2.303RT}\left(\frac{\partial\gamma}{\partial logC}\right)_T \qquad \text{Equation 16}$$

where Γ is the surface excess in (mol/cm^2), R is the gas constant (J/mol.K) and T is the absolute temperature (K). The surface excess was then used to determine the minimum surface area (Equation 17) of each surfactant component molecule and of the mixture together.

$$A_{min} = \frac{10^{19}}{N\Gamma} \qquad \text{Equation 17}$$

where A_{min} is the minimum surface area per molecule (Å^2), and N is Avogadro's number. The minimum surface area per molecule for an ideal mixture of surfactants was calculated using Equation 18 (Zhou & Rosen, 2003).

$$A_{ideal} = X_1 A_1 + (1 - X_1) A_2 \qquad \text{Equation 18}$$

3.5.4 Isothermal titration calorimetry measurements

The TAM III isothermal titration microcalorimeter was used to measure the energy associated with the interaction between collectors and minerals.

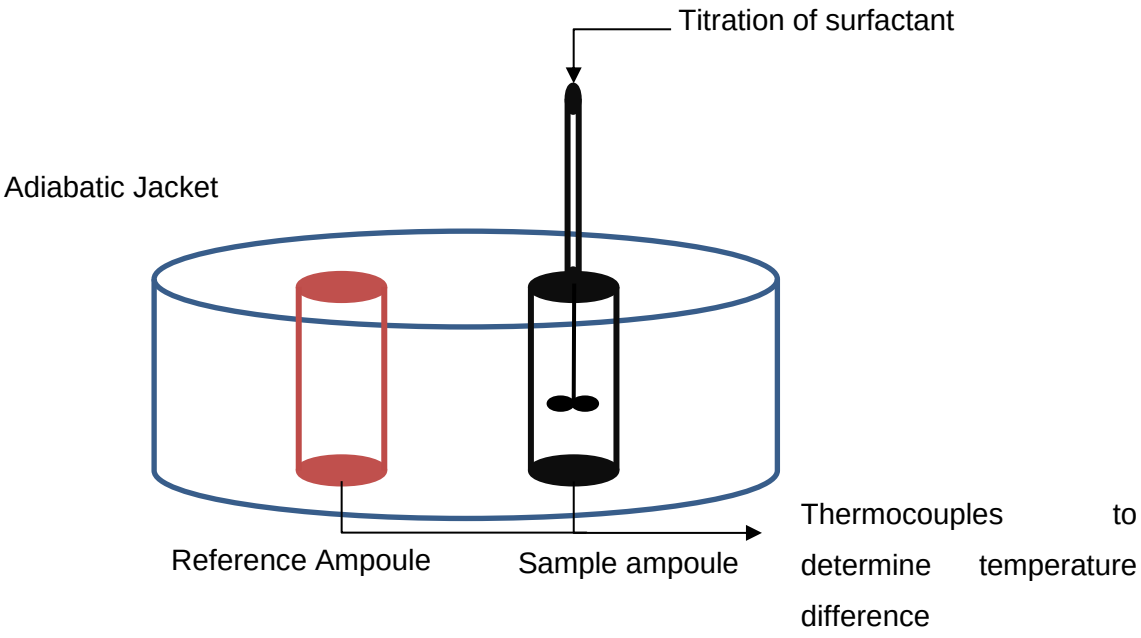

Figure 3.7: Schematic diagram of isothermal titration calorimeter

The ITC unit consists of two ampoules, a sample cell and a reference cell, enclosed in an adiabatic jacket as can be seen from Figure 3.7. When the titrant is titrated into the sample ampoule, the heat evolved changes the temperature, and the thermocouples detect the temperature difference between the ampoules. The amount of heat evolved is measured by measuring the amount of power that is used to maintain a constant temperature between the sample and reference ampoules.

The liquid bath of the calorimeter was set at 25°C which is controlled within 0.0001°C. The calorimeter was operated in heat flow mode where the power inputted into the reference ampoule to maintain a constant temperature between the ampoules can be integrated over time to determine the energy change in the sample ampoule.

A chemical validation was performed using the well-characterized heat of dilution of 10% (by weight) aqueous propan-1-ol in deionized water. Figure 3.8 shows the data output from the validation experiment. The peaks in Figure 3.8 represents the injection of the titrant into the solution. The heat flow was integrated over time to determine the heat of dilution per injection.

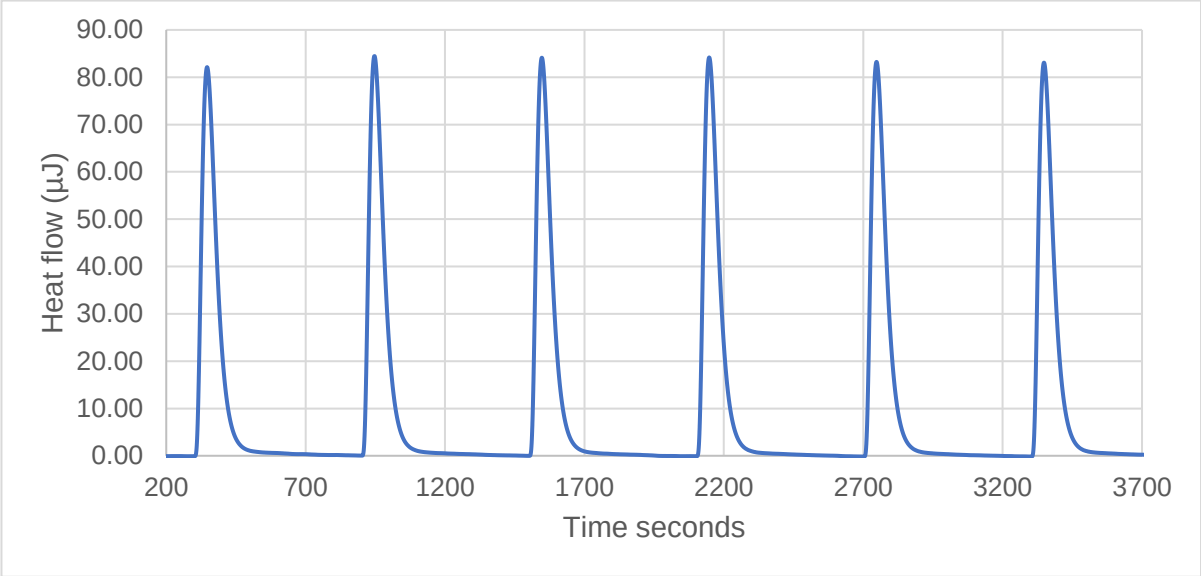

Figure 3.8: Heat flow vs time for the heat of dilution of 10 wt% solution propan-1-ol into deionised water.

Wadsö & Goldberg (2001) found the heat of dilution to be -5.29 ± 0.03mJ when 2.095 µL of aqueous propan-1-ol is diluted in 900mL of deionized water. The same validation was performed, and the heat of dilution was found to be -5.48 ± 0.0038mJ.

For experiments, 200 mg of the -38µm size fraction for each mineral was used in the ampoule with 700 µL of pH 9 water. Surface coverage dosages of collector corresponding to 25% monolayer coverage were used per injection. Heat of dilution tests were performed first, where the collector was titrated into deionized water. The heat of dilution was subtracted from the heat observed when the collector was titrated into the mineral slurry, to obtain the heat of interaction. The pH of the collector solution and the solution was also adjusted to pH 9, to ensure that no heat effects occurred due to differences in pH.

3.6 Hypothesis, Key questions, and Experimental tests to address key questions

Table 3.5: Table summarising which experimental tests address key questions

Hypothesis	Key questions	Experimental tests
Hypothesis I: DTP forms a complex with non-ionic frothers due to the association between the nonpolar and polar parts of the two amphiphilic molecules. The interactions between the molecules are due to hydrogen-bonding between the oxygen atoms on the functional group of DTP and the non-polar part of the frother. The polar parts of the molecule associates through the Van der Waals force, which increases with alkyl chain lengths of the respective reagents.	• Do DTP-frother show greater attractive attractions at the air-water interface compared to other collector-frother mixtures according to the regular solution theory model? • Are the collector-frother interactions dependent on the collector species that forms on the mineral surface?	• Surface tension • Microflotation • ACTA
Hypothesis II: The formation of DTP-non-ionic complexes allows for the co-adsorption of DTP at the air-water interface.	• Do DTP-frother or xanthate-frother mixtures show attractive or repulsive interactions according to the regular solution theory model? • Do DTP-frother or xanthate-frother mixtures lower the CCC with reference to the CCC of the pure components? • Does the presence of a non-ionic frothers influence the adsorption of DTP or xanthate at the sulphide mineral surface?	• Surface tension • Foam stability • Bubble size measurements • UV-Vis photometry
Hypothesis III: When DTP co-adsorbs with non-ionic frothers at the air-water interface, the collector-frother complex can transfer from the air-water interface to the mineral-water interface as the bubble collides with the particle, enhancing the kinetics of film thinning between the bubble and the particle, synergistically enhancing flotation recovery.	• Do bubble-particle interactions reduce the amount of DTP remaining in the pulp, in the presence of a non-ionic frother, compared to when no bubbles are present? • Do DTP-frother or xanthate-frother mixtures synergistically enhance the pulp zone recovery compared to the recoveries obtained for the individual reagents? • Do DTP-frother or xanthate-frother mixtures synergistically enhance the attachment probability in a Glembotsky device compared to the attachment probabilities of the pure reagents?	• UV-Vis photometry with aeration • Microflotation • ACTA

Table 3.5 summarizes the experimental methods that will address each key question and hypothesis. The first hypothesis regarding molecular interactions will be addressed with surface tension, microflotation and ACTA tests. Surface tension tests using regular solution theory will provide insight into the nature of the molecular interactions, i.e., if there are attractive or repulsive interactions. The microflotation and ACTA tests will provide insight on how different minerals and the different collector species that form on these minerals will influence these interactions.

The second hypothesis on the co-adsorption of DTP at the air-water interface will be addressed using surface tension tests, foam stability, bubble size measurements and residual collector concentration using UV-Vis spectrophotometry. These tests will look at how the separate surfactants (DTP and frother) influence the air-water interface compared to the surfactant mixtures.

The third hypothesis on the transfer of the DTP-frother complex from the air-water to the mineral-liquid interface during bubble particle collision will be tested by residual collector concentration using UV-Vis spectrophotometry with aeration, microflotation and the ACTA. The UV-Vis with aeration will provide evidence of the transfer of the collector from the air-water interface to the mineral-liquid interface, and the microflotation and ACTA tests will indicate if this transfer mechanism is synergistically improving recovery and bubble-particle attachment.

4 Results

4.1 Introduction

The results presented in this chapter follow from the project approach. Microflotation tests investigated the effect of collectors, frothers and their mixtures on pulp phase recovery for galena, pyrite, chalcopyrite and chalcocite.

Following the pulp phase recovery tests, the ACTA was used to decouple the hydrodynamic effects that are present in the microflotation cell from the surface forces occurring between the bubble and the particle during attachment. This was to understand whether there is a true synergistic effect between collectors and frother, or whether each of these reagents had separate effects during the sub-processes of bubble-particle attachment.

UV-Vis spectrophotometry and ITC were used to determine the adsorption density and extent of interaction of collectors at the mineral surfaces. The effect of the frother on the extent of collector adsorption was also examined. UV-Vis tests with aeration investigated whether SDEDTP transfers from the air-water interface to the mineral-water interface during bubble-particle collision.

Apart from the mineral-water interface, the air-water interface was examined for interactions between collectors and frothers. Pulp bubble coalescence and foam stability tests were used to evaluate the surface activity of collectors since these techniques are quite sensitive to the typical concentrations used in froth flotation. Dynamic surface tension and the regular solution theory model was then used to quantify the interactions between collectors and frothers at the air-water interface.

4.2 Microflotation

Microflotation tests decouple the froth phase effects from the pulp phase effects and provide insight into the effect of flotation reagents and their mixtures on bubble-particle attachment in the pulp. Microflotation tests were performed on galena, pyrite, chalcopyrite, and chalcocite at pH 9. The experiments were performed in duplicate, and the standard error in the recovery results were less than 5%.

Baseline tests were performed with no reagents to establish the natural floatability of the mineral. Single reagent tests were then used to observe how the reagents affect the recovery of the minerals compared to their natural floatability. Sodium di-ethyl DTP (SDEDTP) and sodium ethyl xanthate (SEX) were used as collectors, and hexanol as the frother. Finally, reagent mixture experiments were performed with each collector mixed with the frother. The

collectors were dosed to cover ~50% of the mineral surface area. Hexanol dosage was 0.12 mM. This is slightly higher than the critical coalescence concentration (CCC) which was reported to be 0.11 mM (Zhang et al, 2012). All these tests are compared to establish if there is any evidence of a synergistic increase in recovery when reagent mixtures were used.

Microflotation tests with other reagents were also conducted. Different frothers, such as longer chain length aliphatic alcohols or polypropylene glycols were used. Longer chain lengths of thiol collectors, and collector-collector-frother mixtures were also investigated. For these tests the dosages of the frothers were approximately at the CCC, and for the collectors were generally ~50% monolayer coverage unless stated otherwise.

The microflotation results are presented as percent recovery vs time plots and the Klimpel model equation (Equation 19) was fitted to the data via the curve_fit method provided from the SciPy Python library (scipy.optimize.curve_fit — SciPy v1.7.0 Manual). The curve_fit method provides the optimally fitted parameters, k (first-order rate constant) and R_∞ (ultimate recovery), as well as the variance of both of these parameters according to the goodness of fit of the model to the data. The variances were used to determine the standard deviation which represents the uncertainty in the fitted parameters. The residual of the fitted model was determined according to the following equation:

$$Residual = \sum_{t=0}^{t=i}(R_{data}(t_i) - R_{fitted}(k_{opt}, R_{\infty_{opt}}, t_i)) \quad \text{Equation 19}$$

Where R_{data} is the experimental recovery data obtained at each time point expressed as % recovery, R_{fitted} is the recovery data obtained from the optimum parameters determined from the fitted model. The points on the graphs show the experimental recovery data with the error bars representing the standard error of each data point. The lines represent the fitted model. The first-order model was also fitted to the results but had a worse goodness of fit when compared to the Klimpel model.

The final microflotation recoveries, the residual of the fitted model, and fitted parameters from the model: k and R_∞, are all subsequently summarised in tables. The recovery vs time curves were plotted with the Matplotlib library from Python.

4.2.1 Microflotation tests using galena

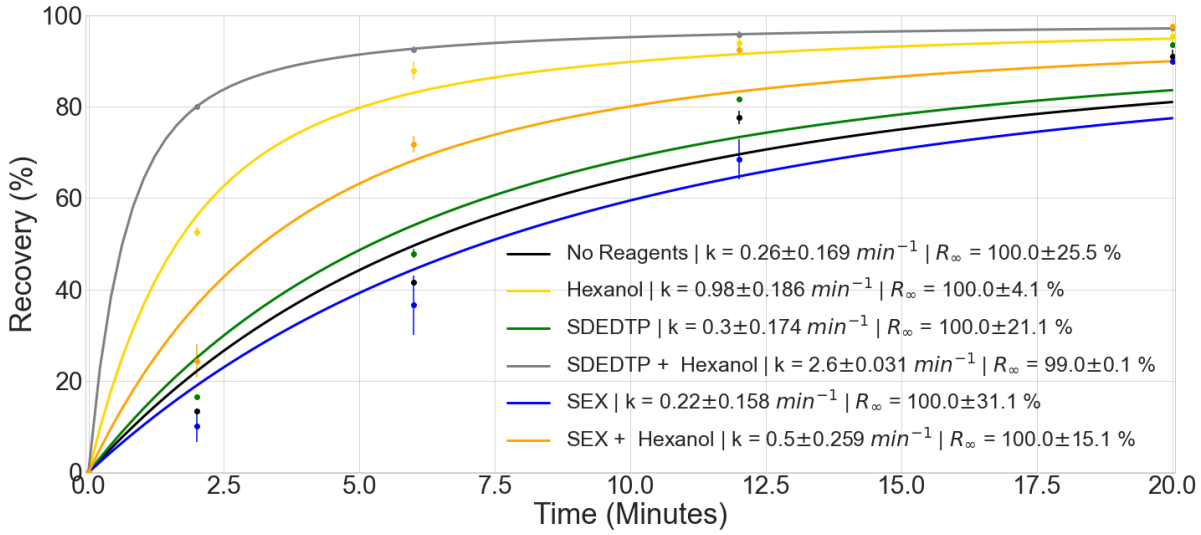

Figure 4.1: Recovery of galena as a function of time at pH9 using single reagents and reagent mixtures. Collectors are dosed at 50% monolayer coverage and the frother is dosed so that the concentration is just above the CCC.

Figure 4.1 illustrates that the natural floatability (no reagents) yielded a galena recovery of 90%, and subsequent tests showed even greater recoveries. Taguta (2015) obtained a similar natural floatability (97.3% recovery) for galena at pH 9.2 using the UCT microflotation cell. As comparing final recoveries in such a narrow range of values would not clearly distinguish the performance of each of the reagents and reagent mixtures, the first order rate constant was used as a performance indicator rather than the recovery, as this parameter provides a clearer variation during the first two minutes of flotation in Figure 4.1. Table 4.1 summarizes the final microflotation recoveries and the fitted first-order Klimpel model parameters for the tests carried out using various collector/frother regimes.

The residuals of the fitted model (Table 4.1) for each reagent condition show that for most reagent conditions the Klimpel models fit the data reasonably well. The residual is quite high for the conditions of SDEDTP (3.44) and SEX + hexanol (8.12), compared to the condition of hexanol (-0.03).

The first order rate constant is directly proportional to the attachment and collision efficiency of the bubble and the particle, where these efficiencies are affected by parameters such as particle density, particle size, bubble size, and bubble velocity (Danoucaras, Vianna & Nguyen, 2013) all of which are incorporated into the microflotation recovery. With a size distribution of -106+38 µm particles, the rate constant can be distributed around the fitted value. There is a distribution of rate constants for each of the particle sizes. This may be the reason for the variations in the goodness of fit in the modelling of the data. Other models such as the classic first order model was fitted to the data but the Klimpel model resulted in the smallest residuals.

Table 4.1: Final microflotation recoveries for galena at pH 9 and fitted parameters for Klimpel equation determined for single reagents and reagent mixtures.

	No Reagents	**Hexanol**	**SDEDTP**	**SDEDTP + Hexanol**	**SEX**	**SEX + Hexanol**
Final microflotation recovery (%)	91.0 ±1.37	95.4 ±2.48	93.5 ±0.36	97.3 ±0.73	89.9 ±0.37	97.6 ±0.59
Model	**Klimpel**					
k - First order rate constant (min^{-1})	0.26 ±0.169	1.49 ±0.122	0.30 ±0.174	2.60 ±0.031	0.22 ±0.158	0.50 ±0.259
R_∞ (%)	100.0 ±25.5	96.1 ±1.3	100.0 ±21.1	99.0 ±0.1	100.0 ±31.1	100.0 ±15.1
Residual	1.54	-0.03	3.44	0.00	-0.47	8.12

Comparing the first order rate constants of the natural floatability (k = 0.26 min^{-1}) of galena where no reagents have been added to case with the addition of collectors, SEX (k = 0.22 min^{-1}) and SDEDTP (k = 0.30 min^{-1}) show that there is no substantial improvement in the rate of flotation, nor a significant difference in the recoveries when these collectors are added. This indicates that either the collectors are not adsorbing onto galena, or there is not enough collector coverage to significantly improve the mineral surface hydrophobicity. However, the addition of the frother, hexanol, gave a 4-fold improvement in the rate of flotation (k = 0.98 min^{-1}) compared to the natural floatability.

Even though the SDEDTP did not significantly increase the floatability of galena, using a mixture of SDEDTP with hexanol improved the rate of flotation by over 2-fold (k = 2.60 min^{-1}), compared to the case where only hexanol was used. This results in 80% of the galena being recovered within the first 2 minutes of flotation when using the mixture of SDEDTP and hexanol. Quantitatively these results indicate that the mixture of SDEDTP and hexanol synergistically improve pulp phase flotation recovery.

In contrast with the synergistic improvements observed for the SDEDTP-hexanol system, the mixture of SEX and hexanol resulted in antagonistic recovery effects. From Table 4.1 it can be seen that the first order rate constant for the SEX-hexanol mixture (k = 0.50 min^{-1}) is half of that of the rate constant when hexanol (k = 0.98 min^{-1}) was used on its own. This is also observed in Figure 4.1 where the recovery of the mixture in the first 10 minutes of flotation is lower than the recovery with hexanol.

4.2.2 Microflotation tests using pyrite

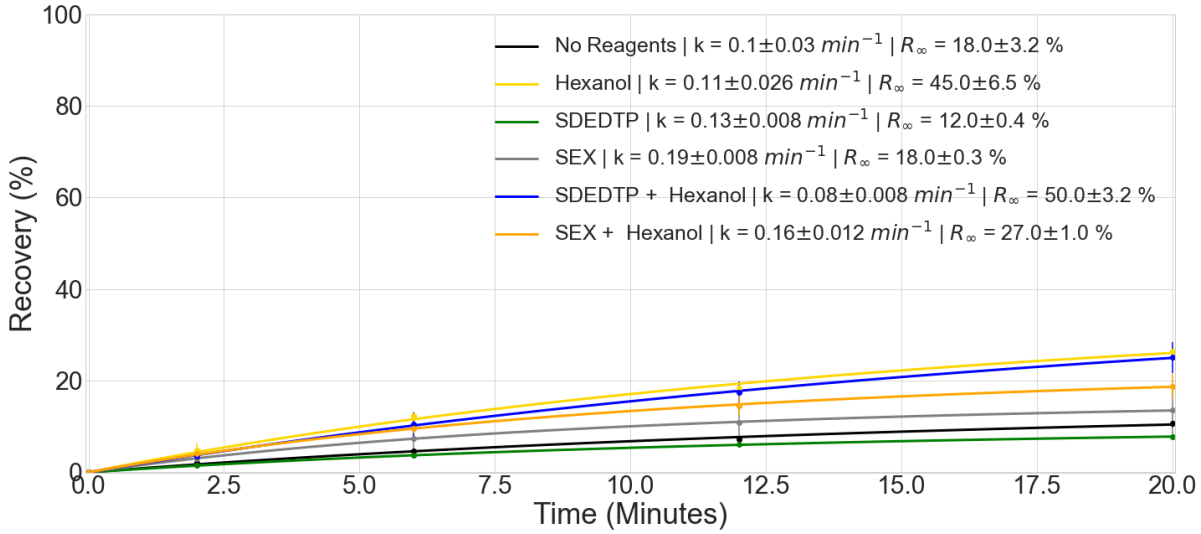

Figure 4.2: Recovery of pyrite as a function of time at pH9 using single reagents and reagent mixtures. Collectors are dosed at 50% monolayer coverage and the frother is dosed so that the concentration is just above the CCC.

Microflotation tests were performed on pyrite at pH 9. Figure 4.2 displays the recovery of pyrite as a function of time using various reagents and reagent mixtures. The final recoveries and the fitted Klimpel model parameters are summarised in Table 4.2.

Table 4.2: Final microflotation recoveries for pyrite at pH 9 and fitted parameters for Klimpel equation parameters determined for single reagents and reagent mixtures.

	No Reagents	**Hexanol**	**SDEDTP**	**SDEDTP + Hexanol**	**SEX**	**SEX + Hexanol**
Final microflotation recovery (%)	11.0 ±0.86	27.5 ±1.41	7.8 ±0.04	25.8 ±3.43	6.9 ±1.08	18.8 ±2.65
Model	**Klimpel**					
k - First order rate constant (min^{-1})	0.10 ±0.030	0.11 ±0.026	0.13 ±0.008	0.08 ±0.008	0.19 ±0.008	0.16 ±0.012
R_∞ (%)	18.2 ±3.2	44.5 ±6.5	12.0 ±0.4	50.3 ±3.2	18.2 ±0.3	26.6 ±1.0
Residual	0.32	0.42	0.03	-0.02	-0.02	0.17

The final recoveries show that neither SDEDTP (7.8%) nor SEX (6.9%) improved the pyrite recovery. They actually resulted in slightly decreased recovery compared to the natural floatability of pyrite, which is 11.0 %. In a study done by Jordaan (2018), the natural floatability of pyrite at pH 9 using the UCT microflotation cell was found to be 35%, which is significantly

higher than the 11% obtained in this study. This suggests that the surface of this sample of pyrite may have been oxidised.

The addition of hexanol improved the recovery of pyrite from 11.0 % to 27.5%, but using a mixture of SDEDTP and hexanol (25.8%) made no significant difference. The SEX-Hexanol mixture results were similar to the results found for the same reagents in the galena system. This mixture decreased the recovery from 27.5% for hexanol to 18.8%. Considering that DTP exhibits weak interaction with the pyrite mineral surface (Taguta, O'Connor & McFadzean, 2017; Nagarj & Brinen, 2001), and interacts at the air-water interface (Jordaan, 2018), it was considered that the surface dosage used in this investigation may have been too low to induce any synergistic effect. A liquid concentration dosage of SDEDTP similar to that of the dosage of frothers was used in subsequent pyrite microflotation tests to test this theory.

A concentration of 0.1 mM was selected for the pulp concentration tests. That concentration corresponds to 39 grams of collector per ton of ore, at 35% weight of solids, which is lower than the typical dosages used in industry. Figure 4.3 compares the effect of dosage of SDEDTP, and its mixture with hexanol on the recovery of pyrite. Table 4.3 summarises the final microflotation recoveries and the fitted parameters for the Klimpel equation for the higher concentrations.

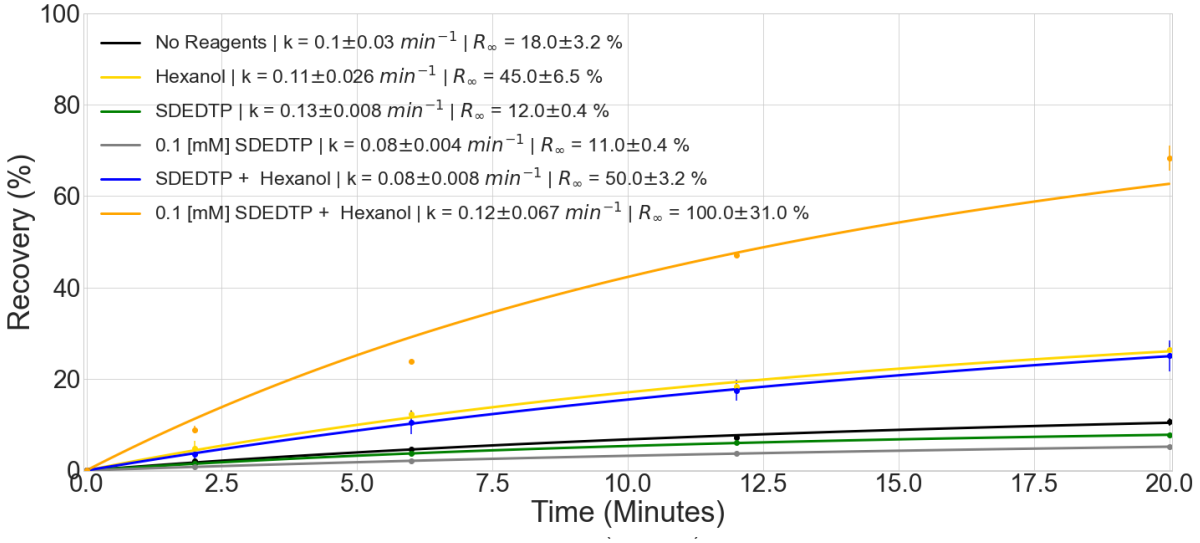

Figure 4.3: Recovery of pyrite as a function of time at pH9 comparing different SDEDTP dosages in the presence of hexanol. The frother is dosed so that the concentration is just above the CCC.

Table 4.3: Final microflotation recoveries for pyrite at pH 9 and fitted parameters for Klimpel equation parameters determined for single reagents and reagent mixtures. The concentration of 0.04 [mM] SDEDTP is equivalent to the 50% monolayer dosage.

	No Reagents	**Hexanol**	**SDEDTP 0.04 [mM]**	**SDEDTP 0.04 [mM] + Hexanol**	**0.1 [mM] SDEDTP**	**0.1 [mM] SDEDTP + Hexanol**
Final microflotation recovery (%)	11.0 ±0.86	27.5 ±1.41	7.8 ±0.04	25.8 ±3.43	5.2 ±0.41	68.3 ±2.74
Model	**Klimpel**					
k - First order rate constant (min^{-1})	0.10 ±0.030	0.11 ±0.026	0.13 ±0.008	0.08 ±0.008	0.08 ±0.004	0.12 ±0.067
R_∞ (%)	18.2 ±3.2	44.5 ±6.5	12.0 ±0.4	50.3 ±3.2	10.6 ±0.4	100.0 ±31.0
Residual	0.32	0.42	0.03	-0.02	-0.03	-2.55

Even though the 0.1 mM SDEDTP is a much higher dosage than the ~50% monolayer dosage, the recovery decreased from 7.8% to 5.2% with the use of the higher dosage of SDEDTP alone. However, the mixture of 0.1mM SDEDTP and hexanol yielded a recovery of 68.3%, compared to the 25.8% recovery when using the ~50% monolayer dosage with hexanol. This revealed that the mixture of SDEDTP and hexanol had a synergistic effect on the recovery of pyrite, similar to the effect observed with galena.

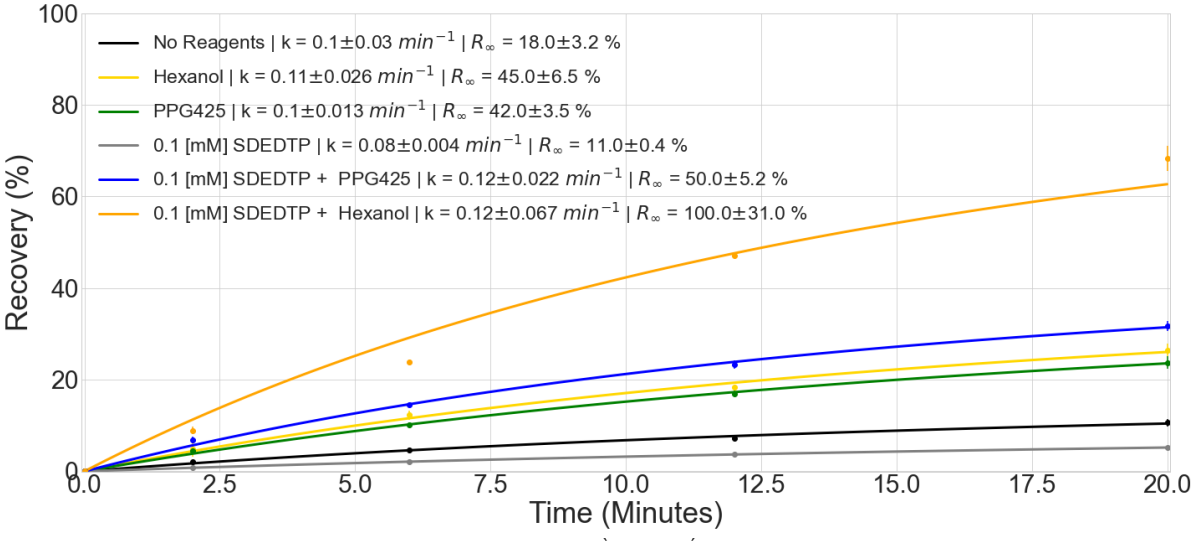

Figure 4.4: Recovery of pyrite as a function of time at pH9 using single reagents and reagent mixtures. SDEDTP is dosed at 0.1mM and the frothers are dosed so that the concentration is just above the CCC.

Following the synergistic reponse observed with SDEDTP and hexanol, another type of non-ionic frother was employed to determine whether a similar synergistic reponse was observed. Tests were performed with PPG425. The recovery responses of PPG425 with SDEDTP are compared to the SDEDTP-hexanol system in Figure 4.4, where the final flotation recoveries and fitted Klimpel equation parameters are summarised in Table 4.4.

The addition of PPG425 improved the natural flotability of pyrite from 11% to 23.7% recovery, which is similar to the response observed in the case of hexanol (27.5%). The addition of SDEDTP to PPG425 improved the recovery from 23.7% to 31.8%, but did not produce as strong a synergistic response as the SDEDTP-hexanol system, which improved the recovery of pyrite from 27.5% to 68.3%. The lower synergistic response might be ascribed to the lower concentration of PPG425 used (0.014mM), compared to hexanol (0.12mM). This was in order to maintain dosages close to the CCC. Higher concentrations of PPG425 were tested in the microflotation cell, but these concentrations affected the normal operation of the microflotation cell due to the formation of a froth phase.

Table 4.4: Final microflotation recoveries for pyrite at pH 9 and fitted parameters for Klimpel equation parameters determined for PPG425, Hexanol, SDEDTP, and mixtures of these reagents.

	No Reagents	**Hexanol**	**0.1 [mM] SDEDTP**	**0.1 [mM] SDEDTP + Hexanol**	**PPG425**	**0.1 [mM] SDEDTP + PPG425**
Final microflotation recovery (%)	11.0 ±0.86	27.5 ±1.41	5.2 ±0.41	68.3 ±2.74	23.7 ±1.34	31.8 ±1.08
Model	**Klimpel**					
k - First order rate constant (min^{-1})	0.10 ±0.030	0.11 ±0.026	0.08 ±0.004	0.12 ±0.067	0.10 ±0.013	0.12 ±0.022
R_∞ (%)	18.2 ±3.2	44.5 ±6.5	10.6 ±0.4	100.0 ±31.0	42.0 ±3.5	50.1 ±5.2
Residual	0.32	0.42	-0.03	-2.55	0.36	0.72

As DTP is used for its selectivity against pyrite (Lotter & Bradshaw, 2010), and it is established that SDEDTP is active at the air-water interface (Jordaan, 2018) rather than the pyrite surface (Taguta, O'Connor & McFadzean, 2017). It was hypothesized that the synergistic mechanism

between SDEDTP in the presence of frother, coupled with the use of SIBX to improve the mineral hydrophobicty would further enhance the synergistic recovery of pyrite. The recovery responses for this system are presented in Figure 4.5. Table 4.5 lists the final microflotation recoveries, along with the fitted Klimpel model data from the recovery data in Figure 4.5.

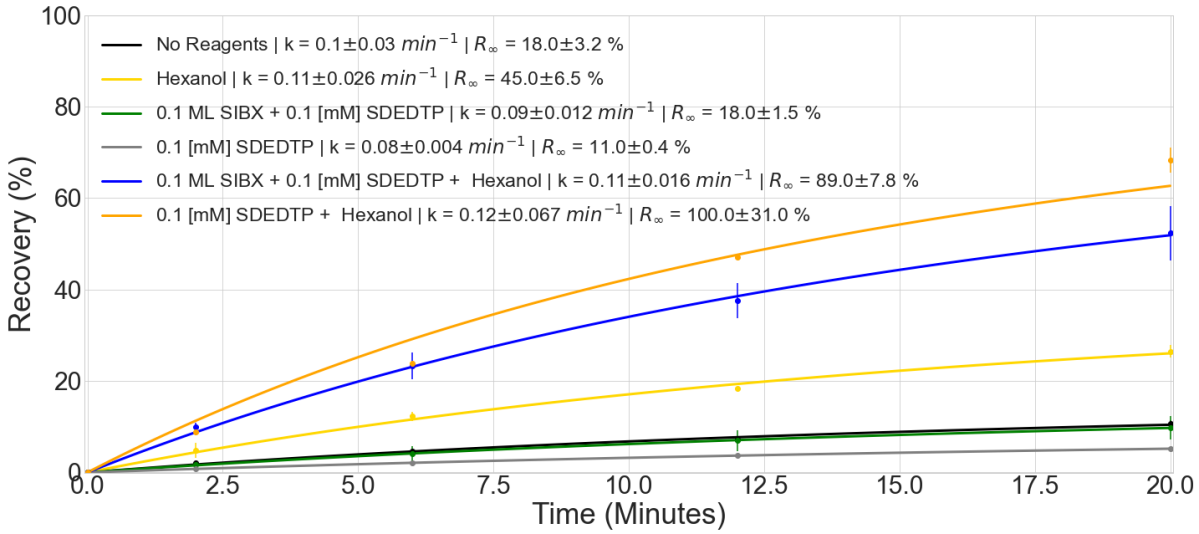

Figure 4.5: Recovery of pyrite as a function of time at pH9 using single reagents and reagent mixtures. SDEDTP is dosed at 0.1mM, SIBX is dosed at 10% monolayer (ML) coverage and the frother is dosed so that the concentration is just above the CCC.

A low surface coverage of SIBX was used (~10% monolayer). SIBX was added first and then SDEDTP, which was used at a pulp concentration of 0.1mM. The recovery of pyrite was 5.2% using SDEDTP only, but it imporoved to 9.8% when SDEDTP was used together with SIIBX. The addition of hexanol to the mixture of both collectors improved the recovery to 52.3%, which is lower than the recovery for the SDEDTP-hexanol system, which was 68.3%. The addition of SIBX had an antagonistic effect on the recovery compared to having only SDEDTP present, together with hexanol.

Table 4.5: Final microflotation recoveries for pyrite at pH 9 and fitted parameters for Klimpel equation parameters determined for SDEDTP, SIBX, hexanol and mixtures of these reagents.

	No Reagents	**Hexanol**	**0.1 [mM] SDEDTP**	**0.1 [mM] SDEDTP + Hexanol**	**0.1 ML SIBX + 0.1 [mM] SDEDTP**	**0.1 ML SIBX + 0.1 [mM] SDEDTP + Hexanol**
Final microflotation recovery (%)	11.0 ±0.86	27.5 ±1.41	5.2 ±0.41	68.3 ±2.74	9.8 ±2.60	52.3 ±5.94
Model	**Klimpel**					
k - First order rate constant (min^{-1})	0.10 ±0.030	0.11 ±0.026	0.08 ±0.004	0.12 ±0.067	0.09 ±0.012	0.11 ±0.016
R_∞ (%)	18.2 ±3.2	44.5 ±6.5	10.6 ±0.4	100.0 ±31.0	17.9 ±1.5	88.5 ±7.8
Residual	0.32	0.42	-0.03	-2.55	0.14	0.84

4.2.3 Microflotation tests using chalcopyrite

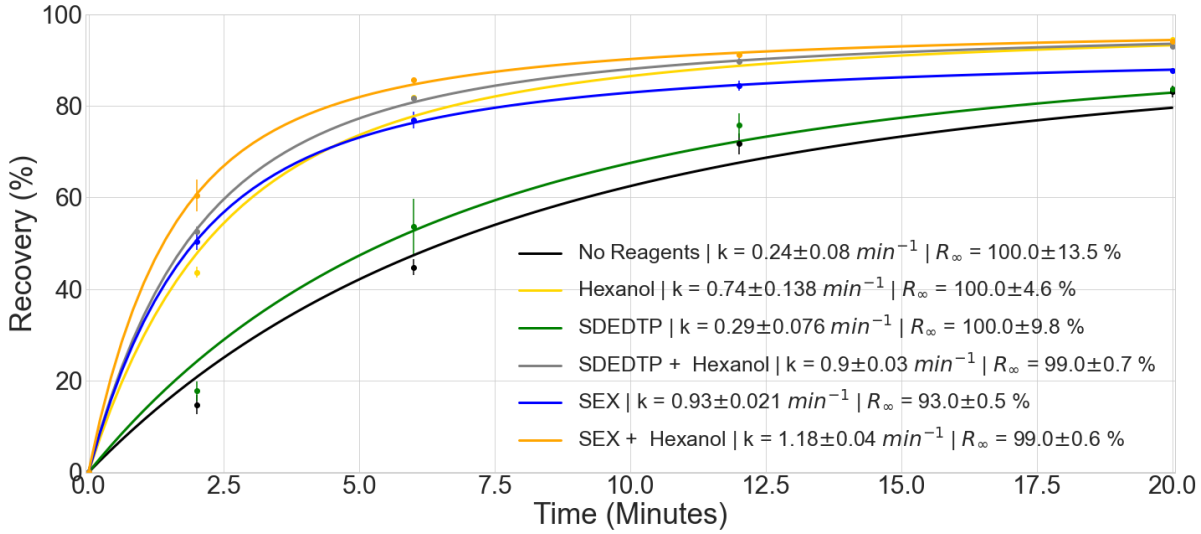

Figure 4.6: Recovery of chalcopyrite as a function of time at pH9 using single reagents and reagent mixtures. Collectors are dosed at 50% monolayer coverage and the frother is dosed so that the concentration is just above the CCC.

Microflotation tests were performed on chalcopyrite at pH 9. The collector dosage for this mineral was the ~50% monolayer coverage. Figure 4.6 shows the recovery of chalcopyrite as a function of time. The final recoveries and the fitted Klimpel model parameters are

summarised in Table 4.6. Without the addition of any reagents, chalcopyrite yielded a high recovery of 83.2%. This is not unusual since it is well known that chalcopyrite demonstrates a high degree of natural hydrophobicity. The first order rate constant was used as a performance indicator to quantitatively assess whether there is a synergistic response for collector-frother mixtures.

The addition of SEX produced a considerable improvement in mineral surface hydrophobicity as the first-order rate constant increased from 0.24 min^{-1} for the natural floatabiltiy to 0.93 min^{-1} for SEX. SDEDTP did not show much improvement relative to the case for the natural floatability, as shown in Table 4.6. Hexanol greatly improved the first order flotation kinetics to 0.74 min^{-1}, relative to the natural hydrophobicity similar to what had been observed with galena in Figure 4.1.

Table 4.6: Final microflotation recoveries for chalcopyrite at pH 9 and fitted parameters for Klimpel equation parameters determined for single reagents and reagent mixtures.

	No Reagents	**Hexanol**	**SDEDTP**	**SDEDTP + Hexanol**	**SEX**	**SEX + Hexanol**
Final microflotation recovery (%)	83.2 ±1.31	94.4 ±0.03	85.2 ±0.21	94.4 ±0.49	87.7 ±0.01	93.1 ±0.18
Model	**Klimpel**					
k - First order rate constant (min^{-1})	0.24 ±0.080	0.74 ±0.138	0.29 ±0.076	0.90 ±0.030	0.93 ±0.021	1.18 ±0.040
R_∞ (%)	100.0 ±13.5	100.0 ±4.6	100.0 ±9.8	99.1 ±0.7	92.9 ±0.5	98.6 ±0.6
Residual	-0.86	3.68	-1.17	-0.07	-0.04	-0.03

The mixtures of both SDEDTP and SEX with hexanol resulted in improvements in the first order rate constant, as can be seen from Table 4.6. The mixture of SEX and hexanol gave the highest first order rate constant of 1.18 min^{-1}, but both SEX and hexanol, on their own, substantially improved the first order flotation kinetics. Thus, it is hard to discern whether the improvements are due to additive effects of each of the reagents, especially since each of these reagents can produce improvements via different mechanisms, where collectors improve mineral surface hydrophicity and frothers can have effects at the air-water interface.

The mixture of SDEDTP and hexanol improved the first order kinetics from 0.74 min^{-1} for hexanol, to 0.90 min^{-1} for the mixture. The strong synergistic effect observed with both galena and pyrite for the DTP-hexanol mixture is as strong as for chalcopyrite in the microflotation cell.

4.2.4 Microflotation tests using chalcocite

DTP is known to have weak interactions with galena, pyrite and chalcopyrite and it has been shown that only sparing amounts of DTP adsorb onto these minerals (Petrus et al., 2011: Grano et al., 1997; McFadzean & O'Connor, 2014; Taguta, O'Connor & McFadzean, 2017). Previous work has shown that SDEDTP adsorbs onto chalcocite at high pulp pH (Woods, Kim & Yoon, 1993; Mielczarski & Minni, 1984), and that 50% monolayer coverage resulted in 90% recovery of the mineral within 1 minute in a microflotation cell (Woods, Kim & Yoon, 1993). The decision was made to use a ~20% monolayer dosage for the following tests, and only record the recovery for the first 2 minutes of flotation to be able to clearly discriminate between the performance of each reagent.

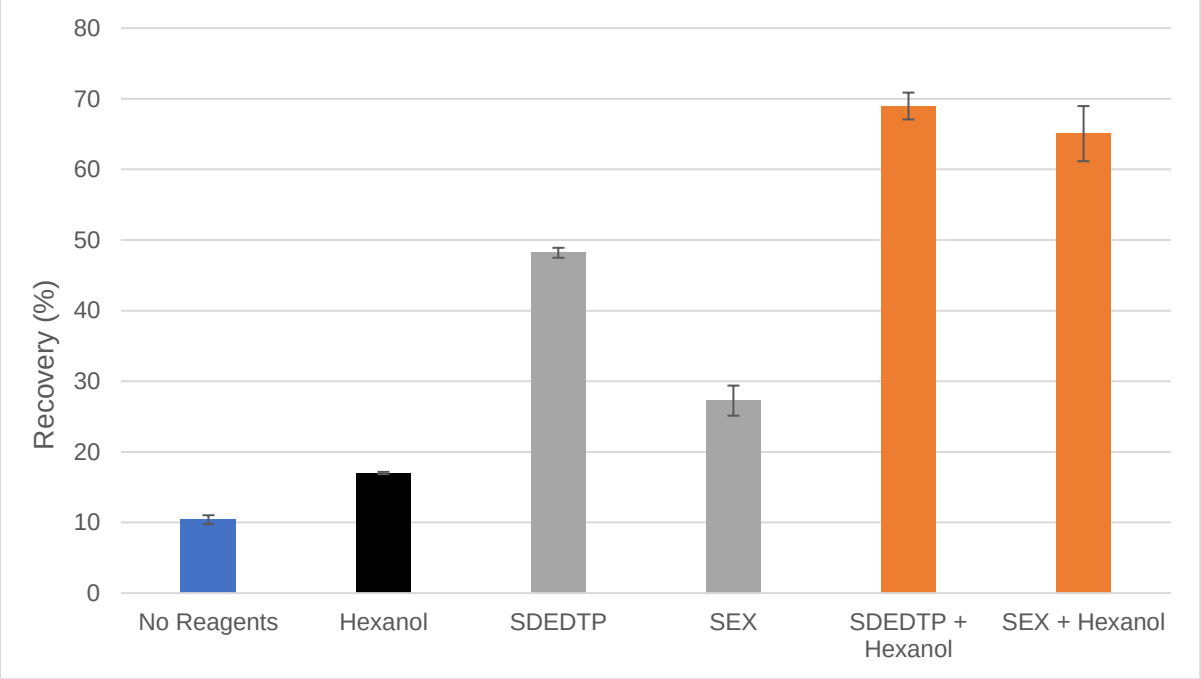

Figure 4.7: Recovery of chalcocite in the first two minutes of flotation at pH 9 using single reagents and reagents mixtures. Collectors are dosed at 20% monolayer coverage and the frother is dosed so that the concentration is just above the CCC.

Figure 4.7 displays the final recovery after 2 minutes for chalcocite at pH 9. The addition of SDEDTP and SEX improved recovery from 10.4% for the natural floatability of chalcocite to 48.2% and 27.3%, respectively. The improvement in recovery corresponds to the results of Woods, Kim & Yoon (1993) which shows that SDEDTP adsorbs onto chalcocite and can

greatly improve floatability at low surface coverages. The use of hexanol only slightly improved the recovery from the natural floatability from 10.4% to 17.0%.

The addition of hexanol to these collectors significantly improved the recovery where SDEDTP and hexanol yielded a recovery of 69%, and SEX and hexanol yielded a recovery of 65.1%. The improvement for the mixture of SEX and hexanol is much greater as SEX on its own did not improve the recovery to the same extent as SDEDTP did. It is not possible to qualitatively determine whether the collector and frother are interacting synergistically in the case of these results. The calculated sum contribution of each reagent is used to quantitatively discern if the improvement in recovery is synergistic or not.

Table 4.7: Mass recovery of chalcocite in the microflotation cell for mixtures of ethyl DTP and xanthate with hexanol compared to the sum contribution of each reagent (collector and hexanol). ML = monolayer

	20% ML SDEDTP + Hexanol	SEX + Hexanol
% Mass recovery of reagent mixture	69.0	65.1
Calculated sum contribution of each reagent	54.8	33.9
Difference	14.2	31.2

Table 4.7 shows that there is a positive difference between the mass recovery of the reagent mixture in the microflotation cell compared to the calculated contribution of each reagent. This positive difference indicates that there is a synergistic improvement for the reagent mixtures compared to the improvements for the reagents on their own. SEX showed a greater difference (31.2) than SDEDTP (14.2).

Further microflotation tests were performed with SDEDTP and hexanol using lower surface-coverage dosages to detect if the improved recovery effect observed for the SDEDTP-hexanol mixture is due to the surface hydrophobicity induced by the collector.

Figure 4.8 demonstrates that the lower dosage which is only ~10% of a monolayer resulted in a decrease in recovery from 48.2% (20% monolayer dosage) to 32.2%. When hexanol is added to the system the recovery only decreased from 69% to 65.1%. Table 4.8 shows the difference between the recovery of the reagent mixture and the calculated sum contribution of each reagent increased from 14.2 to 26.3.

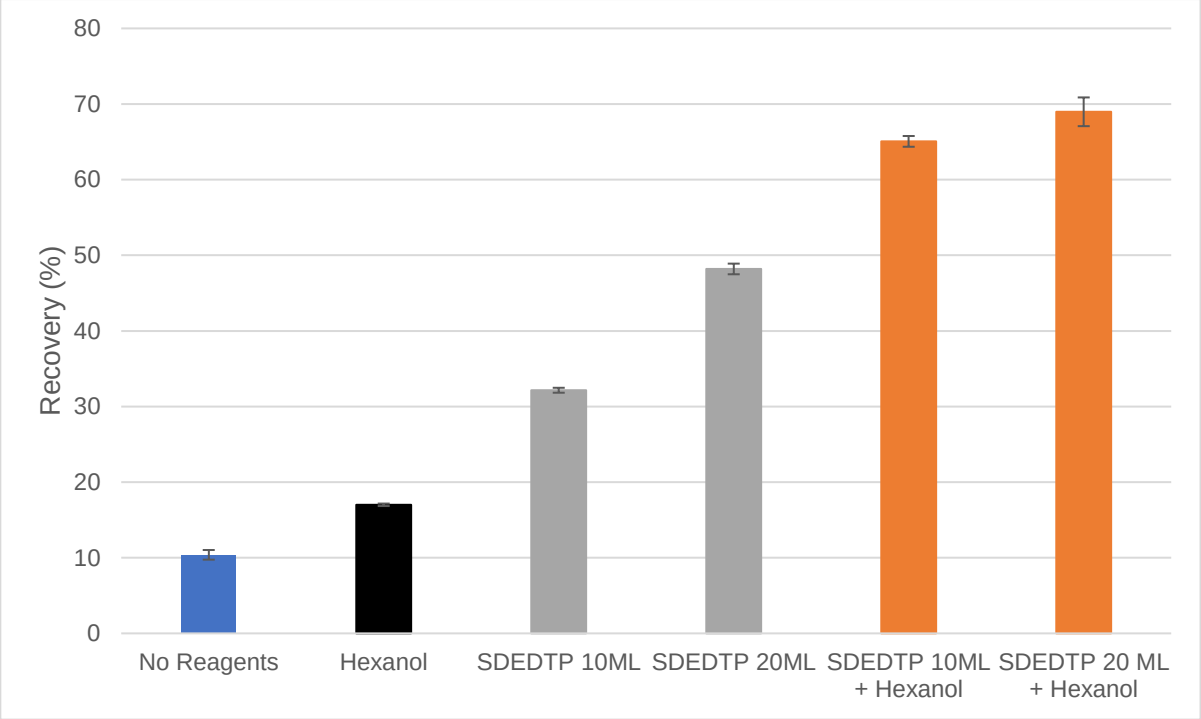

Figure 4.8: Recovery of chalcocite in the first two minutes of flotation at pH 9 comparing the effect of SDEDTP surface coverage. The frother is dosed so that the concentration is just above the CCC. 10ML – 10% monolayer dosage. 20ML – 20% monolayer dosage.

Table 4.8: Mass recovery of chalcocite in the microflotation cell for mixtures of ethyl DTP with hexanol compared to the sum contribution of each reagent (collector and hexanol). ML = monolayer

	20% ML SDEDTP + Hexanol	10% ML SDEDTP + Hexanol
% Mass recovery of reagent mixture	69.0	65.1
Calculated sum contribution of each reagent	54.8	38.8
Difference	14.2	26.3

The lower dosage experiment with SDEDTP and hexanol shows that the synergistic improvement in recovery is not a strong function of the concentration of SDEDTP at the surface. This indicates that it may be the frother that is playing the primary role in improving the mineral recovery.

Lekki & Laskowski (1971) has shown that α-terpineol exponentially improves the induction time of chalcocite coated with ethyl xanthate and proposed that this improvement in induction time is due to the frother destabilizing the thin film between the mineral and the bubble.

4.2.4.1 Microflotation recoveries of longer alkyl chain length collectors

Further microflotation tests were performed using longer chain length DTPs, and mixtures of these DTP's with frothers. Figure 4.9 illustrates the recovery of chalcocite after the first two minutes of flotation for various DTP derivatives and their mixtures with frothers. The most striking result for the longer chain length DTPs is that SDEDTP outperforms all of them, this reagent resulting in a 48.2% recovery compared to 27.7%, 30.8% and 44.9% for SD(N)BDTP (straight chain n-butyl DTP), SD(I)BDTP (branched chain iso-butyl DTP), and SD(I)BDTPINA (branched chain iso-butyl dithiophosphinate), respectively. Generally, for xanthates an increase in alkyl chain length increases mineral surface hydrophobicity and thus floatability (Wark & Wark, 1932; Ackerman et al., 1987) but this is not observed here for DTP. This highlights that DTP does not behave in the same way as standard collectors.

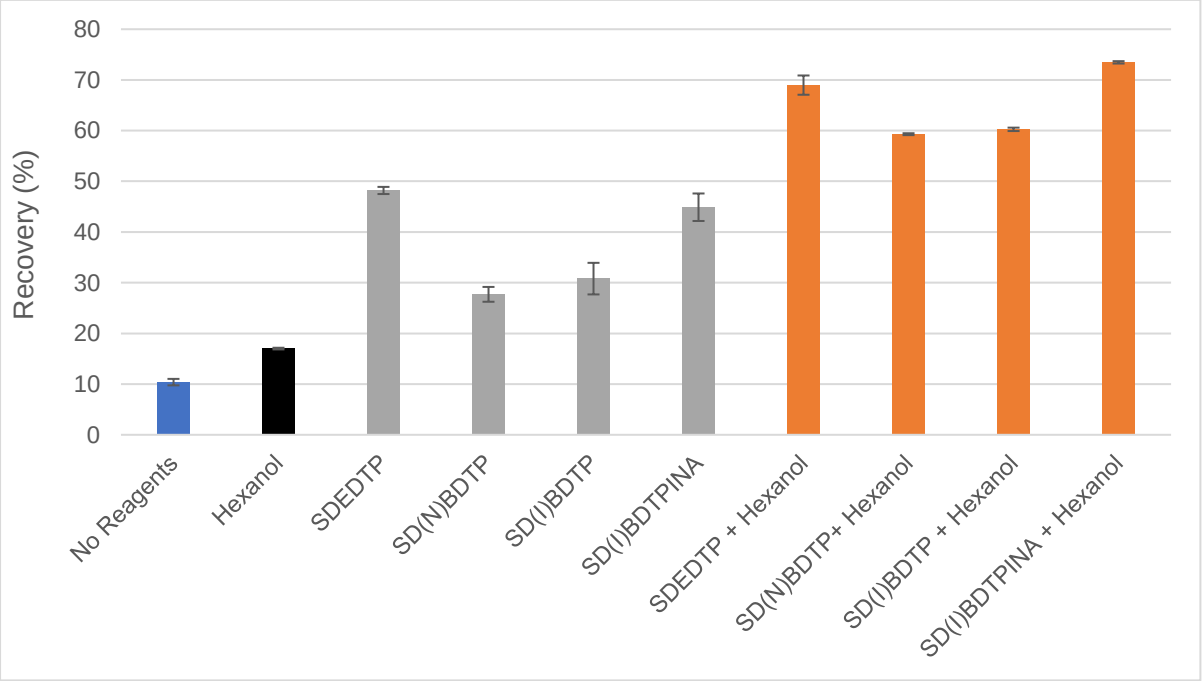

Figure 4.9: Recovery of chalcocite in the first two minutes of flotation at pH 9 using longer chain length DTP collectors and DTP-frother mixtures. Collectors are dosed at 20% monolayer coverage and the frother is dosed so that the concentration is just above the CCC.

Using these collectors in the presence of hexanol produced recoveries of between 60 and 70%, with SDEDTP and SD(I)BDTPINA producing the highest recoveries. This could follow from the fact that these two collectors produced the highest recoveries when comparing the recoveries without the presence of hexanol.

Table 4.9 compares the mass recovery of the reagent mixture to the calculated sum contribution of each reagent.

Table 4.9: Mass recovery of chalcocite in the microflotation cell for mixtures of DTPs with hexanol compared to the sum contribution of each reagent (collector and hexanol). ML = monolayer

	SDEDTP + Hexanol	SD(N)BDTP+ Hexanol	SD(I)BDTP + Hexanol
% Mass recovery of reagent mixture	69.0	59.3	60.3
Calculated sum contribution of each reagent	54.8	34.3	37.4
Difference	14.2	25.0	22.8

All the mixtures of DTP's with hexanol synergistically improved recoveries according to Table 4.9. The longer chain length DTPs exhibited a greater difference showing that there is a stronger synergistic improvement in recovery for these chain lengths.

Similarly to the DTP's, microflotation tests were performed on chalcocite with longer chain length xanthates, and xanthate-hexanol mixtures, as illustrated in Figure 4.10. In this case, increasing the alkyl chain length of the xanthate improved the recovery, with the recovery increasing from 27.3% for SEX to 45.8% for PNBX (straight chain butyl xanthate). Ackerman et al (1987) found that the straight chain xanthate outperforms the branched chain xanthate, and in this case PNBX only slightly outperforms SIBX (branched chain butyl xanthate), but it could be argued that these differences are within experimental error.

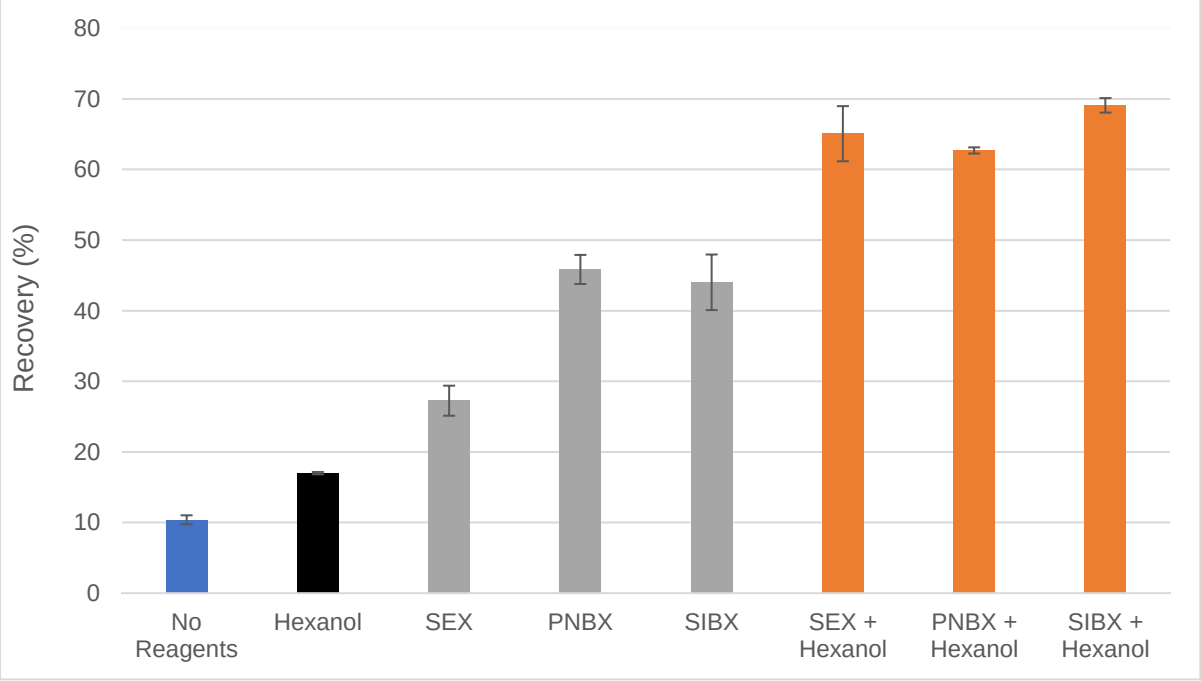

Figure 4.10: Recovery of chalcocite in the first two minutes of flotation at pH 9 using longer chain length xanthate collectors and xanthate-frother mixtures. Collectors are dosed at 20% monolayer coverage and the frother is dosed so that the concentration is just above the CCC.

Corresponding to the results of DTP's, the mixtures of xanthates with hexanol yielded recoveries of between 60 – 70%, even though there was a significant difference between the recovery for SEX compared to PNBX and SIBX, without the presence of hexanol.

Table 4.10 compares the mass recovery of the reagent mixture to the calculated sum contribution of each reagent for xanthates with hexanol. All the mixtures of xanthates with hexanol synergistically improved the recovery. In this case the shorter ethyl chain length xanthate showed the greatest difference compared to the longer chain lengths n-butyl and iso-butyl xanthates.

Table 4.10: Mass recovery of chalcocite in the microflotation cell for mixtures of xanthates with hexanol compared to the sum contribution of each reagent (collector and hexanol). ML = monolayer

	SEX + Hexanol	PNBX + Hexanol	SIBX + Hexanol
% Mass recovery of reagent mixture	65.1	62.7	69.1
Calculated weighted sum contribution of each reagent	33.9	52.5	50.6
Difference	31.2	10.2	18.4

4.2.4.2 Microflotation recoveries in the presence of other frothers

Microflotation tests were conducted with mixtures of DTP and other frothers - PPG425 and octanol. Figure 4.11 illustrates the recoveries for these DTP-frother mixtures. The concentrations of all the frothers were dosed at their CCC. PPG425 was dosed at 0.014 mM, octanol was dosed at 0.062 mM, and hexanol was dosed at 0.12 mM (Zhang et al., 2012). Using hexanol, PPG and octanol individually, recoveries of 17.0%, 15.4% and 13.0% were obtained, as illustrated in Figure 4.11. This indicates that these reagents did not significantly improve the recovery of chalcocite, since the natural floatability of chalcocite was 10.4%.

Subsequent tests were performed with SDEDTP and SD(N)BDTP, together with each of the frothers. The SDEDTP-hexanol mixture produced the highest recovery of 69.0%. For the SDEDTP-PPG425 and SDEDTP-octanol mixtures the recovery was 55.1% and 55.7%, respectively.

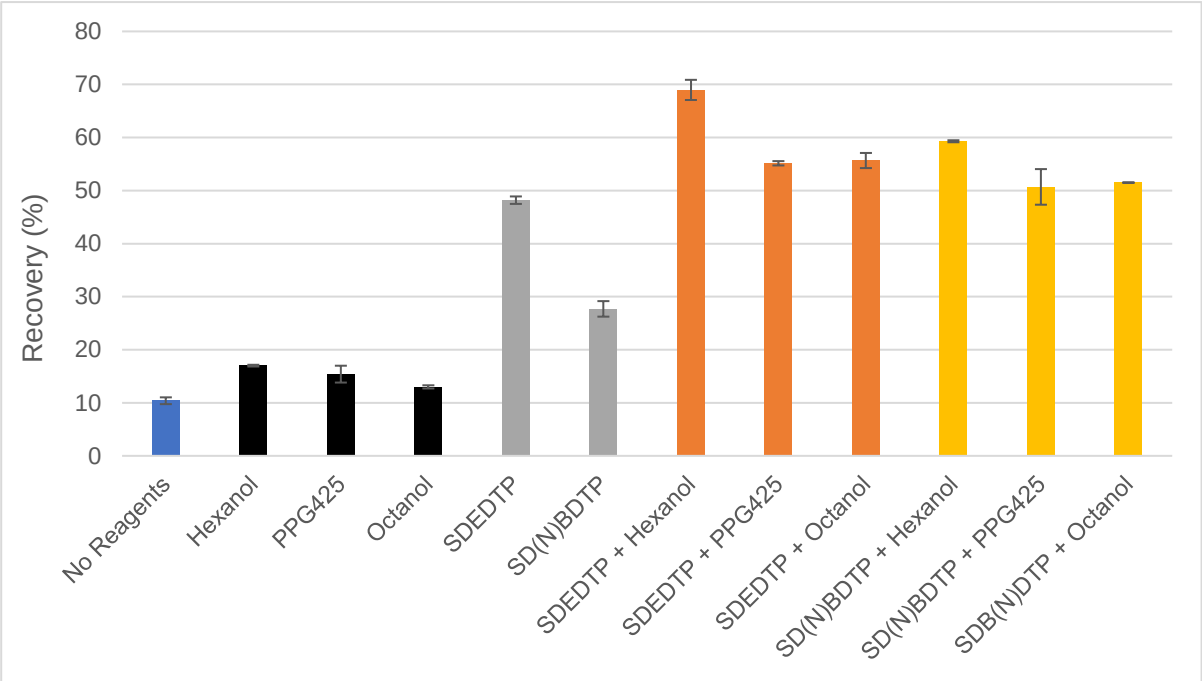

Figure 4.11: Recovery of chalcocite in the first two minutes of flotation at pH 9 using various frothers and DTP-frother mixtures. Collectors are dosed at 20% monolayer coverage and the frothers are dosed so that the concentration is just above the CCC.

Table 4.11: Mass recovery of chalcocite in the microflotation cell for mixtures of DTPs with frothers compared to the sum contribution of each reagent (collector and hexanol). ML = monolayer

	SDEDTP + Hexanol	SDEDTP + PPG425	SDEDTP + Octanol	SD(N)BDTP + Hexanol	SD(N)BDTP + PPG425	SDB(N)DTP + Octanol
% Mass recovery using reagent mixture	69.0	55.1	55.7	59.3	50.7	51.5
Calculated sum contribution of each reagent	54.8	53.2	50.8	34.3	32.7	30.3
Difference	14.2	1.9	4.9	25.0	18.0	21.2

Table 4.11 compares the mass recovery of the reagent mixture to the calculated sum contribution of each reagent. Table 4.11 shows that all the mixtures of SD(N)BDTP and frothers resulted in significant improvements in recovery compared to the mixtures of SDEDTP and frothers. SD(N)BDTP with the straight chain hexanol and octanol exhibited the greatest improvements.

Mixtures of SDEDTP with PPG425 and Octanol did not show a significant synergistic improvement according to Table 4.11, but significant improvements were observed for SDEDTP and hexanol.

Hexanol performed the best for both the cases where SDEDTP and SD(N)BDTP is present. The CCC of hexanol is much higher than that of PPG425 and octanol which indicates that the concentration of the frother may have an effect on the strength of the synergistic mechanism between collectors and frothers.

4.2.5 Quartz

From Figure 4.1 it was illustrated that for galena at pH 9, SDEDTP mixed with hexanol substantially improves the kinetics compared to the baseline, with only hexanol. McFadzean & O'Connor (2014) showed with UV-Vis spectrophotometry and ITC that SDEDTP does not interact or adsorb onto the surface of galena at pH 9. Subsequently, it has been shown that SDEDTP is active at the air-water interface (Jordaan, 2018; Dai, Bradshaw & Harris, 2002, Pienaar et al., 2019). With this in mind further tests were performed on hydrophobized quartz. It was hypothesized that if the mixture of SDEDTP and hexanol is active at the air-water interface, and this interaction at the air-water interface leads to the improved kinetics observed for galena, it can do something similar for quartz, since it is well established that thiol collectors do not adsorb onto oxide minerals (Nagaraj & Brinen, 1996).

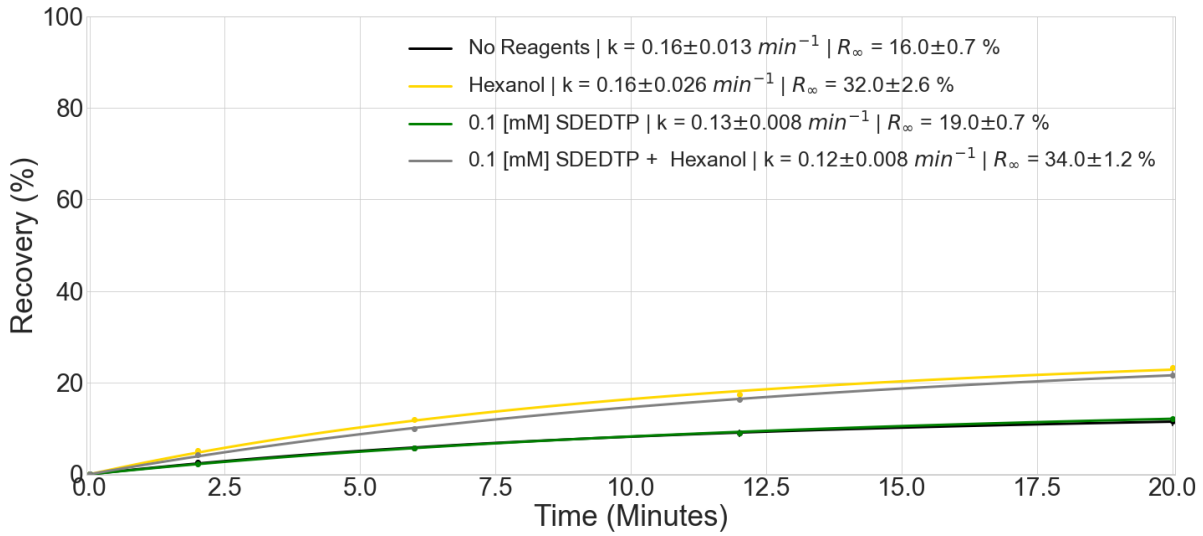

Figure 4.12: The recovery of quartz as a function of time at pH 9 using single reagents and reagents mixtures. Frother is dosed so that the concentration is just above the CCC.

Figure 4.12 shows the recovery of quartz at pH 9 as a function of time. The higher dosage of 0.1mM SDEDTP that was used for pyrite was also used in this experiment. From Table 4.12 it can be seen that the SDEDTP and SDEDTP-hexanol mixture had a minimal effect on the recovery of quartz, compared to the baseline natural floatability and the recovery where only hexanol is present. The first-order rate constant for the mixture was slightly lower than that of hexanol. The fact that the mixture had a minimal effect on recovery and kinetics may indicate that in order for the synergistic mechanism between SDEDTP and hexanol to occur, the

collectors need to be able to somehow interact with the mineral surface and that the presence of the collector and frother at the air-water interface does not have an effect on the mineral recovery.

Table 4.12: Final microflotation recoveries for quartz at pH 9 and fitted parameters for Klimpel equation parameters determined for single reagents and reagent mixtures.

	No Reagents	**Hexanol**	**0.1 [mM] SDEDTP**	**0.1 [mM] SDEDTP + Hexanol**
Final microflotation recovery (%)	11.6 ±1.0	23.3 ±0.4	12.2 ±0.1	21.7 ±0.8
Model	**Klimpel**			
k - First order rate constant (min^{-1})	0.16 ±0.013	0.16 ±0.026	0.13 ±0.008	0.12 ±0.008
R_∞ (%)	16.5 ±0.7	32.4 ±2.6	19.0 ±0.7	34.2 ±1.2
Residual	0.12	0.36	0.06	0.17

4.2.6 Microflotation summary

Table 4.13 summarizes the microflotation outcomes for galena, pyrite, chalcopyrite and chalcocite. The effect of the DTP-hexanol mixture on galena, pyrite and chalcocite is strong, exhibiting large improvements in mineral recovery or first-order kinetics. For chalcopyrite the reagent mixture did not have as strong of an effect.

Xanthate-hexanol mixtures only showed a synergistic response for chalcopyrite and chalcocite, where the extent of this response was much stronger on chalcocite.

Table 4.13: Summary of microflotation outcomes

	Extent of synergistic response to DTP-hexanol	Extent of synergistic response to xanthate-hexanol
Galena	Large	None
Pyrite	Large (at higher DTP dosages)	None
Chalcopyrite	Small	Small
Chalcocite	Large	Large

Tests performed with longer chain length collectors on chalcocite showed that for DTP, increasing the chain length increased the extent of the synergistic response with hexanol, but when the dosage of ethyl DTP was lowered from 20% monolayer dosage to 10% the extent of synergistic response was equivalent to that of the longer chain lengths with hexanol. For xanthate with hexanol, the ethyl chain length gave the strongest synergistic response.

Tests performed with other frothers showed that hexanol performed better than PPG425 and octanol. This was attributed to the concentration of the frother used. As the frothers were dosed at their CCC the concentration of hexanol was the greatest.

Quartz showed no synergistic response when using the SDEDTP-hexanol mixture which indicates that the presence of the SDEDTP and hexanol at the air-water interface does not have an effect on the recovery of the mineral.

4.3 Automated contact time apparatus

The microflotation tests incorporate all the subprocesses of bubble-particle attachment, viz. collision, attachment and detachment probabilities. Frothers may have an impact on bubble size and bubble rise velocity, which would affect the collision by changing the relative velocities between the bubble and the particle. Furthermore, smaller bubbles decrease the induction time of the attachment subprocess of bubble-particle attachment. A Glembotsky device can decouple the collision and attachment subprocesses and control the bubble size to investigate the effect of collectors and frothers on the bubble-particle attachment subprocess.

The automated contact time apparatus developed by Aspiala, Schreithofer & Serna-Guerrero (2018) was used to decouple the effects that frothers have on the collision process, by controlling the bubble size, the approach/recede velocity, and the contact time for bubble particle attachment. This can give an insight into whether the interaction between DTP and frothers is truly synergistic or if each of these molecules is playing a separate role at different interfaces.

4.3.1 Galena

Figure 4.13 shows the attachment probability and mass recovery results for galena at pH 9, with different reagents. As galena is naturally hydrophobic and the recoveries attained in the microflotation cell were ±90% (Figure 4.1), the contact time was set to 20ms which is the shortest contact time that the device was able to attain.

The attachment probability is the ratio of the bubbles with particles attached to them to the number of bubbles that could result in a bubble-particle attachment. The attachment probability is dependent on the operational parameters of the device, such as the contact time,

approach/recede velocity, bubble size, and the pressure of the bubble onto the particle bed. These parameters were kept constant, so the effect of the chemical environment is the only variable parameter that could influence attachment probability.

The number of bubbles that could result in a bubble particle attachment were filtered according to the bubble size. Bubble size was set to 1.77 mm. A squeeze parameter was set to be 0.1 mm, which means that instead of just touching the particle bed the bubble overlaps the touching point by 0.1 mm. The minimum bubble size that could result in bubble-particle attachment was set to be 1.6 mm, so a gap of 70 µm would exist between the bubble and the particle at this size. The upper limit for bubble size was set to 1.9 mm, as anything greater than this would result in bubble-particle attachment probability improving due to the squeezing of the bubble onto the particle bed.

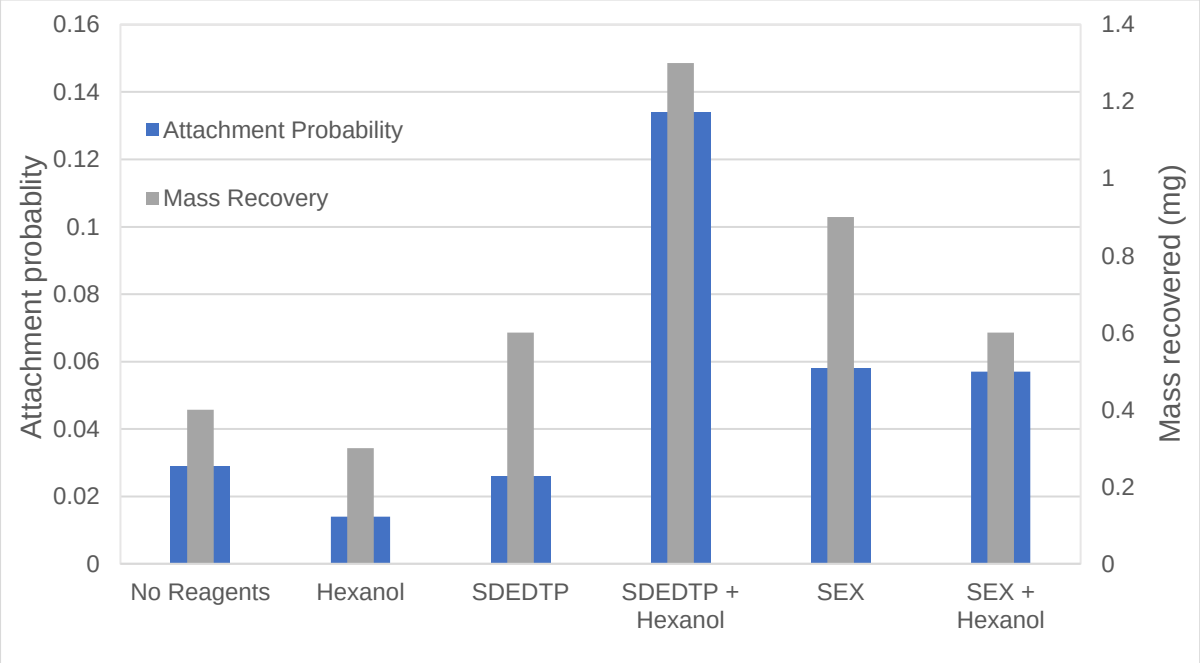

Figure 4.13: Bubble-particle attachment probability and mass recovery of galena (pH9), under various reagent environments. Collectors are dosed at 50% monolayer coverage and the frother is dosed so that the concentration is just above the CCC. (Contact time = 20 ms)

The particles that were attached to bubbles were deposited in a bin and were then collected and weighed. Most of the masses recorded were less than 1 mg and since the lab balance only had a sensitivity of 1 mg these results were not used for the primary analysis. Attachment probability data from images was used to analyze the data.

Table 4.14 presents a summary of the attachment probability, mass recovered, and bubble size data as presented in Figure 4.13. The bubble sizes were between 1.77 and 1.80 mm, with a standard deviation of 0.05 mm. The number of viable bubbles produced in each experiment was greater than 339, which gives a statistically significant sample.

Table 4.14: Summary of ACTA data for galena at pH 9.

	No Reagents	Hexanol	SDEDTP	SDEDTP + Hexanol	SEX	SEX + Hexanol
Attachment probability	0.029	0.014	0.026	0.134	0.058	0.057
Mass recovery (mg)	0.4	0.3	0.6	1.3	0.9	0.6
Number of bubbles	339	355	391	380	386	396
Mean bubble size (mm)	1.773	1.776	1.803	1.794	1.800	1.809
Standard deviation (mm)	0.053	0.054	0.050	0.048	0.047	0.049

Compared to the attachment probability of the condition with no reagents, hexanol roughly halved the attachment probability from 2.9% to 1.4%. This is contrary to the microflotation results in Figure 4.1, where hexanol improved the kinetics of galena flotation 4-fold compared to the natural floatability. This may point to other effects that the frother has on the bubble, such as decreasing the bubble rise velocity, increasing the sliding contact time between the bubble and the particle, or decreasing bubble size and improving attachment kinetics in the microflotation cell.

SDEDTP had no effect on the attachment probability which aligns with both the microflotation results and the adsorption tests where it was found that SDEDTP did not improve the recovery of galena and did not adsorb onto the surface.

The mixture of SDEDTP and hexanol results in a 5-fold improvement in the attachment probability for hexanol. This clearly illustrates that the mixture of SDEDTP and hexanol appears to result in a synergistic improvement in bubble-particle attachment probability, and also synergistically improves flotation recovery (Figure 4.1). Coupling this result with the fact that SDEDTP does not interact with galena as observed in microcalorimetry studies (McFadzean & O'Connor, 2014; Taguta, O'Connor & McFadzean, 2017) indicates that, since SDEDTP does not interact with the mineral surface, it may be interacting with hexanol at the air-water interface.

Figure 4.13 shows that the addition of SEX improves the attachment probability from 0.029 for no reagents to 0.058. This indicates that SEX improved the surface hydrophobicity of galena, but this was not observed in microflotation tests (Figure 4.1). For the mixture of SEX and hexanol there was virtually no change in the attachment probability, indicating that there is no interaction for SEX and hexanol on galena. Interestingly for the mixture of SEX and hexanol, the microflotation results (Figure 4.1) showed an antagonistic response, which lowered the first order kinetics compared to hexanol as the baseline case.

4.3.2 Pyrite

Figure 4.14 shows the attachment probability for pyrite at pH 9. The contact time for these experiments were set to 100ms, as this was the contact time where some particles started to attach to the bubbles for the “no reagent” condition of pyrite. Mass recoveries were not recorded for pyrite, so only the attachment probabilities were used for analysis.

Table 4.15 shows the attachment probability, the bubble size, and the reproducibility of the pyrite experiments. The same bubble squeeze, bubble size and bubble size bounds were used as in the galena experiments. The bubble size varied between 1.74 and 1.80 mm, with a standard deviation of less than 0.05 mm.

The standard deviation of the attachment probabilities for no reagents and hexanol conditions were 0.0005 and 0.0055, respectively. This shows that there was a high level of reproducibility.

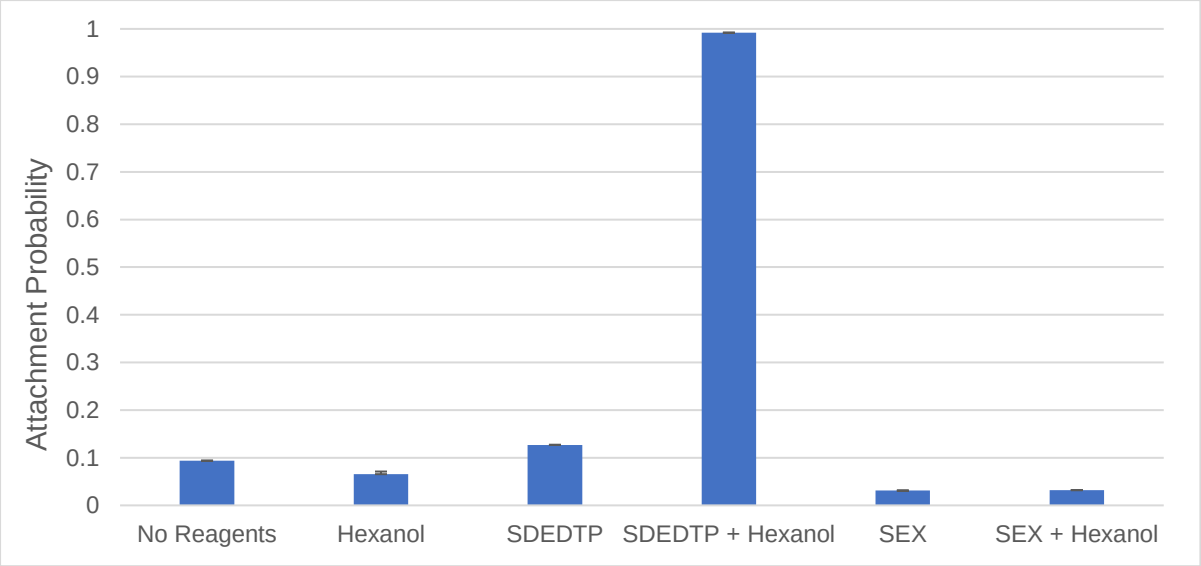

Figure 4.14: Bubble-particle attachment probability of pyrite (pH9), under various reagent environments. Collectors are dosed at 50% monolayer coverage and the frother is dosed so that the concentration is just above the CCC. (Contact time = 100 ms)

Similarly to the galena ACTA data, the presence of hexanol lowered the attachment probability compared to the “no reagents” condition from 0.094 to 0.066. This is contrary to the microflotation results in Figure 4.2 where hexanol improved the recovery of pyrite. The addition of SDEDTP to the mineral improved the attachment probability from 0.094 to 0.127, indicating that there was a slight increase in surface hydrophobicity showing that SDEDTP is present on the mineral surface, but in the microflotation tests (Figure 4.2) SDEDTP lowered the recovery of pyrite. SEX also lowered the recovery in the microflotation tests, but this coincides with ACTA data as the attachment probability is lowered to 0.031. ‘

Table 4.15: Summary of ACTA data for pyrite at pH 9.

	No Reagents		Hexanol		SDEDTP	SDEDTP + Hexanol	SEX	SEX + Hexanol
Repeats	1	2	1	2				
Attachment Probability	0.094	0.093	0.071	0.06	0.127	0.991	0.031	0.032
Number of bubbles	365	388	368	381	386	389	393	386
Mean bubble size (mm)	1.785	1.785	1.788	1.799	1.779	1.779	1.744	1.743
Standard Deviation (mm)	0.048	0.05	0.056	0.057	0.052	0.048	0.035	0.031

The mixture of SDEDTP and hexanol produced a strong synergistic response, increasing the attachment probability from 0.127 for SDEDTP on its own, to 0.991.

Figure 4.15 shows the bubble images from the ACTA and the particle coverage on them. The condition of SDEDTP on its own only showed single particles on bubbles, whereas the condition with SDEDTP mixed with hexanol showed the bubbles were covered with multiple particles. This shows the extent to which the mixture synergistically enhanced bubble-particle attachment.

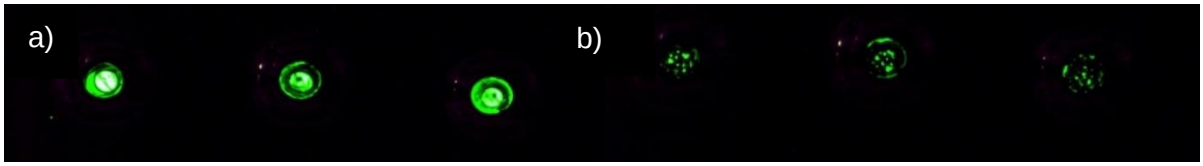

Figure 4.15: Bubble particle coverage for a) SDEDTP and b) SDEDTP and hexanol

The microflotation results in Figure 4.2, which used the same dosage for SDEDTP (calculated by the collector coverage of the mineral surface), did not produce any synergistic effect in the presence of hexanol whereas the ACTA results show 10 times increase in attachment probability for the reagent mixture. This can be explained in terms of the solution concentration. The mass percent solids used in the ACTA is much higher than in the microflotation cell, around 12.3% vs 1.2%. Since the collector is dosed on a surface area basis, this results in a much higher liquid concentration of SDEDTP, assuming that not all of the collector adsorbs onto the mineral surface. In effect the liquid concentration, assuming no SDEDTP adsorbs on the pyrite surface, is around an order of magnitude greater in the ACTA tests than in the microflotation cell. This SDEDTP in the pulp can adsorb at the air-water interface which may lead to the improvement observed when using a higher dosage for the microflotation results in Figure 4.3, when a 0.1 mM dosage of SDEDTP was used. This

indicates that to achieve synergistic interactions between SDEDTP and frother for pyrite, the SDEDTP should be dosed in terms of its liquid concentration rather that solid concentration.

4.3.3 Chalcopyrite

Figure 4.16 shows the mass of chalcopyrite recovered at pH 9. The contact time was set to 20 ms, as this is the shortest contact time that the ACTA can achieve. All the attachment probabilities for each of the reagent conditions resulted in 100% attachment probability so the mass recovery was used as the performance indicator.

Table 4.16 shows a summary of the mass recoveries, corrected mass recoveries and the bubble size data. The bubble sizes and bubble squeeze were set up the same as for previous experiments. As the mass recovery is used as a proxy for performance, the bubble size bounds could not be used as a filter, due to almost every bubble resulting in a bubble particle attachment. The bubble sizes were found to be between 1.75 mm and 1.78 mm, which is not a significant difference, with standard deviation in size being 0.05 mm.

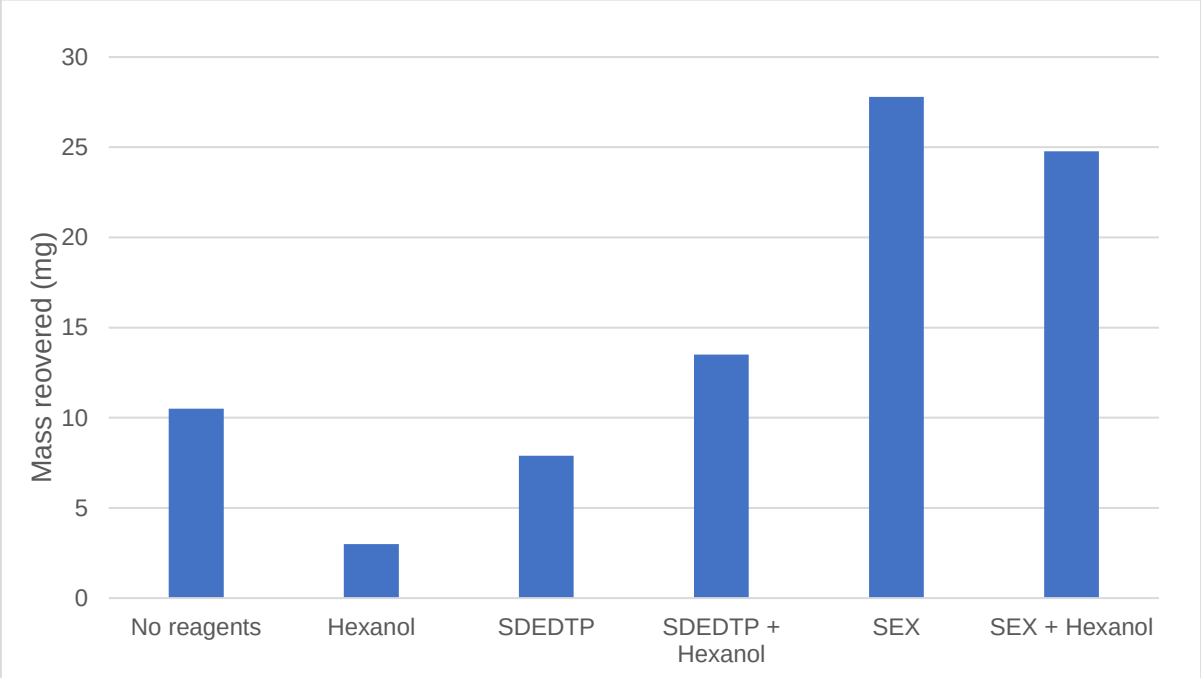

Figure 4.16: Mass recovery and corrected mass recovery of chalcopyrite (pH9), under various reagent environments. Collectors are dosed at 50% monolayer coverage and the frother is dosed so that the concentration is just above the CCC. (Contact time = 20 ms)

During the SDEDTP-hexanol and SEX-hexanol experiments, one of the needles could not produce bubbles and so the number of bubbles produced in those experiments were less than in other tests. This resulted in lower recoveries under these conditions. Therefore, the mass recovered was normalized according to the number of bubbles, and the mass recovered was recalculated for 396 bubble-particle attachment opportunities. The correlated data is labeled as corrected mass recovery (Table 4.16).

The addition of hexanol to chalcopyrite significantly lowered the mass recovered from 10.6 mg to 3.1 mg. Furthermore, the addition of SDEDTP also lowered the mass recovery from 10.6 mg to 7.9 mg. In the microflotation experiments (Figure 4.6) the opposite trend was seen for these reagents, where hexanol improved the first-order kinetics by 3-fold and SDEDTP showed slight improvement. SEX proved to be a strong collector for chalcopyrite, increasing the mass recovery to 28.6 mg, coinciding with the results from microflotation.

Table 4.16: Summary of ACTA data for chalcopyrite at pH 9.

	No reagents	Hexanol	SDEDTP	SDEDTP + Hexanol	SEX	SEX + Hexanol
Mass recovery (mg)	10.5	3.0	7.9	13.5	27.8	24.8
Corrected mass recovery (mg)	10.6	3.1	7.9	15.1	28.6	27.9
Number of bubbles	391	384	396	355	385	351
Mean bubble size (mm)	1.761	1.780	1.759	1.767	1.761	1.753
Standard deviation (mm)	0.045	0.040	0.039	0.041	0.042	0.045

The mixture of SDEDTP and hexanol showed a small synergistic improvement in recovery, improving the recovery from 10.6 mg for no reagents to 15.1 mg for the mixture. The calculated additive effect of hexanol and SDEDTP is 11.0 mg. This is still not as much of an improvement as that observed for SEX on its own which gave 13 mg higher recovery than the mixture of SDEDTP and hexanol. When correcting the mass recovery, the addition of hexanol to SEX did not produce any significant improvement in recovery. This was also observed for the attachment probabilities for galena and pyrite.

4.3.4 Chalcocite

Figure 4.17 shows the mass recovery of chalcocite at pH 9. The contact time was set to 50 ms. Table 4.17 summarizes the attachment probability, mass recovery and bubble size data for chalcocite at each reagent condition.

When collectors were present the attachment probabilities were 100%, so the mass recovered was used as a proxy for these conditions. For the “no reagent” and hexanol condition the attachment probabilities could be determined. Two bubble sets are reported for these conditions. The first set corresponds to the attachment probability, where the upper and lower bounds of bubble sizes have been applied, and the second set corresponds to the mass recovery which includes all the bubbles, similar to the approach with chalcopyrite. The bubble sizes ranged from 1.73 mm to 1.76 mm with a standard deviation of around 0.05 mm.

From Table 4.17 it can be seen that, in common with all the other minerals the addition of hexanol lowered the attachment probability from 0.118 with no reagents to 0.062. The microflotation results in Figure 4.7 show the opposite result, where the mass recovery of chalcocite was improved upon the addition of hexanol.

From Figure 4.17 it can be seen that the addition of SDEDTP and SEX improved the recovery in the ACTA, which was also observed in the microflotation cell. SDEDTP improved the recovery to a much greater extent in the microflotation cell when compared to SEX (almost doubling the recovery), whereas in the ACTA the improvement in recovery of SDEDTP over SEX is only around 16%.

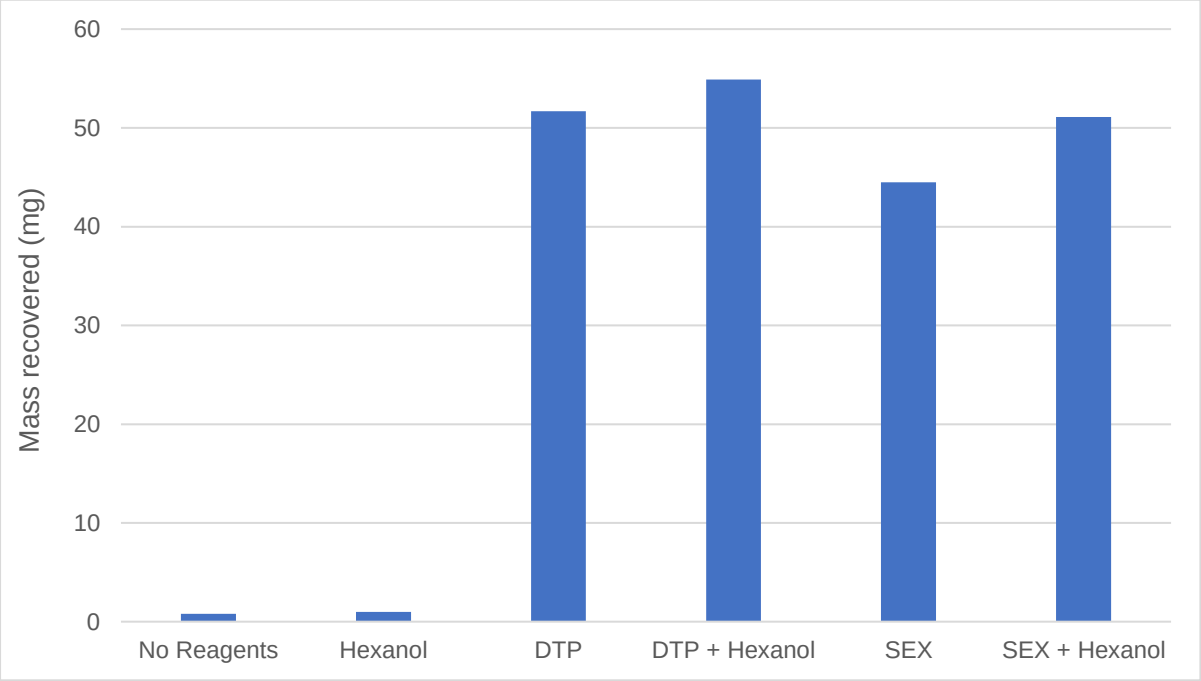

Figure 4.17: Mass recovery of chalcocite (pH9), under various reagent environments. Collectors are dosed at 50% monolayer coverage and the frother is dosed so that the concentration is just above the CCC. (Contact time = 50 ms)

The mixtures of SDEDTP-hexanol, and SEX-hexanol both resulted in improved recoveries. The addition of hexanol resulted in a 6% increase in recovery for SDEDTP, and 15% increase in recovery for SEX. This indicates that the interaction between collectors and frothers are mineral specific. So far SDEDTP and hexanol have interacted synergistically on galena, pyrite and chalcopyrite, where SEX has shown no interaction. On chalcocite, SEX seems to interact synergistically with hexanol, and also to a greater extent than SDEDTP did.

Table 4.17: Summary of ACTA data for chalcocite at pH 9.

	No Reagents	Hexanol	SDEDTP	SDEDTP + Hexanol	SEX	SEX + Hexanol
Mass recovery	0.8	1	51.7	54.9	44.5	51.1
Attachment probability	0.118	0.062	N/A	N/A	N/A	N/A
Number of bubbles	364 / 381	389 / 389	389	393	392	381
Mean bubble size (mm)	1.740/ 1.732	1.758/ 1.758	1.747	1.737	1.736	1.742
Standard deviation (mm)	0.034/ 0.050	0.033/ 0.033	0.037	0.041	0.055	0.050

So far it has been shown that SDEDTP-hexanol mixtures synergistically improve bubble-particle attachment probability for all minerals in this study. For SEX-hexanol mixtures an improvement is only observed with the chalcocite mineral.

4.3.5 Summary ACTA results

Table 4.18 shows the summary of the ACTA outcomes for DTP-hexanol and xanthate-hexanol mixtures. The DTP-hexanol mixture showed a synergistic improvement in bubble-particle attachment for all the minerals in this study.

Table 4.18: Summary of ACTA outcomes

	Extent of synergistic response to DTP-hexanol	Extent of synergistic response to xanthate-hexanol
Galena	Large	None
Pyrite	Large	None
Chalcopyrite	Small	None
Chalcocite	Small	Small

For the xanthate-hexanol mixture a synergistic improvement is only observed for chalcocite. Improvements observed for chalcopyrite in the microflotation results are not observed here. This difference could be attributed to the collector and frother having separate effects on mineral recovery.

4.4 Collector interactions at the mineral-water interface

The extent of surface coverage of collector on the mineral surface and the species that form on the mineral surface can be key indicators in determining whether the collector is increasing hydrophobicity on the mineral surface, and thus improving the floatability of the mineral. The adsorption of collectors onto the mineral surface is influenced by the pulp pH. At high pulp pH the formation of metal hydroxide species on the mineral surface can lower the amount of available adsorption sites, which inhibits the adsorption of the collector. This has been observed for DTP on various sulphide minerals (Petrus et al., 2011: Grano et al., 1997; McFadzean & O'Connor, 2014).

UV-Vis spectrophotometry was used to determine the extent of adsorption of SDEDTP and SEX on the mineral surface by determining the residual concentration in the aqueous phase in order to ascertain if the presence of frother had any effect on the extent of collector adsorption. This was done by measuring the residual concentration of collector in the supernatant, after contact with the mineral. It was assumed that the reduced amount of collector in the supernatant, after contact with the mineral, was adsorbed onto the mineral surface.

Isothermal titration calorimetry (ITC) was used to determine the interaction energy, viz. enthalpy of adsorption, of the collector at the mineral-water interface.

4.4.1 Galena

Table 4.19 shows the molar percentage of collector adsorbing onto the galena mineral surface at pH 9. Collectors were dosed to cover ~50% of the mineral surface to match the microflotation experimental dosages. All of the SEX adsorbed onto the mineral surface and the presence of hexanol did not have an effect on the extent of adsorption of the collector. Interestingly, even though all the SEX adsorbs onto the mineral surface, it did not improve the hydrophobicity of the mineral as was seen in Table 4.1, where the first order rate for SEX with galena did not improve compared to the natural floatability.

On the other hand, none of the SDEDTP adsorbs onto the mineral surface, and similarly to SEX, the presence of hexanol had no effect. This aligns with the results of McFadzean & O'Connor (2014) where it was found that negligible amounts of SDEDTP adsorbed onto the galena surface at pH 9.

Table 4.19: The mole percent of SDEDTP and SEX adsorbed onto galena at pH 9, with or without hexanol present. Collectors were dosed to cover 50% of the mineral surface, and the frother was dosed at the CCC.

	SEX	SEX + Hexanol	SDEDTP	SDEDTP + Hexanol
Collector adsorbed on galena (%)	96.4 ± 0.08	96.4 ± 0.05	~0	1.4 ± 0.89
Monolayer coverage (%)	48.2 ± 0.04	48.2 ± 0.03	~0	0.7 ± 0.45

ITC was performed on galena at pH 9, where a ~50% monolayer dosage was titrated into a slurry of galena with and without the presence of hexanol. Figure 4.18 illustrates the heat of interaction per 50% monolayer injection. The first injection without hexanol produced an enthalpy of -11.7 kJ/mol, with subsequent injections producing heats of -5 kJ/mol or less. This is a higher heat of interaction than was found by McFadzean & O'Connor (2014) and Taguta, O'Connor & McFadzean (2017), where it was found that when the heat of dilution of SDEDTP was subtracted from the heat of titration of SDEDTP onto galena the heat of interaction was found to be ~0 kJ/mol.

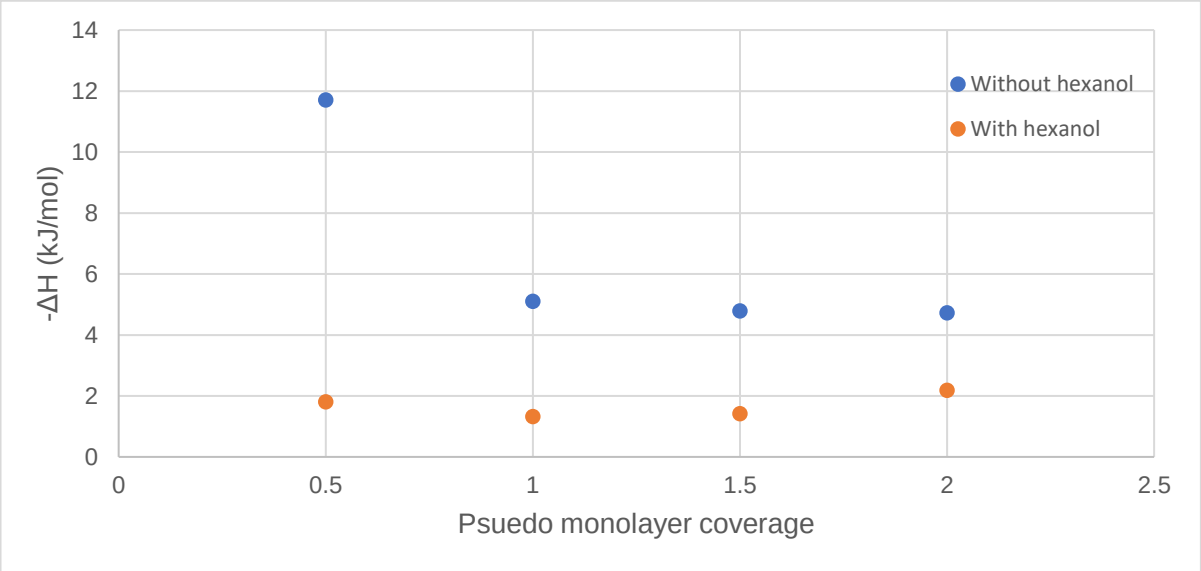

Figure 4.18: The enthalpy of SDEDTP adsorption onto galena at pH 9 in the presence of hexanol and without hexanol as a function of surface area coverage.

The enthalpy of adsorption of SDEDTP with galena in the presence of hexanol was -1.8 kJ/mol. Compared to the enthalpy of adsorption without hexanol, the enthalpy of adsorption with hexanol showed that the presence of hexanol did not improve the interaction energy of SDEDTP with galena but lowered it.

The enthalpy of adsorption of -11.7 kJ/mol for SDEDTP is still relatively low compared to the -35.9 kJ/mol found for SEX onto galena at pH 9.2 (Taguta, 2015). However, the UV-Vis adsorption results from Table 4.19, where no adsorption for SDEDTP was observed, does not correlate with ITC results, where an interaction can be observed. It was noted that the galena had a buffering effect on the pH, lowering the pH. The time scales of the ITC experiments (which happen over hours), compared to the UV-Vis experiments (which occur within minutes) may cause the pH to drop significantly and some of the SDEDTP can adsorb onto the mineral surface. This could explain the discrepancy within the results.

Furthermore, the heat of dilution of SDEDTP into water was found to be 0.56 kJ/mol whereas Taguta (2015) found that the heat of dilution for SDEDTP was 5.7 kJ/mol. This discrepancy might be due to the SDEDTP used in this study was specially purified to remove any other contaminants, whereas in the Taguta (2015) study, Senkol 3 was used which is the commercial version of the reagent. This discrepancy with the heat of dilution might also explain the differences with the results between the two datasets.

4.4.2 Pyrite

Table 4.20 shows the mole percent of SDEDTP and SEX that adsorbed onto pyrite at pH 9, and the effect of hexanol on the extent of the adsorption of these collectors. Similar to the adsorption of SEX onto galena, most of the SEX adsorbed onto the surface of pyrite. Even though SEX adsorbs onto pyrite the microflotation results in Figure 4.2 illustrate that SEX did not improve the recovery of pyrite. The presence of hexanol did not have any significant effect on the extent of SEX adsorption.

Table 4.20: The mole percent of SDEDTP and SEX adsorbed onto pyrite at pH 9, with or without hexanol present. Collectors were dosed to cover 50% of the mineral surface, and the frother was dosed at the CCC.

	SEX	SEX + Hexanol	SDEDTP	SDEDTP + Hexanol
Collector adsorbed on pyrite (%)	88.2 ± 2.21	86.4 ± 2.10	69.3 ± 2.35	41.61 ± 0.92
Monolayer coverage (%)	44.1 ± 1.11	43.2 ± 1.05	34.65 ± 1.18	20.81 ± 0.46

For pyrite, SDEDTP exhibits significant adsorption onto the mineral, with 69.3% of the 50% monolayer dosage adsorbing onto the mineral surface, which translates to a coverage of 34.7%. The microflotation results for pyrite in Figure 4.2, illustrated that SDEDTP did not

significantly improve the recovery of pyrite, so it may be that the species of SDEDTP forming on the mineral surface do not induce hydrophobicity at the mineral surface. With electrochemical techniques Tadie (2015) confirmed that the SDEDTP did not form the dithiolate species on pyrite, so either the chemisorbed (DTP^-_{ads}) or metal thiolate (M-DTP) species is present on pyrite.

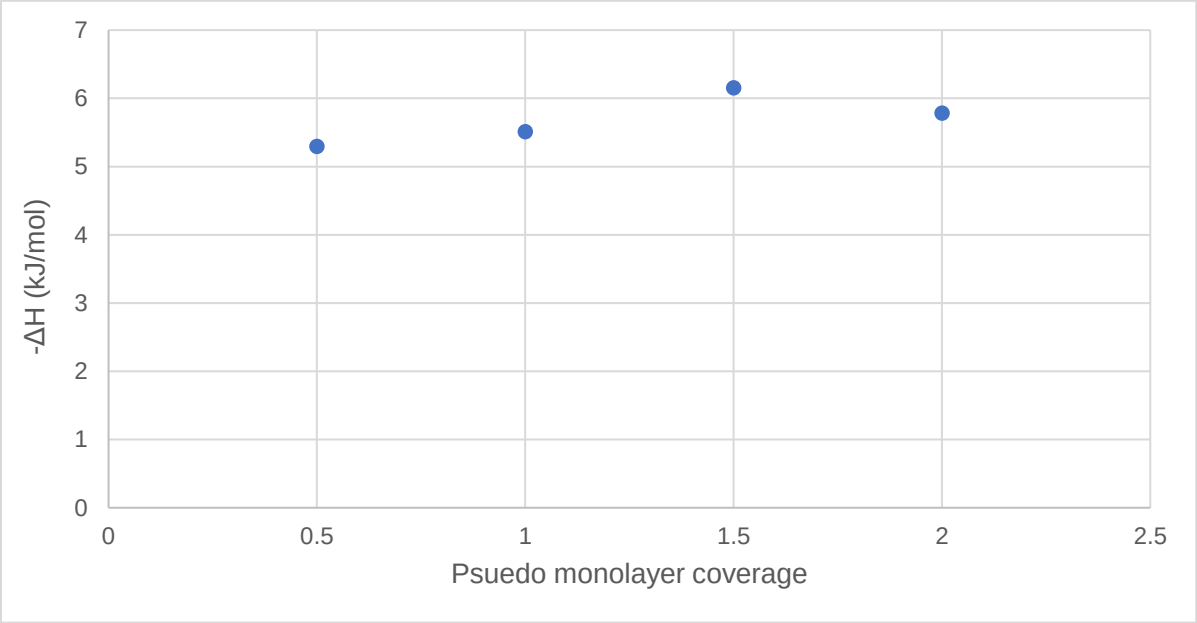

Figure 4.19: The enthalpy of SDEDTP adsorption onto pyrite at pH 9, as a function of surface area coverage

The adsorption of SDEDTP onto pyrite in the presence of hexanol showed significantly lower adsorption densities of SDEDTP, where only 41.6% of the dosage adsorbed onto the mineral, corresponding to a surface coverage of 20.8%. The microflotation results for pyrite in Figure 4.2 illustrated that the recovery using the SDEDTP-hexanol mixture (25.8%) was slightly less compared to the baseline results where only hexanol (27.5%) was used. The lower recovery may correspond to the lower adsorption densities in the presence of hexanol.

Figure 4.19 shows the enthalpy of adsorption for SDEDTP onto pyrite at pH 9. The enthalpy per 50% monolayer dosage varied between -5.3 to -6.1 kJ/mol, which is relatively low compared to the heat of interaction for SEX on pyrite at pH 9, which was determined by Taguta, O'Connor & McFadzean (2017) to be -57.1 kJ/mol. Taguta, O'Connor & McFadzean (2017) also performed a test for the adsorption of SDEDTP onto pyrite at pH 9 which gave a heat of interaction of -6.0 kJ/mol, and they also observed that SDEDTP did not significantly improve the recovery of pyrite in the microflotation cell.

4.4.3 Chalcopyrite

Table 4.21 shows the extent of adsorption of SEX and SDEDTP onto chalcopyrite at pH 9 and the effect of hexanol on the extent of adsorption. The majority of SEX adsorbed onto the mineral surface, and the presence of hexanol did not have much of an effect on the extent of the collector's adsorption. The presence of SEX on chalcopyrite's surface greatly improved the kinetics of chalcopyrite flotation as was observed in kinetic parameters in Table 4.6. The main species responsible for the hydrophobicity with SEX is the metal thiolate (Raju & Forsling, 1997).

Table 4.21: The mole percent of SDEDTP and SEX adsorbed onto chalcopyrite at pH 9, with or without hexanol present. Collectors were dosed to cover 50% of the mineral surface, and the frother was dosed at the CCC.

	SEX	SEX + Hexanol	SDEDTP	SDEDTP + Hexanol
Collector adsorbed on chalcopyrite (%)	74.6 ± 1.13	77.9 ± 0.55	71.2 ± 0.92	64.3 ± 0.54
Monolayer coverage (%)	37.3 ± 0.57	38.96 ± 0.28	35.6 ± 0.46	32.15 ± 0.27

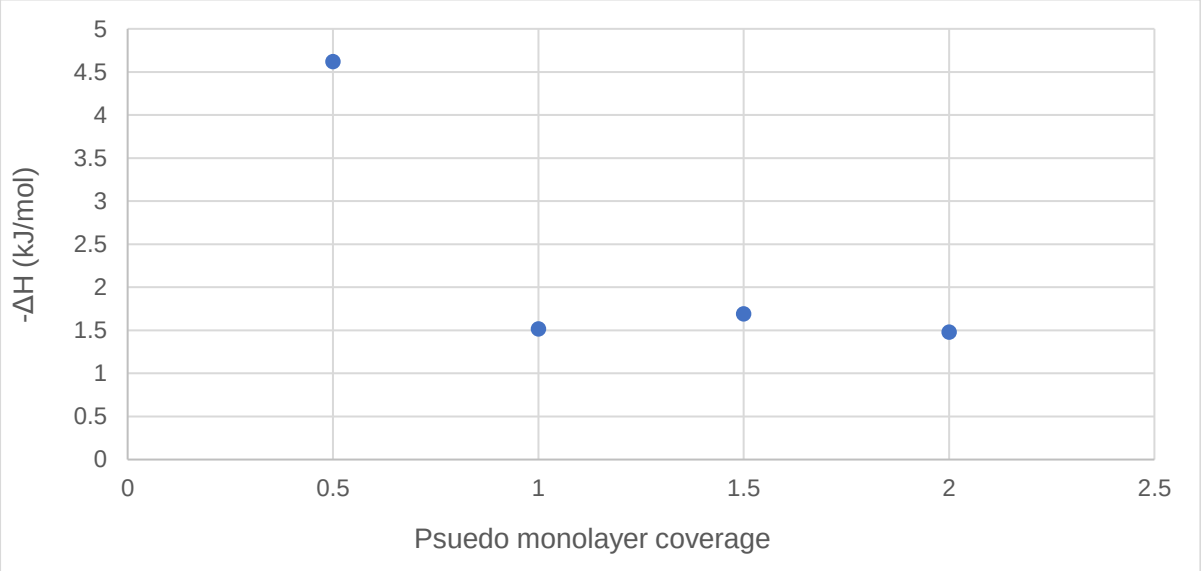

Figure 4.20: The enthalpy of SDEDTP adsorption onto chalcopyrite at pH 9, as a function of surface area coverage

SDEDTP showed similar adsorption densities as SEX on chalcopyrite, but in this case the presence of hexanol slightly decreased the extent of adsorption of SDEDTP – similar to what was observed for pyrite. The SDEDTP that was present on the mineral surface did not significantly improve the hydrophobicity of the mineral surface when comparing the first order

rate constants for the natural floatability (0.1 min^{-1}) of chalcopyrite to the condition with SDEDTP (0.14 min^{-1}). Although Güler et al. (2005), struggled to detect SDEDTP on chalcopyrite's surface at high pulp pH, the main species of SDEDTP detected was the metal thiolate.

The enthalpy of adsorption of SDEDTP onto chalcopyrite at pH 9 is shown in Figure 4.20. The heat of interaction for SDEDTP for the first half monolayer of coverage was found to be -4.6 kJ/mol with subsequent injections only producing heats of around -1.5 kJ/mol. This result is similar to the heat of adsorption observed for SDEDTP onto chalcopyrite (-4.9 kJ/mol) by Taguta, O'Connor & McFadzean (2017).

4.4.4 Chalcocite

Table 4.22 shows the extent of adsorption for SEX and SDEDTP onto chalcocite at pH 9. With or without the presence of hexanol, both collectors completely adsorbed onto the chalcocite surface. Both collectors also significantly improved the recovery of chalcocite as was seen from Figure 4.7. For both SEX and SDEDTP the main species found on the surface of chalcocite in previous studies is the chemisorbed species, which in the case of chalcocite results in high floatability at sub monolayer dosages (Woods, Kim & Yoon, 1993).

Table 4.22: The mole percent of SDEDTP and SEX adsorbed onto chalcocite at pH 9, with or without hexanol present. Collectors were dosed to cover 50% of the mineral surface, and the frother was dosed at the CCC.

	SEX	SEX + Hexanol	SDEDTP	SDEDTP + Hexanol
Collector adsorbed on chalcocite (%)	97.74 ± 0.39	97.66 ± 0.52	97.00 ± 5.78	98.80 ± 5.14
Monolayer coverage (%)	48.87 ± 0.20	48.83 ± 0.26	48.5 ± 2.89	49.4 ± 2.57

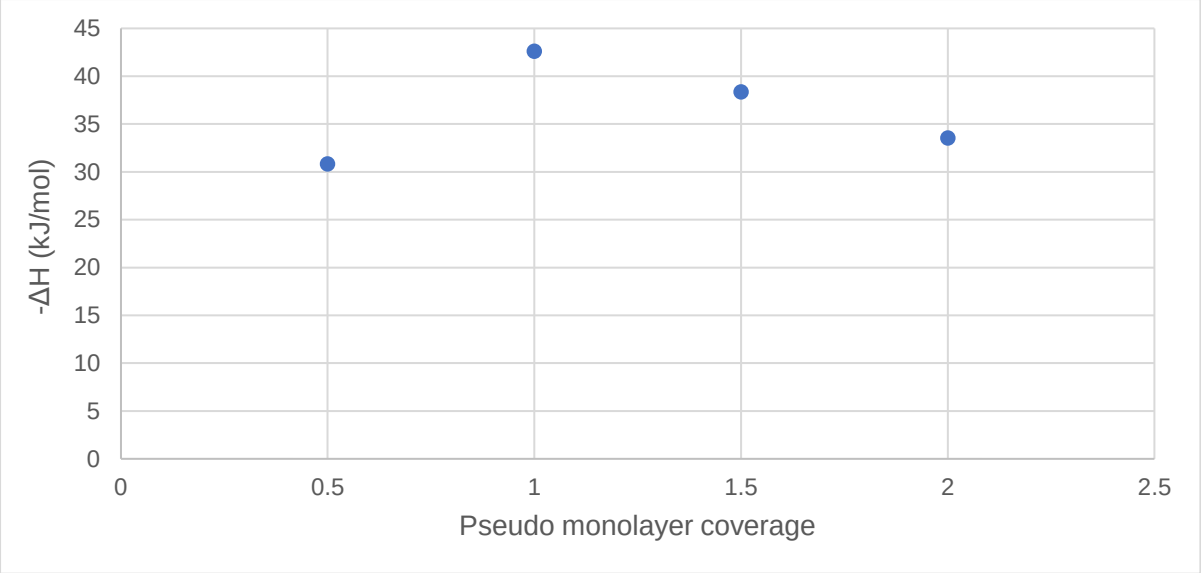

Figure 4.21:The enthalpy of SDEDTP adsorption onto chalcocite at pH 9, as a function of surface area coverage.

Figure 4.21 shows the enthalpy of adsorption of SDEDTP onto chalcocite at pH 9. The heat of interaction of SDEDTP onto chalcocite for the first injection was 30.8 kJ/mol, with next injection giving 42.6 kJ/mol, and subsequent injections decreasing from there. These indicate much greater interactions between SDEDTP and chalcocite than any of the other minerals investigated.

4.5 Adsorption with aeration

It has been shown that SDEDTP hardly adsorbs onto the galena, and only partially onto pyrite and chalcopyrite. In all these cases SDEDTP was also shown to hardly improve the minerals surface hydrophobicity as determined by the ACTA and microflotation results, but the mixture of SDEDTP and hexanol synergistically improved the attachment probability and mass recovery of galena, pyrite, and chalcopyrite.

The mechanism by which SDEDTP and hexanol can improve sulphide mineral recovery is still unclear. Unlike SEX, SDEDTP has been shown to be active at the air-water interface, and it is thought that its activity here could be the key to its synergistic mechanism with frothers. Some authors (Fuerstenau, 2001; Yan, 2016; Wang & Miller, 2018) reported that amine-based collectors adsorb onto the mineral surface by transferring from the air-water interface. This may suggest that a similar mechanism occurs by which SDEDTP and frothers improve sulphide mineral flotation.

To investigate this hypothesis, the adsorption of SDEDTP in a batch flotation cell was investigated using UV-Vis spectrophotometry tests under 4 conditions: with and without the presence of aeration, and with and without the presence of hexanol in the cell.

4.5.1 Galena

Figure 4.22 shows the adsorption behaviour of SDEDTP onto galena at pH 9, with and without aeration. In these tests around 15% of the SDEDTP in the pulp adsorbed onto the mineral (in the absence of aeration), compared to virtually no adsorption as shown previously in Table 4.19. A higher weight percent of solids was used in the batch flotation tests compared to the adsorption results presented in section 4.4 and there was a much higher degree of agitation which may improve the mass transfer of SDEDTP to the mineral surface. The adsorption tests from Table 4.19 were performed in a temperature-controlled bath which was mechanically shaken, which is a much lower energy input than the impeller from a batch flotation cell.

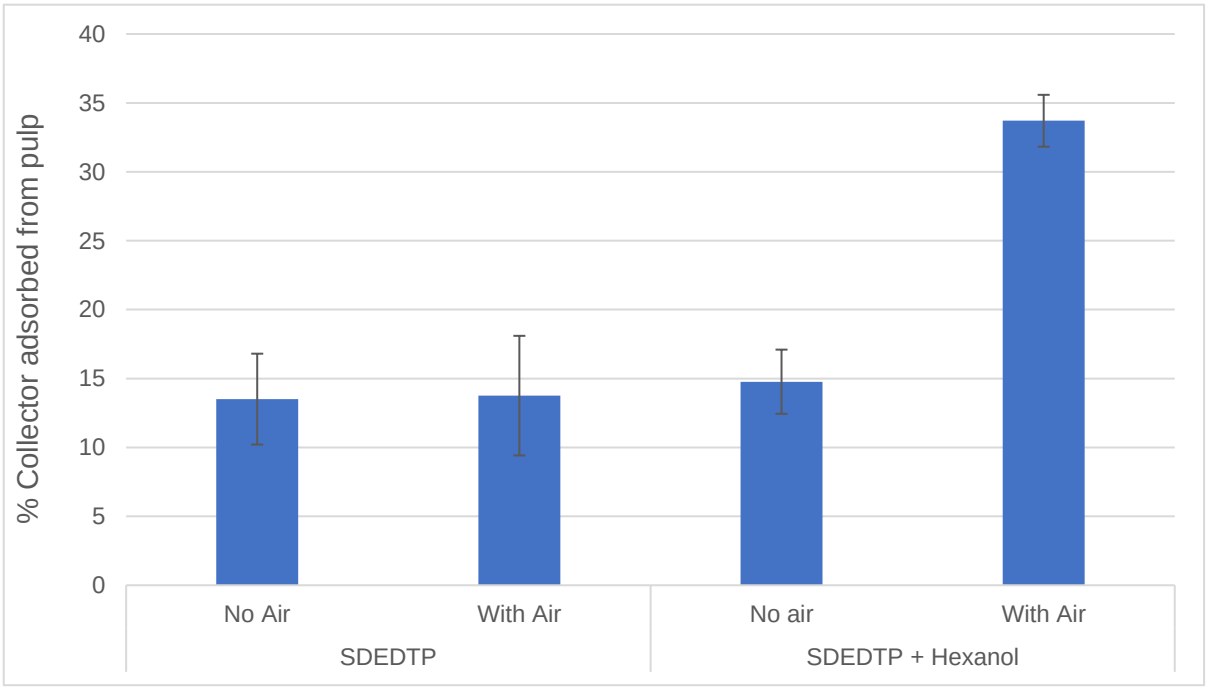

Figure 4.22: The adsorption of SDEDTP onto galena at pH 9 with and without air.

Aeration had little effect on SDEDTP adsorption onto the mineral compared to the tests performed in the absence of aeration. In common with the previous tests presented in Table 4.19, the addition of hexanol did not improve the adsorption of SDEDTP in the absence of aeration. However, in the case of aeration, the SDEDTP-hexanol mixture more than doubled the amount of collector adsorbed from the pulp. This shows that for galena, SDEDTP transfers from the air-water interface to the mineral-water interface in the presence of hexanol.

4.5.2 Pyrite

Figure 4.23 shows similar adsorption results for pyrite at pH 9. The adsorption results show that aeration improved adsorption of SDEDTP onto the mineral surface with or without the presence of hexanol. Similarly to the adsorption results from Table 4.20, the presence of hexanol slightly lowered the extent of SDEDP adsorption onto pyrite. The adsorption in the case of aeration did not increase to the same extent as was observed for galena.

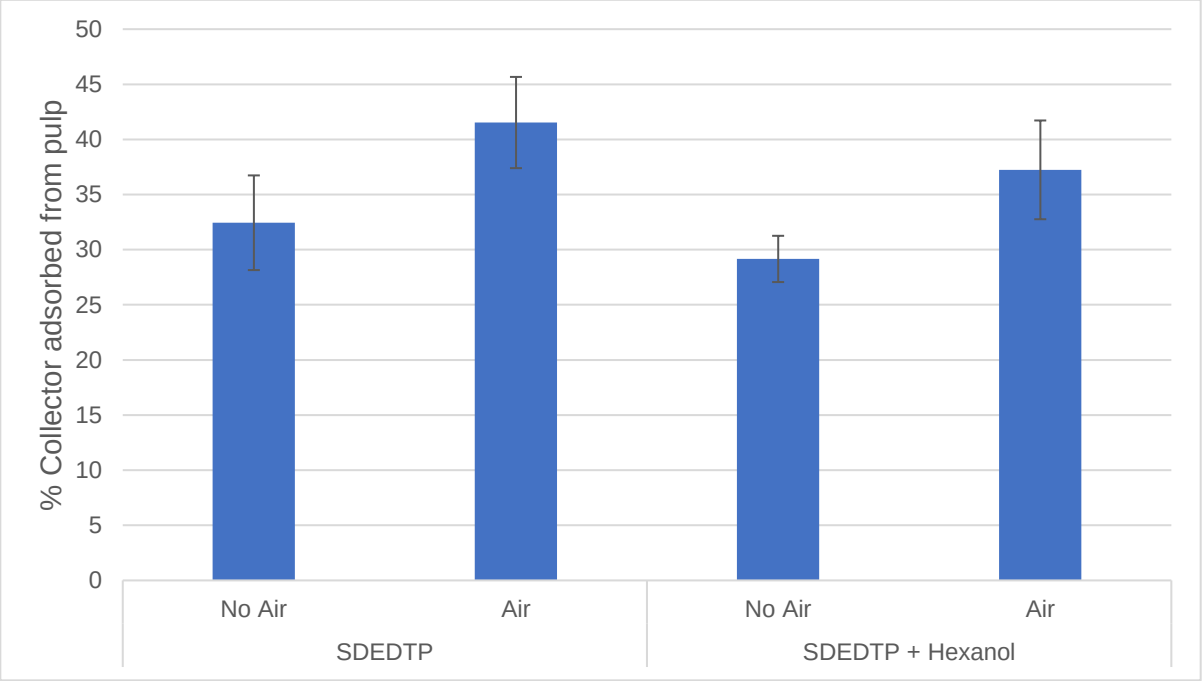

Figure 4.23: The adsorption of SDEDTP onto pyrite at pH 9 with and without air.

4.5.3 Chalcopyrite

Figure 4.24 shows the adsorption of SDEDTP onto chalcopyrite with and without aeration and hexanol. Chalcopyrite seems to exhibit the opposite results of galena and pyrite, where the aeration in the presence of hexanol lowered the extent of SDEDTP adsorption onto the mineral. The ACTA data for chalcopyrite did show that the synergistic improvement for chalcopyrite in the presence of SDEDTP and hexanol, but not to the same extent that galena and pyrite did.

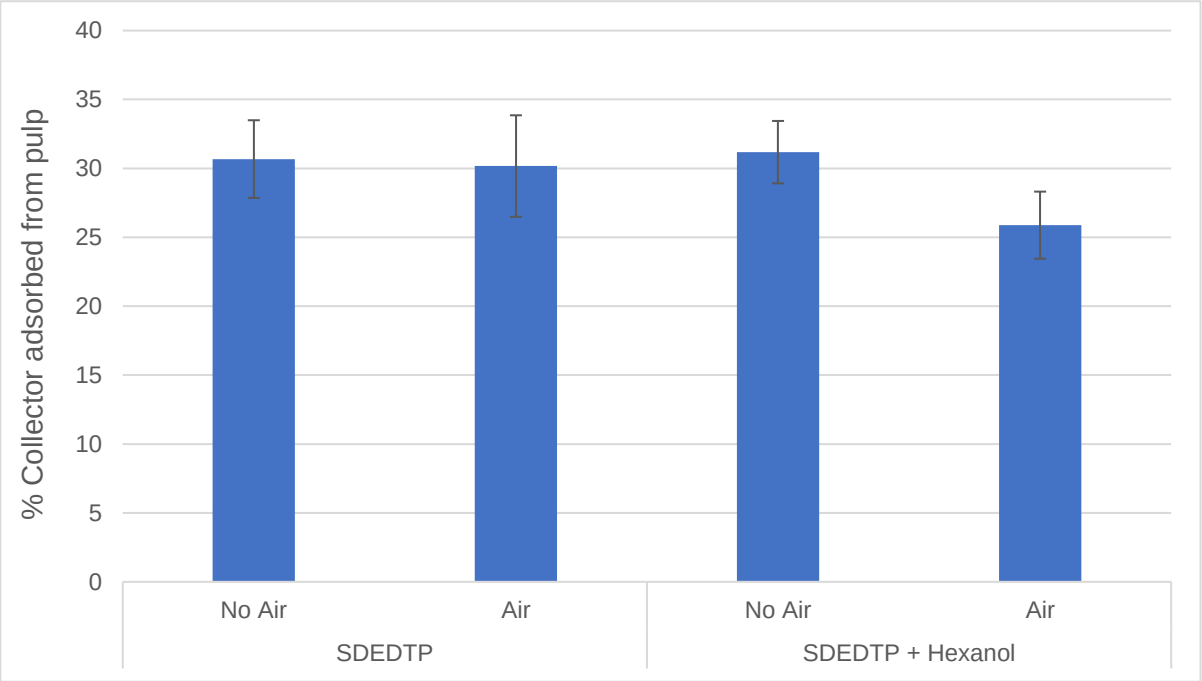

Figure 4.24: The adsorption of SDEDTP onto chalcopyrite at pH 9 with and without air.

4.6 Collector-frother interactions at the air-water interface

The adsorption results so far have indicated that for some minerals like galena, pyrite and chalcopyrite, SDEDTP does not adsorb or only partially adsorbs onto the mineral surface. It follows that the residual SDEDTP in the pulp could adsorb at the air-water interface where it has been shown that SDEDTP is weakly active (Jordaan, 2018; Dai, Bradshaw & Harris, 2002). Since the mixture of SDEDTP and hexanol synergistically improves the recovery of these minerals, further investigation into whether there is an interaction with DTP and frothers at the air-water interface is required.

4.6.1 Critical Coalescence Concentration

Previous investigations (Jordaan, 2018; Dai, Bradshaw & Harris, 2002) investigating the activity of SDEDTP at the air-water interface employed surface tension measurements which only exhibit sensitivity at concentrations that are much higher than is typically used in flotation. Pulp-phase bubble coalescence is sensitive to the low concentrations of reagents which are employed in flotation. The effect of DTP on bubble coalescence was used to determine if DTP synergistically interacts with frothers at the air-water interface.

Figure 4.25 shows the Sauter mean bubble diameter as a function of surfactant concentration. The CCC95 value for hexanol was determined to be 0.10 mM, which corresponds to the 0.11 mM found by Zhang et al. (2012). At concentrations as low as 0.05 mM SDEDTP showed significant activity at the air-water interface, but compared to hexanol, SDEDTP reduced pulp bubble coalescence to a lesser extent.

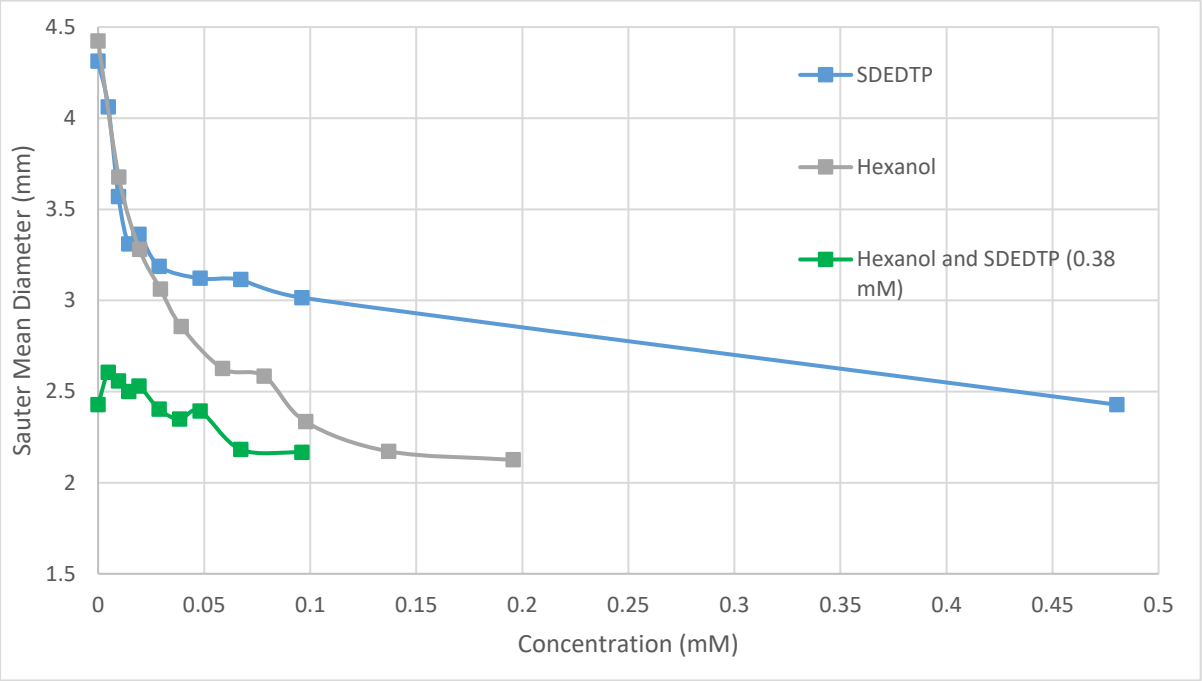

Figure 4.25: Sauter mean diameter as a function of surfactant concentration for hexanol, SDEDTP, and their mixture.

The mixture of hexanol and SDEDTP did not show any synergistic effect. At concentrations lower than the CCC of hexanol, the pulp bubble size of the mixture followed a straight line, which was equivalent to the bubble size of the SDEDTP component (0.38 mM). The addition of hexanol to SDEDTP did not even additively reduce bubble size in this region. At total concentrations higher than the CCC of hexanol, the pulp bubble sizes just follow the same curve as for hexanol on its own, which behaves as if SDEDTP is not present at all. The experiment was not performed for SEX as it has been shown that ethyl xanthate is not active at the air-water interface (Manev & Pugh, 1993; Jordaan, 2018).

The longer chain length di(iso)butyl DTP has perviously been shown to be active at the air-water interface (Dai, Bradshaw & Harris, 2002). Further tests were performed with SDIBDTP to see if the longer chain length collector would exhibit interactions with hexanol. SIBX is used to observe whether xanthates can also interact with frothers at the air-water interface. Figure 4.26 shows the Sauter mean diameter as a function of surfactant concentration for SB(I)BDTP, SIBX and hexanol. From this figure it can be seen that SD(I)BDTP exhibits stronger activity than SIBX at lower concentrations, whereas at higher concentrations these collectors both inhibit bubble coalescence to the same extent at 0.58 mM.

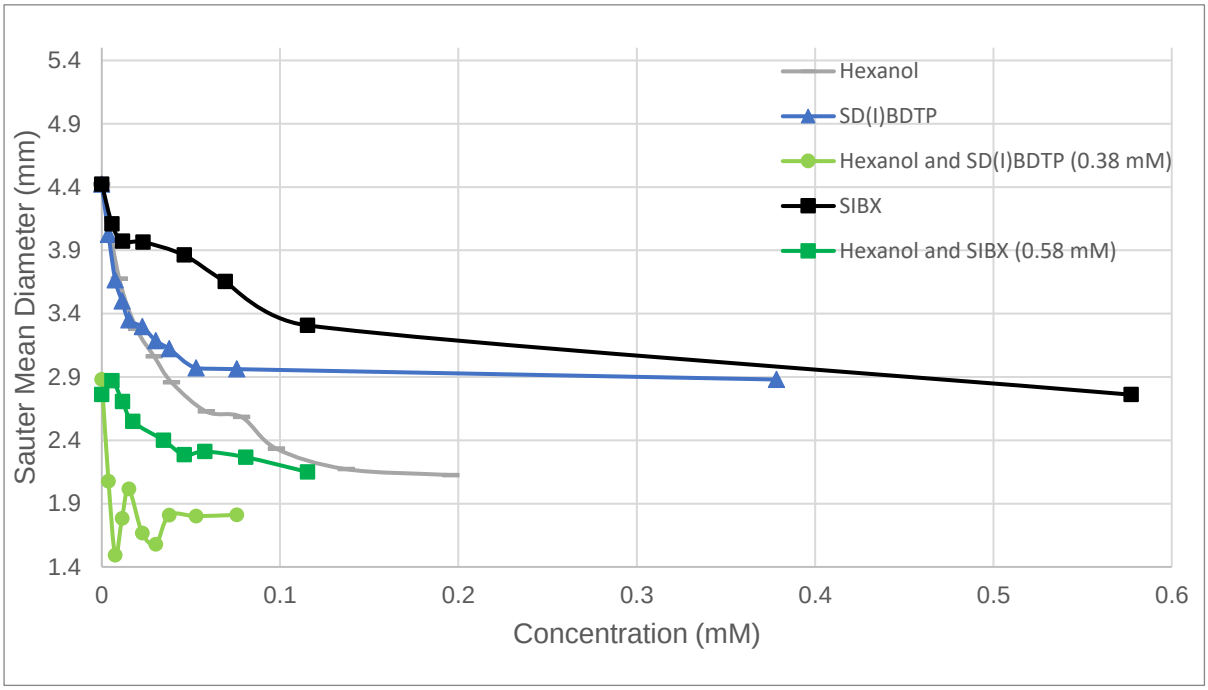

Figure 4.26: Sauter mean diameter as a function of surfactant concentration for hexanol, SD(I)BDTP, SIBX, and their mixtures.

The SIBX and hexanol mixture follows a similar trend to SDEDTP, but in the region before the CCC of hexanol the mixture seems to reduce the pulp bubble size even further. The mixture of hexanol and SD(I)BDTP (0.38 mM) appears to exhibit synergism where the concentrations as low as 0.0098 mM of hexanol in the mixture decrease the bubble size beyond the size at which hexanol inhibits bubble coalescence on its own.

Grau, Laskowski & Heiskanen (2005) observed that the smaller molecule, Dowfroth-200, produced finer bubbles at concentrations beyond the CCC, compared to the larger molecule, Dowfroth-1012. This was attributed to the rate of adsorption of these molecules onto the bubble surface, which can have an effect on bubble breakup and coalescence during dynamic conditions around the impeller region. Some binary surfactant mixtures have exhibited improved rates of diffusion and adsorption at the air-water and mineral-water interface (Leja,

1989). An interaction between SD(I)BDTP and hexanol resulting in a complex formation may exhibit these effects, where improved rates of adsorption may produce smaller bubbles.

4.6.2 Foam stability tests

Similar to pulp bubble coalescence, dynamic foam stability is sensitive to the reagent concentrations typically used in flotation (Sweet et al., 1997). The foam stability was used as a proxy for interfacial activity for flotation frothers and collectors, and to assess whether there are any synergistic interactions between them.

The dynamic foam stability factor (∑) was used to assess the foam stability at each reagent condition. Figure 4.27 shows the dynamic foam stability of single reagents. The concentrations were based on 50 g/ton and 100 g/ton dosage of the frother. The concentration of the collector was selected as the same concentration of the frother on a molar concentration basis. All of the collectors exhibit virtually no ability to enhance the foam stability, whereas hexanol does enhance foam stability, which is expected from a frother.

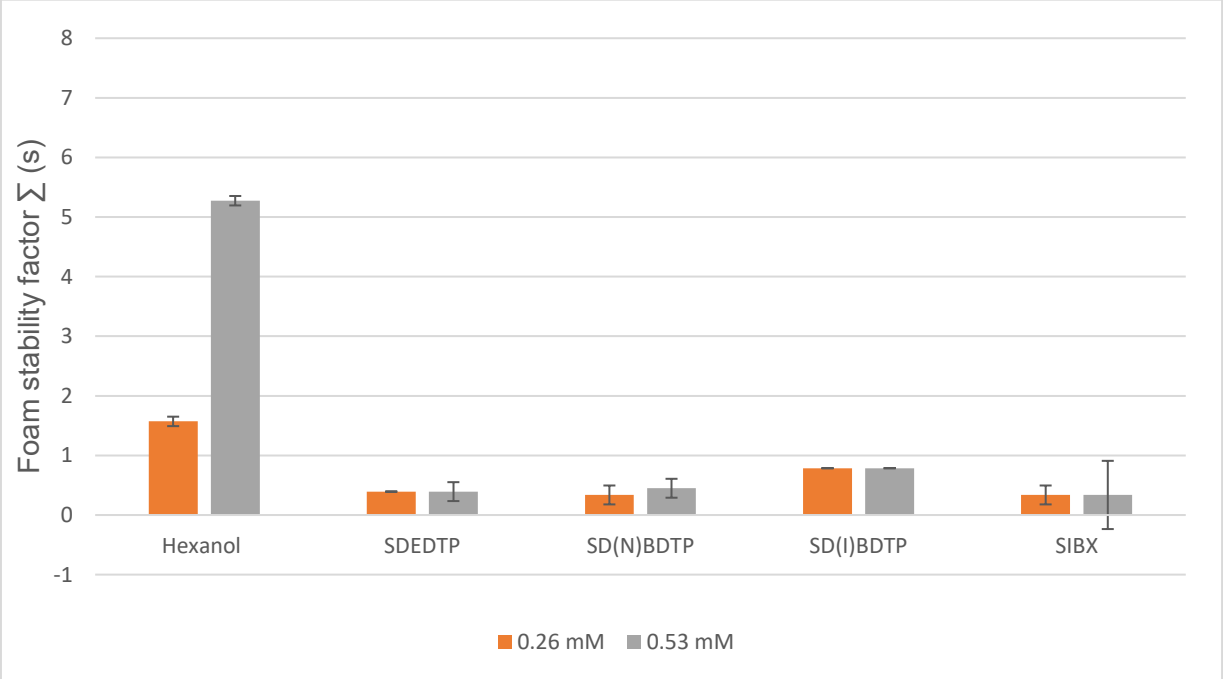

Figure 4.27: The dynamic foam stability of hexanol and various thiol collectors at various concentrations

Figure 4.28 illustrates the foam stability of collector-frother mixtures. The fraction under each grouping shows the mole fraction of collector in the mixture with hexanol, where the concentration below the fraction indicates the total concentration of the mixture in millimoles. The concentrations used in these tests are made up from various combinations of the single reagent concentrations. The dynamic foam stability factor for hexanol on its own is indicated by the orange bar.

Foam stability tests were also conducted with a mixture of SD(N)HDTP and hexanol. The result from this test is not presented as the mixture did not attain an equilibrium height of foam within the column. The foam grew and overflowed over the top of the column.

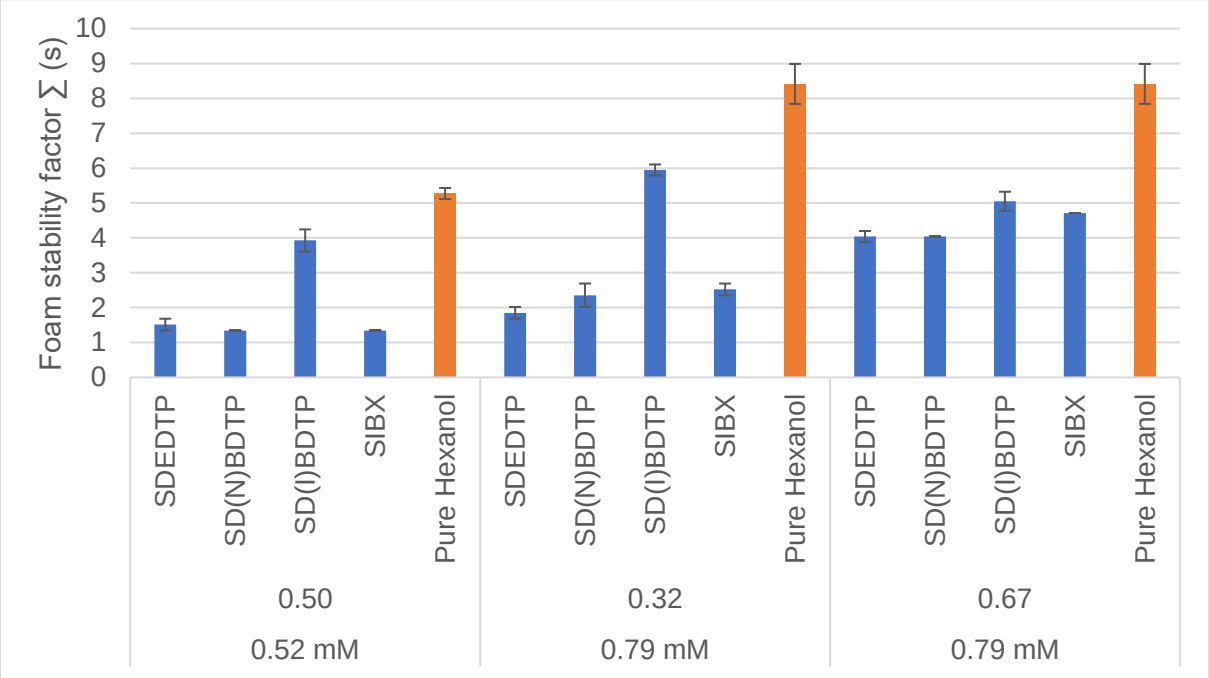

Figure 4.28: The dynamic foam stability of various thiol collectors mixed with hexanol, at different ratios and concentrations.

Table 4.23 compares the calculated dynamic foam stability factors for collector-hexanol mixtures to the experimental values. The calculated values are determined from the single reagent experiments in Figure 4.27, where the dynamic stability factors were linearly combined as a function of the concentration of each reagent (weighted sum contribution). This calculation assumes that the dynamic foam stability factor increases linearly with increasing concentration. Figure 4.29 shows that within the concentrations of hexanol tested the dynamic stability factor was directly proportional to the concentration of the surfactant. For the collectors, the concentration did not have an effect on the dynamic stability factor as illustrated in Figure 4.27. Comparing the calculated dynamic foam stability factors of the collector-hexanol mixtures to the experimental values served as an indication of whether the surfactant mixtures additively, synergistically, or antagonistically affected the dynamic foam stability.

Table 4.23: The dynamic foam stability factors of various thiol collector mixtures with hexanol, at different ratios and concentrations. Additive values represent the mixture stability factor calculated from single reagents experiments.

Mole fraction collector	0.50		0.32		0.67	
Total concentration of surfactants [mM]	0.52		0.79		0.79	
	Dynamic foam stability factor ∑ (s)					
Reagents	∑Calculated	∑Experimental	∑Calculated	∑Experimental	∑Calculated	∑Experimental
SDEDTP + Hexanol	2.0	1.5	5.7	1.9	2.0	4.0
SD(N)BDTP + Hexanol	1.9	1.4	5.6	2.4	2.0	4.0
SD(I)BDTP + Hexanol	2.4	3.9	6.1	6.0	2.4	5.0
SIBX + Hexanol	1.9	1.4	5.6	2.5	1.9	4.7

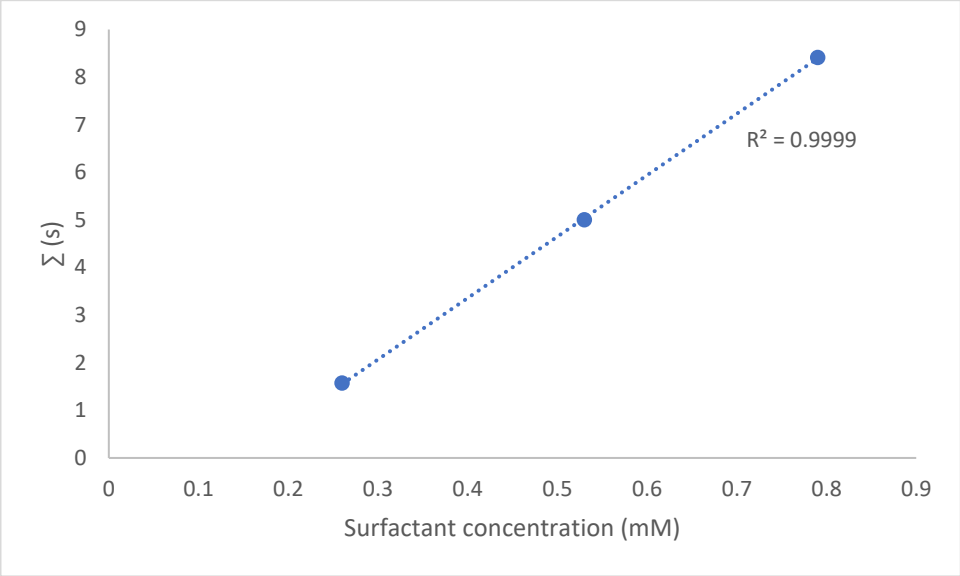

Figure 4.29: Dynamic foam stability factor of hexanol as a function of the concentration of hexanol. A straight line was fit to the data.

At a concentration of 0.52 mM and a 0.50 mole fraction of collector, only SD(I)BDTP and hexanol improved the foam stability compared to the predicted additive values. On its own SD(I)BDTP (0.26 mM) had a dynamic foam stability factor of 0.9s (Figure 4.27), and hexanol (0.26 mM) had a factor of 1.6s (Figure 4.27), which additively would have produced a stability factor of 2.4s, but together they improved stability, giving a value of 3.9s. The other collectors with hexanol showed a decrease in foam stability at these mole ratios and concentrations (Table 4.23). Interestingly, at a concentration of 0.79 mM and a mole fraction of 0.32, SD(I)BDTP and hexanol additively increased the foam stability, whereas the other collectors lowered foam stability. At the higher mole fraction of 0.67, and concentration of 0.79 mM all the collectors exhibited improvements in foam stability compared to the calculated value. SD(I)BDTP showed the greatest improvement.

Table 4.24: The change in the dynamic foam stability factor ($\sum_{Experimental} - \sum_{Calculated}$) for the collector-hexanol mixtures as a function of mole percent of collector.

Mole fraction of collector	Total surfactant concentration [mM]	SDEDTP	SD(N)BDTP	SD(I)BDTP	SIBX
0.32	0.79	-3.8	-3.3	-0.1	-3.1
0.50	0.52	-0.5	-0.6	1.6	-0.6
0.67	0.79	2.1	2.0	2.7	2.8

Table 4.24 shows the change in the dynamic foam stability factor ($\Delta\sum = \sum_{Experimental} - \sum_{Calculated}$). If the change is 0, the surfactants produced no additive effect, whereas if the change is positive a synergistic response was observed, and if the change is negative an antagonistic response was observed.

Table 4.24 shows that all collector-hexanol mixtures can synergistically improve the dynamic foam stability, depending on the mole fraction of collector. It is clear that the increase in synergistic behaviour is driven by the increase in mole fraction of collector since there is a large difference between the 0.32 and 0.67 mole fractions at the same concentration of 0.79 mM. This can be observed qualitatively in Figure 4.28, where an increase in the mole fraction from 0.32 to 0.67 at the same concentration of 0.79 mM increases the foam stability, whereas an increase in the ratio of poorly foam stabilising DTP molecules would be expected to decrease the foam stability. Lower mole fractions of collector and higher mole fractions of hexanol produce an antagonistic response, where the difference between the experimental and calculated dynamic foam stability factor is negative.

The foam rise velocity of some of the mixtures were also measured. Figure 4.30 shows the foam height of the 0.32 mole fraction collector mixture at a concentration of 0.79 mM. In each case results show a peak in the initial foam height, which decreases to an equilibrium height. SD(I)BDTP gave the greatest peak, following SD(N)DTP, SIBX and SDEDTP (giving no peak at all). It was hypothesized that as water drains out of the foam during the initial rise in foam height, the collector molecules elutriate back into the pulp with the draining water which causes the foam to collapse to an equilibrium value. Further tests were conducted on longer time scales to see if the foam would regenerate.

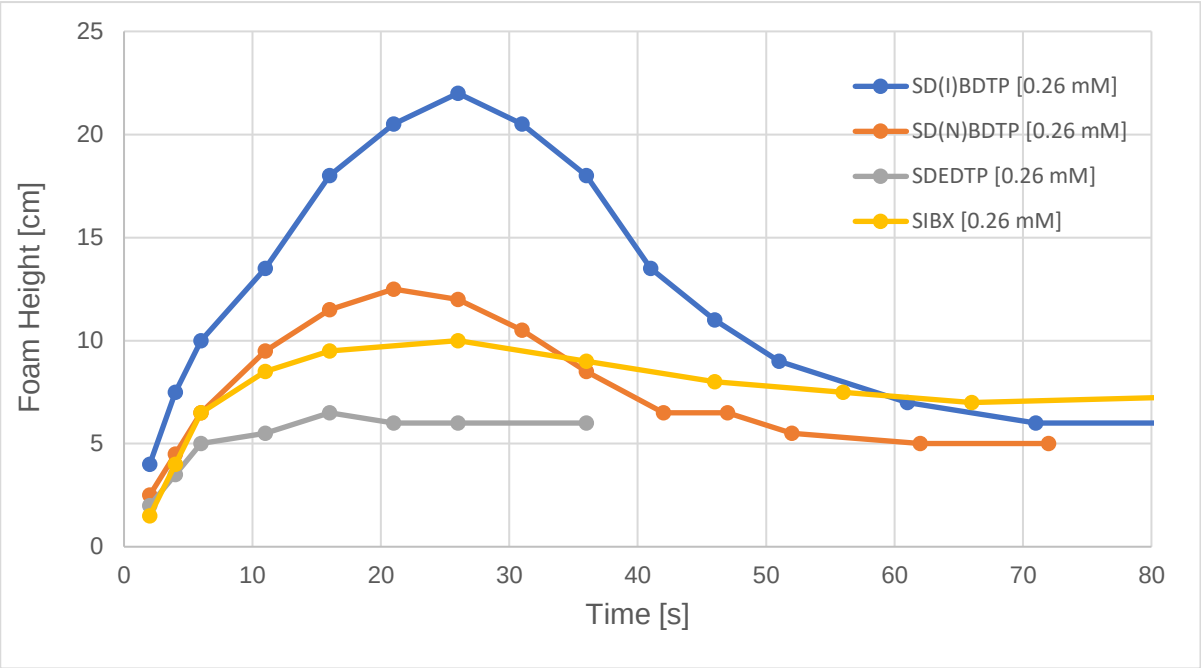

Figure 4.30: The foam height as a function of time. A collector-frother mixture with 32 mole percent collector was used and the total concentration of surfactants was 0.79 mM.

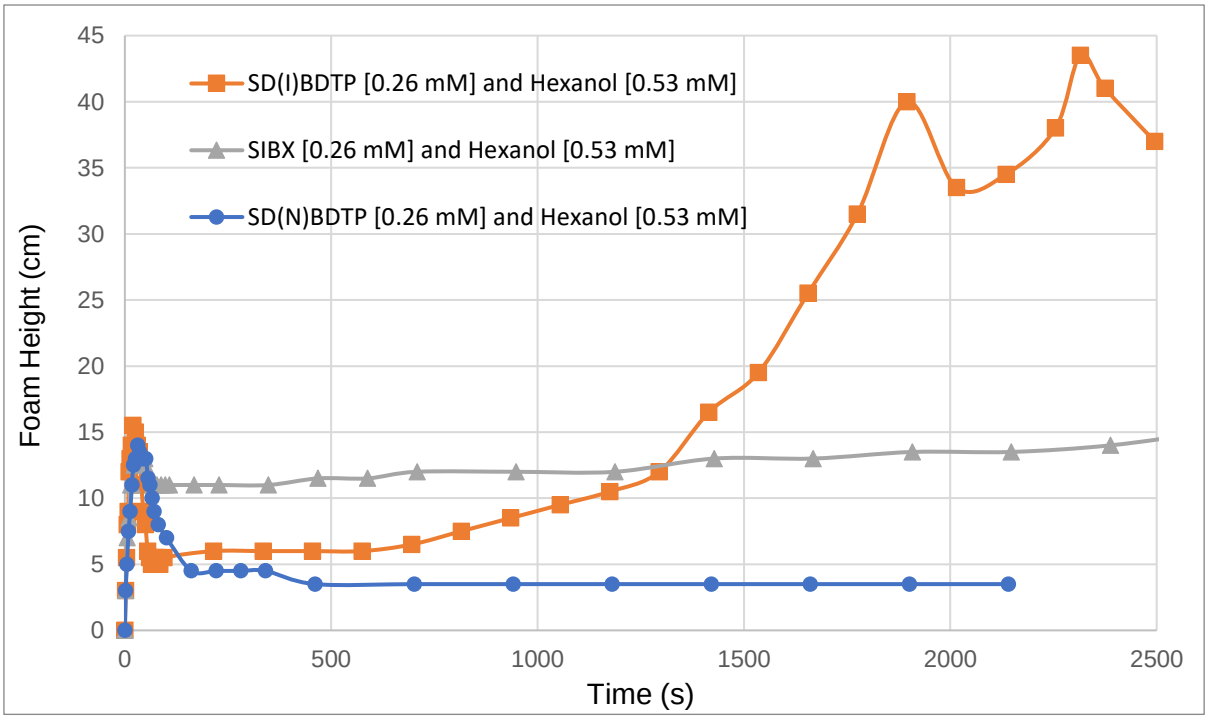

Figure 4.31: Foam height as a function of time (Test was performed over the period of 40 min). A collector-frother mixture with a mole fraction of 0.32 collector was used and the total concentration of surfactants was 0.79 mM.

Figure 4.31 shows the foam height as a function of time for SD(I)BDTP, SD(N)DTP and SIBX. Each collector constitutes 32 mol percent of the collector-hexanol mixtures and the total surfactant concentration is 0.79 mM. For the mixture of SD(I)BDTP and hexanol a synergistic improvement in foam height is observed although this only occurs after 1000s and ultimately the foam height reaches 43.5 cm. The experiments were performed using medical grade air, so that no contaminants could affect the results. The foam height for SD(N)BDTP remained completely stable when equilibrium was attained, whereas for SIBX the foam grew slightly from 11 cm to around 15 cm.

A test was performed where the solution of SD(I)BDTP and hexanol was reused after a period of 30 minutes. Figure 4.32 shows that the foam height quickly grew back to the original height found in Figure 4.31, and the foam exhibited oscillating behaviour with a maximum height around 38 cm and a minimum height around 30 cm.

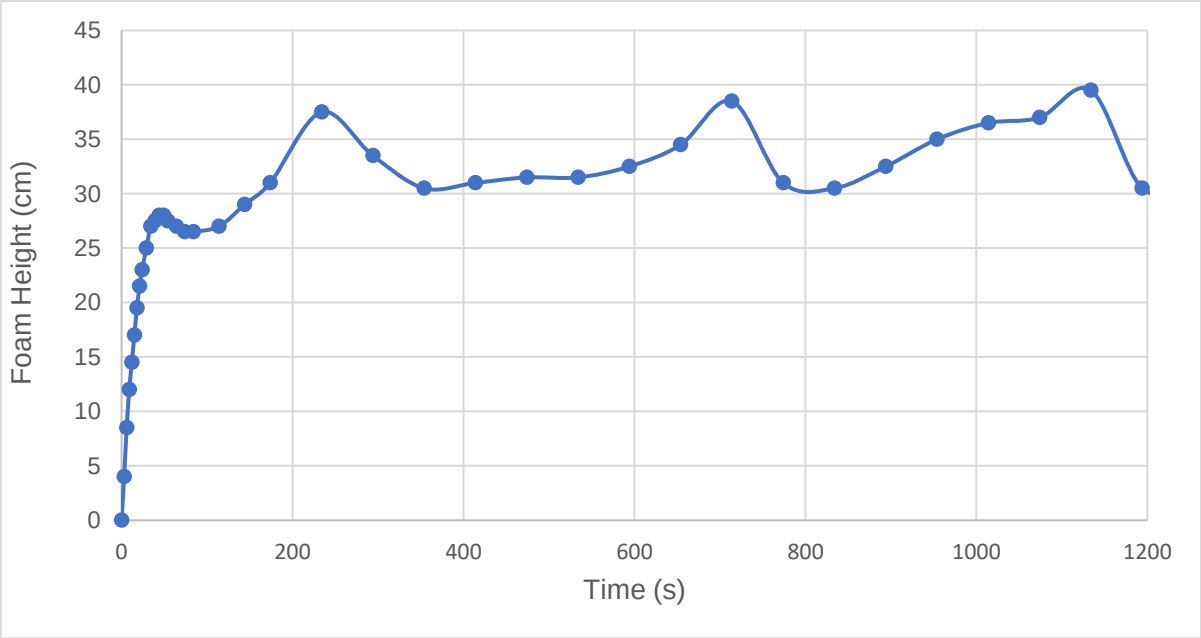

Figure 4.32: Foam height as a function of time (Test was performed over the period of 20 min). A SD(I)BDTP-hexanol mixture with 32 mole % collector was used and the total concentration of surfactants was 0.79 mM.

These results may not seem to have practical applications to froth stability since the residence time within a flotation cell is much less than the time regimes reflected above. These tests do however show a strong synergistic interaction between SD(I)BDTP and hexanol. Between the test performed in Figure 4.31 and Figure 4.32, where the solution was reused, it appears that there was a change in the behaviour of the two surfactants. The foam rose to its maximum

height in Figure 4.31 over 30 minutes, whereas Figure 4.32 it grew to a similar height in 4 minutes.

Leja & Schumann (1954) speculated that the associated complexes that collectors and frothers form have different functional properties. Figure 4.32 seems to show that the SD(I)BDTP interacts with the hexanol at the air-water interface over a relatively long period time, but once these molecules have associated, they form a complex that responds at a much faster rate.

Crozier & Klimpel (1989) have explained that some mining companies use collectors and frothers that are preblended and this was found to reduce collector consumption by up to 40%. This reduction in consumption was attributed to the improved efficacy of the complex that was formed in the concentrated collector-frother blend. It may be that at the air-water interface both SD(I)BDTP and hexanol can concentrate and form these complexes, improving the efficacy in foam stability. A concentrated blend of these molecules could allow them to associate, and thus be immediately effective.

4.6.3 Regular solution theory

With the interpretation of foam stability and CCC data so far, the improvements observed for the collector-frother mixtures have been mostly qualitatively evaluated from the data. This can often be misleading as there are difficulties in discerning whether the contributions of each of the components are additive or if they are due to synergism - producing effects that are greater than the sum of each of the contributions. To be able to quantitatively provide information on collector-frother synergism, the regular solution theory model was applied to surface tension data. The β parameter calculated from this model will indicate if there is an attractive or repulsive interaction between the surfactants, relative to their interaction with themselves. The conditions for true synergism are that β is a negative value and that Equation 20 is satisfied. The parameters C_1^O and C_2^O are the concentrations of surfactant 1 and surfactant 2 at a constant surface tension.

To obtain this concentration a horizontal line was drawn across the graph at the same value of surface tension that was used to determine the β parameter. The points where this line intersects the lines for surfactant 1 and surfactant 2 are the concentrations C_1^O and C_2^O.

$$|\boldsymbol{\beta}| > \left| ln\left(\frac{C_1^0}{C_2^0}\right) \right| \qquad \text{Equation 20}$$

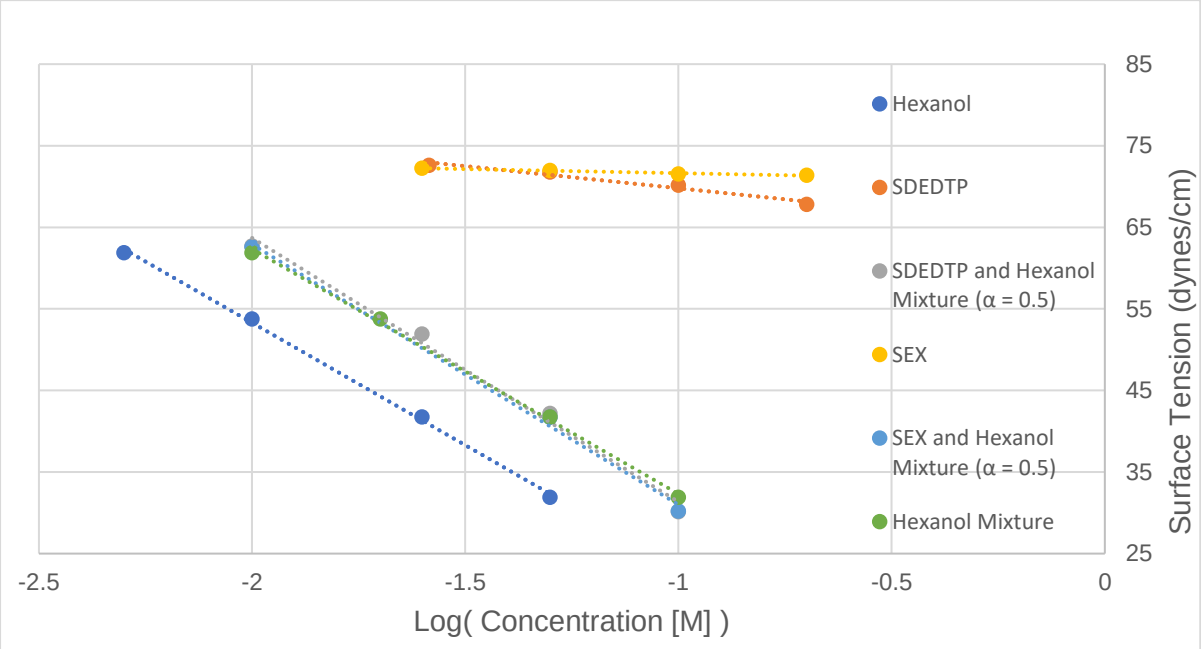

Figure 4.33: Surface tension vs Log concentration for SEX, SDEDTP, hexanol, and the mixtures of 50 mole percent of the collectors and hexanol.

The surface tension vs the log of the concentration is presented in Figure 4.33. The graph shows the surface tension data for the pure reagents, viz. SDEDTP, SEX, hexanol, and 50 mole percent of each reagent in a mixture of the collector and frother. Figure 4.33 shows that there is no decrease in surface tension with increasing SEX concentration. This shows that SEX is not active at the air-water interface, which is consistent with results found by Manev & Pugh (1993), and Jordaan (2018). For SDEDTP weak surface activity is observed which was also previously found by Jordaan (2018), and Dai, Bradshaw & Harris (2002).

The line labelled hexanol mixture represents the contribution of the pure hexanol to reducing the surface tension in the mixture. It is the surface tension contribution of hexanol at the concentration found in the mixture plotted vs the total surfactant concentration in the solution. When comparing the mixtures of SDEDTP-hexanol, and SEX-hexanol to the hexanol mixture line, all lie on top of each other. This shows that the collectors are making no contribution to the reducing surface tension – thus the weak interfacial activity of SDEDTP does not show any interaction that is detectable at the concentrations investigated.

The β parameter could not be calculated for SEX as the surface tension range of the SEX line and the hexanol line do not overlap when drawing a line through the data at a constant surface tension, this is depicted in Figure 4.34. This is mostly due to SEX having no surface activity, and thus the surface tension vs concentration line would be horizontal.

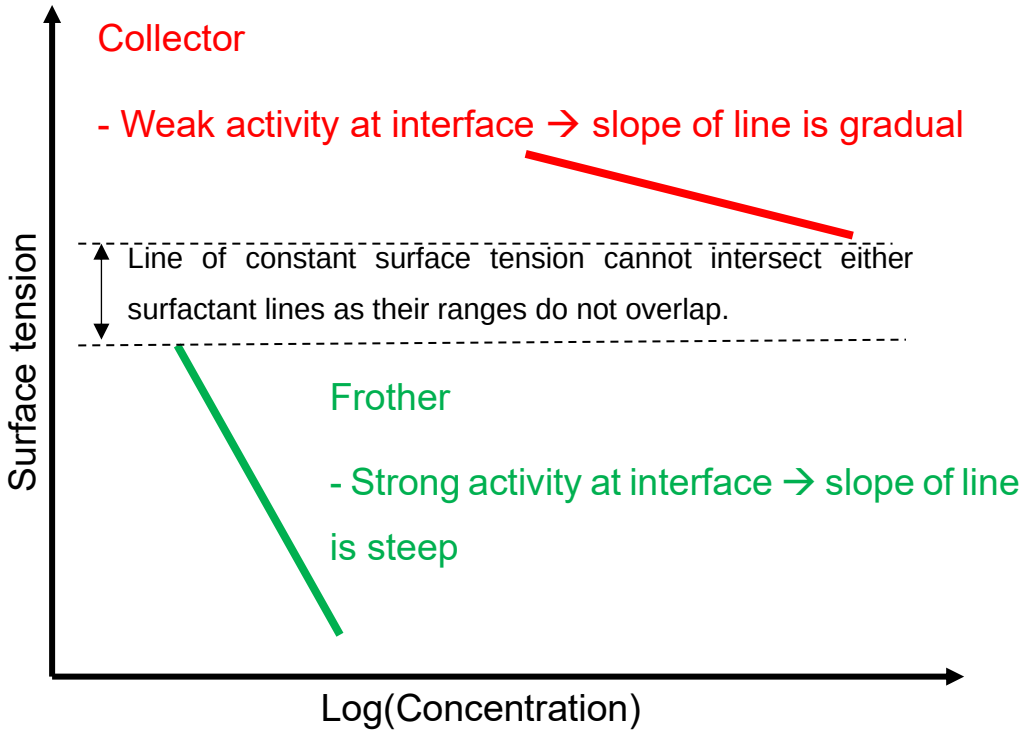

Figure 4.34: Surface tension vs Log concentration depicting when the surface tension domains of different surfactant lines do not overlap.

Furthermore, the β parameters could not be calculated for SDEDTP. The surface tension ranges do not overlap but even if the SDEDTP line is extrapolated so that a straight line of surface tension can be drawn through the data to find the parameters to solve the equations, no solution to Equation 14 could be found. SDEDTP is such a weak surfactant that where a line of constant surface tension intersects the lines for SDEDTP and hexanol, the concentration of SDEDTP is so high compared to that of hexanol at the same surface tension value, that the surface mole fraction of SDEDTP tends to 1 ($X_{DTP} \rightarrow 1$).

Longer chain length thiol collectors, which have stronger activity at the air-water interface, were then tested.

Figure 4.35 shows the surface tension vs log concentration of the butyl thiol collectors, hexanol, and their mixtures. Compared to the ethyl chain lengths on their own in Figure 4.33, both SD(N)BDTP and PNBX show significantly greater interfacial activity. At 200 mM SD(N)BDTP and PNBX reduced the surface tension to 41.3 and 65.4 dynes/cm, respectively. This is compared to SDEDTP which lowered the surface tension to 67.8 dynes/cm and SEX,

which showed no activity at the air-water interface. The stronger activity that SD(N)BDTP exhibits at the air-water interface compared to PNBX may be due to the dual alkyl chain structure of DTPs, where xanthates only have one alkyl chain.

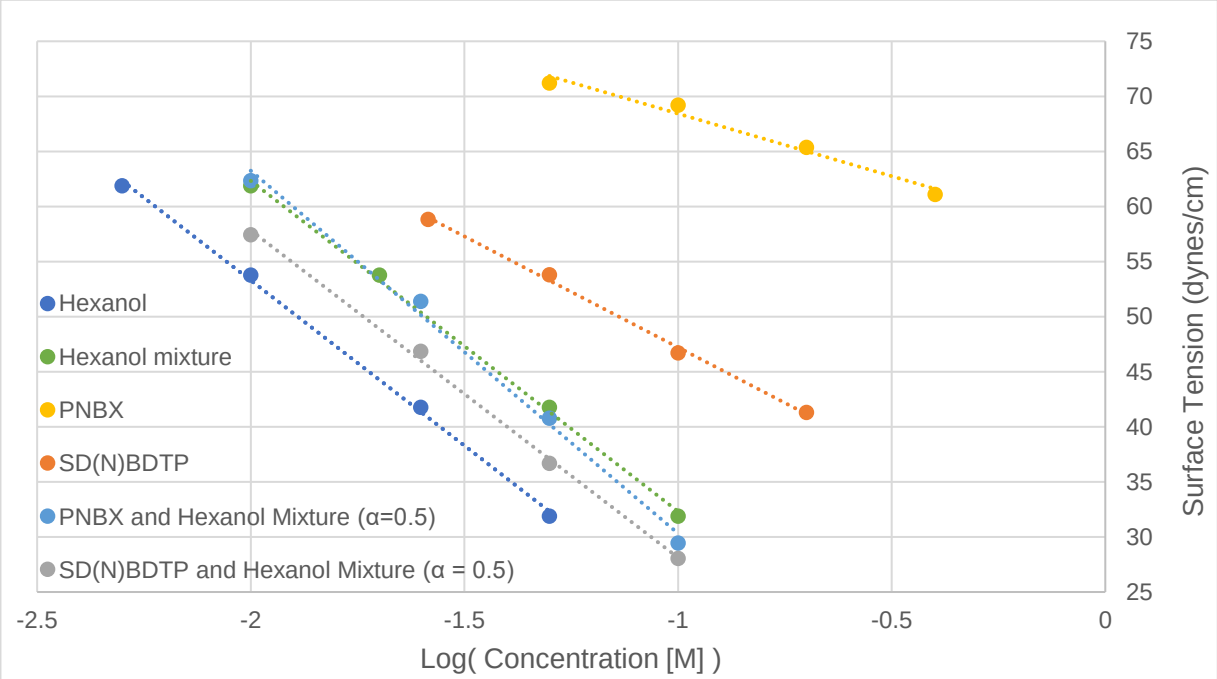

Figure 4.35: Surface tension vs Log concentration for PNBX, SD(N)BDTP, hexanol, and the mixtures of 50 mole percent of the collectors and hexanol.

The β parameter for PNBX could not be calculated due to the weak activity. A solution to Equation 14 could not be found, and this was also a problem for SIBX and PAX. For the xanthate collectors, the information is qualitatively analyzed in the graphs by comparing the mixture of xanthate and hexanol to the surface tension reduction that hexanol, alone, would exhibit in the mixture. This line is labelled “Hexanol mixture”, and if the collector-hexanol line lies on top of the hexanol mixture line it can be inferred that xanthate does not interact with hexanol at the air-water interface, viz. there is no synergistic effect. In Figure 4.35 the PNBX-hexanol line does lie on top of the hexanol mixture line, but at higher concentrations seems to deviate away from this line, adding to interfacial reduction ability and indicating that the concentration of the collector is playing a role.

Table 4.25 shows the β parameter analysis for the various DTP collectors mixed with frothers. The table also shows experimental and ideal area per molecule for each collector, frother and collector-frother mixture.

Table 4.25: β parameters calculated for mixtures of various chain length thiol collectors and frothers

					Mixture			
Collector	**Frother**	β	$A_{collector}$ (Å^2)	$A_{frother}$ (Å^2)	A_{exp} (Å^2)	A_{ideal} (Å^2)	A_{exp} - A_{ideal} (Å^2)	Synergistic interaction
SD(N)BDTP	Hexanol	-0.66	47.04	31.59	31.91	35.62	-3.71	×
PNBX	Hexanol	-	47.04	31.59	31.31	-	-	×
SD(I)BDTP	Hexanol	-1.57	68.18	31.59	34.18	43.50	-9.32	✓
SIBX	Hexanol	-	91.96	31.59	29.77	-	-	×
SD(I)BDTPINA	Hexanol	-1.40	80.90	31.59	36.68	47.32	-10.64	✓
SD(N)HDTP	Hexanol	-2.13	53.47	31.59	39.07	44.10	-5.03	✓
PAX	Hexanol	-	69.43	31.59	30.06	-	-	×
SD(N)BDTP	PPG425	-3.92	47.04	118.06	80.36	86.71	-6.35	✓

From Table 4.25 the β parameter calculated for SD(N)BDTP is -0.66. A negative β parameter indicates that there is an attractive interaction between SD(N)BDTP and hexanol, relative to the two reagents alone. To determine if there is a synergistic interaction between SD(N)BDTP and hexanol the inequality in Equation 20 needs to be satisfied. The right-hand side of the equation was found to be 1.36 which is greater than the absolute value of the β parameter (0.66), so the interaction between these surfactants is not synergistic. These calculations for the other molecules tested, showed that there was an attractive interaction between SD(I)BDTP, SD(I)BDTPINA and SD(N)HDTP with hexanol, as well as SD(N)BDTP with PPG425. None of the xanthate molecules showed any attractive interactions with hexanol. The various interactions will be discussed in further detail in the following sections.

Noting the difference between the experimental and ideal surface areas per molecule for the mixture of SD(N)BDTP and hexanol, there is a difference of -3.71 Å^2. As SD(N)BDTP is an ionic surfactant there is electrostatic self-repulsion between the polar head groups of the molecules when they are adsorbed at the air-water interface. When this ionic surfactant is mixed with a non-ionic surfactant like hexanol, the non-ionic molecule can dilute the electrostatic self-repulsion effect (Zhou & Rosen, 2003), causing the mixture of collector and frother molecules to pack more tightly at the air-water interface. This tighter packing could explain the discrepancy between the ideal and experimental surface areas, where the experimental values take into account the interactions which change the packing behavior at the air-water interface This observation was made throughout for all of the collector-frother

mixtures, as all the collectors that were used were ionic, and all the frothers that were used were non-ionic.

4.6.3.1 Branching Alkyl Chain

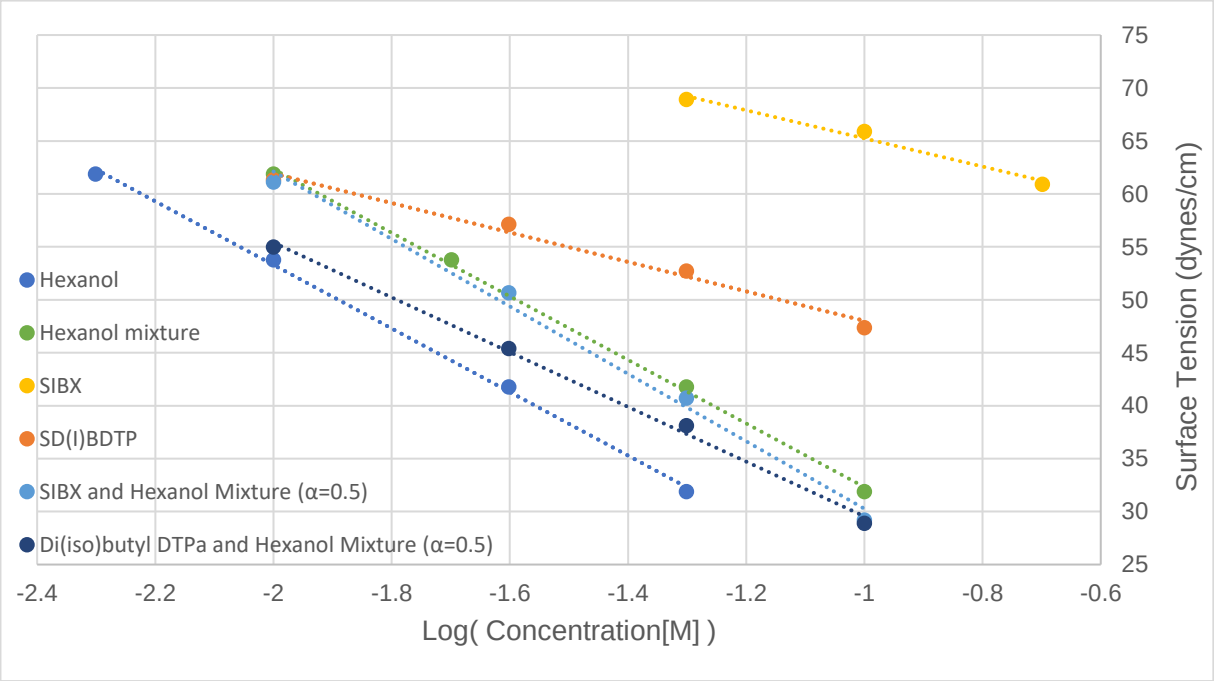

Figure 4.36: Surface tension vs Log concentration for SIBX, SD(I)BDTP, hexanol, and the mixtures of 50 mole percent of the collectors and hexanol.

Figure 4.36 compares the surface tension of pure isobutyl thiols and their mixtures with hexanol as a function of their concentration. Comparing the surface tension, i.e., the interfacial activity, of SIBX to PNBX shows that SIBX is slightly more active at the air-water interface than PNBX. At 200 mM, SIBX reduced the surface tension to 60.9 dynes/cm, compared to the 65.4 dynes/cm of PNBX (shown in Figure 4.35). The mixture of SIBX and hexanol did not reduce the surface tension to a much greater extent than the case of hexanol on its own at equivalent hexanol concentrations.

The β parameter of SD(I)BDTP was determined to be -1.57 as can be seen in Table 4.25Table 4.25: β parameters calculated for mixtures of various chain length thiol collectors and frothers, revealing an attractive interaction between the collector and frother. The inequality in Equation 20 was satisfied, where the right-hand side of the equation was determined to be 1.27, less than the absolute value of the β parameter. This indicates that there is a synergistic interaction between SD(I)BDTP and hexanol.

Comparing the β parameters of SD(N)BDTP (β = -0.66) and SD(I)BDTP (β = -1.57), a stronger and synergistic interaction between the branched chain molecule and hexanol is observed. This is also reinforced by the larger deviation between the ideal and experimental molecular

cross-sectional area for SD(I)BDTP (-9.32 Å^2), compared to SD(N)BDTP (-3.71 Å^2). The branching alkyl chains of SD(I)BDTP significantly increase the area per molecule, viz. 68.2 Å^2, compared to the value for the straight chain SD(N)BDTP, viz. 47.4 Å^2. Even though there is a strong steric self-repulsion for the branched chain molecule, it still shows a stronger interaction with hexanol than with the straight chain.

Branched alkyl chains impose stronger inductive effects on the head group of the molecules than straight alkyl chains (Clayden, Greeves & Warren, 2012). Inductive effects could play a role in the interactions between the head group of the DTP molecules and the frother, which may negate the steric repulsive effects for the alkyl chain.

4.6.3.2 Increasing alkyl chain length

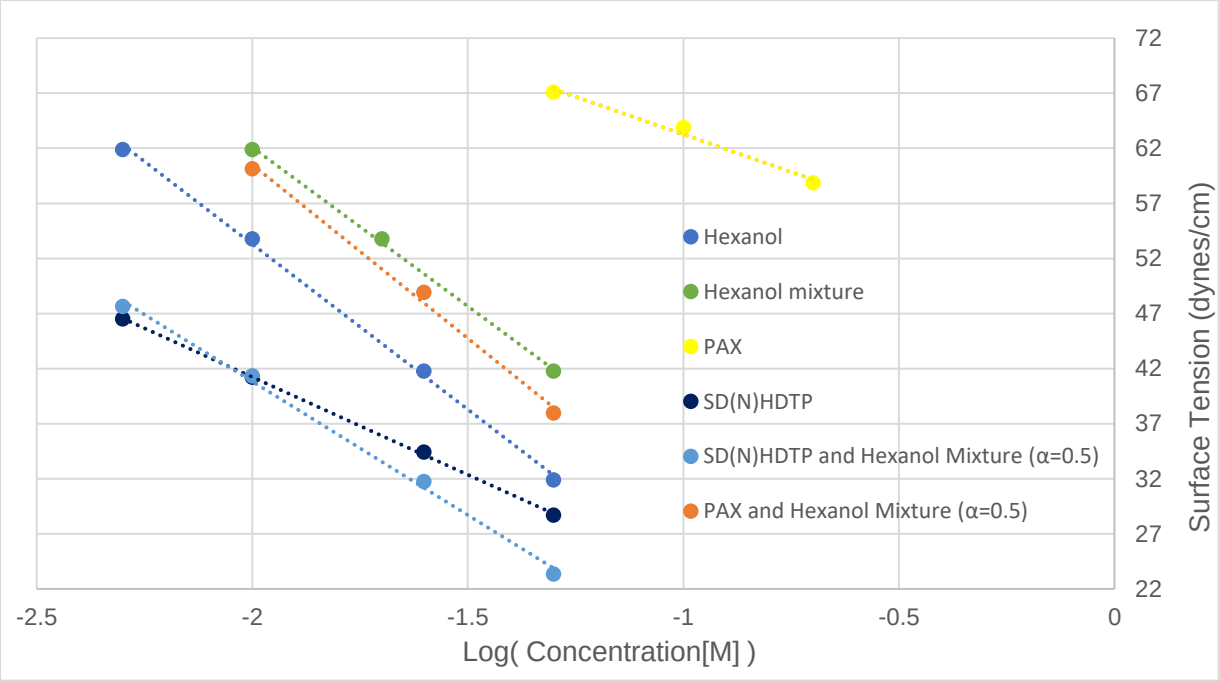

Figure 4.37: Surface tension vs Log concentration for PAX, SD(N)HDTP, hexanol, and the mixtures of 50 mole percent of the collectors and hexanol.

Figure 4.37 compares the surface tension of the longer chain length thiol collectors, and mixtures of these with hexanol as a function of the log of the concentrations. PAX showed greater interfacial activity than SIBX or PNBX. The mixture of PAX and hexanol showed a reduction of interfacial tension, compare to the hexanol mixture line.

The longer chain length, SD(N)HDTP (β = -2.13), showed a greater attractive interaction compared to SD(N)BDTP (β = -0.66) and SD(I)BDTP (β = -1.57). The inequality in Equation 20 also showed that the interaction between SD(N)HDTP and hexanol is synergistic, as the right-hand side of the equation was found to be 0.59 – less than the absolute value of the β parameter.

Table 4.25 shows that even though the interaction between SD(N)HDTP and hexanol is greater than the interaction between SD(I)BDTP, the difference between the experimental and calculated molecular surface areas for SD(I)BDTP and SD(N)HDTP, is -9.32 and -5.03, respectively. This can be attributed SD(I)BDTP having a greater molecular surface area than SD(H)DTP due to the branched chain.

Similarly, to the branched chain DTP, longer alkyl chain lengths can also increase the inductive effects on the head group of the molecule. This may influence the interactions between the collector and the frother. Longer alkyl chain lengths can also increase the Van der Waals forces between the alkyl chains, whether between self-associating molecules or associating in mixtures, which can enhance the attractive interactions.

4.6.3.3 Alcohol vs polypropylene glycol frothers

Polypropylene glycol (PPG) frothers are much more soluble than aliphatic alcohol frothers, mainly due to their heterogenous distribution of alternating polar and non-polar components. These frothers form a different structure at the air-water interface compared to alcohols, where PPG forms a polymeric matrix which tends to lie flat on the bubble surface (Gupta et al., 2007). The mixture of SD(N)DTP and PPG425 was investigated to observe if similar interactions are present between DTP and other frothers.

The β parameter for the mixture of PPG425 and SD(N)BDTP (β = -3.92) shows that there is a strong attractive interaction between these reagents, when compared to hexanol and SD(N)BDTP (β = -0.66). The inequality in Equation 20 is also satisfied, where the right-hand side of the equation produces a value of 0.69, so the interaction between PPG425 and SD(N)BDTP is synergistic. The difference in packing of these frothers could play a large role in how they interact with DTP at the air-water interface.

4.6.3.4 Difference in structure for functional group of DTP

It has been proposed that the interaction between thiol collectors with non-ionic frothers is through hydrogen bonding via the oxygen atoms in the functional group of the collector (Bradshaw & O'Connor, 1998). From Figure 2.4 in the literature review section 2.2.3, it can be observed that the DTP molecule has two oxygen atoms, which might make it possible for interactions with frother molecules. To test if this hypothesis is plausible, tests were performed with mixtures of SD(I)BDTPINA and hexanol. SD(I)BDTPINA has a similar structure to SD(I)BDTP, except that it does not have the oxygen atoms and, instead the alkyl chains link directly to the phosphorus atom (Figure 4.38).

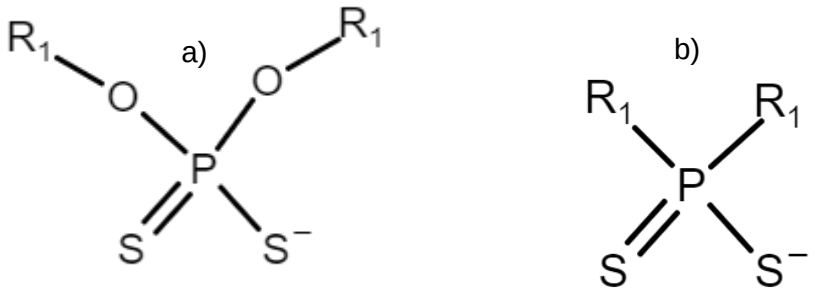

Figure 4.38: The molecular structure of a) dithiophosphate and b) dithiophosphinate

Table 4.25 shows that the β parameters for SD(I)BDTPINA (β = -1.40) and SD(I)BDTP (β = -1.57) with hexanol are relatively similar with both mixtures producing a synergistic interaction. SD(I)BDTPINA is as active at the air-water interface as SD(I)BDTP, but SIBX is still not as active as either of these molecules. It could be that the stronger activity of these molecules at the air-water interface provides an opportunity for the frother molecules to interact with them. It is not clear if the interaction between DTP and non-ionic frothers are through the oxygen atoms in the headgroup of the molecule.

4.6.3.5 Regular solution theory summary

The regular solution theory approach shows that there are attractive molecular interactions between DTP and non-ionic frothers. The β parameters demonstrate that increasing the alkyl chain length of DTP increases the strength of the molecular interactions between these molecules. Branching the alkyl chain of DTP also further increases the strength of the molecular interactions.

The experimental and ideal cross sectional surface area shows that the experimental area is less than the ideal surface area for DTP-frother mixtures. This also supports the attractive molecular interactions between DTP and non-ionic frother molecules.

No interactions were observed between xanthate and hexanol using the regular solution theory approach. Furthermore, xanthate consistently exhibited lower surface activity at the air-water interface compared to DTP.

5 Discussion

This section of the thesis will discuss the results presented in chapter 4. The results will be related to the key objectives.

The discussion will be structured as follows:

- Collectors (in the absence of frothers):
    - Bubble-particle attachment results,
    - Microflotation recovery results,
    - Adsorption results
    - For each mineral, viz., Galena, Pyrite, Chalcopyrite and Chalcocite
- Frothers (in the absence of collectors):
    - Bubble-particle attachment results,
    - Microflotation recovery results,
    - For each mineral, viz., Galena, Pyrite, Chalcopyrite and Chalcocite
- Collector-frother mixtures: Effect of synergistic interaction between these reagents on:
    - Recovery and bubble-particle attachments,
    - Molecular interactions between the respective reagents
        - At the air-water and,
        - Mineral-water interface,
    - Mechanism of collector transfer from the air-water interface.

The effect of each reagent on the pulp phase will firstly be evaluated separately. This will focus on the effect of collectors on pulp phase recovery and bubble-particle attachment and on the adsorption of collectors on the mineral surface. Furthermore, the effect of frothers on pulp-phase recovery and bubble-particle attachment will be discussed. After the effects of each reagent is quantified, the effect of collector-frother mixtures on pulp phase recovery and bubble-particle attachment will be evaluated to observe if there is a synergistic improvement in pulp-phase recovery or if each of the reagents have separate roles in the improvement of pulp-phase recovery. The molecular interactions between collectors and frothers at the air-water and mineral-water interface will be discussed along with aeration adsorption results to explain the mechanism whereby the mixture of these reagents improve pulp-phase recovery.

5.1 Collectors

The function of the collector is to adsorb at the mineral-water interface to control the hydrophobicity of the mineral surface so as to facilitate bubble-particle attachment. The hydrophobicity that the collector induces at the mineral-water interface is governed by many factors such as its reactivity with the mineral surface, the chemical structure of the collector, the surface collector species that form, and the oxidation state of the mineral surface.

This section on collectors will review interactions between collectors and sulphide minerals, in the absence of frothers, to establish the differences between the behaviour of DTP and xanthate. Although collector interactions with sulphide minerals are relatively well established in the literature, it is important to carefully characterise the interaction between the single reagents at each interface (mineral-water and air-water) in order to use that information in the analysis of the collector-frother mixture results.

5.1.1 The effect of collectors on pulp phase recovery and bubble-particle attachment

Pulp-phase recovery is the most direct way to measure if a collector effectively induces hydrophobicity on the mineral surface. In this section the microflotation and automated contact time apparatus results will be compared to collector adsorption results. These results are compared to understand if the collector is present on the mineral surface (UV-Vis adsorption results to determine residual concentrations after contact with the mineral), the reactivity of the collector species with the mineral surface (heat of adsorption results) and if the species that formed on the mineral surface are inducing hydrophobicity at the mineral surface (microflotation and ACTA results).

The natural flotation behaviour of each mineral will be compared to the results where SDEDTP and SEX, respectively, are present. Xanthate was used as benchmark comparison to DTP as xanthate is the most common thiol collector used in sulphide mineral flotation operations and its behaviour is well documented. In most cases, the ethyl chain length derivative is used, unless otherwise stated.

5.1.1.1 Galena

In order for a collector to improve mineral flotation, it first needs to adsorb at the mineral surface to induce hydrophobicity which then facilitates bubble-particle attachment and recovery to the froth phase. It is well established from literature that the ethyl homologue of

DTP does not adsorb onto galena's surface at basic pH's and does not improve mineral recovery (Buckley & Woods, 1991; McFadzean, Castelyn & O'Connor, 2012; McFadzean & O'Connor, 2014; Sutherland and Wark, 1955; Taguta 2015; Wark and Cox, 1934).

Table 5.1: Summary of microflotation, ACTA and adsorption results for SDEDTP and SEX on galena at pH 9. SEX heat of adsorption data obtained from Taguta (2015).

	No reagents	**SDEDTP**	**SEX**
Collector adsorbed (mol %)	N/A	~0	96.4 ± 0.08
Heat of adsorption (kJ/mol)	N/A	-11.7	-35.9
Recovery (%)	91 ± 1.37	93.5 ± 0.36	89.9 ± 0.37
First order rate constant, k (min^{-1})	0.26 ± 0.169	0.30 ± 0.174	0.22 ± 0.158
Attachment Probability	0.029	0.026	0.058

From the UV-Vis adsorption and isothermal titration calorimetry results summarised in Table 5.1, it can be observed that negligible amounts of SDEDTP adsorb onto the galena surface at pH 9, and that the heat of adsorption of SDEDTP is relatively low (-11.7 kJ/mol) compared to that of SEX (-35.9 kJ/mol).

Sutherland & Wark (1955) determined the residual concentration of SDEDTP remaining in the pulp for galena as a function of pH. The critical pH (the pH at which the collector does not adsorb onto the mineral or induce hydrophobicity on the mineral surface) was found to be 6, similar to the 6.2 determined by Wark & Cox (1934). So, the results in Table 5.1 are consistent showing as they do that SDEDTP does not interact with galena at pH 9.

McFadzean & O'Connor (2014) and Taguta (2015) found that the heat of interaction between SDEDTP and galena at pH 9 was negligible which supports the findings discussed above. However, the value determined from this study was -11.7 kJ/mol. As the duration of these experiments are of the order of hours and the pulp concentration of pure minerals in the test ampoule is quite high (23% by weight) it was observed that the mineral buffered and lowered the pH. The lowering of the pH may have allowed for interaction of SDEDTP with the mineral producing a slightly greater heat of interaction.

Buckley & Woods (1991) performed cyclic voltammetry tests and Auger electron spectroscopy (AES) with galena and ethyl DTP at pH 5 which is lower than the critical pH of SDEDTP on galena (Sutherland & Wark, 1955). AES showed that even though the pH was below the critical pH, no DTP was present on the mineral surface, even on freshly fractured surfaces. Further investigation with voltammograms suggested that the metal thiolate formed on the

mineral surface but due to the high solubility of the metal thiolate it dissolved back into the aqueous phase. McFadzean & O'Connor (2014) observed that SDEDTP produced a high heat of dilution relative to SEX when performing ITC with galena. The higher heat was attributed to a stronger interaction of SDEDTP with water relative to SEX, which correlates with the solubility of the lead thiolates, viz 5.2 x 10^{-11} M for SDEDTP (Buckley & Woods, 1991) and 1.7 x 10^{-17} M for SEX (Kakovskii, 1957). In the case of SEX, the formation of the metal thiolate occurs in the aqueous phase, where the low solubility of the complex results in its precipitation on the mineral surface (McFadzean & O'Connor, 2014).

The microflotation tests that were conducted showed that galena was naturally floatable at pH 9, achieving a recovery of 91%. The high floatability of galena has been observed in other studies (Taguta, 2015; Kelebek & Yoruk, 2002). The natural floatability of galena thus made it difficult to discern the effect of SDEDTP or SEX on galena recovery. In some instances, the first order rate constant was used as a proxy to observe the effects of these reagents.

The relative absence of SDEDTP on the mineral surface is clearly reflected in the contact time results. Table 5.1 shows negligible improvements in the attachment probability in the presence of SDEDTP compared to the mineral without any reagents. Similarly, the difference in the recovery and first-order rate constant (determined from the fitting on the Klimpel model) in the microflotation cell were negligible (within experimental error). Other studies (McFadzean, Castelyn & O'Connor, 2012; Taguta, 2015) have similarly shown that SDEDTP did not have any significant impact on galena microflotation at pH 9.

The adsorption of SEX onto galena is well established, where the metal thiolate is the species present on the mineral surface (Alison et al., 1972; Finkelstein & Goold, 1972; Finkelstein & Poling, 1977; Woods & Gardner, 1997). The results from Table 5.1 show that 96.4% of the dosage adsorbed onto the mineral surface, which is equivalent to a coverage of half a monolayer on the mineral surface. Nevertheless, such a coverage of SEX on galena did not affect the microflotation recovery compared to the natural floatability of galena.

Taguta, O'Connor & McFadzean (2017) found that the adsorption of SEX onto galena produced a heat of adsorption of -35.9 kJ/mol, but SEX did not improve the microflotation recovery compared to collectorless conditions. Taguta (2015) concluded that the heat of interaction of the collector with the mineral surface was not an indicator for mineral surface hydrophobicity, but rather only provides information about the reactivity and the mechanism of interaction between the collector and the mineral. So even though SEX adsorbs onto the mineral surface it does not improve mineral surface hydrophobicity to an extent that can be detected in microflotation tests at these dosages.

Contact time tests showed improvement in the attachment probability (5.7%) for SEX compared to the attachment probability of galena without any reagents (2.9%). The attachment probability for these tests were, however, relatively low as the contact time chosen was quite short (20ms), the limit at which the ACTA could operate. The improvements observed in the attachment probability for SEX are not reflected in the microflotation results.

This discrepancy may be due to differences in bubble-particle attachment subprocesses in each device. Flotation in the microflotation cell is controlled by all subprocesses of bubble-particle attachment – collision, attachment, and detachment. In the ACTA the collision probability is effectively set to 1 as the bubble is squeezed onto the particle bed. The detachment probability will also be much lower in the ACTA as the energy input into the system is much lower compared to the microflotation cell.

Neither SDEDTP nor SEX result in improvements in galena recovery but interact with the mineral surface differently. The lack of adsorption of SDEDTP and the complete adsorption of SEX onto galena, is governed by the structure of the head groups of these thiol collectors. DTP has two electron withdrawing oxygen atoms which withdraw electron density from the dithiol head group giving it the most non-ionic character. Xanthate on the other hand only has one oxygen atom in its thiol head group, resulting in higher electron density in the dithiol headgroup and greater extent of reactivity with the mineral surface. This may explain the differences in the heat of adsorption between these two reagents.

5.1.1.2 Pyrite

Very little research has been conducted on measuring the interaction of DTP and pyrite, but this may be due to industry practice as DTP is typically used for its selectivity against pyrite (Lotter & Bradshaw, 2010).

Table 5.2 summarises the adsorption and microflotation studies performed on pyrite. UV-Vis adsorption of reagent in the pulp showed that ~70% of the dosage of SDEDTP adsorbed onto the mineral creating ~35% monolayer coverage. Even though UV-Vis shows that SDEDTP is present on the mineral surface, the heat of interaction shows that the interaction is -5.3 kJ/mol relative to the -57.1 kJ/mol of SEX on pyrite (results from Taguta et al. (2017)). This result indicates that SDEDTP physisorbs onto the surface of pyrite. Wang & Zeng (2012) characterised interaction energies of less than -40 kJ/mol as physisorption reactions. The heat of interaction in the case of pyrite with SDEDTP, -5.3 kJ/mol, is significantly less negative than the threshold value -40 kJ/mol.

Table 5.2: Summary of microflotation, ACTA and adsorption results for SDEDTP and SEX on pyrite at pH 9. SEX heat of adsorption data obtained from Taguta (2015). NP – Not performed.

	No reagents	***50 % Monolayer SDEDTP***	***[0.1 mM] SDEDTP***	***SEX***	***0.1 Monolayer SIBX + 0.1 [mM] SDEDTP***
% Collector adsorbed (mol %)	N/A	69.3 ± 2.35	NP	88.2 ± 2.10	NP
Heat of adsorption (kJ/mol)	N/A	-5.3	NP	-57.1	NP
Recovery %	11.0 ± 0.86	7.8 ± 0.04	5.1 ± 0.41	6.9 ± 1.08	9.8 ± 2.60
First order rate constant, k (min^{-1})	0.1 ± 0.03	0.13 ± 0.01	0.08 ± 0.01	0.19 ± 0.01	0.09 ± 0.12
Attachment Probability	0.094 ± 0.0004	0.127	NP	0.031	NP

Even though SDEDTP is present on the pyrite surface, it did not improve mineral floatability. The natural floatability of pyrite at pH 9 resulted in 11% recovery, whereas the presence of SDEDTP decreased the recovery to 7.8%. Similarly, Taguta, O'Connor & McFadzean (2017) and Jordaan (2018) observed that SDEDTP had no effect on the microflotation recovery of pyrite at pH 9. In the ACTA tests improvements in the attachment probability of pyrite was observed upon addition of SDEDTP, with the attachment probability of pyrite at pH 9 increasing from 9.4% to 12.7% in the presence of SDEDTP. These small improvements in the ACTA may not reflect in the microflotation cell as the contact time used in the ACTA was 100 ms, whereas back calculated contact times in the UCT microflotation cell were on the order of 10 ms (Min & Nguyen, 2012).

The UV-Vis adsorption tests for pyrite showed that 88.2% of the SEX dosage adsorbed onto the mineral resulting in 44.1% monolayer coverage. However, this did not improve the recovery or attachment probability of pyrite compared to the condition where no reagents are present. This is similar to the results for galena, where 96% of the SEX adsorbed, but produced no improvement in attachment probability.

Hanson & Fuerstenau (1993) found, similarly that the floatability of pyrite at pH 9 in the presence of SEX is strongly dependent on the concentration of the collector in the pulp, with collector concentrations of around 1 x 10^{-5} M only yielding a recovery of 10%. In this study,

SEX shows similar behaviour. The concentration of SEX used was 5 x 10^{-5} M which yielded a pyrite recovery of 6.9 %.

From both the adsorption data and the flotation results it can be concluded that the collector species (for both SDEDTP and SEX) that form on the surface of pyrite do not induce sufficient hydrophobicity to induce improved flotation recovery.

5.1.1.3 Chalcopyrite

Many authors have concluded that the interaction of DTP with the chalcopyrite is dependent on pH (Güler et al., 2005; Petrus et al., 2011; Grano et al., 1997). At more alkaline conditions the formation of ferric hydroxide species on the mineral surface may inhibit the adsorption of DTP.

Table 5.3 summarises the adsorption and floatability results of chalcopyrite in the presence of SDEDTP. UV-Vis adsorption tests showed that 71.2% of the dosage of SDEDTP adsorbed onto the mineral surface, resulting in 35.6% monolayer coverage. Similarly to the behaviour on pyrite, the heat of adsorption of SDEDTP onto chalcopyrite was very low, viz. -4.6 kJ/mol. The critical pH of SDEDTP at which the residual concentration begins to increase was found to be around 9.5 for chalcopyrite (Sutherland & Wark, 1955). The tests conducted in this study were performed at pH 9, which is slightly below the critical pH, so some adsorption of SDEDTP is expected.

Table 5.3: Summary of microflotation, ACTA and adsorption results for SDEDTP and SEX on chalcopyrite at pH 9. SEX heat of adsorption data obtained from Taguta (2015).

	No reagents	**SDEDTP**	**SEX**
% Collector adsorbed	N/A	71.2 ± 0.92	74.6 ± 1.13
Heat of adsorption	N/A	-4.6	-33.4
Recovery %	83.2 ± 1.31	85.2 ± 0.21	87.7 ± 0.01
First order rate constant k (min^{-1})	0.24 ± 0.08	0.29 ± 0.08	0.92 ± 0.02
Mass Recovered (mg)	10.5	7.9	28.6

Most investigations into the adsorption of ethyl DTP onto chalcopyrite at pH 9 detect low surface concentrations of SDEDTP (Güler et al., 2005; Petrus et al., 2011; Grano et al., 1997) compared to xanthate, while the species that form on the surface have not been agreed upon. Güler et al. (2005) suggested that SDEDTP may oxidize into its radical form ($DEDTP^0$) which chemisorbs onto the mineral surface. This mechanism proposed for SDEDTP and chalcopyrite has also been observed on chalcocite (Buckley & Woods, 1993; Chander & Fuerstenau,

1974). This may not be the case in the present study as both minerals exhibit completely different flotation responses to the addition of SDEDTP. Chalcopyrite shows no significant improvement in recovery or kinetics compared to the condition where no reagents are present, which has been observed in this study and other studies (Taguta et al., 2017; Güler et al., 2005; Petrus et al., 2011), whereas chalcocite showed a strong recovery response to the addition of SDEDTP (Figure 4.7).

In common with the effect of SDEDTP on the recovery of pyrite, the presence of SDEDTP on the surface of chalcopyrite did not enhance the natural floatability of chalcopyrite, only showing very slight improvements in final recovery. The fitted Klimpel first-order rate constant showed an improvement in the kinetics, but when looking at the recovery time curves for the microflotation of chalcopyrite in Figure 4.6, SDEDTP does not discernibly improve kinetics within experimental error. Results from the ACTA indicate that the presence of SDEDTP lowers the recovery without any reagents, from 10.5 mg to 7.9 mg. Microflotation and ACTA results indicate that the species present on the surface of chalcopyrite are not contributing to raising the hydrophobicity of the mineral to the critical concentration required for attachment to occur.

The behaviour of SDEDTP on chalcopyrite is very similar to that of SDEDTP on pyrite. On both minerals SDEDTP adsorbs to some extent but showed very low heats of adsorption. The resultant species that form on the surface of these minerals do not seem to influence the critical hydrophobicity of the mineral surface required for bubble-particle attachment, having no significant impact on pulp phase recovery as indicated by microflotation.

Taguta et al (2017) found that the heat of adsorption of SDEDTP onto chalcopyrite at pH 9.2 was -4.9 kJ/mol which is similar to the heat of adsorption obtained in this study. This low heat of adsorption indicates that SDEDTP physisorbs onto chalcopyrite.

From Table 5.3, the adsorption density of SEX onto chalcopyrite was similar to that of SDEDTP, where SEX formed a monolayer coverage of 37.3%. Taguta et al (2017) found that the heat of interaction of SEX with chalcopyrite at pH 9 was -33.4 kJ/mol, which is significantly greater than that for SDEDTP. The interaction of chalcopyrite with xanthate results in the formation of the metal thiolate (Finkelstein & Goold, 1972; Raju & Forsling, 1997), the dithiolate (Alison et al., 1972; Leppinen, Basilio & Yoon, 1989) or a mixture of these species (Leppinen, 1990). These species deposit onto the surface of the mineral and are responsible for the hydrophobicity on the mineral surface.

SEX does not have a large effect on chalcopyrite final recovery since it is naturally floatable, yielding a recovery of 83.2% in the absence of the collector. However, the first-order rate constant shows that SEX has a significant effect on the kinetics. From Table 5.3 it can be seen that the first order rate constant increased from 0.24 min^{-1} for the natural floatability of chalcopyrite to 0.92 min^{-1} when using SEX. Similarly, the ACTA results showed that chalcopyrite recovery increased from 10.5 mg to 28.6 mg in the presence of SEX. The improved kinetics observed in the microflotation cell and the greater mass recovered in the ACTA upon the addition of SEX show that SEX improves the mineral surface hydrophobicity.

5.1.1.4 Chalcocite

The interaction of SDEDTP with chalcocite has been established in literature (Woods, Kim & Yoon, 1993; Buckley & Woods, 1993; Mielczarski & Minni, 1984), where the collector species that form on the surface of chalcocite have been shown to improve mineral recovery.

Table 5.4 shows that of the 50% monolayer dosage of SDEDTP almost completely adsorbs onto chalcocite's surface at pH 9 and that the heat of adsorption of SDEDTP with chalcocite was -30.8 kJ/mol, which is substantially higher than for any of the other minerals tested, and is very similar to SEX heat of adsorption onto galena and chalcopyrite. Buckley & Woods (1993) have shown that SDEDTP adsorbs onto the surface of chalcocite, where the species present on the mineral surface is the chemisorbed form as the collector was found to deposit onto the mineral surface at potentials below that required for the formation of CuDTP. Chemisorption is when the collector bonds to a metal atom that is still a part of the surface of the mineral. The reaction is described by Equation 2 and 3 under section 2.3.1.1

Table 5.4: Summary of microflotation, ACTA and adsorption results for SDEDTP and SEX on chalcopyrite at pH 9. NP – Not performed.

	No reagents	**SDEDTP**	**SEX**
% Collector adsorbed	N/A	97.0 ± 5.78	97.7 ± 0.39
Heat of adsorption (kJ/mol)	N/A	-30.8	NP
Recovery %	10.4 ±	48.2 ± 0.64	27.3 ± 2.13
Mass recovery (mg)	0.8	51.7	44.5

The chemisorbed diethyl DTP on the surface of chalcocite has a strong effect on chalcocite recovery. From Table 5.4 it can be seen that 20% monolayer dosage of SDEDTP used improved the recovery relative to the natural floatability, increasing the recovery from 10.4% to 48.2% within the first 2 minutes. The recovery results from the ACTA, where 50% monolayer dosages were used, also showed large increases in recovery. SDEDTP yielded a recovery of 51.7 mg chalcocite, whereas without any reagents the recovery was only 0.8 mg. These results are consistent with the results obtained by Woods, Kim & Yoon (1993), where 50% monolayer dosage resulted in 90% recovery in 1 minute in a microflotation cell.

Typically, with metal thiolates the hydrophobic character of the complex is influenced by the metal atom, where the electronegativity of the metal atom determines the hydrophobicity. The greater the relative electronegativity difference between the sulfur atom of the collector and the metal ion, the less the hydrophobic character (Rao, 2013:483). This is due to the inductive effects. Electronegative metal ions draw electron density from the alkyl chain making them more polar in character, which would be especially prevalent in short chain collectors. Since it is shown that SDEDTP interacts with copper atoms bonded in the lattice of the mineral (Buckley & Woods, 1993), they may not have the same degree of electronegativity as copper ions in the bulk solution.

In the case of SEX, most of the 50% monolayer dosage adsorbed onto chalcocite, the same as for SDEDTP. According to Woods, Young & Yoon (1990) the mechanism of adsorption is similar, with the formation of chemisorbed SEX on the chalcocite surface. Microflotation results show that the 20% monolayer dosage increased the natural floatability of chalcocite from 10.4% to 27.3%, and in the ACTA an increase in recovery from 0.8 mg to 44.5 mg chalcocite.

Interestingly this is one of the few cases where DTP outperforms xanthate as a collector. Due to its structure, xanthate is more reactive with minerals and generally forms metal thiolates or dithiolates that are much less soluble than those of DTP. The difference in the performance of the two collectors in the case of chalcocite might be attributed to DTP having two alkyl chains giving a greater hydrophobic character, whereas xanthate only has one alkyl chain.

5.1.1.4.1 Longer chain lengths

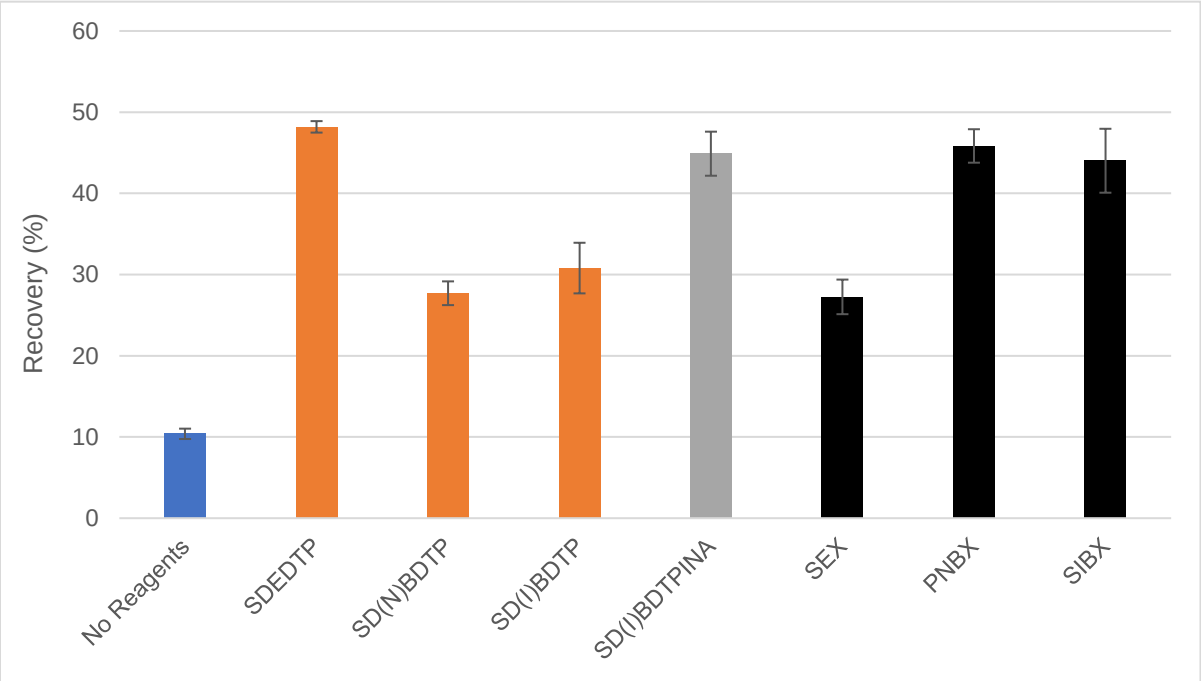

Figure 5.1: Recovery of chalcocite in the first two minutes of flotation at pH 9 using longer chain length thiol collectors. Collectors are dosed at 20% monolayer coverage.

Figure 5.1 summarises the effect of longer chain length DTP's and xanthates on chalcocite microflotation recovery. SD(I)BDTPINA was also used due to its similar headgroup structure to DTP (Figure 4.38). UV-Vis adsorption tests showed that there were no traces of the longer chain length homologues of collectors remaining in the pulp.

Generally longer chain length collectors impart a greater degree of hydrophobicity on the mineral surface. From Figure 5.1 this trend is observed for the xanthate homologues. SEX produces the lowest recovery, with PNBX and SIBX producing similar recoveries. In the case of DTP this is not observed. The ethyl chain length in SDEDTP yielded much higher recoveries than the butyl or isobutyl homologues. The reason for this behaviour of DTP is not clear. It is possible that the longer chain homologues form the metal thiolate instead of the chemisorbed form which can have an impact on the hydrophobicity of the species formed on the mineral surface.

The improved recovery of SD(I)BDTPINA relative to SD(I)BDTP can be attributed to the difference in molecular structure. The DTP headgroup has the two electron withdrawing oxygens which inductively draw electron density away from the reactive thiol headgroup, whereas with the DTPINA the oxygen atoms are absent so the collector should be much more reactive with the mineral.

5.1.2 Summary

Table 5.5 summarises the results observed on the addition of ethyl DTP to the various sulphide minerals in the absence of frother. These results were compared to those of the equivalent chain length ethyl xanthate collector in the absence of frother. The general observation is that for galena, pyrite, and chalcopyrite, SDEDTP is not an effective collector. Even when the collector is present on the mineral surface it does not form surface species that impart sufficient hydrophobicity at the mineral surface to be observed in the microflotation and ACTA results. Similar results were observed for SEX with galena and pyrite, where SEX did not improve the recovery or attachment probability of these minerals compared to the condition where no reagents were present. However, SEX was an effective collector for chalcopyrite. The ethyl homologue of both collectors is not effective in most cases in improving mineral recovery. The SDEDTP interaction with chalcocite was found to be different to the other minerals in that a strong improvement in bubble-particle attachment was noticed for both the ACTA and microflotation experiments. The significance of these observations, in the absence of frother, will be discussed further when the collector-frother interactions are discussed in Section 5.3.

Examining the headgroup structure of DTP and xanthate may explain the difference in adsorption energies and the hydrophobicity of the species that form on the mineral surface when contacted with the collectors. However, the metal thiolate species that form also have a significant impact on the hydrophobicity. Decreasing electronegativity of the metal ion increases the hydrophobic character of metal thiolate (Rao, 2013:483). Therefore, the thiol collectors would be most effective on the copper sulphides compared to lead and iron sulphides, which is what is observed for chalcocite (for DTP and xanthate collectors) and chalcopyrite (for SEX).

The results from microflotation and ACTA show similar trends where increases in hydrophobicity are reflected in both devices. The ACTA can detect more subtle changes in hydrophobicity, which may be due to the device decoupling the subprocesses of bubble-particle attachment, observing only the attachment step. In the microflotation cell all the subprocesses of bubble-particle attachment occur (collision, attachment, detachment), so if one of these is a rate limiting step, only the overall effect of the reagent on bubble-particle attachment will be observed.

Table 5.5: Summary of the interaction of the thiol collectors with the sulphide minerals studied, and the effect of the thiol collectors on bubble particle attachment.

	Galena		Pyrite		Chalcopyrite		Chalcocite	
	SEX	SDEDTP	SEX	SDEDTP	SEX	SDEDTP	SEX	SDEDTP
Adsorption / Interaction with mineral?	✓	✗	✓	✓	✓	✓	✓	✓
Improvement in bubble-particle attachment?	✗	✗	✗	✗	✓	✗	✓	✓

5.2 Frothers

Frothers are added to the flotation system to reduce bubble coalescence in the pulp and to improve froth stability, but some authors have reported that frothers can have a strong effect on bubble-particle attachment kinetics (Lekki & Laskowski, 1971; Leja & He, 1984; Mukai, Wakamatsu & Takahashi, 1972; Dai, Bradshaw & Harris, 2001; Jordaan, 2018).

5.2.1 Effect of frothers on bubble-particle attachment

The effect of hexanol on bubble particle attachment is summarised in Table 5.6. The results from the microflotation tests show that hexanol improved mineral recovery and also the rate of flotation for galena, pyrite, chalcopyrite, and chalcocite without the presence of any collector. This section will examine the effects of frothers on various aspects of flotation performance in the absence of collectors.

In the ACTA tests, where the attachment subprocess is decoupled from the collision and detachment subprocess, there is a decrease in attachment probability observed upon the addition of hexanol. The attachment probability for each mineral basically halves compared to the attachment probability where no reagents are present (Chalcopyrite had 100% attachment

probability so the mass of the mineral recovered was used as a proxy, but the same trend was observed). In the ACTA tests the bubble size was controlled so the decrease in attachment probability was not due to a change in bubble size. The effect that is observed is purely due to the interfacial chemistry at the air-water interface, the mineral-water interface and the intervening thin film.

Table 5.6: A summary on the effect of hexanol on bubble-particle attachment for galena, pyrite, chalcopyrite and chalcocite at pH 9.

	Galena		*Pyrite*		*Chalcopyrite*		*Chalcocite*	
Reagents	No reagents	Hexanol	No reagents	Hexanol	No reagents	Hexanol	No reagents	Hexanol
Microflotation								
Recovery %	91.0 ±1.37	95.4 ±2.48	11.0 ±0.86	27.5 ±1.41	83.2 ±1.31	94.4 ±0.03	10.4 ±0.64	17.0 ±0.16
First-order rate constant (min^{-1})	0.26 ±0.169	2.60 ±0.031	0.10 ±0.030	0.11 ±0.026	0.24 ±0.080	0.74 ±0.138	N/A	N/A
ACTA								
Attachment Probability	0.029	0.014	0.094 ±0.005	0.065 ±0.0055	N/A	N/A	0.118	0.062
Recovery (mg)	0.4	0.3	NP	NP	10.5	3	0.8	1

The differences observed in the microflotation cell compared to the ACTA could be due to many factors. In the microflotation cell variables such as bubble-rise velocity and bubble size are not controlled for which could be affected by the addition of the frother. These will be discussed in further detail below.

5.2.1.1 Decrease in bubble-particle attachment probability.

The lower attachment probabilities observed for bubble-particle attachment relative to the case where no reagents are present can be explained by the same theory that describes why bubble-bubble interactions do not result in coalescence. During bubble-bubble interactions the frother can create a kinetic resistance to the drainage of the thin film between the bubbles. This happens due to hydrogen bonding between the polar group of the frother and the water molecules. This hydrogen bonding interaction can form a stable immobile film around the bubble that can resist bubble coalescence in the pulp and froth (Rodel, 1981).

Similarly, during bubble-particle attachment, the thin film between the particle and bubble starts to drain. The interaction of the polar group of the frother and the water molecules in the thin film can resist the drainage, reducing the chances of the film reaching critical thickness and the rupture of the thin film. Furthermore, the Marangoni effect, which is a restorative force can further stabilise the film against drainage.

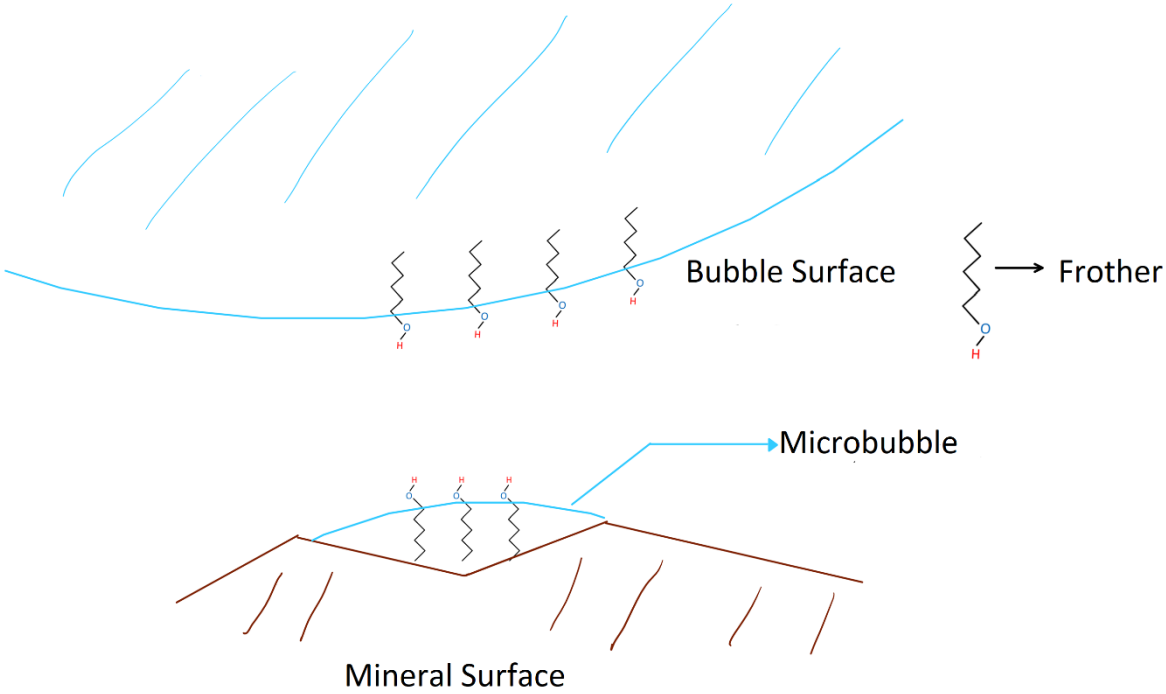

Figure 5.2: Diagram depicting microbubbles at the mineral surface

Microbubbles at the solid-water interface have also been shown to increase the induction time in the presence of a non-ionic frother. Flotation frothers are thought to adsorb onto these bubbles and during bubble-particle interaction, the entrapped micro bubbles at the mineral surface (depicted in Figure 5.2) and colliding bubble can resist drainage of the thin film between them, increasing the induction time (Kosior et al., 2013).

Both theories stem from the same principle that the frother at the air-water interface stabilizes a thin film of water around it. Without the presence of the collector, the interaction between the bare mineral surface and the frother coated bubble is analogous to a bubble-bubble interaction. When the bubble-particle interaction occurs in the microflotation cell this effect is not apparent anymore and improvements in recovery and kinetics are observed.

5.2.1.2 Improvement in bubble-particle attachment kinetics – microflotation

When looking at the effects that surface chemistry has on the bubble-particle attachment in the ACTA, a decrease in attachment probability is observed. Therefore, the improvements in recovery in the microflotation cell must be due to the physical effects the frother has on bubble-

particle interactions in the pulp i.e., the collision efficiency between the bubble and the particle. These will be mainly determined by the bubble size or the bubble rise velocity, in this case, since other parameters such as energy input remain constant.

5.2.1.2.1 Bubble rise velocity

A decrease in the bubble rise velocity can enhance the bubble-particle attachment probability as it lengthens the sliding contact time of a bubble over a particle (Nguyen & Schulze, 2004).

In the microflotation cell it is unlikely that the bubble reaches terminal velocity. The distance from the capillary where the bubble is generated to the pulp zone in the microflotation is 1.5 cm. Kowalczuk, Zawala & Drzymala (2017) showed that the velocity profile of a bubble in an aqueous solution of 1-pentanol depends on its concentration, where the bubble may reach terminal velocity anywhere between 5 to 30 cm.

The bubble terminal rise velocity was calculated from the following empirical equation (Kowalczuk, Zawala & Drzymala, 2017):

$$v = v_{min} + (v_{max} - v_{min})e^{-3\left(\frac{c}{CMV}\right)^2} \quad \text{Equation 21}$$

Where c is the concentration of the frother in solution CMV is the concentration at the minimum bubble rise velocity, v is the terminal rise velocity of the bubble at the concentration of the frother in solution, v_{min} and v_{max} is the minimum terminal velocity at the CMV and maximum terminal velocity in distilled water. The relationship and the fitting parameters were obtained from Kowalczuk, Zawala & Drzymala (2017).

Data from various studies is summarised in Table 5.7 below where microflotation recoveries of chalcocite in the presence of MIBC, Dow 200 and terpineol at various concentrations are compared to the rise velocities used. For all the frothers the rise velocity does not change significantly between the concentrations used, viz. 5.0 x 10^{-5} M and 1.0 x 10^{-4} M, but the recovery of the mineral increases by around 10 to 20% when the concentration is increased from the 5.0 x 10^{-5} M to 1.0 x 10^{-4} M.

From this it can also be concluded that the rise velocity does not have a significant impact on the recovery in the microflotation cell. It is possible that bubbles in the microflotation cell do not reach their terminal rise velocity or that the rise velocity does not have a significant impact on the sliding contact time as proposed by Nguyen & Schulze (2004). Possibly it could rather be the bubble size that has an impact on microflotation recovery.

5.2.1.2.2 Bubble size

Table 5.7: Comparison between microflotation recovery, frother concentration, rise velocity and CCC on chalcocite at pH 9.

Reference for microflotation data	Dai, Bradshaw & Harris (2001)							Lekki & Laskowski (1971)		
	MIBC			Dow 200		Terpineol		Terpineol		
CCC [M]	1.1E-04			4.9E-04		1.6E-04				
Concentration [M]	0	5.0E-05	1.0E-04	5.0E-05	1.0E-04	5.0E-05	1.0E-04	0	6.5E-05	1.3E-04
Recovery %	36.4	38.9	52.5	40.4	51.6	41.4	57.9	22.5	49.5	73
Rise velocity (cm/s)	35	34.1	31.6	35	35	15.3	15	35	15	15
Reference for rise velocity	Tan et al. (2013)			Tan & Finch (2016)		Kosior et al. (2013)				
Reference for CCC	Laskowski (2004)			Zhang et al. (2012)		Szyszka et al. (2006)				

Table 5.7 summarises the CCC, microflotation and rise velocity values taken from various references for MIBC, Dow 200 and terpineol at various concentrations. The purpose of the following discussion is to illustrate that the improvements in microflotation recovery noted, upon increase in frother concentration, were mostly related to an increase in bubble size in these studies.

The increase in recovery (Table 5.7) upon the addition of 5.0×10^{-5} M MIBC and Dow 200 is only around 2 – 5%, compared to no reagent being present. The CCC value of these frothers are much greater than 5.0×10^{-5} M as can be seen from Table 5.7. When increasing the concentration to 1.0×10^{-4} M, which is above the CCC for MIBC, the recovery is increased by 13.6%. For Dow 200 and terpineol the recovery increases as the concentration of the frother approaches the CCC.

Higher microflotation recoveries for chalcocite were observed for increasing concentrations of terpineol in the Lekki & Laskowski (1971) study compared to the Dai, Bradshaw & Harris (2001) study (Table 5.7). This can be attributed to the cell design used in that study (Figure 2.15). The Hallimond microflotation cell was used in Lekki and Laskowski (1971), which uses a glass frit of the same diameter as the cell to produce a swarm of bubbles. The swarm of bubbles increases the probability of bubble-bubble interaction in the pulp and the chance of coalescence and so low concentrations of frother can have a significant impact on reducing the bubble size. The UCT microflotation cell, which is used in the Dai, Bradshaw & Harris

(2001) study, uses a needle to produce a single stream of bubbles which may lower the probability of bubble coalescence, so the effect of the frother on recovery is not to the same extent.

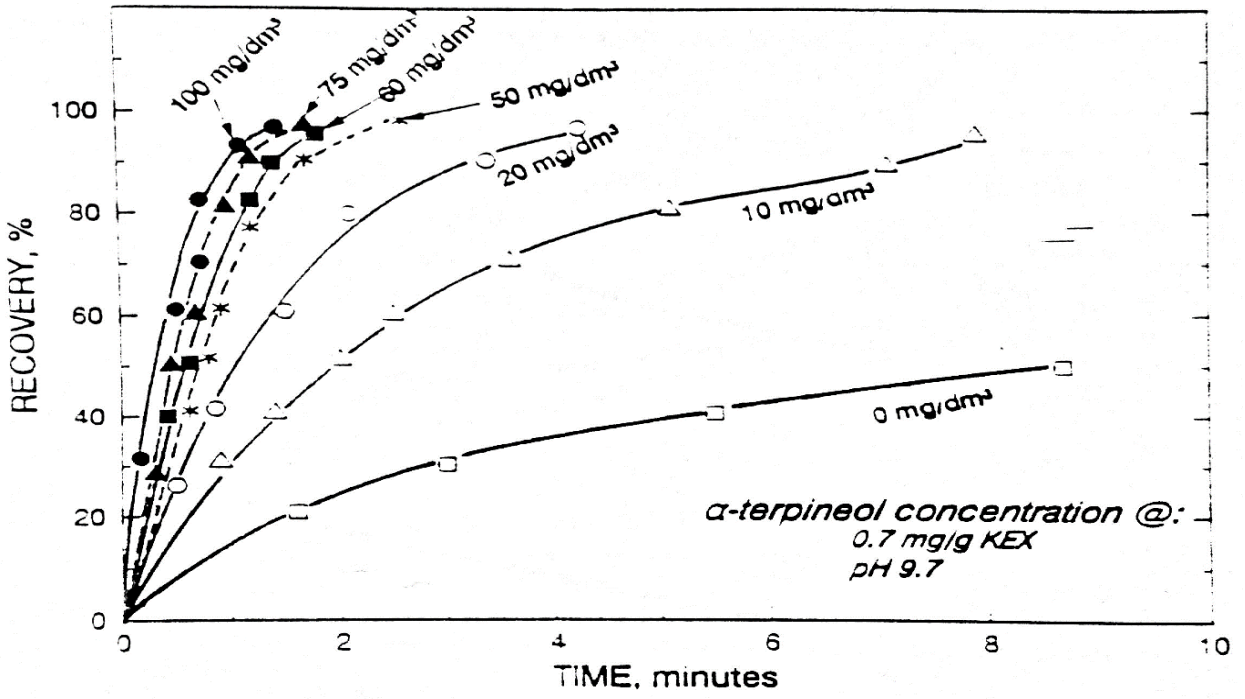

Figure 5.3: The recovery of chalcocite at pH 9.2 as a function of time. Each recovery curve represents an increase in the concentration of terpineol. (Lekki & Laskowski, 1971)

Figure 5.3 shows the effect that concentrations of terpineol greater than the CCC of the frother have on the recovery of chalcocite (Lekki & Laskowski, 1971). At dosages greater than 50 mg/L the rates of flotation are fairly similar. The CCC of terpineol is 24.26 mg/L, so the increase in recovery from 20 mg/L to 50 mg/L is because the concentration of terpineol is greater than the CCC value, the bubble size does not change, and under these conditions of fairly constant bubble size there is little change in the rates of recovery.

In contrast to the Lekki & Laskowski (1971) study, in the current microflotation study, all frothers were dosed just above the CCC of the frother. In particular for chalcocite two frothers were used, hexanol and octanol. Thesewere dosed at their CCC and, so the bubble sizes should be approximately the same in both cases (Cho & Laskowski, 2002). In the concentration ranges of the CCC of these frothers the surface tension is not affected so the size of the bubble produced at the capillary of the needle should be the same for both frothers, meaning that the bubble size is controlled through the mechanism of coalescence (Cho & Laskowski, 2001; Sweet et al., 1997). Improvements in recovery are observed relative to the natural floatability, but octanol does not improve the recovery to the same extent as hexanol.

As frothers affect many different aspects of the flotation process it is difficult to decouple the effects that the reagent has on the process and identify which effect is leading to an improvement in the recovery or bubble-particle attachment kinetics. From the perspective of the ACTA, where we observe the interactions between the bubble and the particle, the effect of the frother at the air-water interface during bubble-particle interaction is analogous to bubble-bubble interaction. In the microflotation cell where all the subprocesses of bubble-particle attachment are incorporated, frothers increase the recovery and this was attributed to the effect of frothers on bubble size and, therefore, an increase in the collision efficiency. The effect of bubble size was greater on recovery than the decrease observed for bubble-particle attachment probability in the ACTA, but other frothers, such as octanol, may exhibit a greater decrease in bubble particle attachment probability. This may account for the decrease in microflotation recovery observed when using octanol compared to hexanol, when bubble sizes were constant (Figure 4.11).

5.3 Collector-frother mixtures

Both the effect of the thiol collectors used in this study and the effect of the frothers have been characterised in the previous sections. The following section will focus on the mixtures of collectors and frother, their effect on bubble-particle attachment, and their effect on adsorption at the mineral-water and air-water interface. Furthermore, the mechanism of how interactions between collectors and frothers at the air-water or mineral-water interface can improve bubble-particle attachment and mineral recovery, will be discussed. The interaction between DTP and frothers will be compared to xanthate and frothers as the behaviour of xanthate has been well characterised in literature.

5.3.1 The effect of collector-frother mixtures on bubble-particle attachment for various minerals

5.3.1.1 Galena

The ACTA results and microflotation results are summarised in the following figures for the single reagents and reagent mixtures to assess whether they produce any synergistic effect. The ACTA data is used to observe if the effect is due to the surface chemistry at the interfaces that improves the bubble-particle attachment subprocess. The microflotation data showed that the effects observed in the ACTA studies are reflected in the kinetics of flotation in the microflotation cell.

From Figure 5.4 it is evident that in the case of galena the mixture of SDEDTP and hexanol had a synergistic effect. This effect is both observed in the first order rate constant which was fitted to the microflotation results, and the attachment probability. Even though the SDEDTP-hexanol mixture synergistically improves bubble-particle attachment probability and the first-order rate constant, adsorption tests show that SDEDTP does not adsorb onto the surface of galena (Table 4.19). This is true even in the presence of hexanol.

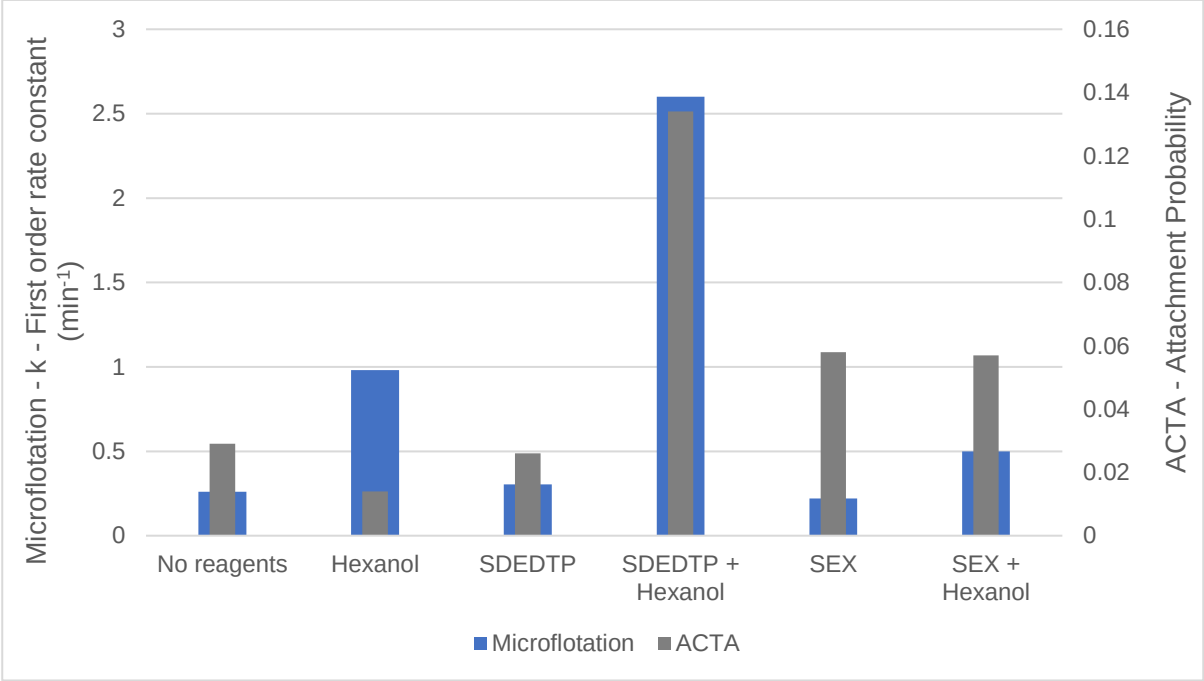

Figure 5.4: The ACTA and Microflotation results for galena at pH 9. The dosage of each collector is at 50% monolayer dosage and the concentration of hexanol is 0.12 mM.

On the other hand, the SEX-hexanol mixture did not show any such synergistic effect. The SEX-hexanol mixture had no effect on the attachment probability relative to the attachment probability where SEX was used on its own. The SEX-hexanol mixture produces an antagonistic effect in the microflotation cell where there is a decrease in rate of bubble-particle attachment relative to the case where only hexanol is present. As the presence of hexanol does not affect the adsorption of SEX onto galena (Table 4.19), it is not evident as to why this antagonistic effect occurs.

5.3.1.2 Pyrite

Figure 5.5 shows the microflotation and ACTA results for pyrite at pH 9 and Table 5.8 compares the mass recovery of DTP-frother mixtures to the sum of the contribution of each reagent to the microflotation recovery. The collectors were all dosed at 50% surface coverage unless specified. The difference between the mass recovery obtained from results and the calculated sum of the contribution of each reagent in

Table 5.8 represents the improvement due to interactions between the collector and the frother.

The 0.1mM SDEDTP microflotation results are shown in Figure 5.5, instead of the 50% monolayer dosage. The dosage of 0.1 mM dosage in the microflotation cell is closer to the actual concentrations used in the ACTA as can be seen from Table 3.4.

Figure 5.5 demonstrates that the mixture of SDEDTP and hexanol synergistically improvement the attachment probability and microflotation recovery for pyrite. The ACTA results show that there is a 10-fold improvement in attachment probability when using the SDEDTP-hexanol mixture compared to the baseline where only SDEDTP is present. In the microflotation cell this improvement was not as large but still a significant improvement. The greater improvement in the ACTA may be due to the long contact time used in the ACTA, which was 100ms. Contact times in the microflotation cell are on the order of 10 ms (Min & Nguyen, 2012), so the synergistic effect may not be as strong when compared to the ACTA.

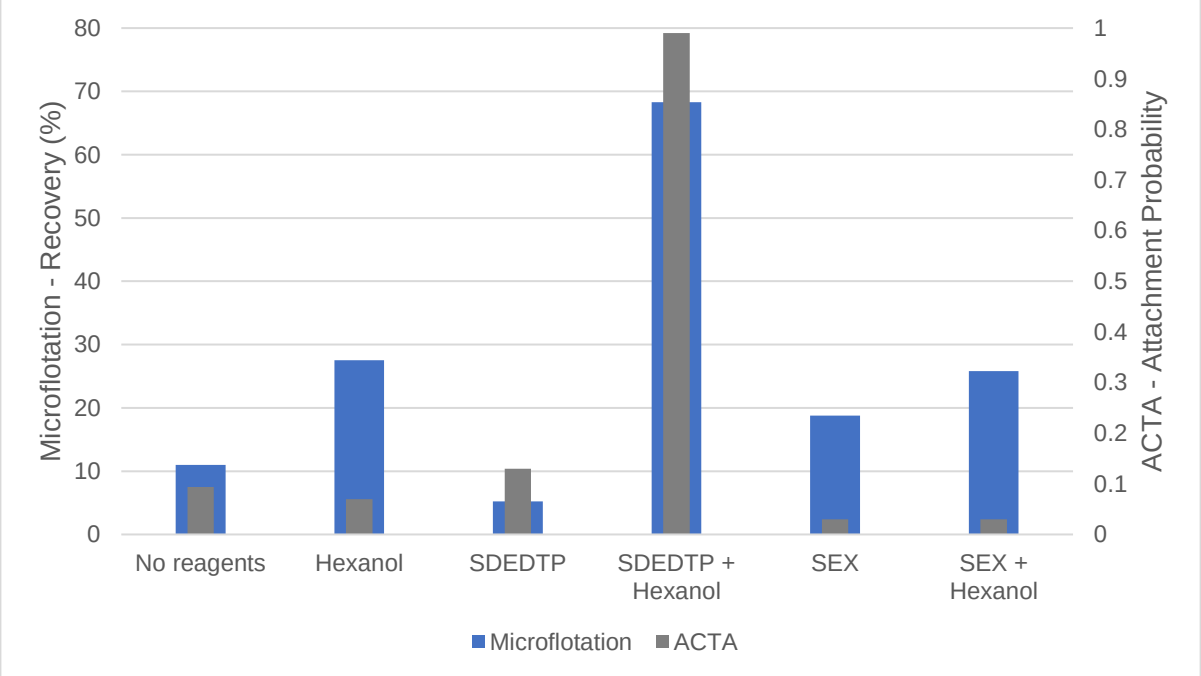

Figure 5.5: The ACTA and Microflotation results for pyrite at pH 9. The dosage of SEX is at 50% monolayer coverage, SDEDTP is dosed at a concentration of 0.1mM and the concentration of hexanol is 0.12 mM

The use of PPG425 with SDEDTP did not result in such a improvement as hexanol with SDEDTP. The differences between the microflotation recovery of the reagent mixture and the calculated sum of the contribution of each reagent in Table 5.8 demonstrate this. The difference for SDEDTP-hexanol (46.5 %) is greater than for SDEDTP-PPG425 (13.8 %). This can be attributed to the lower concentration of PPG425 used. The CCC was used as the dosage for frothers in each case and the CCC of PPG425 is lower than the CCC for hexanol.

Pienaar et al. (2019) observed ~90% recoveries for pyrite using SDEDTP-PPG425 and SDEDTP-hexanol mixtures at higher concentrations of these frothers.

SEX does not show a synergistic interaction with hexanol. A decrease in microflotation recovery for the mixture is shown compared to the microflotation recovery of pyrite in the presence of hexanol, indicating an antagonistic effect which is also demonstrated in Table 5.8.

A mixture of SDEDTP-SIBX-hexanol also did not perform as well as only SDEDTP and hexanol. Table 5.8 demonstrates that the SIBX has an antagonistic effect on the synergistic effect which SDEDTP and hexanol exhibits.

Table 5.8: Mass recovery for pyrite in microflotation cell for mixtures of DTP and frothers compared to the sum of contribution of each reagent (collector and hexanol) in microflotation cell.

	SDEDTP 0.5 ML + Hexanol [0.12mM]	SEX 0.5 ML + Hexanol [0.12mM]	SDEDTP [0.1mM] + Hexanol [0.12mM]	SDEDTP [0.1mM] + PPG [0.014mM]	SIBX 0.1 ML + SDEDTP [0.1mM] + Hexanol [0.12mM]
% Mass recovery of reagent mixture	25.1	18.8	68.3	31.8	52.3
Calculated sum contribution of each reagent	24.3	23.4	21.7	17.9	26.3
Difference	0.7	-4.6	46.5	13.8	26.0

5.3.1.3 Chalcopyrite

Figure 5.6 summarises the microflotation and ACTA results for chalcopyrite at pH 9. A clear synergistic effect is present in the ACTA results as both SDEDTP and hexanol, alone, lowered the mass recovered but together, SDEDTP and hexanol, improved the mass recovered to a greater extent than the case where no reagents are present. Qualitatively it does not seem to be such a strong effect compared to those observed for galena and pyrite. The other notable difference between chalcopyrite and the previous minerals discussed is that SEX alone produced a higher ACTA recovery than the SDEDTP mixture, but the addition of hexanol to SEX had no effect at all relative to the recovery of SEX in the ACTA. This indicates that the SEX-hexanol mixture on chalcopyrite does not demonstrate any synergistic effects.

The microflotation results demonstrate the same synergistic phenomena as the ACTA results for the SDEDTP-hexanol mixture, but compared to galena and pyrite the effect is not as strong.

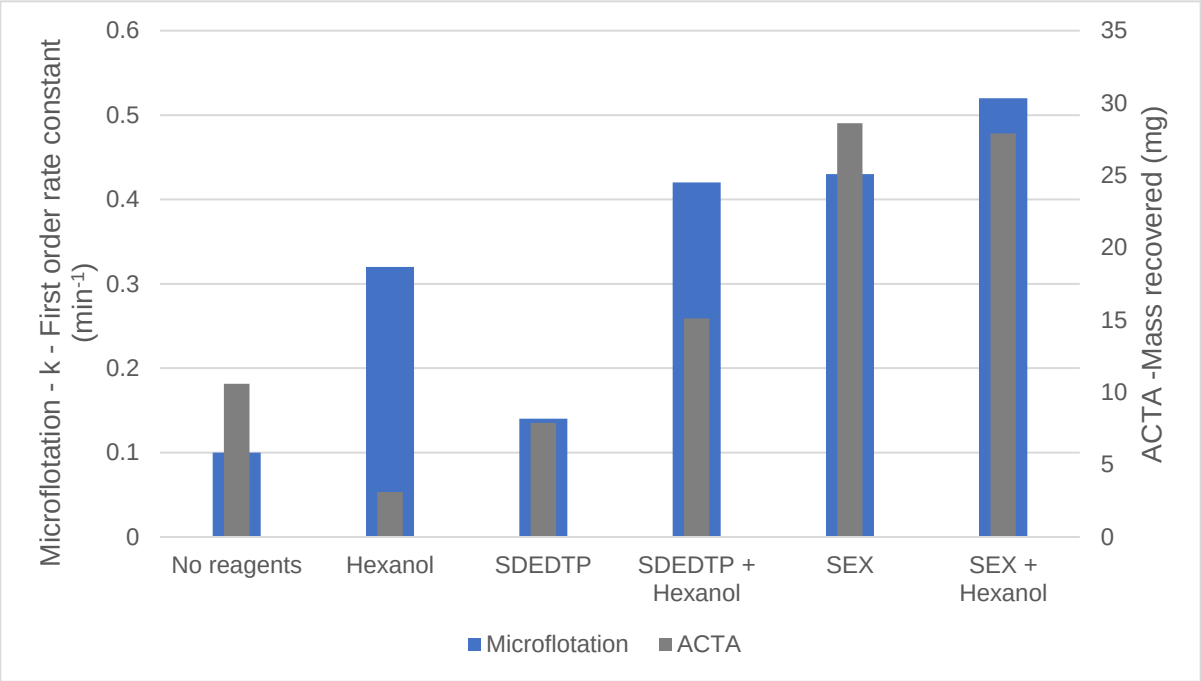

Figure 5.6: The ACTA and Microflotation results for chalcopyrite at pH 9. The dosage of each collector is at 50% monolayer dosage and the concentration of hexanol is 0.12 mM

The mixture of SEX and hexanol demonstrated improvements in the first-order rate constant, but as the reagents both exhibited improvement in the first-order rate constant on their own, the improvements are attributed to separate effects of each reagent. This is further substantiated by the ACTA results which show no synergistic effect when using the mixture of SEX and hexanol.

5.3.1.4 Chalcocite

Figure 5.7 summarises the ACTA and microflotation results for chalcocite at pH 9. The behaviour of chalcocite is different from the other minerals investigated, in that SDEDTP shows clear improvements for both microflotation recovery and ACTA mass recovery in the absence of frother. Furthermore, all the collectors used in this study show complete adsorption onto the mineral surface. This indicates that if molecular interactions occur between collectors and frothers on chalcocite they would be at the mineral-water interface.

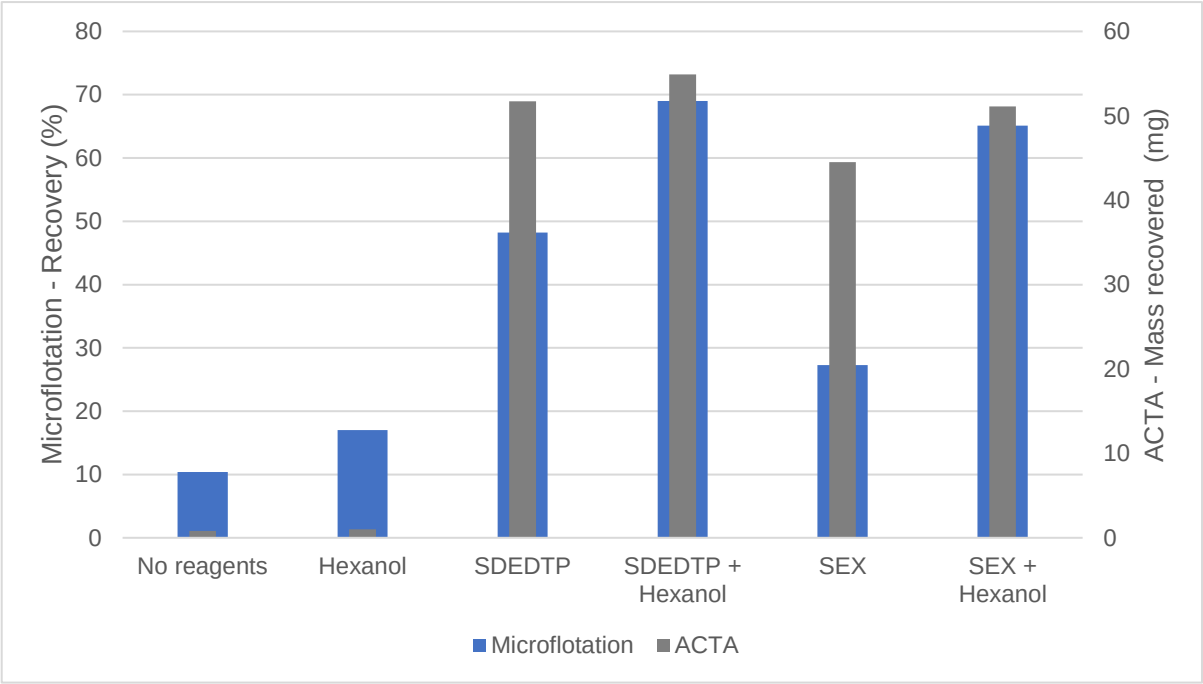

Figure 5.7: The ACTA and Microflotation results for chalcocite at pH 9. The dosage of each collector is at 50% monolayer dosage and the concentration of hexanol is 0.12 mM

Table 5.9 compares the mass recovered for the collector-frother mixtures in the ACTA to the calculated sum of the contribution of each of the reagents (collector and frother) in the ACTA. Both mixtures showed an improvement beyond the contribution of each reagent. The effect of the SDEDTP-hexanol mixture is not as apparent as for galena and pyrite, where the synergy between SDEDTP and frother could be clearly seen in the data. However, this is the first mineral where the SEX-hexanol mixture showed improvements compared to the SEX alone. Lekki & Laskowski (1971) had similar observations for SEX-terpineol mixtures in the Glembotsky device where this mixture demonstrated improvements in the induction time.

Table 5.9: Mass recovered in ACTA for mixture of SDEDTP and SEX with hexanol compared to the sum of contribution of each reagent (collector and hexanol) in ACTA.

	SDEDTP + Hexanol	SEX + Hexanol
Mass recovered in ACTA (mg)	54.9	51.1
Calculated sum of contribution of each reagent in ACTA (mg)	51.9	44.7

High masses were recovered with a 50% monolayer dosage in the ACTA chalcocite tests. To observe clearer differences in recovery, a 20% and a 10% monolayer dosage was used for the microflotation tests. These results showed that the recovery of chalcocite with SDEDTP decreased from 48.2% at 20% monolayer dosage to 32.2% at 10% monolayer dosage (Figure

4.8). The recovery of the SDEDTP-hexanol mixture only decreased from 69.0% (20% monolayer dosage) to 65.1% (10% monolayer dosage). Even though the recovery dropped by 16% when using SDEDTP alone, in the mixture it only dropped by 3.9%, indicating that the improvement in recovery for chalcocite when using a mixture of SDEDTP and hexanol is not a strong function of the hydrophobicity, but the improvement is rather due to the molecular interaction occurring between SDEDTP and hexanol.

5.3.1.5 Summary

Table 5.10 provides a summary of the SDEDTP-hexanol and SEX-hexanol mixtures' response to bubble-particle attachment probability or microflotation recovery. A synergistic improvement in bubble-particle attachment kinetics is observed for the SDEDTP and hexanol mixture on all the minerals used in this study. These improvements carried through to the microflotation response in all minerals except chalcopyrite. SEX-hexanol mixtures only show synergistic improvements in recovery and bubble-particle attachment with chalcocite. Chalcocite seems to be an outlier within this collection of minerals as SDEDTP increases the mineral surface hydrophobicity and the SEX-hexanol mixture exhibits synergistic improvements in recovery, contrary to the results with all the other minerals tested. These results indicate that the extent of synergistic effect is mineral specific.

Table 5.10: Minerals for which SDEDTP-hexanol and SEX-hexanol mixtures synergistically improved the bubble-particle attachment probability or microflotation recovery.

	Galena		Pyrite		Chalcopyrite		Chalcocite	
ACTA	SEX	SDEDTP	SEX	SDEDTP	SEX	SDEDTP	SEX	SDEDTP
	✗	✓	✗	✓	✗	✓	✓	✓
Microflotation	SEX	SDEDTP	SEX	SDEDTP	SEX	SDEDTP	SEX	SDEDTP
	✗	✓	✗	✓	✗	✓	✓	✓

5.3.2 The interactions of collectors and frothers at the air-water interface

The improvements in recovery and bubble-particle attachment kinetics observed in collector-frother systems have been attributed to molecular interactions between collectors and frothers (Leja & Schulman, 1954; Mukai, Wakamatsu & Takahashi, 1972; Dai, Bradshaw & Harris, 2001; Jordaan, 2018; Pienaar et al., 2019). Surfactants are used in mixtures as the interactions between surfactants have been shown to synergistically improve performance compared to the use of one surfactant on its own (Rosen, 1986).

In the previous section synergistic improvements in bubble-particle attachment kinetics and mineral recovery were determined for mixtures of SDEDTP and hexanol. These improvements in bubble-particle are attributed to molecular interactions between SDEDTP and hexanol. The main objective of this section is to attempt to understand the nature of the interactions between DTP and frothers.

Foam stability is sensitive to the concentration ranges used in flotation. In section 4.6.2, Table 4.24, the difference between the experimental and the calculated dynamic foam stability factors were calculated ($\sum_{Experimental} - \sum_{Calculated}$). The difference demonstrates the departure of the dynamic foam stability from ideal behaviour. The SDEDTP-hexanol mixture containing 0.67 mole percent SDEDTP showed a positive difference for the dynamic foam stability factor which demonstrates that the mixture synergistically improves the foam stability. These improvements were also observed for mixtures of SD(N)BDTP and SD(I)BDTP with hexanol. SD(I)BDTP demonstrated the greatest improvement.

The regular solution model did not show an attractive interaction between SDEDTP and hexanol. The activity of SDEDTP at the air-water interface is quite weak compared to the longer alkyl chain DTP collectors used (Table 4.25 – Section 4.6.3). The relatively high concentrations of hexanol used in these experiments could displace or block the adsorption of SDEDTP at the air-water interface. At the concentrations used in flotation the interface is diffuse and both SDEDTP and hexanol can co-adsorb, but no changes in surface tension could be detected in these concentration ranges.

Leja & Schulman (1954) used insoluble collectors and frothers that have alkyl chains longer than 12 carbons to study molecular interactions at the air-water interface and used froth stability results to substantiate that the interactions are occurring between shorter chain length soluble collectors and frothers.

The longer chain length DTP's (n-butyl, iso-butyl, and n-hexyl) mixed with hexanol all showed attractive interactions at the air-water interface by the regular solution theory approach, according to Table 4.25. SD(N)HDTP which was the longest alkyl chain length (C6) used in this study showed the strongest interaction with hexanol. Interactions among surfactant alkyl chains are due to van der Waals forces between these groups. Increasing the alkyl chain length of the molecule increases the attraction between self-associating surfactants or surfactant mixtures, and generally show the greatest interaction when the surfactants have similar length alkyl chains (Leja & Schulman, 1954).

The attractive synergistic interactions predicted by regular solution theory for SD(I)BDTP and hexanol was confirmed in foam stability and bubble size tests. The effect of SD(I)BDTP and hexanol on bubble size in Figure 4.26 shows that the reagent mixture decreases the bubble size beyond the size at which hexanol inhibits bubble coalescence on its own.

No interactions were observed in the case where xanthate was used as the collector in surface tension and bubble size tests. The surface tension results shown in section 4.6.3 showed that xanthates were not as active at the air-water interface compared to DTPs. SEX exhibited no activity at the air-water interface as indicated by surface tension results (Figure 4.33), and this has been observed by other authors (Jordaan, 2018; Manev & Pugh, 1993). These results indicate that the activity of xanthates at the air-water interface is too weak to determine if an interaction is present between xanthates and frother. Surface tension tests are also only conducted in two phase systems where concentrations of the reagents were much greater than those used in the microflotation or the ACTA tests. At the lower concentrations used in the foam stability tests, compared to the concentrations used in surface tension tests, SIBX-hexanol mixtures did show synergistic improvements in foam stability at higher mole fractions of collector in the mixture (Table 4.24).

A synergistic improvement in recovery and bubble-particle attachment is observed for all minerals when using SDEDTP with hexanol, and DTP and hexanol has exhibited molecular interactions at the air-water interface. Xanthate does not show synergistic improvements for all minerals, only chalcocite. Furthermore, xanthate has not shown clear interactions with frothers. The evidence observed for DTP supports the fact that interaction with the frother is due to the structure of the DTP molecule as even though the extent of the interaction may be mineral specific as previously stated, the general presence of improvements are not mineral specific. Bradshaw & O'Connor (1998) proposed that the interaction between the collector and the frother could be due the oxygen group in the thiol headgroup.

Table 5.11:The electronegativities of the elements found in thiol collectors

	Carbon	Oxygen	Sulphur	Phosphorus
Electronegativity	2.55	3.44	2.58	2.19

It could be that the electronegativity between the oxygen atoms and other groups in the atom can induce dipole-dipole interactions between the polar group of the frother and the collector. From Table 5.11 it can be seen the difference in electronegativity between the phosphorus and the oxygen atom in DTP, viz. 1.25, is greater than the difference in electronegativity of the carbon atom and oxygen atom in xanthate, viz.0.89.

Furthermore, as can be seen from Figure 5.8, the molecular structure of DTP contains two oxygen atoms so inductively the electronegative oxygen atoms have an even greater effect in terms of reduced electron density on the thiol head group and the phosphorus atom. This would result in dipole-dipole interactions between the polar group of the frother molecule and the phosphorus group on DTP as demonstrated in Figure 5.8 .

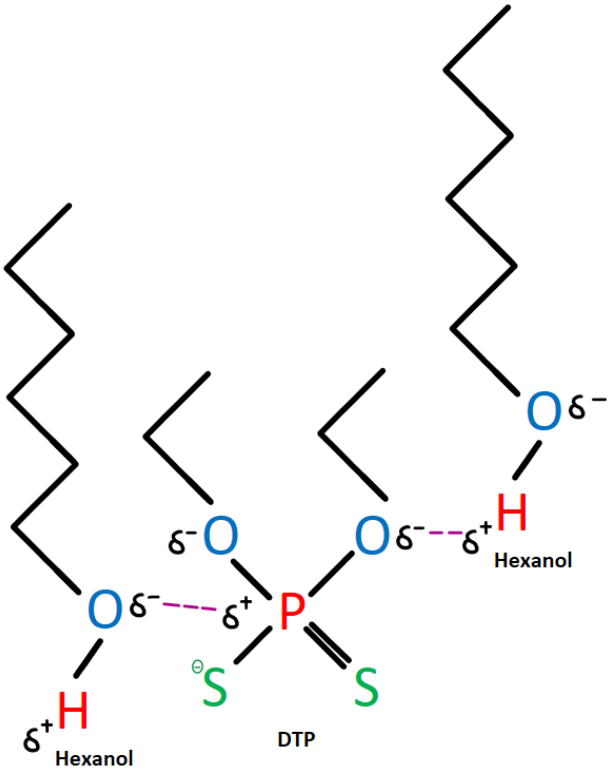

Figure 5.8: The mechanism of interaction between hexanol and DTP

5.3.3 The interaction of collectors with frothers at the mineral-water interface

In the penetration theory proposed by Leja & Schulman (1954), molecular interactions between the collector and the frother at the air-water and mineral-water interface, and the interpenetration of these two mixed films were envisioned to improve bubble-particle attachment by increasing the amount of collector at the mineral-water interface by forming a condensed, mixed layer of collector and frother.

In the discussion under the frother section (Section 5.2.1) it was established that frothers do not adsorb onto the mineral surface without the presence of collector. It has been established in literature that the co-adsorption of a non-ionic surfactant onto a solid interface only occurs through interaction with another surfactant that has been adsorbed onto the interface (Leja & Schulman, 1954; Bansal, 1975; Mukai, Wakamatsu & Takahashi, 1972; Hadler, Aktas & Cilliers, 2006).

In considering the first scenario, which is the co-adsorption of collector, with frother, onto the mineral surface, the results for the adsorption tests in the absence of air, performed on all the minerals are summarised in Table 5.12 In the case of galena and chalcocite, the presence of hexanol does not affect the adsorption of both SEX and SDEDTP. However, in the case of pyrite and chalcopyrite, the adsorption of SDEDTP is significantly affected by the presence of hexanol. The amount of collector adsorbed is significantly lowered in the presence of hexanol. This result shows that there is no co-adsorption of collector, with the addition of frother, onto the mineral surface.

Table 5.12: Summary of the adsorption results of SDEDTP and SEX in the presence of hexanol. The percentage collector adsorbed represents the amount of the 50% monolayer dosage that has been adsorbed onto the mineral.

	Collector adsorbed (%)			
Reagent	Galena	Pyrite	Chalcopyrite	Chalcocite
SDEDTP	0	69.3	71.2	97
SDEDTP + Hexanol	1.4	41.61	64.3	98.8
SEX	96.4	88.2	74.6	97.7
SEX + Hexanol	96.4	86.4	77.9	97.7

In considering the alternative scenario, which is the co-adsorption of frother, with collector, onto the mineral surface, there is no direct evidence available from this study. However, the

following reasoning is applied to this possibility. The collectors in the current study are dosed at 20-50% monolayer coverage which makes the interface diffuse, and the collectors have a short chain length (2 carbon chain). The hydrophobicity of the collectors at diffuse surface coverage is mainly attributed to the solubility of the species that forms on the mineral surface (Wark & Wark, 1932; Kim et al., 2012). As discussed in Section 5.1 the solubility of metal thiolate species is of the order of 10^{-11} M to 10^{-17} M, whereas the solubility of hexanol is 5.78×10^{-2} M. These values are different by several orders of magnitude, so it is unlikely that at diffuse adsorption densities there is an increase in surface hydrophobicity due to the co-adsorption of these frothers on the mineral surface. Furthermore, co-adsorption of frothers onto a collector coated surface does not change the contact angle if a diffuse film of surfactants is formed (Rao, 2013:667).

Since it has been shown that it is unlikely that SDEDTP-hexanol complexes on the surface of the mineral are affecting the hydrophobicity, the question remains what is the possible mechanism by which these molecular interactions can improve mineral recovery? Lekki & Laskowski (1971) have proposed that frothers can improve the film thinning kinetics of the water film between the bubble and particle by transferring from the air-water interface to the mineral-water interface. In order for frothers to co-adsorb onto the mineral surface the presence of a collector on the surface is required (Leja & Schulman, 1954; Bansal, 1975; Mukai, Wakamatsu & Takahashi, 1972; Hadler, Aktas & Cilliers, 2006).

If the transfer of the frother between the air-water and mineral-water interface is improving the film thinning kinetics and mineral recovery, the type of frother and its concentration will likely have an effect on the mineral recovery. Furthermore, it has been shown that longer chain lengths of DTP show stronger molecular interactions with hexanol (Section 5.3.2) which may also have an effect on mineral recovery. The extent of molecular interactions and the effect of different frother types on mineral recovery will be explored in the following sections.

5.3.3.1 Effect of molecular interactions at the mineral-water interface on mineral recovery

The longer chain lengths of DTP and xanthate were tested on chalcocite. The collectors were tested on chalcocite as all chain lengths from ethyl to isobutyl DTPs and xanthate's exhibit complete adsorption onto the mineral and it was therefore guaranteed that any interactions that were observed would be at the mineral-water interface. Leja & Schulman (1954) and Mukai, Wakamatsu & Takahashi (1972) demonstrated that the strength of the molecular interactions between xanthate and frothers increased with increasing alkyl chain length. This study similarly showed that the β parameter increased with increasing and branching alkyl

chain length of DTP. Tests with longer and branching alkyl chain lengths would reveal if the strength of these interactions at the mineral-water interface have an effect on the recovery of chalcocite.

Table 5.13: Mass recovery of chalcocite in microflotation cell for mixtures of DTP and xanthate with hexanol compared to the sum contribution of each reagent (collector and hexanol) in microflotation cell.

	20% ML SDEDTP + Hexanol	10% ML SDEDTP + Hexanol	SD(N)BDTP+ Hexanol	SD(I)BDTP + Hexanol	SEX + Hexanol	PNBX + Hexanol	SIBX + Hexanol
% Mass recovery of reagent mixture	69.0	65.1	59.3	60.3	65.1	62.7	69.1
Calculated weighted sum contribution of each reagent	54.8	38.8	34.3	37.4	33.9	52.5	50.6
Difference	14.2	26.3	25.0	22.8	31.2	10.2	18.4

Table 5.13 compares the calculated weighted sum of the contribution of each reagent (collector and frother) to the microflotation recovery of chalcocite and the mass recovery of the reagent mixture. The collectors were all dosed at 20% surface coverage unless otherwise specified. The difference between the mass recovery obtained and the calculated sum of the contribution of each reagent represents the improvement due to synergistic interactions between the collector and the frother.

In the case of the DTP collectors (Table 5.13), the microflotation tests on chalcocite showed that the mixtures of SD(N)BDTP and SD(I)BDTP with hexanol yielded the greatest improvement in recovery whereas SDEDTP shows the least improvement. When lowering the dosage of SDEDTP to 10% monolayer dosage the difference increases to values similar to that of SD(N)BDTP and SD(I)BDTP. For xanthate, the mixture of PNBX or SIBX with hexanol showed the least improvement compared to the contribution of each reagent, with SEX showing the greatest improvement.

Although all combinations of DTP chain length with hexanol showed clear synergistic improvements in flotation recovery, there seems to be no clear correlation between those improvements and the β values shown in Table 4.25. Notably, the recoveries obtained for all the collector-hexanol mixtures were relatively similar - between 60 - 70%. This may suggest

that the strength of interaction between the collector and frother does not have a strong effect on the recovery.

Since it is suggested that the improvement in recovery is controlled by the transfer of the frother from the air-water interface to the mineral-water interface by improving the kinetics, the strength of the molecular interaction may not have a strong influence on this transfer mechanism, it should simply be present.

This mechanism is further supported by the result where the dosage of SDEDTP is lowered from 20% monolayer coverage to 10%. Halving the dosage of SDEDTP in the presence of hexanol only lowered the recovery by 3.9%. The synergistic improvement observed with SDEDTP and hexanol on chalcocite does not seem to be a strong function of the amount of SDEDTP on the surface of chalcocite. This suggests that as long as there is enough SDEDTP on the surface of the mineral the transfer of frother will improve bubble-particle attachment kinetics.

The synergistic improvement in film thinning kinetics via the transfer of frother is supported by batch flotation tests. McFadzean, Mhlanga & O'Connor (2013) did not observe a synergistic improvement for pyrite with SDEDTP and DOW200 even though they observed synergistic improvements for galena with this reagent mixture. Pyrite is not naturally hydrophobic and SDEDTP does not improve its hydrophobicity so the bubble-particles aggregates cannot be stabilized in the turbulent batch flotation system even though the kinetics are enhanced. When a mixture of SEX and SDEDTP (10% of the dosage was SEX and 90% of the dosage was SDEDTP) with DOW200 was used, McFadzean, Mhlanga & O'Connor (2013) observed a synergistic improvement in the recovery of pyrite. The low dosage of xanthate provided the hydrophobicity to stabilize bubble-particle aggregates and the SDEDTP interacted with the frother to facilitate the transfer of the frother, which enhances the film thinning kinetics. This resulted in the improvement in recovery. The synergistic improvement was observed for galena as it is naturally hydrophobic, so the bubble-particle aggregates were stabilized and the bubble-particle attachment kinetics were enhanced.

5.3.3.2 Effect of frother type on molecular interactions and mineral recovery

If the improvement in recovery is controlled by the transfer of the frother from the air-water to the mineral-water interface, the interactions may be a function of the concentration of the frother or the type of frother.

The recovery of chalcocite was, therefore, tested with different frothers and DTP. Table 5.14 compares the microflotation recovery of the reagent mixtures to the calculated weighted sum contribution of each reagent.

Table 5.14: Mass recovery for chalcocite in microflotation cell for mixtures of DTP and frothers compared to the sum of contribution of each reagent (collector and hexanol) in microflotation cell.

	SDEDTP + Hexanol	SDEDTP + PPG425	SDEDTP + Octanol	SD(N)BDTP + Hexanol	SD(N)BDTP + PPG425	SDB(N)DTP + Octanol
% Mass recovery of reagent mixture	69.0	55.1	55.7	59.3	50.7	51.5
Calculated weighted sum contribution of each reagent	54.8	53.2	50.8	34.3	32.7	30.3
Difference	14.2	1.9	4.9	25.0	18.0	21.2

Table 5.14 shows that for both the ethyl and n-butyl chain length of DTP, the mixture with hexanol produced the greatest improvement, followed by octanol and then PPG425. These microflotation results are contrary to the regular solution theory results which showed that SD(N)BDTP had the strongest interaction with PPG425 (β = -3.92) compared to hexanol (β = -0.66).

In the case of pyrite, SDEDTP and PPG425 only yielded half the recovery of that of SDEDTP and hexanol (Figure 4.4). Therefore, it was found that hexanol produced the greatest synergistic interactions with SDEDTP out of the various frother types tested.

As the frothers were dosed at their CCC, the concentration of PPG425 and octanol are much lower than hexanol. The concentration of PPG425 was 0.014mM which is 8 times lower than the concentration of hexanol, and the molar concentration of octanol was about half that of hexanol. Higher concentrations of these frothers may also induce a synergistic effect. Pienaar et al. (2019) performed tests with SDEDTP and various frothers at higher concentrations than the CCC of the frothers and observed a strong synergistic improvement in recoveries for pyrite and galena. Lekki & Laskowski (1971) demonstrated that the induction time exponentially decreased as the concentration of the frother increased in the presence of KEX (cf Figure 2.17).

These results indicate that the synergistic mechanism is dependent on the concentration of the frother used which further supports the theory of Lekki & Laskowski (1971) explaining the role of non-ionic frothers in bubble-particle attachment. This is a very interesting since it illustrates that the role of frother is more than just its role as an inhibitor of bubble coalescence, important as that role is.

5.3.4 Transfer of SDEDTP from the air-water to mineral-water interface

It was proposed in section 5.3.3 that when collectors are at the mineral-water interface the improvements in recovery ascribed to collector-frother interactions are due to the transfer of the frother from the air-water interface to the mineral-water interface, which improves the film thinning kinetics.

The mechanism by which a synergistic interaction between a collector and a frother at the air-water interface improves mineral recovery and bubble-particle attachment is unclear in the case of galena. No adsorption of SDEDTP was found on the mineral surface, even in the presence of hexanol. Yet, a strong synergistic increase in recovery and bubble-particle attachment is observed leading to the question of the effect DTP-frother mixtures have on the air-water interface. The improvement in foam stability and reduction in pulp bubble coalescence for DTP-frother mixtures show that the interaction between DTP and frothers stabilizes the thin film around the bubble to a greater extent than each of the individual reagents. Frothers which have the same effect on the air-water interface were shown to decrease the bubble-particle attachment probability of all the minerals tested in the ACTA. If frothers decrease bubble-particle attachment probability and DTP-frother mixtures stabilize the thin film around the bubble as shown by improvements in foam stability, it thus begs the question as to why DTP-frother mixtures do not show a decrease in bubble-particle attachment probability. They show the opposite trend a synergistic improvement in bubble-particle attachment probability.

It has been shown through foam stability tests and the regular solution theory model that there is an attractive interaction between DTP and frothers at the air-water interface. It is proposed that the SDEDTP-frother mixture at the air-water interface interacts with the mineral surface during bubble-particle collision, thus destabilising the thin film and improving bubble-particle attachment kinetics.

In order to test this theory, tests were conducted to show the amount of collector adsorbing with and without aeration of the slurry, which contained respectively collector with no frother and collector with frother.

Table 5.15: Percent of SDEDTP adsorbing onto the mineral surface, with and without the presence of aeration. The dosage of SDEDTP was 0.1 mM in each case, whereas the dosage of hexanol was 0.12 mM

	SDEDTP		SDEDTP + Hexanol	
	No Air	With Air	No air	With Air
Galena	13.5	13.8	14.8	33.7
Pyrite	32.4	41.5	29.2	37.2
Chalcopyrite	30.7	30.2	31.2	25.9

Table 5.15 shows the percent adsorption of SDEDTP onto various minerals in the presence and absence of hexanol and aeration. SDEDTP shows improved adsorption onto galena only in the presence of air and hexanol, in all other cases the percentage of SDEDTP adsorbed does not change. This supports the theory put forward that SDEDTP and hexanol interact at the air-water interface and transfers onto the mineral surface during bubble-particle collision, improving bubble-particle attachment kinetics.

The adsorption of SDEDTP onto pyrite improves in the presence of aeration but the addition of hexanol does not have a significant impact in this case and in fact slightly reduces adsorption. Microflotation results for pyrite support this finding, viz. that SDEDTP is transferred from the air-water interface to the mineral-water interface.

Chalcopyrite shows lower adsorption density after contact with hexanol and air, whereas at all other conditions the adsorption is constant. Wang & Miller (2018) showed that dodecyl amine transferred to the quartz surface during bubble-particle attachment, but when the bubble is detached from the surface most of the dodecyl amine is stripped from the surface. Since the interaction of SDEDTP with the chalcopyrite surface is very weak (-4.9 kJ/mol), it follows that in a similar manner the complex that forms between the collector and frother at the mineral-water interface may detach and transfer back to the bubble surface as it is not stable on the mineral surface. The transfer only in the presence of the frother may be due to the frother being in a lower energy state (higher stability) at the air-water interface than on the mineral surface. This is supported by the work of Kondratyev & Ryaboy (2016) who postulated that metal dithiophosphate complexes that precipitate on the mineral surface can desorb from the mineral surface and transfer to the air-water interface, destabilising the intervening thin film and enhancing bubble-particle attachment kinetics. Thus, even though there is not enhanced collector attachment at the mineral surface, the bubble-particle attachment can still be improved by this mechanism.

The microflotation tests performed with hydrophobized quartz further supports the transfer mechanism of DTP (cf. Figure 4.12). The SDEDTP-hexanol mixture had no effect on the recovery of quartz at all. It is well established that thiol collectors do not interact with oxide minerals, and Nagaraj & Brinen (1996) have shown that SDEDTP does not adsorb onto the quartz surface at all. The fact that SDEDTP-hexanol mixture had no effect on the recovery of quartz and that SDEDTP does not interact with the surface of quartz shows that the interaction of the reagents and their effect on the air-water interface is not causing the improvement in recovery. It is rather a dynamic transfer of reagents from the air-water interface to the mineral-water interface during bubble-particle collision, as opposed to static adsorption of reagents at one of the interfaces.

5.3.5 The synergistic mechanism for increasing the bubble-particle attachment probability.

In the above sections it was shown that, for various collector-frother-mineral systems there were synergistic effects occurring in which the flotation performance of the mixture was greater than the weighted sum of the contributions of the respective components based on their individual performance. The manner in which this is proposed to occur is presented in this section. Since this study has primarily focused on the synergistic effects of SDEDTP, the discussion will focus on this reagent. Other alkyl chain lengths and collectors were introduced for comparative purposes and are discussed separately:

SDEDTP was shown to be weakly active at the air-water interface. During the bubble-particle collision process SDEDTP can diffuse through the thin film between the air-water and mineral-water interface and adsorb onto the high energy sites on the mineral surface. This was shown to be the case for galena and pyrite. Since SDEDTP is very soluble due to its strong interaction with water (McFadzean and O'Connor, 2014), it does not cause the destabilization of the thin film as described by Lekki and Laskowski (1971) for frothers diffusing through the thin film. Therefore, SDEDTP alone will not cause an increase in the kinetics of film thinning. However, it has been shown that frother molecules such as hexanol interact with DTP at the air-water interface. During the collision process between the bubble and the particle, DTP can diffuse through the thin stable film, pulling the frother along with it (due to the attractive interactions between the two molecules). The movement of large frother molecules with long alkyl chains through the thin film causes destabilization of the film, leading to rupture and formation of 3

phase contact. Thus, the presence of DTP and frother together can increase the kinetics of film thinning, enhance bubble-particle attachment and hence improve flotation performance.

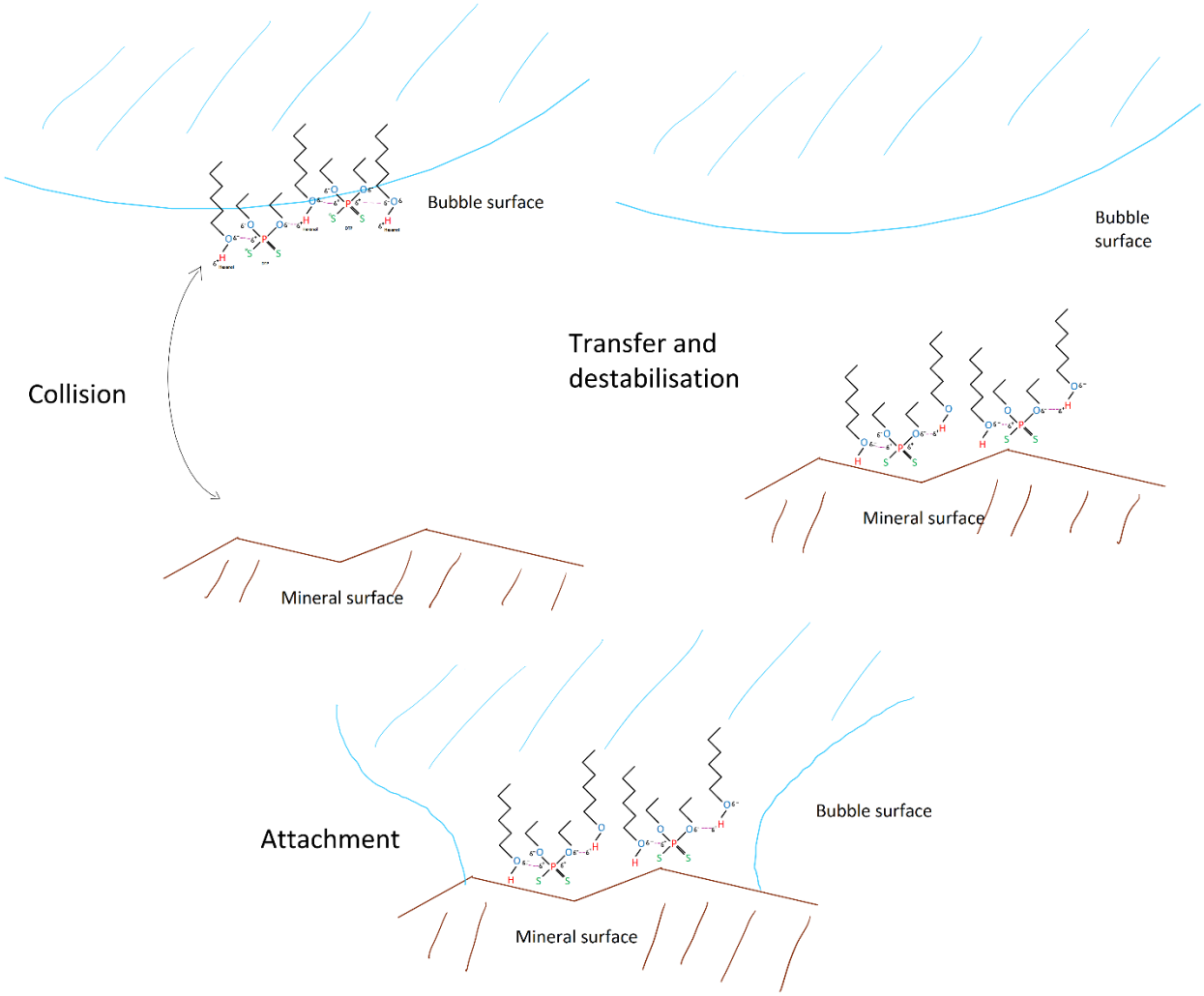

Figure 5.9: Depiction of the interaction of SDEDTP and hexanol at the air-water interface, and the transfer of this collector frother complex to the mineral-water interface

If the collector is already present at the mineral surface, the frother can still transfer from the air-water interface to the mineral-water interface to interact with collector adsorbed at the mineral-water interface, as is the case for chalcocite interactions.

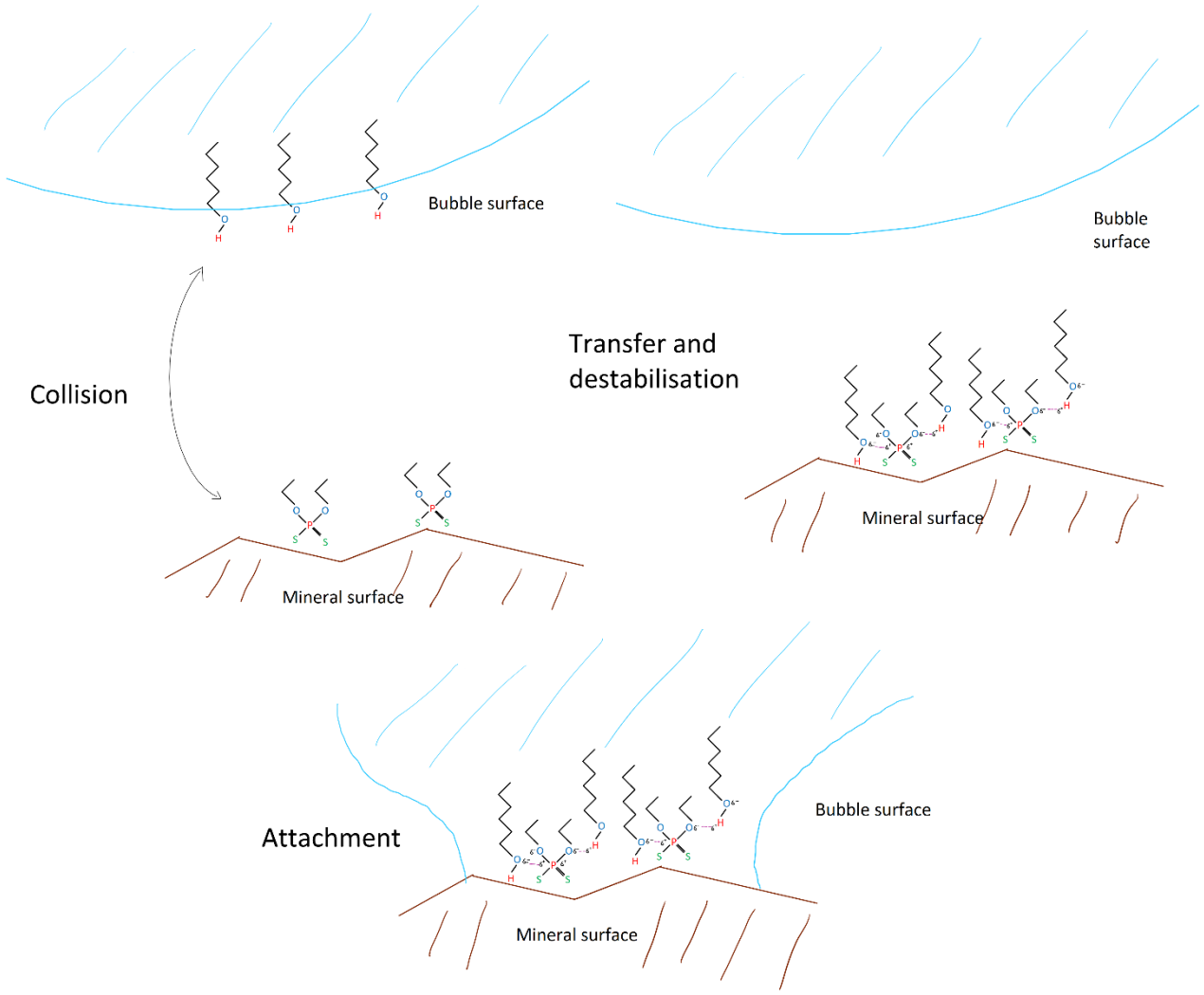

Figure 5.10: Depiction of the transfer of hexanol from the air-water interface to the mineral-water interface, and its interaction with SDEDTP at the mineral-water interface.

It is proposed that the attractive interactions that were found between DTP and frother molecules during the surface tension and foam stability tests is the underlying mechanism for all mineral types, whether the DTP molecule adsorbs from the bulk solution onto the mineral surface or not. If the DTP adsorbs from the bulk solution onto the mineral surface (as is the case for chalcocite), then the frother molecule will transfer from the bubble surface and through the thin film during collision due to the attractive forces present between it and the DTP, as in the cartoon shown in Figure 5.9. This will destabilise the thin film and increase attachment kinetics. If the DTP molecule does not adsorb onto the mineral surface in the bulk solution, it may still adsorb during bubble-particle collision when instantaneous concentrations are higher. In this case, the frother molecule will transfer across the interface with the DTP molecule due to the attractive forces between them, with the same resultant increase in attachment kinetics, as in the carton shown in Figure 5.10. It was shown in Table 5.12, that it requires very little DTP on the mineral surface in order to show synergistic improvements once the frother is added.

6 Conclusions

DTP has been shown to synergistically increase flotation recovery in the presence of frothers (Pienaar et al., 2018) but it has also been shown that DTP does not adsorb onto the sulphide mineral surface (Nagaraj & Brinen, 2001; McFadzean & O'Connor, 2014; Petrus et al., 2011; Grano et al., 1997; Guler et al., 2006; Taguta, O'Connor & McFadzean, 2017) as occurs with conventional collectors. If DTP does not adsorb onto the mineral surface and improve hydrophobicity it was not clear what the role of DTP is in the flotation process. This research aimed to identify the role of DTP in the sulphide mineral flotation.

It was found that DTP in the presence of a non-ionic frother synergistically improved sulphide mineral recovery. This improvement was attributed to attractive molecular interactions which were found to occur between the collector and the frother. The interaction facilitated the transfer of the frother between the air-water and mineral-water interface which destabilised the film between the bubble and the particle improving film thinning kinetics and synergistically enhanced mineral recovery. When DTP did not adsorb onto the mineral surface the collector co-adsorbed with the frother at the air-water interface and transferred with the frother onto the mineral surface during bubble-particle collision.

6.1 Key outcomes

SDEDTP did not adsorb onto galena, and when it adsorbed onto pyrite and chalcopyrite it did not improve mineral surface hydrophobicity. The collector did adsorb onto and improve the hydrophobicity and floatability of chalcocite. Even in the cases where SDEDTP did not adsorb or improve mineral hydrophobicity, the collector demonstrated a synergistic improvement in bubble-particle attachment for all minerals in this study when in the presence of hexanol or other non-ionic frothers.

SEX adsorbed onto all minerals in this study. It did not show improvements in mineral surface hydrophobicity for galena and pyrite but did improve floatability of chalcopyrite and chalcocite. The collector did not show synergistic improvements in bubble-particle attachment for galena, pyrite, and chalcopyrite when in the presence of a frother, but in the case of chalcocite it did. This result indicated that the interaction between xanthate and frothers is mineral specific and may be dependent on the collector species formed on the mineral surface. It was also clear that xanthate-frother interactions were far less pronounced than in the case of DTP.

Pulp bubble coalescence, foam stability and the regular solution theory approach demonstrated that attractive interactions occur between DTP and frothers at the air-water interface. These interactions were not found between xanthate and frothers, showing that the

molecular interactions present between these molecules are due to the molecular structure of the collector. It was argued that the interactions between DTP and frothers are through dipole-dipole interactions between the polar head groups of the molecules. These tests support hypothesis I and II which state that the interaction of DTP with frothers is due to the structure of the collector and that the attraction between DTP and frothers can promote co-adsorption at the air-water interface.

Adsorption tests with aeration showed that the adsorption of SDEDTP is dynamic in nature. For galena, the collector only adsorbed in the presence of hexanol and aeration, whereas with chalcopyrite the opposite effect occurred where the adsorption density decreased only in the presence of hexanol and aeration. SDEDTP exhibited increased adsorption onto pyrite in the presence of aeration, the presence of hexanol had no effect.

The dynamic adsorption in the presence of aeration and hexanol supports the mechanism whereby SDEDTP synergistically improves the recovery of minerals like galena where no adsorption is observed without aeration.

The dynamic adsorption of SDEDTP in the presence of aeration and synergistic improvements in bubble-particle attachment and mineral recovery in the presence of SDEDTP-hexanol mixtures support hypothesis III. This hypothesis proposed that the transfer of DTP-frother complex from the air-water to the mineral-water interface will enhance the kinetics of film thinning between the bubble and the particle and synergistically enhance the recovery of flotation.

6.2 Contribution to knowledge

Many studies have quantitatively tried to show that there are interactions between collectors and frothers at the air-water interface using surface tension results (Manev & Pugh, 1993; Pienaar et al., 2019; Dai, Bradshaw & Harris, 2001), but is challenging to discern if these are due to molecular interactions or if these effects are due to the sum of the contribution of the effect of each reagent. This study has used the regular solution theory model to quantify these interactions and has shown how varying the structure of the alkyl chain can affect the strength of these interactions.

Frothers have been shown to improve bubble-particle attachment kinetics and mineral recovery. Leja & He (1984) have proposed theories of how frothers can improve bubble-particle attachment kinetics. This study has given deeper insight into the role of frothers without the presence of collectors on bubble-particle attachment. Hexanol showed a decrease in bubble-particle attachment probability in this study. This is the opposite to what was theorized by Leja & He (1984) which suggested an improvement in kinetics. It was argued that

the presence of frother at the air-water interface stabilizes the thin film around the bubble which inhibits drainage during collision. The improvements in mineral recovery observed were attributed to the effect of frothers on bubble size.

The synergistic mechanism whereby SDEDTP and hexanol improves the recovery of galena is unique and this research is the first to describe this mechanism. In oxide mineral flotation, authors (Fuerstenau, 2001; Yan, 2016; Wang & Miller, 2018) have shown that collectors can transfer from the air-water interface to the mineral-water interface, but this mechanism is unique in that the frother facilitates the adsorption of the collector onto the mineral surface during bubble-particle collision.

6.3 Recommendations

The regular solution theory approach showed strong synergistic interactions between SD(I)BDTP and hexanol at the air-water interface and these synergistic interactions with these reagents were clearly observed in foam stability and pulp bubble size coalescence tests. The regular solution theory technique may find applications in froth stability. Finding what mixtures of frothers have the strongest molecular interactions may help with the development of frother blends that could reduce reagent consumption.

It was argued that the interactions between DTP and frothers are through dipole-dipole interactions between the polar head groups of the molecules. Further investigation into this interaction using techniques such as density functional theory or other computational chemistry techniques should be able to model the nature of these interactions and the strength of these interactions at the air-water interface or when adsorbed onto different mineral types. The knowledge of how these reagents interact could help design collectors with the right chemical structure to utilise this synergistic effect.

Tracking the adsorption of the frother onto the mineral surface was not performed in this study. Total organic carbon analysis was performed but it was found not to be sensitive to the concentrations of frother used in this study. More sensitive techniques such as studying thin film micro interference might give insight into the transfer of the frother between the air-water and mineral-water interface.

The ACTA is quite sensitive to changes in the chemical environment. Further studies using this device to study the concentration ranges at which collectors and frothers maximize the synergistic effect should be performed and the type of frothers that should be used.

It was proposed that the transfer mechanism of the frother between the air-water and mineral-water interface that destabilizes the thin film between the mineral and the bubble and

synergistically enhances bubble-particle attachment. It was also discussed that the DTP-frother complex on the mineral surface may not be significantly improving the hydrophobicity of the mineral surface. If that is the case, strong bubble-particle aggregates will not form. Tests looking at the effect of energy input on mineral recovery in the presence of DTP-frother systems will provide insight into hydrophobicity that the collector-frother complex induces on the mineral surface. It may be that DTP-frother mixtures only enhance the kinetics of bubble-particle attachment and the addition of xanthate will be required to provide the hydrophobicity at the mineral surface to stabilize bubble-particle aggregates.

7 References

Ackerman, P. K.; G.H. Harris; R. R. Klimpel; & F.F. Aplan. 1987. Evaluation of Flotation Collectors for Copper Sulfides and Pyrite, III. Effect of Xanthate Chain Length and Branching. *International Journal of Mineral Processing*. 21:141–156

Albijanic, B., Ozdemir, O., Nguyen, A. & Bradshaw, D. 2010. A review of induction and attachment times of wetting thin films between air bubbles and particles and its relevance in the separation of particles by flotation. *Advances in Colloid and Interface Science*. 159(1):1-21. DOI: 10.1016/j.cis.2010.04.003.

Allison, S., Goold, L., Nicol, M. & Granville, A. 1972. A determination of the products of reaction betweer various sulfide minerals and aqueous xanthate solution, and a correlation of the products with electrode rest potentials. *Metallurgical Transactions*. 3(10):2613-2618. DOI: 10.1007/bf02644237.

Aspiala, M., Schreithofer, N. & Serna-Guerrero, R. 2018. Automated contact time apparatus and measurement procedure for bubble-particle interaction analysis. *Minerals Engineering*. 121:77-82. DOI: 10.1016/j.mineng.2018.02.018.

Bagci, E., Ekmekci, Z. & Bradshaw, D. 2007. Adsorption behaviour of xanthate and dithiophosphinate from their mixtures on chalcopyrite. *Minerals Engineering*. 20(10):1047-1053. DOI: 10.1016/j.mineng.2007.04.011.

Bansal, V. 1975. Collector frother interaction in a flotation system. *PhD. Indian Institute of Technology Kanpur.*

Barbian, N., Ventura-Medina, E. & Cilliers, J.J. 2003. Dynamic froth stability in froth flotation. *Minerals Engineering*. 16(11):1111-1116.

Bellers, T. 2017. Development of the experimental method for a new attachment timer apparatus as a diagnostic tool in mineral flotation studies. *MSc. Aalto University.*

Bezuidenhout, J. 2011. An investigation into the role of DTP as a co-collector in the flotation of a South African PGM ore. *MSc. University of Cape Town.*

Bikerman, J. 1973. Foams. *In: Applied Physics and Engineering, Springer-Verlag, Berlin*.10.

Blake, P. & Ralston, J. 1985. Controlled methylation of quartz particles. *Colloids and Surfaces*. 15:101-118. DOI: 10.1016/0166-6622(85)80059-7.

Bradshaw, D. & Connor, C. 1996. Measurement of the sub-process of bubble loading in flotation. *Minerals Engineering*. 9(4):443-448. DOI: 10.1016/0892-6875(96)00029-5.

Bradshaw, D. & O'Connor, C. 1994. The flotation of pyrite using mixtures of dithiocarbamates and other thiol collectors. *Minerals Engineering*. 7(5-6):681-690. DOI: 10.1016/0892-6875(94)90099-x.

Bradshaw, DJ, Harris, PJ & O'Connor, C.T. 1998. Synergistic interactions between reagents in sulphide flotation. *Journal of the Southern African Institute of Mining and Metallurgy*. 98(4):189-193.

Buckenham, M.H., Schulman, J.H. 1963. Molecular associations in flotation.*Trans. A.I.M.E*. 226:1-6.

Buckley, A. & Woods, R. 1991. Adsorption of ethyl xanthate on freshly exposed galena surfaces. *Colloids and Surfaces*. 53(1):33-45. DOI: 10.1016/0166-6622(91)80034-l.

Buckley, A. & Woods, R. 1993. Underpotential deposition of dithiophosphate on chalcocite. *Journal of Electroanalytical Chemistry*. 357(1-2):387-405. DOI: 10.1016/0022-0728(93)80393-v.

Buckley, A.N. & Woods, R. 1997. Chemisorption—the thermodynamically favoured process in the interaction of thiol collectors with sulphide minerals. *International journal of mineral processing*/ 51(1-4):15-26. DOI: 10.1016/S0301-7516(97)00016-1

Bueno-Tokunaga, A., Pérez-Garibay, R. & Martínez-Carrillo, D. 2015. Zeta potential of air bubbles conditioned with typical froth flotation reagents. *International Journal of Mineral Processing*. 140:50-57. DOI: 10.1016/j.minpro.2015.04.028.

Chander, S. & Fuerstenau, D. 1974. The effect of potassium diethyldithiophosphate on the electrochemical properties of platinum, copper and copper sulfide in aqueous solutions. *Journal of Electroanalytical Chemistry and Interfacial Electrochemistry*. 56(2):217-247. DOI: 10.1016/s0022-0728(74)80330-x.

Cho, Y. & Laskowski, J. 2002. Effect of flotation frothers on bubble size and foam stability. *International Journal of Mineral Processing*. 64(2-3):69-80. DOI: 10.1016/s0301-7516(01)00064-3.

Clayden, J., Greeves, N. & Warren, S. 2012. Organic chemistry. *Oxford: Oxford University Press*.

Comley, B., Harris, P., Bradshaw, D. & Harris, M. 2002. Frother characterisation using dynamic surface tension measurements. *International Journal of Mineral Processing*. 64(2-3):81-100. DOI: 10.1016/s0301-7516(01)00065-5.

Corin, K., Bezuidenhout, J. & O'Connor, C. 2012. The role of dithiophosphate as a co-collector in the flotation of a platinum group mineral ore. *Minerals Engineering*. 36-38:100-104. DOI: 10.1016/j.mineng.2012.02.019.

Crozier, R. & Klimpel, R. 1989. Frothers: Plant Practice. Mineral Processing and Extractive Metallurgy Review. 5(1-4):257-279. DOI: 10.1080/08827508908952652.

Dai, Z., Bradshaw, D. & Harris, P. 2001. Collector-frother interactions in chalcocite flotation. In *Annual conference of metallurgists of CIM*. Toronto: Met Soc. 181-198.

Dannhauser, W. 1968. Dielectric Relaxation in Isomeric Octyl Alcohols. *The Journal of Chemical Physics*. 48(5):1918-1923. DOI: 10.1063/1.1668990.

Danoucaras, A., Vianna, S. & Nguyen, A. 2013. A modeling approach using back-calculated induction times to predict recoveries in flotation. *International Journal of Mineral Processing*. 124:102-108. DOI: 10.1016/j.minpro.2013.04.013.

Derjaguin, B.V., & Du Dukhin, S.S. 1961. The theory of flotation of small and medium-sized particles. *Trans. Inst. Min. Metall.* 70:221-246

Dhar, P., Thornhill, M. & Kota, H. 2019. Investigation of Copper Recovery from a New Copper Deposit (Nussir) in Northern Norway. *Mineral Processing and Extractive Metallurgy Review*. 40(6):380-389. DOI: 10.1080/08827508.2019.1635475.

Finch, J., Nesset, J. & Acuña, C. 2008. Role of frother on bubble production and behaviour in flotation. *Minerals Engineering*. 21(12-14):949-957. DOI: 10.1016/j.mineng.2008.04.006.

Finkelstein, N.P. & Goold, L.A. 1972. The reaction of sulphide minerals with thiol compounds. *National Institute for Metallurgy*.

Finkelstein, N.P. & Poling, G.W. 1977. The role of dithiolates in the flotation of sulphide minerals. *Mintek*.

Fornasiero, D., Eijt, V. & Ralston, J. 1992. An electrokinetic study of pyrite oxidation. *Colloids and Surfaces*. 62(1-2):63-73. DOI: 10.1016/0166-6622(92)80037-3.

Fornasiero, D., Li, F. & Ralston, J. 1994. Oxidation of Galena. *Journal of Colloid and Interface Science*. 164(2):345-354. DOI: 10.1006/jcis.1994.1176.

Fuerstenau, D. 2001. Excess nonequilibrium collector adsorption and flotation rates. *Mining, Metallurgy & Exploration*. 18(2):83-86. DOI: 10.1007/bf03402876.

Glembotsky, V.A. 1953. The time of attachment of bubbles to solid particles in flotation and its measurement. *Izv. Akad Nauk USSR otdel. Tekhn. Nauk*. 1524-31.

Grano, S., Cnossen, H., Skinner, W., Prestidge, C. & Ralston, J. 1997. Surface modifications in the chalcopyrite-sulphite ion system, II. Dithiophosphate collector adsorption study. *International Journal of Mineral Processing*. 50(1-2):27-45. DOI: 10.1016/s0301-7516(97)00003-3.

Grau, R., Laskowski, J. & Heiskanen, K. 2005. Effect of frothers on bubble size. *International Journal of Mineral Processing*. 76(4):225-233. DOI: 10.1016/j.minpro.2005.01.004.

Gu, G., Sean Sanders, R., Nandakumar, K., Xu, Z. & Masliyah, J. 2004. A novel experimental technique to study single bubble–bitumen attachment in flotation. *International Journal of Mineral Processing*. 74(1-4):15-29. DOI: 10.1016/j.minpro.2003.08.002.

Gu, G., Xu, Z., Nandakumar, K. & Masliyah, J. 2003. Effects of physical environment on induction time of air–bitumen attachment. *International Journal of Mineral Processing*. 69(1-4):235-250. DOI: 10.1016/s0301-7516(02)00128-x.

Güler, T. & Hiçyilmaz, C. 2004. Hydrophobicity of chalcopyrite with dithiophosphate and dithiophosphinate in electrochemically controlled condition. *Colloids and Surfaces A: Physicochemical and Engineering Aspects*. 235(1-3):11-15. DOI: 10.1016/j.colsurfa.2004.01.009.

Güler, T., Hiçyılmaz, C., Gökağaç, G. & Ekmekçi, Z. 2005. Electrochemical behaviour of chalcopyrite in the absence and presence of dithiophosphate. *International Journal of Mineral Processing*. 75(3-4):217-228. DOI: 10.1016/j.minpro.2004.08.009.

Gupta, A., Banerjee, P., Mishra, A., Satish, P. & Pradip. 2007. Effect of alcohol and polyglycol ether frothers on foam stability, bubble size and coal flotation. *International Journal of Mineral Processing*. 82(3):126-137. DOI: 10.1016/j.minpro.2006.09.002.

Hadler, K., Aktas, Z. & Cilliers, J. 2005. The effects of frother and collector distribution on flotation performance. *Minerals Engineering*. 18(2):171-177. DOI: 10.1016/j.mineng.2004.09.014.

Hanson, J.S. & Fuerstenau, D.W. 1993. The mechanism of xanthate adsorption on pyrite. *In 18th International Mineral Processing Congress (IMPC).* Parkville, Australia.

Hernandez-Aguilar, J., Coleman, R., Gomez, C. & Finch, J. 2004. A comparison between capillary and imaging techniques for sizing bubbles in flotation systems. *Minerals Engineering*. 17(1):53-61. DOI: 10.1016/j.mineng.2003.09.011.

Jordaan, T. 2018. Investigating the role of dithiophosphate in the flotation of base metal sulfides. *MSc. University of Cape Town*.

Kakovskii, I., Ryazantseva, B. & Serebryakova, O. 1959. Redox potentials of dithiophosphates. *Zhurnal Fizicheskoi Khimii*. 33(8):1830-1839.

Kakovsky, I.A. 1957. Second International Congress of Surface Activity. *by JH Schulman, Butterworth Scientific Publications*. London, p.225-237

Kelebek, S. & Yoruk, S. 2002. Bubble contact angle variation of sulphide minerals in relation to their self-induced flotation. *Colloids and Surfaces A: Physicochemical and Engineering Aspects*. 196(2-3):111-119. DOI: 10.1016/s0927-7757(01)00822-6.

Kloppers, L., Maree, W., Oyekola, O. & Hangone, G. 2016. Froth flotation of a Merensky Reef platinum bearing ore using mixtures of SIBX with a dithiophosphate and a dithiocarbamate. *Minerals Engineering*. 87:54-58. DOI: 10.1016/j.mineng.2015.12.003.

Kondratyev, S.A. & Ryaboy V.I. 2016. Influence of desorbed species of xanthates and dialkyldithiophosphates on their collecting ability. *In IMPC 2016-28th International Mineral Processing Congress*.

Kosior, D., Zawala, J., Krasowska, M. & Malysa, K. 2013. Influence of n-octanol and α-terpineol on thin film stability and bubble attachment to hydrophobic surface. *Physical Chemistry Chemical Physics*. 15(7):2586. DOI: 10.1039/c2cp43545d.

Kowalczuk, P.B., Zawala, J. & Drzymala, J. 2017. Concentration at the minimum bubble velocity (CMV) for various types of flotation frothers. *Minerals*. 7(7):118. DOI: https://doi.org/10.3390/min7070118

Kunjappu, J. & Rosen, M. 2013. Surfactants and interfacial phenomena. *Hoboken, N.J.: Wiley.*

Laskowski, J. & Kitchener, J. 1969. The hydrophilic—hydrophobic transition on silica. *Journal of Colloid and Interface Science*. 29(4):670-679. DOI: 10.1016/0021-9797(69)90219-7.

Laskowski, J. 2004. Testing flotation frothers. *Physicochemical Problems of Mineral Processing*. 38:13-22.

Leja, J. & He, B. 1984. The role of flotation frothers in the particle-bubble attachment process. *Australian IMM*. 73-39.

Leja, J. & Schulman, J. H. 1954. Flotation theory: molecular interactions between frothers and collectors at solid–liquid–air interfaces. *Trans. A.I.M.E.*, 199:221–228.

Leja, J. 1989. Interactions Among Surfactants. *Mineral Processing and Extractive Metallurgy Review*. 5(1-4):1-24. DOI: 10.1080/08827508908952642.

Lekki, J. & Laskowski, J. (1976). Dynamic interaction in particle-bubble attachment in flotation. *Hydrosols and Rheology*. 331-345. DOI: 10.1016/b978-0-12-404504-0.50029-0.

Lekki, J. & Laskowski, J. 1971. On the dynamic effect of frother-collector joint action in flotation. *Transactions of the Institute of Mining and Metallurgy*. (80):174 - 179.

Leppinen, J. 1990. FTIR and flotation investigation of the adsorption of ethyl xanthate on activated and non-activated sulfide minerals. *International Journal of Mineral Processing*. 30(3-4):245-263. DOI: 10.1016/0301-7516(90)90018-t.

Leppinen, J., Basilio, C. & Yoon, R. 1989. In-situ FTIR study of ethyl xanthate adsorption on sulfide minerals under conditions of controlled potential. *International Journal of Mineral Processing*. 26(3-4):259-274. DOI: 10.1016/0301-7516(89)90032-x.

Lotter, N. & Bradshaw, D. 2010. The formulation and use of mixed collectors in sulphide flotation. *Minerals Engineering*. 23(11-13):945-951. DOI: 10.1016/j.mineng.2010.03.011.

Manev, E. & Pugh, R. 1993. Frother/collector interactions in thin froth films and flotation. *Colloids and Surfaces A: Physicochemical and Engineering Aspects*. 70(3):289-295. DOI: 10.1016/0927-7757(93)80302-u.

Manono, M., Matibidi, K., Otunniyi, I., Thubakgale, C., Corin, K. & Wiese, J. 2020. The Behaviour of Mixtures of Sodium Iso-Butyl Xanthate and Sodium Di-Ethyl Dithiophosphate during the Flotation of a Cu-Ni-Pt Ore in Degrading Water Quality. *Minerals*. 10(2):123. DOI: 10.3390/min10020123.

Matsuoka, I. & Ichikoku, T. 1982. Study on collection of galena by dithiophosphates. *J. Min. Metall. Inst. Jpn*. 98(1131):423-428.

McFadzean, B. & O'Connor, C. 2014. A thermochemical study of thiol collector surface reactions on galena. *Minerals Engineering*. 65:54-60. DOI: 10.1016/j.mineng.2014.04.010.

McFadzean, B., Castelyn, D. & O'Connor, C. 2012. The effect of mixed thiol collectors on the flotation of galena. *Minerals Engineering*. 36-38:211-218. DOI: 10.1016/j.mineng.2012.03.027.

McFadzean, B., Mhlanga, S. & O'Connor, C. 2013. The effect of thiol collector mixtures on the flotation of pyrite and galena. *Minerals Engineering*. 50-51:121-129. DOI: 10.1016/j.mineng.2013.06.018.

Mielczarski, J. & Minni, E. 1984. The adsorption of diethyldithiophosphate on cuprous sulphide. *Surface and Interface Analysis*. 6(5):221-226. DOI: 10.1002/sia.740060504.

Min, M. & Nguyen, A. 2013. An exponential decay relationship between micro-flotation rate and back-calculated induction time for potential flow and mobile bubble surface. *Minerals Engineering*. 40:67-80. DOI: 10.1016/j.mineng.2012.09.017.

Mukai, S., Wakamatsu, T. & Takahashi, K. 1972. Mutual interaction between collectors and frothers in flotation. *Mem. Fac. Eng. Kyoto Univ.* 34:279–288.

Nagaraj, D. & Brinen, J. 1996. SIMS study of adsorbed collector species on mineral surfaces. *In SME Annual Meeting.*

Nagaraj, D. & Brinen, J. 2001. SIMS study of adsorption of collectors on pyrite. *International Journal of Mineral Processing*. 63(1):45-57. DOI: 10.1016/s0301-7516(01)00043-6.

Nguyen, A. & Schulze, H. 2004. *Colloidal science of flotation*. New York: Marcel Dekker.

Nguyen, A., Schulze, H. & Ralston, J. 1997. Elementary steps in particle—bubble attachment. *International Journal of Mineral Processing*. 51(1-4):183-195. DOI: 10.1016/s0301-7516(97)00030-6.

Petrus, H., Hirajima, T., Sasaki, K. & Okamoto, H. 2011. Study of diethyl dithiophosphate adsorption on chalcopyrite and tennantite at varied pHs. *Journal of Mining Science*. 47(5):695-702. DOI: 10.1134/s1062739147050194.

Pienaar, D., Jordaan, T., McFadzean, B. & O'Connor, C. 2019. The synergistic interaction between dithiophosphate collectors and frothers at the air-water and sulphide mineral interface. *Minerals Engineering*. 138:125-132. DOI: 10.1016/j.mineng.2019.04.038.

Raju, G. & Forsling, W. 1997. Adsorption of thiol collectors on chalcopyrite. *Journal of Surface Science Technology*. 13(1):25-37.

Rao, S. R. 2013. Surface Chemistry of Froth Flotation: Volume 1 & Volume 2. *Springer Science & Business Media.*

Rödel, K. 1981. Proof of boundary surface water and its effect on colloidal-chemical properties: IR spectroscopy of foam films. *Tenside Det*. 18(3):141-148.

Rosen, M.J., 1986. Phenomena in mixed surfactant systems. *ACS symposium series. American Chemical Society Washington, DC.*

scipy.org. scipy.optimize.curve_fit — SciPy v1.7.0 Manual. [online] Available at: <https://docs.scipy.org/doc/scipy/reference/generated/scipy.optimize.curve_fit.html>

Somasundaran, P. & Nagaraj, D. 1984. Chemistry and application of chelating agents in flotation and focculation. *IMM Transactions*. 209-219.

Sutherland, K. & Wark, I. 1955. Principles of flotation. *Australian IMM*.

Sweet, C., Van Hoogstraten, J., Harris, M. & Laskowski, J. 1997. The effect of frothers on bubble size and frothability of aqueous solutions. *In Processing of Complex Ores. Montreal: Int. Symp. Metallurgical Society of CIM*. 235-245.

Szyszka, D., Drzymała, J., Łuczyński, J., Wilk, K.A. & Patkowski, J. 2006. Concentration of α-terpineol and (2-dodecanoyloxyethyl) trimethylammonium bromide required for prevention of air bubble coalescence in aqueous solutions. *Physicochemical Problems of Mineral Processing*. 40:53-59.

Tadie, M. 2015. An electrochemical investigation of platinum group minerals. *PhD. University of Cape Town.*

Taguta, J. 2015. The thermochemical behaviour of thiol collectors and collector mixtures with sulphide minerals. *MSc. University of Cape Town.*

Taguta, J., O'Connor, C. & McFadzean, B. 2017. The effect of the alkyl chain length and ligand type of thiol collectors on the heat of adsorption and floatability of sulphide minerals. *Minerals Engineering*. 110:145-152. DOI: 10.1016/j.mineng.2017.04.021.

Tan, Y.H., Rafiei, A.A., Elmahdy, A. & Finch, J.A. 2013. Bubble size, gas holdup and bubble velocity profile of some alcohols and commercial frothers. *International Journal of Mineral Processing*. 119:1-5.

Usul, A. & Tolun, R. 1974. Electrochemical study of the pyrite-oxygen-xanthate system. *International Journal of Mineral Processing*. 1(2):135-140. DOI: 10.1016/0301-7516(74)90009-x.

Wadsö, I. & Goldberg, R. 2001. Standards in isothermal microcalorimetry (IUPAC Technical Report). *Pure and Applied Chemistry*. 73(10):1625-1639. DOI: 10.1351/pac200173101625.

Wang, W., Zhou, Z., Nandakumar, K., Masliyah, J. & Xu, Z. 2005. An induction time model for the attachment of an air bubble to a hydrophobic sphere in aqueous solutions. *International Journal of Mineral Processing*. 75(1-2):69-82. DOI: 10.1016/j.minpro.2004.04.009.

Wang, X. & Miller, J. 2018. Dodecyl amine adsorption at different interfaces during bubble attachment/detachment at a silica surface. *Physicochemical Problems of Mineral Processing*. 54.

Wark, E.E & Wark, I.W. 1932. The Physical Chemistry of Flotation III. *J.Phys. Chem*. 37(1):805–814.

Wark, I. & Cox, A. 1934. Principles of flotation, III. *Trans. AIME*. (112):267 - 301.

Winter, G. & Woods, R. 1973. The Relation of Collector Redox Potential to Flotation Efficiency: Monothiocarbonates. *Separation Science*. 8(2):261-267. DOI: 10.1080/00372367308058000.

Woods, R., Kim, D. & Yoon, R. 1993. The potential dependence of flotation of chalcocite with diethyl dithiophosphate. *International Journal of Mineral Processing*. 39(1-2):101-106. DOI: 10.1016/0301-7516(93)90055-f.

Woods, R., Young, C. & Yoon, R. 1990. Ethyl xanthate chemisorption isotherms and Eh-pH diagrams for the copper/water/xanthate and chalcocite/water/xanthate systems. *International Journal of Mineral Processing*. 30(1-2):17-33. DOI: 10.1016/0301-7516(90)90065-7.

Yan, H. 2016. Collector transfer between bubble and particle collision. *MSc. University of British Columbia.*

Yoon, R. & Luttrell, G. 1989. The Effect of Bubble Size on Fine Particle Flotation. *Mineral Processing and Extractive Metallurgy Review*. 5(1-4):101-122. DOI: 10.1080/08827508908952646.

Zembala, M. & Pomianowski, A. 1970. Adsorption of flotation frothers on a surface of mercury. *In 9th—symposium on physicochemical problems of mineral processing*. Gliwice.

Zhang, W., Nesset, J., Rao, R. & Finch, J. 2012. Characterizing Frothers through Critical Coalescence Concentration (CCC)95-Hydrophile-Lipophile Balance (HLB) Relationship. *Minerals*. 2(3):208-227. DOI: 10.3390/min2030208.

Zhang, W., Tan, Y.H. and Finch, J.A., 2016. Synthesis and characterization of alkyl, propoxy, ethoxy-based frothers. *Minerals Engineering*. 95:66-73.

Zhou, Q. & Rosen, M. 2003. Molecular Interactions of Surfactants in Mixed Monolayers at the Air/Aqueous Solution Interface and in Mixed Micelles in Aqueous Media: The Regular Solution Approach. *Langmuir*. 19(11):4555-4562. DOI: 10.1021/la020789m.

8 Appendices

All data not available in the appendices are available at the following link: https://figshare.com/s/a8dff54b525a9a3a1a3e

8.1 Microflotation data

8.1.1 Galena

Reagents Condition	Samples	Mass Recovery Run 1	Mass Recovery Run 2
No Reagents	Concentrate 1	0.4121	0.3873
	Concentrate 2	0.8124	0.8502
	Concentrate 3	1.0964	1.0389
	Concentrate 4	0.3081	0.4843
	Tailings	0.302	0.2257
0.12 mM Hexanol	Concentrate 1	1.5189	1.5725
	Concentrate 2	1.001	1.0669
	Concentrate 3	0.156	0.1974
	Concentrate 4	0.0523	0.0337
	Tailings	0.2087	0.0628
SDEDTP	Concentrate 1	0.483	0.4738
	Concentrate 2	0.88	0.9424
	Concentrate 3	1.01754	0.9398
	Concentrate 4	0.3495	0.3372
	Tailings	0.179	0.1988
SDEDTP + 0.12 mM Hexanol	Concentrate 1	2.4029	2.3784
	Concentrate 2	0.3637	0.3774
	Concentrate 3	0.0961	0.0977
	Concentrate 4	0.0466	0.0441
	Tailings	0.1035	0.0582
SEX	Concentrate 1	0.4035	0.1981
	Concentrate 2	0.8685	0.7097
	Concentrate 3	0.8761	1.0238
	Concentrate 4	0.5162	0.7656
	Tailings	0.2856	0.3139
SEX + 0.12 mM Hexanol	Concentrate 1	0.621	0.8388
	Concentrate 2	1.4706	1.3584
	Concentrate 3	0.6446	0.5836
	Concentrate 4	0.1982	0.1118
	Tailings	0.0539	0.0888

8.1.2 Pyrite

Reagents	Samples	Mass Recovery Run 1	Mass Recovery Run 2
No Reagents	Concentrate 1	0.0732	0.0565
	Concentrate 2	0.0654	0.0884
	Concentrate 3	0.054	0.1034
	Concentrate 4	0.0922	0.1079
	Tailings	2.6372	2.7488
0.12 mM Hexanol	Concentrate 1	0.0917	0.1921
	Concentrate 2	0.2316	0.2045
	Concentrate 3	0.1979	0.1569
	Concentrate 4	0.2777	0.1985
	Tailings	2.0671	2.2492
0.014 mM PPG425	Concentrate 1	0.1486	0.0977
	Concentrate 2	0.172	0.1519
	Concentrate 3	0.2054	0.1694
	Concentrate 4	0.2205	0.1571
	Tailings	2.2326	1.9981
SDEDTP	Concentrate 1	0.0416	0.0486
	Concentrate 2	0.0681	0.0565
	Concentrate 3	0.0767	0.0645
	Concentrate 4	0.0436	0.0594
	Tailings	2.7053	2.7267
0.1 mM SDEDTP	Concentrate 1	0.0169	0.0261
	Concentrate 2	0.0368	0.0447
	Concentrate 3	0.0434	0.0501
	Concentrate 4	0.0428	0.0445
	Tailings	2.7926	2.7894
0.1 ML SIBX + 0.1 mM SDEDTP	Concentrate 1	0.0723	0.0341
	Concentrate 2	0.1014	0.0395
	Concentrate 3	0.1049	0.0658
	Concentrate 4	0.092	0.0763
	Tailings	2.6214	2.7874

Reagents	Samples	Mass Recovery Run 1	Mass Recovery Run 2
0.1 mM SDEDTP + 0.12 mM Hexanol	Concentrate 1	0.2547	0.2594
	Concentrate 2	0.3829	0.4872
	Concentrate 3	0.5857	0.7611
	Concentrate 4	0.6433	0.5662
	Tailings	0.7626	1.0912
0.1 ML SIBX + 0.1 mM SDEDTP + 0.12 mM Hexanol	Concentrate 1	0.3206	0.2673
	Concentrate 2	0.4481	0.3377
	Concentrate 3	0.4442	0.3953
	Concentrate 4	0.4941	0.3777
	Tailings	1.2223	1.592
SEX	Concentrate 1	0.059	0.1119
	Concentrate 2	0.0671	0.1865
	Concentrate 3	0.0695	0.1297
	Concentrate 4	0.0532	0.0965
	Tailings	2.7177	2.2828
SEX + 0.12 mM Hexanol	Concentrate 1	0.1368	0.102
	Concentrate 2	0.1751	0.1418
	Concentrate 3	0.175	0.1144
	Concentrate 4	0.1411	0.1048
	Tailings	2.2987	2.4036
0.1 mM SDEDTP + 0.014 mM PPG425	Concentrate 1	0.2325	0.1785
	Concentrate 2	0.2089	0.2492
	Concentrate 3	0.2456	0.2809
	Concentrate 4	0.2563	0.2529
	Tailings	2.1302	1.9651

8.1.3 Chalcopyrite

Reagents	Samples	Mass Recovery Run 1	Mass Recovery Run 2
No Reagents	Concentrate 1	0.5111	0.3743
	Concentrate 2	0.785	1.0046
	Concentrate 3	0.7941	0.8185
	Concentrate 4	0.3736	0.3098
	Tailings	0.545	0.4597
0.12 mM Hexanol	Concentrate 1	1.2751	1.3312
	Concentrate 2	1.1849	1.0958
	Concentrate 3	0.2967	0.2715
	Concentrate 4	0.0823	0.1037
	Tailings	0.166	0.1656
SDEDTP	Concentrate 1	0.5771	0.4684
	Concentrate 2	1.1579	0.9614
	Concentrate 3	0.5378	0.7652
	Concentrate 4	0.1505	0.3247
	Tailings	0.4776	0.4815
SDEDTP + 0.12 mM Hexanol	Concentrate 1	1.6118	1.6486
	Concentrate 2	0.9547	0.8458
	Concentrate 3	0.2564	0.2434
	Concentrate 4	0.0977	0.1066
	Tailings	0.2	0.2271
SEX	Concentrate 1	1.496	1.4249
	Concentrate 2	0.7557	0.7779
	Concentrate 3	0.195	0.2398
	Concentrate 4	0.0613	0.1276
	Tailings	0.3526	0.3613
SEX + 0.12 mM Hexanol	Concentrate 1	1.6892	1.9079
	Concentrate 2	0.829	0.6647
	Concentrate 3	0.1776	0.1566
	Concentrate 4	0.0877	0.0846
	Tailings	0.1794	0.1697

8.1.4 Chalcocite

Reagents	Samples	Mass Recovery Run 1	Mass Recovery Run 2
No Reagents	Concentrate 1	0.3314	0.2706
	Tailings	2.6742	2.5047
SDEDTP	Concentrate 1	1.4674	1.4087
	Tailings	1.5336	1.5578
SD(N)BDTP	Concentrate 1	0.8587	0.7727
	Tailings	2.0856	2.1722
SD(I)BDTP	Concentrate 1	0.8236	0.9877
	Tailings	2.1512	1.9245
10 ML SDEDTP	Concentrate 1	0.9583	0.9406
	Tailings	1.9924	2.0148
SD(I)BDTPINA	Concentrate 1	1.4189	1.2691
	Tailings	1.562	1.7401
SEX	Concentrate 1	0.7364	0.8824
	Tailings	2.1947	2.1206
PNBX	Concentrate 1	1.2948	1.43554
	Tailings	1.6627	1.5614
SIBX	Concentrate 1	1.4259	1.1916
	Tailings	1.5475	1.7812
0.12 mM Hexanol	Concentrate 1	0.5043	0.5151
	Tailings	2.4906	2.4855
0.014 mM PPG425	Concentrate 1	0.4713	0.4203
	Tailings	2.3022	2.6224
0.062 mM Octanol	Concentrate 1	0.3348	0.4259
	Tailings	2.1826	2.929
SDEDTP + 0.12 mM Hexanol	Concentrate 1	1.9854	2.0889
	Tailings	0.9746	0.8584
SD(N)BDTP + 0.12 mM Hexanol	Concentrate 1	1.6484	1.8837
	Tailings	1.1228	1.3033
SD(I)BDTP + 0.12 mM Hexanol	Concentrate 1	1.7937	1.761
	Tailings	1.1668	1.1782
10 ML SDEDTP + 0.12 mM Hexanol	Concentrate 1	1.925	1.9102
	Tailings	1.0017	1.0582
SD(I)BDTPINA + 0.12 mM Hexanol	Concentrate 1	2.2101	2.2231
	Tailings	0.7886	0.8127

Reagents	Samples	Mass Recovery Run 1	Mass Recovery Run 2
SEX + 0.12 mM Hexanol	Concentrate 1	1.8361	2.0517
	Tailings	1.1376	0.8981
PNBX + 0.12 mM Hexanol	Concentrate 1	1.8717	1.6968
	Tailings	1.0931	1.0287
SIBX + 0.12 mM Hexanol	Concentrate 1	2.0678	2.1615
	Tailings	0.9709	0.9215
SDEDTP + 0.014 mM PPG425	Concentrate 1	1.64624	1.6544
	Tailings	1.3171	1.368
SD(N)BDTP + 0.014 mM PPG425	Concentrate 1	1.6353	1.4197
	Tailings	1.3903	1.5794
SDEDTP + 0.062 mM Octanol	Concentrate 1	1.677	1.4761
	Tailings	1.2605	1.2454
SD(N)BDTP + 0.062 mM Octanol	Concentrate 1	1.6162	1.5582
	Tailings	1.5179	1.4714

8.1.5 Quartz

Reagents	Samples	Mass Recovery Run 1	Mass Recovery Run 2
No Reagents	Concentrate 1	0.0708	0.0772
	Concentrate 2	0.0832	0.1009
	Concentrate 3	0.0843	0.101
	Concentrate 4	0.0683	0.0775
	Tailings	2.601	2.4779
0.12 mM Hexanol	Concentrate 1	0.1313	0.1683
	Concentrate 2	0.2016	0.1805
	Concentrate 3	0.1346	0.1762
	Concentrate 4	0.1851	0.1446
	Tailings	2.1086	2.2642
0.1 mM SDEDTP	Concentrate 1	0.0675	0.0679
	Concentrate 2	0.098	0.1078
	Concentrate 3	0.1068	0.0887
	Concentrate 4	0.0879	0.0923
	Tailings	2.5629	2.6032
0.1 mM SDEDTP + 0.12 mM Hexanol	Concentrate 1	0.1194	0.1233
	Concentrate 2	0.1768	0.1576
	Concentrate 3	0.1758	0.1867
	Concentrate 4	0.1717	0.1342
	Tailings	2.217	2.2844

8.2 Isothermal Titration Calorimetry

8.2.1 Galena and SDEDTP

Section name	Duration	Mean	Slope	Peak Area
Units	**s**	**Watts**	**Watts/s**	**J**
Initial baseline	298.84724	-1.679E-07	-1.733E-10	
Titration 1	2701.6327	3.12E-07	-3.147E-10	0.0011292
Baseline 1	897.56193	-4.359E-08	-5.115E-11	
Titration 2	2702.8263	2.827E-07	-2.192E-10	0.0006167
Baseline 2	896.36836	1.535E-07	1.102E-10	
Titration 3	2703.4754	2.481E-07	-1.818E-10	0.0003627
Baseline 3	900.56995	7.473E-08	-1.144E-10	
Titration 4	2699.9666	1.553E-07	-1.644E-10	0.0003974
Baseline 4	899.22808	-5.815E-08	-1.685E-10	
Titration 5	2702.1626	5.451E-08	-1.347E-10	0.0003675
Baseline 5	897.0321	-1.044E-07	-7.932E-11	
Titration 6	2703.583	2.765E-08	-5.22E-11	0.0001683
Baseline 6	900.4623	3.556E-08	-3.323E-11	
Titration 7	2699.9238	3.013E-08	-1.547E-10	0.0001354
Baseline 7	899.27085	-7.572E-08	1.608E-10	

8.2.2 Galena, Hexanol and SDEDTP

Section name	Duration	Mean	Slope	Peak Area
Units	**s**	**Watts**	**Watts/s**	**J**
Initial baseline	298.8038	-6.36E-08	1.17E-10	
Titration 1	2700.848	6.27E-08	-4.62E-11	0.000184
Baseline 1	898.0989	5.30E-08	-9.14E-12	
Titration 2	2703.029	5.05E-08	-1.41E-10	8.49E-05
Baseline 2	895.9181	-1.48E-08	-9.36E-11	
Titration 3	2704.346	2.79E-08	-1.07E-10	0.000121
Baseline 3	899.4513	-1.87E-08	-1.14E-11	
Titration 4	2700.957	1.48E-08	-1.14E-10	7.65E-05
Baseline 4	897.9904	-8.22E-09	-3.97E-11	
Titration 5	2702.492	2.83E-08	-8.19E-11	0.000128
Baseline 5	896.455	-3.01E-08	2.93E-11	
Titration 6	2703.861	1.03E-08	-9.40E-11	8.31E-05
Baseline 6	899.937	-1.06E-08	6.09E-11	
Titration 7	2700.329	1.08E-07	-5.24E-11	0.000147
Baseline 7	898.6179	1.18E-07	-6.72E-11	
Titration 8	2701.844	9.10E-08	-1.51E-10	0.000179
Baseline 8	901.6251	-6.76E-08	3.57E-11	

8.2.3 Pyrite and SDEDTP

Section name	Duration	Mean	Slope	Peak Area
Units	**s**	**Watts**	**Watts/s**	**J**
Initial baseline	294.33337	1.729E-06	-5.826E-11	
Titration 1	2705.4812	7.156E-07	-1.267E-09	-0.0001012
Baseline 1	900.71616	-2.243E-07	-7.046E-11	
Titration 2	2699.5193	-3.99E-08	-5.6E-10	0.0006876
Baseline 2	900.62738	-3.64E-07	1.707E-10	
Titration 3	2700.2321	-7.099E-08	-4.897E-10	0.0008127
Baseline 3	899.91458	-3.792E-07	-7.254E-12	
Titration 4	2700.9866	2.738E-08	-4.371E-10	0.0007813
Baseline 4	899.16004	-1.437E-07	5.126E-12	
Titration 5	2701.2311	2.963E-07	-4.201E-10	0.0008707
Baseline 5	898.91552	9.242E-08	1.087E-10	
Titration 6	2702.1797	5.177E-07	-4.446E-10	0.0009087
Baseline 6	897.96701	2.712E-07	1.652E-11	
Titration 7	2702.2742	5.851E-07	-4.257E-10	0.0007874
Baseline 7	897.87248	3.172E-07	5.647E-11	
Titration 8	2703.0625	5.988E-07	-4.922E-10	0.0008852
Baseline 8	897.08412	2.257E-07	-9.133E-11	
Titration 9	2703.1477	4.292E-07	-4.937E-10	0.0009046
Baseline 9	896.99896	-3.644E-08	-1.469E-10	
Titration 10	2704.0422	1.079E-07	-5.333E-10	0.0007685
Baseline 10	901.44099	-3.166E-07	-1.571E-10	

8.2.4 Chalcopyrite and SDEDTP

Section name	Duration	Mean	Slope	Peak Area
Units	**s**	**Watts**	**Watts/s**	**J**
Initial baseline	298.24865	1.923E-07	1.305E-10	
Titration 1	2702.2353	3.669E-07	-3.341E-10	0.000767
Baseline 1	897.20411	-2.528E-08	-5.391E-11	
Titration 2	2703.1197	2.19E-07	-1.919E-10	0.000669
Baseline 2	896.31976	-3.065E-08	-1.009E-10	
Titration 3	2704.5284	1.829E-08	-1.247E-10	0.000218
Baseline 3	899.76202	-9.363E-08	-1.633E-11	
Titration 4	2701.2754	4.429E-08	-8.54E-11	0.000255
Baseline 4	898.16402	-6.112E-09	-4.719E-12	
Titration 5	2702.2476	1.139E-07	-8.579E-11	0.000265
Baseline 5	897.19187	3.803E-08	-2.101E-11	
Titration 6	2704.0238	1.611E-07	-7.326E-11	0.000261
Baseline 6	900.26659	9.12E-08	-4.01E-11	
Titration 7	2700.1299	1.552E-07	-1.03E-10	0.000233
Baseline 7	899.30951	4.667E-08	-6.95E-11	
Titration 8	2701.8269	6.544E-08	-1.161E-10	0.000227
Baseline 8	901.42507	-8.401E-08	-8.843E-11	

8.2.5 Chalcocite and SDEDTP

Section name	Duration	Mean	Slope	Peak Area
Units	**s**	**Watts**	**Watts/s**	**J**
Initial baseline	294.98232	2.252E-07	-2.051E-10	
Titration 1	5404.9133	6.825E-07	-1.087E-09	0.0040755
Baseline 1	1794.3597	-3.658E-07	-1.191E-10	
Titration 2	5406.9844	1.493E-06	-1.036E-09	0.0084954
Baseline 2	1792.2886	2.144E-07	-4.081E-11	
Titration 3	5407.8588	1.885E-06	-9.747E-10	0.0088009
Baseline 3	1791.4142	3.038E-07	-1.356E-10	
Titration 4	5409.5419	1.82E-06	-8.857E-10	0.0085795
Baseline 4	1799.3816	1.663E-07	-1.312E-10	
Titration 5	5400.4429	1.553E-06	-8.139E-10	0.0081649
Baseline 5	1798.8301	-8.124E-08	-1.809E-10	
Titration 6	5401.7897	1.147E-06	-7.151E-10	0.0074786
Baseline 6	1797.4833	-3.928E-07	-1.141E-10	
Titration 7	5403.4774	1.004E-06	-5.881E-10	0.0069948
Baseline 7	1795.7956	-1.875E-07	-1.472E-10	
Titration 8	5404.4996	1.296E-06	-4.861E-10	0.0066829
Baseline 8	1801.1289	3.102E-07	-1.727E-11	

8.2.6 Validation Propan-1-ol

Section name	Duration	Mean	Slope	Peak Area
Units	**s**	**Watts**	**Watts/s**	**J**
Initial baseline	299.2299	-5.11E-08	-2.98E-10	
Titration 1	450.8586	1.20E-05	-1.10E-07	0.005378
Baseline 1	150.1414	1.27E-07	-1.03E-09	
Titration 2	450.2487	1.22E-05	-1.14E-07	0.005476
Baseline 2	149.7513	7.96E-08	-1.26E-09	
Titration 3	450.4962	1.21E-05	-1.13E-07	0.005452
Baseline 3	150.5038	-5.58E-08	-6.77E-10	
Titration 4	449.8354	1.21E-05	-1.14E-07	0.005485
Baseline 4	150.1646	-5.52E-08	-1.79E-09	
Titration 5	450.0961	1.19E-05	-1.12E-07	0.005417
Baseline 5	149.9039	-7.15E-08	-1.43E-09	
Titration 6	450.4513	1.20E-05	-1.11E-07	0.005419
Baseline 6	300.8746	4.00E-08	-4.03E-10	

8.3 UV-Vis with aeration

Absorbance of SDEDT at 225 nm for different minerals and conditions

	No reagents air	No reagents without air	SDEDTP with air	SDEDTP without air	Hexanol with air	Hexanol without air	SDEDTP+ Hexanol with air	SDEDTP + Hexanol without air
Galena	0.269	0.281	0.463	0.468	0.302	0.282	0.454	0.467
	0.28	0.286	0.47	0.478	0.306	0.276	0.45	0.465
Pyrite	0.164	0.167	0.308	0.309	0.164	0.159	0.295	0.319
	0.17	0.152	0.29	0.314	0.155	0.157	0.31	0.314
Chalcopyrite	0.166	0.163	0.317	0.319	0.139	0.153	0.309	0.312
	0.15	0.157	0.32	0.312	0.145	0.158	0.31	0.308

8.4 Foam Stability

8.4.1 Foam stability of single reagents

Foam height in cm. NP – Not Performed

Reagents	**Concentration**	**0.13**	**0.26**	**0.53**
Hexanol	Run 1	NP	2	9
	Run 2	NP	2.5	7.5
	Run 3	NP	2.5	7
SDEDTP	Run 1	0.5	0.75	0.5
	Run 2	0.5	0.5	0.5
	Run 3	0.5	0.5	0.75
SD(N)BDTP	Run 1	0.5	0.5	1
	Run 2	0.5	0.5	0.5
	Run 3	0.5	0.5	0.5
SD(I)BDTP	Run 1	1	1.5	1.5
	Run 2	1	1	1
	Run 3	1	1	1
SIBX	Run 1	0.5	0.5	0.5
	Run 2	0.5	0.5	0.5
	Run 3	0.5	0.5	0.5

8.4.2 Foam stability of reagent mixtures

Total Concentration	0.52 mM				0.79 mM				0.79 mM			
Mole Fraction	0.50				0.32				0.67			
	SDEDTP	SD(N)BDTP	SD(I)BDTP	SIBX	SDEDTP	SD(N)BDTP	SD(I)BDTP	SIBX	SDEDTP	SD(N)BDTP	SD(I)BDTP	SIBX
Foam Height (cm)	2.5	2	5.5	2	6.5	6	8	7	2.5	4	8.5	3.5
	2	2	5.5	2	6	6	7	7	3	3	9	4

8.4.3 Foam rise velocity

Foam rise velocity of different collectors in the presence of 0.53 mM hexanol

SDEDTP [0.26 mM]		SD(N)BDTP [0.26 mM]		SD(I)BDTP [0.26 mM]		SIBX [0.26 mM]	
Time (s)	Height (cm)	Time (s)	Height (cm)	Time (s)	Height (cm)	Time (s)	Height (cm)
2	2	2	2.5	2	4	2	1.5
4	3.5	4	4.5	4	7.5	4	4
6	5	6	6.5	6	10	6	6.5
11	5.5	11	9.5	11	13.5	11	8.5
16	6.5	16	11.5	16	18	16	9.5
21	6	21	12.5	21	20.5	26	10
26	6	26	12	26	22	36	9
36	6	31	10.5	31	20.5	46	8
		36	8.5	36	18	56	7.5
		42	6.5	41	13.5	66	7
		47	6.5	46	11	96	7.5
		52	5.5	51	9		
		62	5	61	7		
		72	5	71	6		
				81	6		

Foam rise velocity of different collectors over longer time periods in the presence of 0.53 mM hexanol.

SD(N)BDTP [0.26 mM]		SD(I)BDTP [0.26 mM]		SIBX [0.26 mM]	
Time (s)	Height (cm)	Time (s)	Height (cm)	Time (s)	Height (cm)
0	0	0	0	0	0
2	3	2	3	2	3
5	5	4	5.5	6	7
9	7.5	6	8	10	8.5
13	9	8	9	14	11
17	11	10	12	18	11
21	12.5	13	13	23	12.5
26	13	16	14	28	13.5
31	14	20	15.5	33	13.5
36	13.5	25	15	38	12.5
41	13	30	14	43	13.5
46	13	35	13.5	48	13
51	13	40	11	58	12
56	11.5	45	9	68	11
61	11	50	8	78	11
66	10	55	6	88	11
71	9	60	5.5	98	11
81	8	65	5	108	11
101	7	70	5	168	11
161	4.5	75	5.5	228	11
221	4.5	80	5.5	348	11
281	4.5	85	5	468	11.5
341	4.5	95	5.5	588	11.5
461	3.5	215	6	708	12
701	3.5	335	6	948	12
941	3.5	455	6	1188	12
1181	3.5	575	6	1428	13
1421	3.5	695	6.5	1668	13
1661	3.5	815	7.5	1908	13.5
1901	3.5	935	8.5	2148	13.5
2141	3.5	1055	9.5	2388	14
		1175	10.5	2628	15
		1295	12		
		1415	16.5		
		1535	19.5		
		1655	25.5		
		1775	31.5		
		1895	40		
		2015	33.5		
		2255	38		

Solution reused			
SD(I)BDTP [0.26 mM] + Hexanol [0.53 mM]			
Time (s)	Height (cm)	Time (s)	Height (cm)
0	0	174	31
3	4	234	37.5
6	8.5	294	33.5
9	12	354	30.5
12	14.5	414	31
15	17	474	31.5
18	19.5	534	31.5
21	21.5	594	32.5
24	23	654	34.5
29	25	714	38.5
34	27	774	31
39	27.5	834	30.5
44	28	894	32.5
49	28	954	35
54	27.5	1014	36.5
64	27	1074	37
74	26.5	1134	39.5
84	26.5	1194	30.5
114	27	1254	31
144	29		

8.5 Surface tension

Surface tension in dynes per cm

Concentration [M]	Hexanol	SDEDTP	SEX	SDEDTP + Hexanol	SEX + Hexanol
0.001	70.42	74	73.29	72.81	72.72
0.005	61.88	73.69	72.48	68.75	68.11
0.01	53.76	73.31	72.51	62.7	62.57
0.025	41.77	72.58	72.26	51.93	NP
0.05	31.89	71.78	71.95	42.17	41.7
0.1		70.16	71.54	30.14	30.22
0.2		67.79	71.39		

Concentration [M]	SD(N)BDTP	PNBX	SD(N)BDTP + Hexanol	PNBX + Hexanol
0.001	70.42	73.6	70.65	73.06
0.005	66.55	73.37	62.65	68.77
0.01	63.61	72.99	57.44	62.34
0.026	58.82	72.1	46.86	51.38
0.05	53.8	71.22	36.68	40.78
0.1	46.71	69.2	28.06	29.44
0.2	41.31	65.36		
0.4		61.11		

Concentration [M]	SD(I)BDTP	SIBX	SD(I)BDTPINA	SD(I)BDTP + Hexanol	SIBX + Hexanol	SD(I)BDTPINA + Hexanol
0.001	67.94	71.81	68.81	66.96	NP	69.08
0.005	63.65	71.38	63.94	60.4	66.84	61.05
0.01	61.32	71.17	60.73	54.59	61.12	54.99
0.025	57.12	70.25	56.08	44.82	50.66	45.4
0.05	52.72	68.92	52.8	35.48	40.7	38.1
0.1	47.36	65.88	48.92	27.09	29.19	28.9
0.2		60.92	44.23			

Concentration [M]	SDHDTP	PAX	SDHDTP + Hexanol	PAX + Hexanol
0.001		71.39	NP	
0.005	46.5	70.72	47.63	66.14
0.01	41.22	70.12	41.32	60.11
0.025	34.42	68.78	31.74	48.9
0.05	28.67	67.06	23.34	37.94
0.1		63.88		
0.2		58.84		

Concentration [M]	PPG425	SD(N)BDTP + PPG425
1.00E-03	58.19	59.35
5.00E-03	53.32	53.28
1.00E-02	51.31	50.71
2.50E-02	48.52	46.8
5.00E-02	46.02	43.94
0.1	43.27	38.58

8.6 Collector purity sheet

Sample ID		% (w/w) Active by Iodine	Composition by GC/FID area% [2]			
No.	DTP [1]		Component [3]	% rel. [4] of active	% rel.[4] of total	Figure
UCT-2	di-ethyl	46.6	Sodium O,O'-diethyl thiophosphate	4.0	3.96	1
			Sodium O,O'-diethyl dithiophosphate	96.0	95.66	
			O,O',S-triethyl dithiophosphate	-	0.37	
UCT-3	di-(*n*-butyl)	48.4	di-Sodium O- butyl dithiophosphate	0.39	0.37	2
			Sodium O,O'-dibutyl thiophosphate	4.45	4.27	
			Sodium O,O'-dibutyl dithiophosphate	95.16	91.38	
			O,O',O"-tributyl thiophosphate	-	3.22	
			O,O',S-tributyl dithiophosphate	-	0.75	
UCT-4	di-(*iso*-propyl)	44.5	Sodium O,O'-di-(*iso*-propyl) thiophosphate	5.79	5.77	3
			Sodium O, O'-di-(*iso*-propyl) dithiophosphate	94.21	93.79	
			O,O',O"-tri-(*iso*-propyl) thiophosphate	-	0.44	
UCT-5	di-cyclohexyl	45.6	cyclohexanol		10.39	4
			di-Sodium O-cyclohexyl dithiophosphate	0.93	0.83	
			Sodium O,O'-di-cyclohexyl thiophosphate	5.98	5.36	
			Sodium O, O'-di-cyclohexyl dithiophosphate	93.09	83.42	
UCT-6	di-(*iso*-butyl)	45.3	Sodium O,O'-di-(*iso*-butyl) thiophosphate	5.87	5.65	5
			O,O',O"-tri-(*iso*-butyl) thiophosphate	-	3.82	
			Sodium O, O'-di-(*iso*-butyl) dithiophosphate	93.91	90.32	
			Sodium O-butyl- O'-(*iso*-butyl) dithiophosphate	0.23	0.22	
UCT-7	di-cresyl	44.9	m-cresol	-	5.04	6
			di-Sodium O- cresyl dithiophosphate	0.93	0.88	
			Sodium O,O'-di-(*m*-cresyl) thiophosphate	7.97	7.57	
			Sodium O, O'-di-(*m*-cresyl) dithiophosphate	89.67	85.15	
			Sodium O-(*m*-cresyl)-O'-(*p*-cresyl) dithiophosphate	1.46	1.35	
UCT-8	di-(*n*-hexyl)	15.6	n-hexanol	-	7.27	7
			Sodium O,O'-dihexyl thiophosphate	2.52	2.24	
			Sodium O,O'-dihexyl dithiophosphate	97.48	86.53	
			O,O',O"-trihexyl thiophosphate	-	3.95	

8.7 Image size analysis code

```
import Pkg
Pkg.activate(mktempdir())
Pkg.add([
    Pkg.PackageSpec(name="ImageIO", version="0.5"),
    Pkg.PackageSpec(name="ImageShow", version="0.2"),
    Pkg.PackageSpec(name="FileIO", version="1.6"),
    Pkg.PackageSpec(name="PNGFiles", version="0.3.6"),
    Pkg.PackageSpec(name="ImageMagick", version="1"),
    Pkg.PackageSpec(name="ImageFiltering", version="0.6"),
    Pkg.PackageSpec(name="Colors", version="0.12"),
    Pkg.PackageSpec(name="ColorVectorSpace", version="0.8"),
    Pkg.PackageSpec(name="PlutoUI", version="0.7"),
    Pkg.PackageSpec(name="Plots", version="1"),
    Pkg.PackageSpec(name="ImageView"),
    Pkg.PackageSpec(name="ImageFeatures")

])

using Images, ImageView
using Colors, ColorVectorSpace, ImageShow, FileIO
using ImageFiltering
using Plots, PlutoUI
using ImageFeatures
using Statistics, LinearAlgebra  # standard libraries available in any
environment

function resize_img(img)
    bi_r, bi_c = size(img)
    window_row(x) = Int64(bi_r/2 - bi_r*x):1:Int64(bi_r/2 + bi_r*x)-450
    image_resize = copy(img[window_row(0.25),1:bi_c])
    return image_resize
end

bubble_image = load("CYCLE 1_LED.JPG")
bubble_image_resize = resize_img(bubble_image)
```

```
function bubble_detect(img,α)
    brightness(image,α=1) = image.*α
    bubble_gray = Gray.(brightness.(img,α))
    img_edges = canny(bubble_gray, (Percentile(99), Percentile(80)))
    dx, dy=imgradients(bubble_gray, KernelFactors.sobel)
    img_phase = phase(dx, dy)
    centers, radii = hough_circle_gradient(img_edges, img_phase, 75:250)
    return centers,radii,img_phase,img_edges
end

function circle_plot(img,radii,centers,line_width)
    img_plot = copy(RGB.(img))
    L = line_width
    for (c,r) in zip(centers,radii)
        a = c[1] #x coordinate of center point
        b = c[2] #y coordinate of center point
        #Plotting the center point of the cirlce
        [img_plot[i,j] = RGB(1,0,0) for i=a-L:a+L,j=b-L:b+L]
        #Plotting the circle around the center point
        for angle in 0:360
            i = ceil(Int64,r*sin(deg2rad(angle)) + a)
            j = ceil(Int64,r*cos(deg2rad(angle)) + b)
            [img_plot[k,l] = RGB(1,0,0) for k= i-L:i+L,l=j-L:j+L]
        end
    end
    return img_plot
end

centers, radii, img_phase, img_edges = bubble_detect(bubble_image_resize,1)

circle_plot(bubble_image_resize,radii,centers,2)
```